

ISSUES INVOLVED IN SEISMIC RETROFIT OF
REINFORCED CONCRETE FRAMES
USING INFILLED WALLS

APPROVED BY
DISSERTATION COMMITTEE:



Michael E. Kreger, Co-Chairman



James O. Jirsa, Co-Chairman



Michael D. Engelhardt



Jose M. Roesset



Stelios Kyriakides

**Copyright
by
Rajalingam Valluvan
1993**

In dedication to my mother, father, wife and teachers

**ISSUES INVOLVED IN SEISMIC RETROFIT OF
REINFORCED CONCRETE FRAMES
USING INFILLED WALLS**

by

RAJALINGAM VALLUVAN, B.E., D.I.C., M.Sc.

DISSERTATION

Presented to the Faculty of the Graduate School of
The University of Texas at Austin
in Partial Fulfillment
of the Requirements
for the Degree of

DOCTOR OF PHILOSOPHY

THE UNIVERSITY OF TEXAS AT AUSTIN
December 1993

ACKNOWLEDGEMENT

The dissertation study was funded by the National Science Foundation under Grant No. BCS-8820502. The research was conducted at Ferguson Structural Engineering Laboratory of University of Texas at Austin under the direct supervision of Dr. Michael E. Kreger and Dr. James O. Jirsa. The technical collaborator was Mr. Loring A. Wyllie, Jr. of H. J. Degenkolb Associates, San Francisco. I gratefully acknowledge all the assistance received by me during the course of this study.

I would like to thank Dr. Michael E. Kreger and Dr. James O. Jirsa who served as co-supervisors on my dissertation research program. The study would not have been fruitful and complete but for their counsel and support. I admire Dr. Kreger's friendly nature. I also consider myself as fortunate to have worked with Dr. Jirsa whose constructive criticism and dedication helped develop my career. The role of Dr. Michael D. Engelhardt, Dr. Jose M. Roesset and Dr. Stellos Kyriakides as members of my dissertation committee is gratefully acknowledged. I would also like to thank Dr. John E. Breen, Dr. Ned H. Burns, Dr. Engelhardt, Dr. Karl H. Frank, Dr. Richard W. Furlong, Dr. Richard E. Klingner and Dr. Joseph A. Yura for their generous advice and support during my stay here.

The contributions made by Emad Ahmed, Randall Bravo, Julio Jimenez and Mohamad Najah are gratefully acknowledged. The assistance provided by the staff of the Ferguson Structural Engineering Laboratory made this research possible and is acknowledged with gratitude. My thanks go to Gautam Arun, Patrick Ball, Michael Cobb, Sharon Cunningham, Johaan Ernest, Wayne Fontenot, Jean Gerhke, Laurie Golding, Ryan Green, April Jenkins, Wayne Little, Raymond Madonna, Blake Stasney and Alec Tahmassebi. I would also like to thank Carole Reese and Lena Brooks for their kind assistance.

My friends (too many to name) helped me make this place my home. Their kindness and hospitality made my entire stay here enjoyable and memorable. I feel indebted to all of them. I sincerely hope that our friendship will continue to flourish as the years go by.

I can only express my indebtedness to my mother and father for their continued dedication and sacrifice throughout my life. My brother and sisters filled my life with

affection and cheer. I consider myself as the luckiest to have been blessed with Nimmy (my wife) who, through her dedication, affection and undying support, has made my life meaningful. My gratitude also goes to her parents for being our parents. I finally pay my gratitude to the almighty God for having blessed me with a challenging and meaningful life.

Rajalingam Valluvan

Austin, Texas, U.S.A.

December, 1993

**ISSUES INVOLVED IN SEISMIC RETROFIT OF
REINFORCED CONCRETE FRAMES
USING INFILLED WALLS**

Publication No. _____

Rajalingam Valluvan, Ph.D.

The University of Texas at Austin, 1993

Supervisors: Michael E. Kreger and James O. Jirsa

Buildings in the United States, designed and constructed in the late 1950's and early 1960's in accordance with prevalent standards, are often found to be inadequate to withstand major earthquakes. Gravity loading was the primary concern in the design of these buildings, and as a result, they may not possess adequate lateral strength and ductility. Addition of infill walls is a widely-used scheme for seismic retrofit of non-ductile reinforced concrete moment-resisting frames (RCMRF) which have been identified as a type of structural system that poses significant potential hazard to life safety and may result in major financial loss.

The current experimental study focussed on issues associated with seismic retrofit of non-ductile RCMRF using infilled walls. Issues investigated were: (1) retrofit techniques for strengthening column lap splices which may control the performance of retrofitted RCMRF; and (2) the shear transfer mechanism across frame-wall interfaces.

Investigation of retrofit techniques for column lap splices involved strengthening column-splice specimens using a variety of selected retrofit techniques and testing the

performance of retrofitted splices in terms of splice tensile strength and ductility. The retrofit techniques used included: confinement of the splice region with steel angles and straps or reinforcing bar ties; and welding of spliced bars. They were intended to supplement confinement in the splice region to delay/prevent splitting of concrete cover in the splice region or to provide continuity between spliced bars. Retrofitted column-splice specimens were subjected to axial load reversals simulating the action of seismic forces on the boundary elements (columns) of a frame-wall system. Providing confinement or continuity improved splice tensile strength and ductility in most cases.

The study of the shear transfer mechanism across a frame-wall interface involved constructing test specimens that were representative of a portion of the frame-wall interface and subjecting the specimen interface to different load patterns in direct shear. Variables investigated in the test program included: type of shear loading (reversed cyclic vs monotonic), level of external compression across the specimen interface, number of dowels (the dowels were not anchored to develop yield) as shear connectors across the specimen interface, strength of concrete in the frame segment of the test specimen, and procedure used for construction of the specimen interface. Test results provided information for establishing (1) the benefit of cyclic compression across frame-wall interfaces resulting from seismic loads, (2) the number of dowels that must be provided across the interface for satisfactory performance, (3) the influence of strength of concrete in the existing frame, and (4) the strength to be assigned to grouted (dry-packed) frame-wall joints. Test results were used to verify and extend the application of shear-friction provisions currently incorporated in Sect. 11.7 of ACI 318-89.

TABLE OF CONTENTS

| | |
|--|-----|
| LIST OF TABLES | xv |
| LIST OF FIGURES | xvi |
| | |
| CHAPTER 1 INTRODUCTION | 1 |
| 1.1 GENERAL | 1 |
| 1.2 RESEARCH OBJECTIVES | 3 |
| 1.2.1 Retrofitting of Column Splices | 3 |
| 1.2.2 Shear Transfer Across Frame-Wall Interfaces | 3 |
| 1.3 RESEARCH SCOPE | 4 |
| 1.3.1 Retrofitting of Column Splices | 4 |
| 1.3.2 Shear Transfer Across Frame-Wall Interfaces | 4 |
| | |
| CHAPTER 2 RESEARCH BACKGROUND AND LITERATURE REVIEW | 7 |
| 2.1 RESEARCH BACKGROUND | 7 |
| 2.2 LITERATURE REVIEW | 8 |
| 2.2.1 Column Lapped Splices | 8 |
| 2.2.2 Direct Shear Transfer | 11 |
| | |
| CHAPTER 3 RETROFITTING OF COLUMN SPLICES - EXPERIMENTAL PROGRAM | 28 |
| 3.1 INTRODUCTION | 28 |
| 3.2 RETROFITTING TECHNIQUES | 28 |
| 3.2.1 Retrofitting Methodology | 28 |
| 3.2.2 Techniques for Supplementing Confinement in the Splice Region | 28 |
| 3.2.3 Technique for Making Spliced Bars Continuous | 29 |
| 3.3 TEST SPECIMENS | 29 |
| 3.3.1 Existing (Unstrengthened) Column Specimen | 29 |

| | | |
|---------|---|----|
| 3.3.2 | Retrofitted Column Specimens | 29 |
| 3.3.2.1 | Nomenclature for Column Specimens | 29 |
| 3.3.2.2 | Column Specimens Retrofitted Using Steel Angles and Straps | 30 |
| 3.3.2.3 | Column Specimens Retrofitted Using External Reinforcing Bar Ties | 30 |
| 3.3.2.4 | Column Specimen Retrofitted Using Additional Internal Ties | 30 |
| 3.3.2.5 | Column Specimens Retrofitted with Welded Splices | 31 |
| 3.3.3 | Characteristics of Materials | 31 |
| 3.3.3.1 | Concrete | 31 |
| 3.3.3.2 | Steel | 31 |
| 3.3.3.3 | Cement Grout | 32 |
| 3.3.3.4 | Welds | 32 |
| 3.4 | TEST SETUP AND TESTING PROCEDURE | 32 |
| 3.4.1 | Test Setup | 32 |
| 3.4.2 | Loading History | 32 |
| 3.4.3 | Instrumentation | 33 |
| 3.4.4 | Data Acquisition System | 33 |

CHAPTER 4 **RETROFITTING OF COLUMN SPLICES - TEST RESULTS**

| | | |
|-------|---|----|
| 4.1 | EXISTING (UNSTRENGTHENED) COLUMN SPECIMEN | 47 |
| 4.1.1 | Column Specimen U-B-1 | 47 |
| 4.2 | COLUMN SPECIMENS RETROFITTED USING STEEL ANGLES AND STRAPS | 47 |
| 4.2.1 | Column Specimen U-SS6-UG-1 | 47 |
| 4.2.2 | Column Specimen U-SS6-UG-2 | 47 |
| 4.2.3 | Column Specimen U-SS6-UG-3 | 48 |
| 4.2.4 | Column Specimen U-SS6-G-4 | 48 |
| 4.2.5 | Column Specimen U-SS6-G-5 | 48 |

| | | |
|-------|---|----|
| 4.3 | COLUMN SPECIMENS RETROFITTED USING EXTERNAL REINFORCING BAR TIES | 48 |
| 4.3.1 | Column Specimen U-ES3-G-1 | 48 |
| 4.3.2 | Column Specimen U-ES3-UG-2 | 49 |
| 4.3.3 | Column Specimen U-ES3-PG-3 | 49 |
| 4.4 | COLUMN SPECIMEN RETROFITTED USING ADDITIONAL INTERNAL TIES | 49 |
| 4.4.1 | Column Specimen U-AT8-1 | 49 |
| 4.5 | COLUMN SPECIMENS RETROFITTED WITH WELDED SPLICES | 50 |
| 4.5.1 | Column Specimen S-WS-1 | 50 |
| 4.5.2 | Column Specimen S-WS-2 | 50 |

| | | |
|------------------|--|-----------|
| CHAPTER 5 | RETROFITTING OF COLUMN SPLICES - DISCUSSION OF TEST RESULTS AND THEIR IMPLICATIONS - SUMMARY, CONCLUSIONS AND RECOMMENDATIONS | 86 |
| 5.1 | EXISTING (UNSTRENGTHENED) COLUMN SPECIMEN | 86 |
| 5.2 | CONFINEMENT WITH STEEL ELEMENTS (ANGLES & STRAPS) | 86 |
| 5.3 | CONFINEMENT WITH EXTERNAL REINFORCING BAR TIES | 87 |
| 5.4 | CONFINEMENT WITH ADDITIONAL INTERNAL TIES | 87 |
| 5.5 | CONTINUITY USING WELDED SPLICES | 88 |
| 5.6 | SUMMARY AND CONCLUSIONS | 88 |
| 5.7 | RECOMMENDATIONS BASED ON TEST RESULTS | 89 |
| 5.7.1 | Pros and Cons of Schemes Investigated and Final Choice .. | 89 |
| 5.7.2 | Recommended Features for Additional Confinement Schemes | 90 |
| 5.7.3 | Offsets in Spliced Bars | 91 |
| 5.8 | SUGGESTIONS FOR FURTHER RESEARCH | 92 |

| | | |
|------------------|---|-----------|
| CHAPTER 6 | SHEAR TRANSFER ACROSS FRAME-WALL INTERFACES - EXPERIMENTAL PROGRAM | 99 |
| 6.1 | INTRODUCTION | 99 |

| | |
|--|------------|
| 6.2 TEST VARIABLES | 99 |
| 6.3 TEST SPECIMENS AND MATERIALS | 99 |
| 6.4 TEST SETUP AND TESTING PROCEDURE | 101 |
| | |
| CHAPTER 7 SHEAR TRANSFER ACROSS FRAME-WALL INTERFACES - TEST RESULTS - MEASUREMENTS AND SPECIMEN BEHAVIORS | 119 |
| 7.1 INTRODUCTION | 119 |
| 7.2 LOAD AND DEFORMATION MEASUREMENTS | 119 |
| 7.2.1 Shear Stresses | 119 |
| 7.2.2 Interface Slips | 119 |
| 7.2.3 Interface Uplifts | 120 |
| 7.3 BEHAVIOR OF TEST SPECIMENS | 120 |
| 7.3.1 Pull Out Failure of Dowels | 121 |
| 7.3.2 Aggregate Interlock Failure | 121 |
| 7.3.3 Failure Due to Disintegration of Concrete or Grout Around the Dowels | 122 |
| | |
| CHAPTER 8 SHEAR TRANSFER ACROSS FRAME-WALL INTERFACES - DISCUSSION OF TEST RESULTS AND THEIR IMPLICATIONS, SUMMARY, CONCLUSIONS AND RECOMMENDATIONS | 136 |
| 8.1 INTRODUCTION | 136 |
| 8.2 DISCUSSION OF TEST RESULTS AND IMPLICATIONS | 136 |
| 8.2.1 Influence of Loading Pattern in Shear | 136 |
| 8.2.2 Influence of External Compression Across Specimen Interface | 137 |
| 8.2.2.1 Level of Compression | 137 |
| 8.2.2.2 Pattern of Compression (Constant vs Cyclic) | 138 |
| 8.2.3 Influence of Dowels Across the Specimen Interface | 139 |

| | |
|---|-----|
| 8.2.4 Influence of Strength of Concrete in the Frame Segment . . . | 141 |
| 8.2.5 Influence of Procedures Used for Interface Construction . . . | 142 |
| 8.3 SUMMARY, CONCLUSIONS AND RECOMMENDATIONS | 144 |
| 8.4 SUGGESTIONS FOR FURTHER RESEARCH | 146 |

| | |
|---|------------|
| CHAPTER 9 A REVIEW ON SHEAR-FRICTION PROVISIONS IN SECTION 11.7 OF ACI 318-89 | 180 |
| 9.1 INTRODUCTION | 180 |
| 9.2 EVALUATION OF ACI SHEAR-FRICTION PROVISIONS USING CURRENT TEST RESULTS | 182 |
| 9.2.1 Shear-Friction Hypothesis in Section 11.7.7 of ACI Code | 184 |
| 9.2.2 Friction Coefficients μ Specified in ACI Code | 186 |
| 9.2.3 Upper Limit on Shear Strength Specified by ACI Code | 187 |
| 9.2.4 Useful Upper Limit on Amount of Shear-Friction Reinforcement | 189 |
| 9.3 MODIFIED SHEAR-FRICTION PROVISIONS FOR SECTION 11.7 OF ACI 318-89 | 191 |
| 9.4 COMPARISON OF TEST RESULTS FROM CURRENT AND PREVIOUS RESEARCH WITH MODIFIED SHEAR-FRICTION PROVISIONS | 199 |
| 9.5 USE OF MODIFIED FRICTION COEFFICIENTS μ AND MODIFIED STRENGTH UPPER LIMITS FOR RETROFIT SCHEMES | 200 |
| 9.6 SUMMARY, CONCLUSIONS AND RECOMMENDATIONS | 201 |

| | |
|---|------------|
| CHAPTER 10 CONCLUSIONS AND RECOMMENDATIONS | 215 |
|---|------------|

| | |
|---|------------|
| APPENDIX A RETROFITTING OF COLUMN SPLICES - DESIGN OF RETROFIT SCHEMES | 218 |
| A.1 DESIGN CRITERIA | 218 |
| A.2 STEEL ANGLES AND STRAPS | 218 |
| A.3 EXTERNAL REINFORCING BAR TIES | 220 |

| | | |
|-------------------|---|------------|
| A.4 | ADDITIONAL INTERNAL TIES | 221 |
| A.5 | WELDED SPLICES | 222 |
| APPENDIX B | SHEAR TRANSFER ACROSS FRAME-WALL INTERFACES - LOAD-DEFORMATION RELATIONSHIPS FOR ALL TEST SPECIMENS .. | 226 |
| APPENDIX C | SHEAR TRANSFER ACROSS FRAME-WALL INTERFACES - PULL OUT TEST RESULTS | 278 |
| C.1 | PULL OUT TESTS | 278 |
| C.2 | PULL OUT TEST RESULTS | 278 |
| APPENDIX D | SHEAR-FRICTION PROVISIONS IN SECTION 11.7 OF ACI 318-89 | 283 |
| REFERENCES | | 290 |
| VITA | | 294 |

LIST OF TABLES

| TABLE | | PAGE |
|-------|---|------|
| 3.1 | Test specimen nomenclature | 34 |
| 3.2 | Compressive strength of concrete at different ages | 35 |
| 4.1 | Summary of test results - column splices | 51 |
| 6.1 | Summary of test program - shear tests | 102 |
| 7.1 | Summary of test results - shear tests | 124 |
| 9.1 | Comparison of test results from current study with ACI 318-89 provisions on shear-friction | 202 |
| 9.2 | Comparison of current test results with modified shear-friction equation ... | 204 |
| 9.3 | Comparison of test results from current study with modified shear-friction provisions | 205 |
| C.1 | Summary of pull out test results | 279 |

LIST OF FIGURES

| FIGURE | PAGE |
|--------|---|
| 1.1 | Weak column lap splices subjected to large tensile forces due to frame-wall action 6 |
| 1.2 | Compression across frame-wall interfaces from gravity loads and seismic forces 6 |
| 2.1 | Frame-wall specimens tested by Gaynor 13 |
| 2.2 | Performance of frames retrofitted by Gaynor with shotcrete infill walls 14 |
| 2.3 | Shotcrete wall separations and voids 15 |
| 2.4 | Finished epoxied interface 15 |
| 2.5 | Reinforcement layout for test specimen retrofitted by Shah with cast-in-place infill wall and supplementary tensile reinforcement in boundary element region 16 |
| 2.6 | Performance of test specimens by Shah and Gaynor 17 |
| 2.7 | Wall and encasing reinforcement for frame retrofitted by Jimenez 18 |
| 2.8 | Performance of test specimens by Jimenez and Gaynor 19 |
| 2.9 | Retrofit schemes for low-rise building investigated analytically by Jordan 20 |
| 2.10 | Retrofit schemes for medium-rise building investigated analytically by Jordan 21 |
| 2.11 | Low-rise, unstrengthened building investigated analytically by Pincheira 23 |
| 2.12 | Eccentrically braced steel frames for retrofit of low-rise buildings investigated analytically by Bouadi 24 |
| 2.13 | Tests for direct shear transfer by Hofbeck and Mattock 25 |
| 2.14 | Tests on direct shear transfer across concrete-to-concrete interfaces by Paulay 26 |
| 2.15 | Design recommendations by Birkeland based on direct shear tests by Anderson, Hanson, and Mast 27 |
| 3.1 | Example of non-contact lap splices 36 |
| 3.2 | Test specimen with existing splice details 37 |
| 3.3 | Column reinforcement cage with contact lap splices 38 |

| | | |
|------|---|----|
| 3.4 | Welding of steel straps to angles | 39 |
| 3.5 | Cement grout between column face and steel elements | 40 |
| 3.6 | Welded external reinforcing bar ties | 40 |
| 3.7a | UngROUTED external reinforcing bar ties | 41 |
| 3.7b | Grouted external reinforcing bar ties | 41 |
| 3.7c | Partially-grouted external reinforcing bar ties | 42 |
| 3.8 | Additional internal ties | 42 |
| 3.9 | Welded splices with an additional tie | 43 |
| 3.10 | Test setup | 44 |
| 3.11 | Typical loading history for the test specimens | 45 |
| 3.12 | Measurement of axial deformation in splice region using a displacement transducer | 46 |
| 4.1 | Column specimen U-B-1 at failure | 52 |
| 4.2 | Crack pattern in specimen U-B-1 at failure | 53 |
| 4.3 | Performance of column specimen U-B-1 | 54 |
| 4.4 | Crack pattern in specimen U-SS6-UG-1 at failure | 55 |
| 4.5 | Column specimen U-SS6-UG-1 at failure | 56 |
| 4.6 | Performance of column specimen U-SS6-UG-1 | 57 |
| 4.7 | Crack pattern in specimen U-SS6-UG-2 | 58 |
| 4.8 | Performance of column specimen U-SS6-UG-2 | 59 |
| 4.9 | Performance of column specimen U-SS6-UG-3 | 60 |
| 4.10 | Confinement of column ends with steel channels and mild steel rods | 61 |
| 4.11 | Large cracks outside the splice region demonstrating yielding of column reinforcing bars | 62 |
| 4.12 | Crack pattern in specimen U-SS6-G-4 | 63 |
| 4.13 | Performance of column specimen U-SS6-G-4 | 64 |
| 4.14 | Performance of column specimen U-SS6-G-5 | 65 |
| 4.15 | Column specimen U-ES3-G-1 at failure | 66 |
| 4.16 | Crack pattern in specimen U-ES3-G-1 at failure | 67 |
| 4.17 | Performance of column specimen U-ES3-G-1 | 68 |
| 4.18 | Column specimen U-ES3-UG-2 at failure | 69 |
| 4.19 | Crack pattern in specimen U-ES3-UG-2 at failure | 70 |

| | | |
|------|---|-----|
| 4.20 | Performance of column specimen U-ES3-UG-2 | 71 |
| 4.21 | Column specimen U-ES3-PG-3 at failure | 72 |
| 4.22 | Crack pattern in specimen U-ES3-PG-3 at failure | 73 |
| 4.23 | Performance of column specimen U-ES3-PG-3 | 74 |
| 4.24 | Crack pattern in specimen U-AT8-1 at failure | 75 |
| 4.25 | Column specimen U-AT8-1 at failure | 76 |
| 4.26 | Monolithic behavior between existing concrete and replacing cement grout in specimen U-AT8-1 | 76 |
| 4.27 | Performance of column specimen U-AT8-1 | 77 |
| 4.28 | Crack pattern in specimen S-WS-1 | 78 |
| 4.29 | Spalling of concrete cover in specimen S-WS-1 | 79 |
| 4.30 | Opening of 90 degree hook in specimen S-WS-1 | 79 |
| 4.31 | Prying action of outer spliced bar in specimen S-WS-1 | 80 |
| 4.32 | Performance of column specimen S-WS-1 | 81 |
| 4.33 | Performance of column specimen S-WS-2 | 82 |
| 4.34 | Development of cracks in specimen S-WS-2 upon yielding of additional tie .. | 83 |
| 4.35 | Cracks in specimen S-WS-2 developed by offset forces in spliced bars | 83 |
| 4.36 | Spalled cover in specimen S-WS-2 produced by offset forces in spliced bars | 84 |
| 4.37 | Crack pattern in specimen S-WS-2 | 85 |
| 5.1 | Measured responses of specimens strengthened with steel angles and straps | 93 |
| 5.2 | Measured responses of specimens strengthened with external reinforcing bar ties | 94 |
| 5.3 | Measured responses of specimens strengthened with welded splices | 95 |
| 5.4 | Performance of unstrengthened specimen vs retrofitted specimens | 96 |
| 5.5 | Force transfer mechanism in lap spliced bars and forces initiating cover splitting | 97 |
| 5.6 | Forces produced by offsets in lap spliced bars | 98 |
| 6.1 | Frame-wall interfaces | 104 |
| 6.2 | Test specimen details | 105 |
| 6.3 | Frame reinforcement cage inside wooden form | 106 |

| | | |
|------|---|-----|
| 6.4 | Casting of frame segments | 107 |
| 6.5 | Sandblasted frame-wall interface | 108 |
| 6.6 | Drilling of holes in frame segments for placement of dowels | 109 |
| 6.7 | Wall reinforcement cage tied to dowels | 109 |
| 6.8 | Wall reinforcement cage supported by chairs | 110 |
| 6.9 | Casting of wall segments | 110 |
| 6.10 | Gap in top frame-wall connection after casting frame and wall segments . . . | 111 |
| 6.11 | Completed test specimen | 112 |
| 6.12 | Test setup | 113 |
| 6.13 | Schematic of loads applied on each test specimen | 114 |
| 6.14 | Load histories for test specimens | 115 |
| 6.15 | Load history LH3 for test specimen B9 | 117 |
| 6.16 | Displacement transducer locations | 118 |
| 7.1 | Interface slip for both sides of interface | 126 |
| 7.2 | Interface slip at locations along interface | 127 |
| 7.3 | Interface uplift for both sides of interface | 128 |
| 7.4 | Performance of shear specimen A6 | 129 |
| 7.5 | Peak strength of specimen B1 controlled by pull out failure of dowels | 130 |
| 7.6 | Appearance of interface upon pull out failure of dowels | 131 |
| 7.7 | Peak strength of specimen B3 controlled by aggregate interlock failure | 132 |
| 7.8 | Appearance of interface upon failure of aggregate interlock | 133 |
| 7.9 | Peak strength of specimen A4 controlled by disintegration of low-strength concrete around dowels | 134 |
| 7.10 | Peak strength of specimen B8 controlled by disintegration of dry-packed grout around dowels | 135 |
| 8.1 | Performance of test specimens without compressive stress for different loading patterns | 147 |
| 8.2 | Performance of test specimens with compressive stress for different loading patterns | 148 |
| 8.3 | Performance of test specimens with dowels for different levels of compressive stress | 149 |

| | | |
|------|---|-----|
| 8.4 | Performance of test specimens without dowels for different levels of compressive stress | 152 |
| 8.5 | Performance of test specimens with lower frame strength for different levels of compressive stress | 155 |
| 8.6 | Peak strengths and residual capacities of test specimens for different levels of compressive stress | 158 |
| 8.7 | Performance of test specimens with different patterns of compressive stress | 159 |
| 8.8 | Performance of test specimens without compressive stress for different number of dowels | 162 |
| 8.9 | Performance of test specimens with compressive stress for different number of dowels | 165 |
| 8.10 | Performance of test specimens without compressive stress for different frame strengths | 168 |
| 8.11 | Performance of test specimens with compressive stress for different frame strengths | 171 |
| 8.12 | Performance of test specimens without compressive stress for frame-wall interfaces constructed using different procedures | 174 |
| 8.13 | Performance of test specimens with compressive stress for frame-wall interfaces constructed using different procedures | 177 |
| 9.1 | Comparison of test results with ACI recommended upper limits for nominal shear stress | 207 |
| 9.2 | Influence of amount of shear-friction reinforcement on interface shear transfer as established from tests by Hofbeck | 208 |
| 9.3 | Comparison of current test results with modified shear-friction provisions | 209 |
| 9.4 | Comparison of current ACI code and modified code provisions based on current test results | 210 |
| 9.5 | Comparison of test results by Hofbeck and Mattock with modified shear-friction provisions | 211 |
| 9.6 | Comparison of current ACI code and modified code provisions based on test results by Mattock | 212 |
| 9.7 | Comparison of test results by Bass with modified shear-friction provisions | 213 |

| | | |
|------|---|-----|
| 9.8 | Comparison of current test results with modified friction coefficients for retrofit purposes | 214 |
| A.1 | Details of retrofit scheme with steel angles and straps | 224 |
| A.2 | Details of welded lap splices | 225 |
| B.1 | Performance of shear specimen A2 | 227 |
| B.2 | Interface uplift on north side of shear specimen A2 | 228 |
| B.3 | Interface uplift on south side of shear specimen A2 | 229 |
| B.4 | Performance of shear specimen A3 | 230 |
| B.5 | Interface uplift on north side of shear specimen A3 | 231 |
| B.6 | Interface uplift on south side of shear specimen A3 | 232 |
| B.7 | Performance of shear specimen A4 | 233 |
| B.8 | Interface uplift on north side of shear specimen A4 | 234 |
| B.9 | Interface uplift on south side of shear specimen A4 | 235 |
| B.10 | Performance of shear specimen A5 | 236 |
| B.11 | Interface uplift on north side of shear specimen A5 | 237 |
| B.12 | Interface uplift on south side of shear specimen A5 | 238 |
| B.13 | Performance of shear specimen A6 | 239 |
| B.14 | Interface uplift on north side of shear specimen A6 | 240 |
| B.15 | Interface uplift on south side of shear specimen A6 | 241 |
| B.16 | Performance of shear specimen A7 | 242 |
| B.17 | Interface uplift on north side of shear specimen A7 | 243 |
| B.18 | Interface uplift on south side of shear specimen A7 | 244 |
| B.19 | Performance of shear specimen A8 | 245 |
| B.20 | Interface uplift on north side of shear specimen A8 | 246 |
| B.21 | Interface uplift on south side of shear specimen A8 | 247 |
| B.22 | Performance of shear specimen B1 | 248 |
| B.23 | Interface uplift on north side of shear specimen B1 | 249 |
| B.24 | Interface uplift on south side of shear specimen B1 | 250 |
| B.25 | Performance of shear specimen B2 | 251 |
| B.26 | Interface uplift on north side of shear specimen B2 | 252 |
| B.27 | Interface uplift on south side of shear specimen B2 | 253 |
| B.28 | Performance of shear specimen B3 | 254 |

| | | |
|------|--|-----|
| B.29 | Interface uplift on north side of shear specimen B3 | 255 |
| B.30 | Interface uplift on south side of shear specimen B3 | 256 |
| B.31 | Performance of shear specimen B4 | 257 |
| B.32 | Interface uplift on north side of shear specimen B4 | 258 |
| B.33 | Interface uplift on south side of shear specimen B4 | 259 |
| B.34 | Performance of shear specimen B5 | 260 |
| B.35 | Interface uplift on north side of shear specimen B5 | 261 |
| B.36 | Interface uplift on south side of shear specimen B5 | 262 |
| B.37 | Performance of shear specimen B6 | 263 |
| B.38 | Interface uplift on north side of shear specimen B6 | 264 |
| B.39 | Interface uplift on south side of shear specimen B6 | 265 |
| B.40 | Performance of shear specimen B7 | 266 |
| B.41 | Interface uplift on north side of shear specimen B7 | 267 |
| B.42 | Interface uplift on south side of shear specimen B7 | 268 |
| B.43 | Performance of shear specimen B8 | 269 |
| B.44 | Interface uplift on north side of shear specimen B8 | 270 |
| B.45 | Interface uplift on south side of shear specimen B8 | 271 |
| B.46 | Performance of shear specimen B9 | 272 |
| B.47 | Interface uplift on north side of shear specimen B9 | 273 |
| B.48 | Interface uplift on south side of shear specimen B9 | 274 |
| B.49 | Performance of shear specimen B10 | 275 |
| B.50 | Interface uplift on north side of shear specimen B10 | 276 |
| B.51 | Interface uplift on south side of shear specimen B10 | 277 |
| C.1 | Pull out test setup | 280 |
| C.2 | Pull out failure patterns of dowels | 281 |

CHAPTER 1

INTRODUCTION

1.1 GENERAL

Buildings in the United States, designed and constructed in the 50's and 60's in accordance with prevalent standards, are often found to be inadequate to withstand major earthquakes. Gravity loading was the primary concern in the design of these buildings and, as a result, they may not possess adequate lateral strength and ductility.

Non-ductile reinforced concrete moment-resisting frames (RCMRF) are identified as one of the types of structural systems that poses significant potential hazard to life safety and may result in major financial loss. Strengthening of such frames typically involves (1) addition of infill walls, (2) use of steel bracing, (3) jacketing of frame elements, or (4) a combination of these techniques. Selection of a rehabilitation technique is based on correcting the deficiencies in the structure as well as satisfying other factors including desired performance level, economy, aesthetics, and construction feasibility.

Addition of infill walls is a widely-used scheme for seismic retrofit of non-ductile RCMRF. In using the scheme, two specific issues must be given due consideration. One, the existing weak links in the frame must be eliminated so that the performance requirements of retrofitted RCMRF can be realized. One weak link in an existing frame may be the tensile capacity of column lap splices, originally designed for little or no flexure in combination with axial compression. The short lap splices are typically located at the base of the columns just above a construction joint, and column ties in the splice region are often widely-spaced. In the retrofitted structure, existing columns act as boundary elements for the new walls. As a result, some columns may be subjected to large, axial tensile forces (Fig. 1.1) and inelastic deformations. The performance of a retrofitted RCMRF may therefore be limited by the premature failure of column splices unless they are strengthened to develop the tensile strength of column reinforcement and significant inelastic deformation. Experimental studies by Gaynor [13], Shah [33], and Jimenez [17] verify the significance of strengthening column splices to enable the retrofitted frames to perform adequately during major earthquakes. Also, analytical studies by Bouadi [11], Jordan [19], and

Pincheira [30] show the role of inadequate column splices in limiting the benefits of different strengthening procedures.

Two, monolithic behavior between the existing frame and the newly added infill wall must be achieved. Monolithic behavior of a frame-wall system demands effective shear transfer between the existing frame and the new infill wall. Typically, infill walls are integrated with the existing frames by sandblasting frame-wall interface in the frame, drilling and cleaning holes in the existing concrete, setting dowels as shear connectors by grouting them using a suitable material such as epoxy, and connecting the wall reinforcement to the dowels. The infill wall can be cast in place or shotcreted. The following issues need investigation in order to ensure effective shear transfer across frame-wall interfaces and also achieve economy:

(1) Compression across frame-wall interfaces. Compression across frame-wall interfaces from gravity loads, and seismic forces (Fig. 1.2) would improve the interface shear capacity so that a shear can be transferred with a minimum number of dowels crossing the interface. In retrofit schemes, a reduction in the number of dowels as shear connectors may result in significant savings in retrofit costs since installation of dowels may be labor intensive and expensive. Extensive tests were conducted by Bass [7, 8, 9] on shear transfer strength of concrete-to-concrete interfaces. The roles of reinforcing bar dowels as interface shear reinforcement and different procedures for roughening the interface were studied in detail. However, the influence of external compression on the interface shear transfer strength was not investigated in the study. As a result, the relative influences of shear reinforcement and external compression on shear transfer strength could not be established from the study.

(2) Dowels. Dowels installed as shear connectors across frame-wall interfaces must be anchored on both sides of the shear plane to develop tensile yield. Code provisions for estimating connection shear capacity are based on developing the tensile yield strength of shear-friction reinforcement across the shear plane [3]. However, embedment lengths inadequate to develop tensile yield are typical in retrofit schemes where it is not possible to anchor the dowels into the existing frame to develop yield strength. In some cases, the difficulties arise from congestion of reinforcement in the existing structural

elements. It is therefore important to study the behavior of shear planes that have dowels with inadequate embedment to develop yield strength.

(3) **Strength of concrete in the existing frame.** Frames constructed more than 30 years ago may have concrete of very low compressive strength [16]. Very little is known about interface shear transfer in low strength concrete materials.

(4) **Grouted top frame-wall connections.** In some cases, the top frame-wall connections are constructed by dry-packing the gap between the top of the infill and the bottom of the frame element with a suitable grout. Since it may be difficult to cast concrete directly against the bottom of the beam, a gap is left. Performance of such grouted connections needs to be investigated.

1.2 RESEARCH OBJECTIVES

1.2.1 Retrofitting of Column Splices. The major objective of the first phase of the experimental study was to develop, and test techniques that would improve the tensile strength and deformation capacity (ductility) of short lap splices present in the columns.

1.2.2 Shear Transfer Across Frame-Wall Interfaces. The objective of the second phase of the experimental investigation was to study the role of the following factors on the shear transfer mechanism in frame-wall interfaces: external compression across the interface, dowels not anchored sufficiently to develop tensile yield, concrete of different (low) compressive strength in the existing frame, and dry-packed grout at the gap between the frame and the top of the infill wall.

The test results were used to verify and extend the application of shear-friction provisions currently incorporated in Sect. 11.7 of ACI 318-89 [3].

1.3 RESEARCH SCOPE

1.3.1 Retrofitting of Column Splices. Twelve two-thirds scale specimens with column splice details typical of ordinary moment-resisting frames were constructed. Eleven of them were strengthened using two approaches. The first consisted of supplementing confinement in the column splice region to improve bond along the spliced bars. The second involved making spliced bars continuous so that forces could be transferred directly without relying on surrounding concrete and confinement to develop bond between spliced bars. The strengthening procedures included confinement of the splice region with steel elements such as angles and straps, addition of steel reinforcing bar ties externally or internally in the splice region, and welding of spliced bars. They were intended to confine the bars to prevent splitting of concrete cover in the splice region or to provide continuity. Retrofit schemes designed to supplement confinement externally were studied with different grouting conditions between column faces and externally confining steel elements. This was done to determine the influence of grout on the effectiveness of retrofit schemes.

All test specimens were subjected to repeated cycles of axial load reversals that would be predominant in boundary elements of frame-wall systems subjected to seismic loads. The performance of retrofitted specimens was evaluated based on the capacity of column splices to enable the column longitudinal reinforcing bars to develop the tensile yield strength, and permit significant inelastic deformation in the column region.

1.3.2 Shear Transfer Across Frame-Wall Interfaces. Seventeen test specimens were constructed. The test specimen was designed to represent a segment of a frame-wall interface. Reinforcement details in the frame and wall segments were kept similar in all test specimens. Variables investigated in the test program included; pattern of loading in shear (reversed cyclic vs monotonic), level of external compression across the specimen interface, number of dowels with inadequate anchorage to develop yield as shear connectors across the specimen interface, strength of concrete in the frame segment of test specimen, and procedure used for the construction of specimen interface.

All test specimens were subjected to either reversed cyclic or monotonic loading in direct shear. Loading histories consisted of reversed cycles of increasing magnitude. The cycles were load-controlled until the test specimens reached the peak shear capacity and

were displacement-controlled thereafter. The performance of test specimens was evaluated based on three major criteria; shear strength, shear stiffness, and residual shear capacity (post-failure capacity).

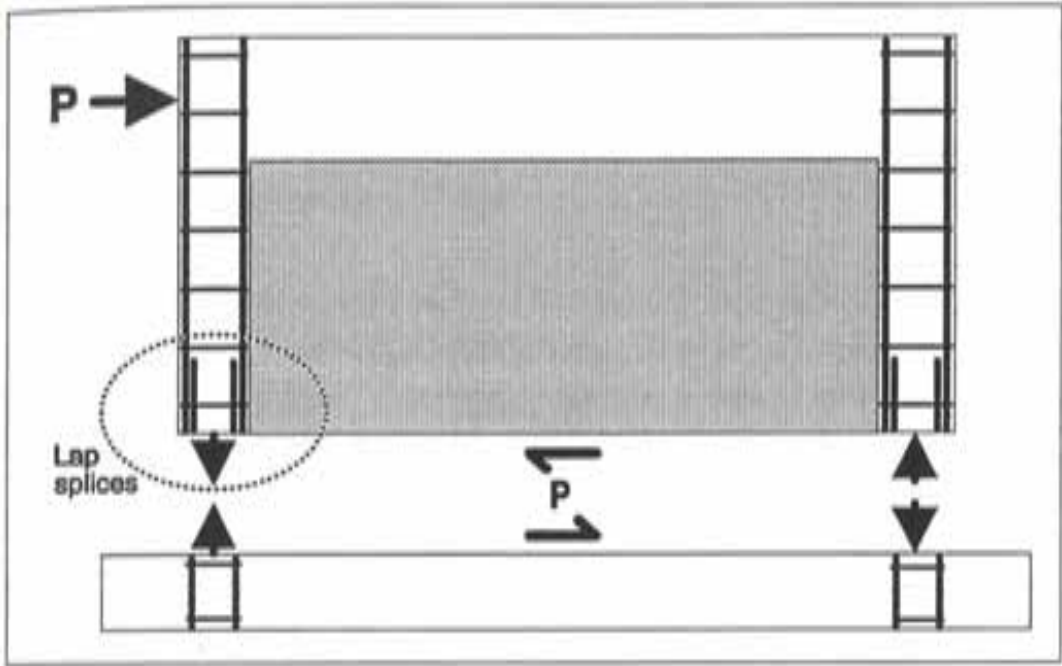


Figure 1.1 Weak column lap splices subjected to large tensile forces due to frame-wall action

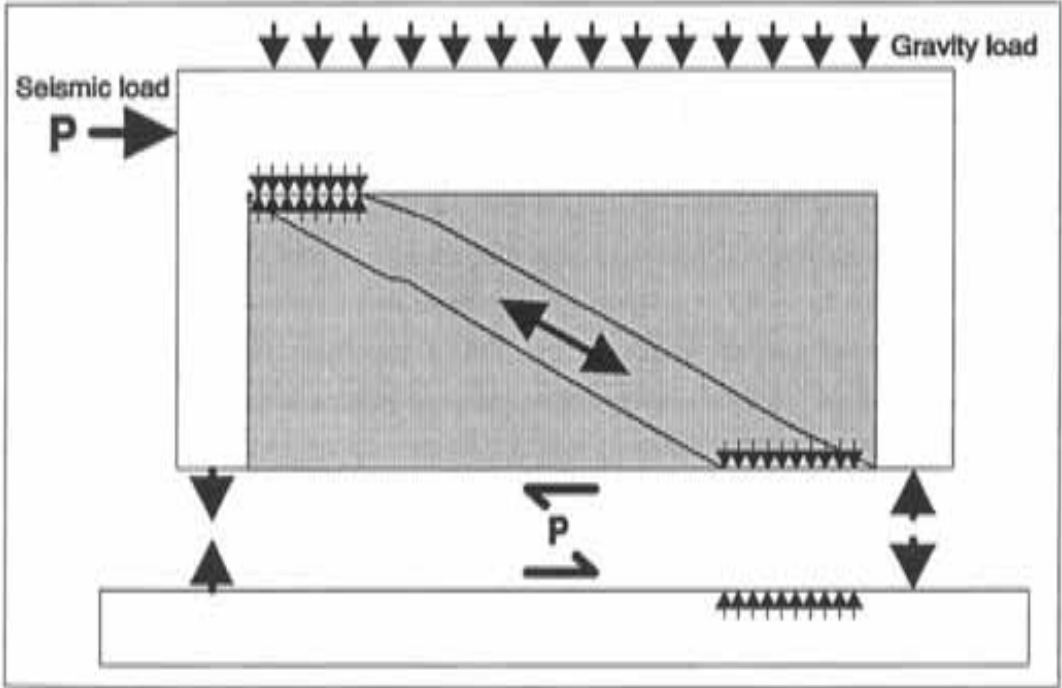


Figure 1.2 Compression across frame-wall interfaces from gravity loads and seismic forces

CHAPTER 2

RESEARCH BACKGROUND AND LITERATURE REVIEW

2.1 RESEARCH BACKGROUND

During the past decade a variety of techniques for repairing and retrofitting non-ductile reinforced concrete moment-resisting frames (RCMRF) have been investigated at University of Texas at Austin. Techniques investigated included addition of infill walls, jacketing of frame elements, and addition of steel bracing.

An experimental investigation involving the addition of shotcreted infill walls to strengthen non-ductile RCMRF was carried out by Gaynor [13]. In the study, three two-thirds scale single-story, single-bay frames representative of late 1950's and early 1960's construction were designed and constructed. The frame had typical details of that period such as short lap splices at the base of the columns and minimal ties along the column including the splice region. The column splices were 24 bar diameters long and the tie spacing was 12 inches. These details conform to ACI 318-56 [1] and ACI 318-63 [2]. The frames were strengthened using shotcrete infill walls. One frame-wall specimen had a solid infill wall, the second had an infill with a door opening centered in the frame, and the third had an infill with a window opening centered in the frame (Fig. 2.1). The frame-wall specimens were subjected to cyclic reversals of in-plane lateral loads simulating the effects of earthquake ground motions. The strength of test specimens which had a solid infill and an infill with a door opening was controlled by anchorage failure of column splices in tension. The specimen which had an infill with a window opening failed in shear. The envelopes of load vs drift plots of all three specimens are shown in Fig. 2.2. Although the addition of infill walls did improve the lateral force resistance of the frames, the benefit of strengthening two of the three frames was limited by tensile failure of the column splices resulting from overturning forces on the frame-wall specimens.

Also during construction of the walls, the shotcrete procedure did not completely fill the interface between the frame and the top of the wall (Fig. 2.3). The shotcrete rebounded off the bottom of the beam and the plywood used to form the back surface of each wall. The flaw at the top of each wall ranged in size from a small separation to a

sizeable void. An epoxy grout was injected to fill the small separations and used to patch the voids (Fig. 2.4). The repaired interface did not exhibit any distress during the tests.

Shah [33] retrofitted a two-thirds scale frame specimen that was similar in details as the frame specimens constructed by Gaynor [13]. The frame was strengthened by infilling with a cast-in-place wall with a door opening. The weak column splice in the test specimen was supplemented by adding continuous steel in the wall near the columns (Fig. 2.5). The performance of the retrofitted frame was better than that of the frame specimen strengthened by Gaynor [13] using a shotcrete infill wall with a door opening (Fig. 2.6).

Jimenez [17] investigated retrofitting a frame using an eccentric wall and column jackets. The two-thirds scale frame was similar in detail to the frame specimens constructed by Gaynor [13] and Shah [33]. The wall was connected to the concrete frame through epoxy-grouted dowels and reinforced concrete jackets around the frame columns (Fig. 2.7). The eccentric wall was cast in place. The column jackets improved the behavior of weak column splices, allowing steel strains well beyond yield without failing. The vertical wall and column reinforcement at the base was well into the yield range and the load-deflection curve was nearly flat indicating that the ultimate load in flexure was almost reached. The performance of the retrofitted specimen and the specimen strengthened by Gaynor [13] using a shotcrete infill wall are compared in Fig. 2.8.

2.2 LITERATURE REVIEW

2.2.1 Column Lapped Splices

An analytical investigation was performed by Jordan [19] to evaluate the effectiveness of different retrofit schemes for existing non-ductile RCMRF. In the investigation, a low-rise and a medium-rise building representative of American design and construction in the 1950's and 60's were analyzed. The study revealed that a short compression lap splice, inadequate to permit tensile yielding of column longitudinal reinforcement, was one of the major weak links in the existing buildings. The schemes considered for retrofitting both structures were addition of infill walls and jacketing of frame elements (beams and columns). The study showed the importance of strengthening column

splices, in the strengthened and unstrengthened frames of the buildings, to enable the retrofitted structures to perform adequately during major earthquakes (Figs. 2.9 and 10).

Pincheira [30] investigated analytically the performance of post-tensioned bracing system as an alternate retrofit technique for strengthening RCMRF. Variables considered in the study were building characteristics (low and medium rise), soil conditions (soft and firm), and various ground motion records representing major earthquakes. The study revealed that the lateral strength of low-rise, unstrengthened building was inadequate to withstand major earthquakes and was controlled by the failure of short lap splices in the existing columns (Fig. 2.11).

Ongoing research by Bouadi [11] on the use of steel eccentrically braced frames (EBFs) for seismic retrofit of RCMRF shows the vulnerability of short column splices in controlling the lateral strength of RCMRF in existing low-rise buildings and leading to their total collapse during major earthquakes (Fig. 2.12).

A series of experimental investigations was carried out at Cornell University. In one of the studies, the performance of column lap splices subjected to repeated, reversed cyclic loads was investigated by Lukose [22]. Splices in fourteen full-scale specimens were subjected to a combination of bending and shear force. The relationship between splice length and the spacing of confining reinforcement (ties) was studied in some detail. The study also included, but to a lesser extent, concrete cover effects, and compression splice behavior. Sivakumar [34, 35] continued the study and investigated transverse steel requirements for specimens with more than two splices in a layer, effects of offsets in spliced bars, effect of concrete strength on splice strength and behavior, and strength of epoxy-repaired splices. The extended study consisted of ten full-scale and three small-scale test specimens. Panahshahi [27] investigated the behavior of lap splices experimentally and analytically, incorporating additional parameters such as splice bar diameter and yield strength, and the splice spacing. Investigations by Sagan [32] focussed on studying the behavior of noncontact lap splices, and formulating suitable design guidelines.

Orangun [26] developed an equation for calculating the splice lengths of deformed bars based on the bond strength between the bars and the surrounding concrete. The equation considers the effects of concrete cover; splice bar diameter; splice length; size, spacing, and yield strength of transverse (confining) reinforcement; and strength of concrete surrounding the splice. The equation is given below:

$$\begin{aligned}
 u'_{cal} &= u_{cal} + u_{tr} & (2-1) \\
 &= \left[1.2 + \frac{3C}{d_b} + \frac{50d_b}{l_s} + \frac{A_{tr}f_{yt}}{500sd_b} \right] \sqrt{f'_c}
 \end{aligned}$$

where,

$$\frac{u_{tr}}{\sqrt{f'_c}} = \frac{A_{tr}f_{yt}}{500sd_b} \leq 3 \quad (2-2)$$

- and
- u'_{cal} = bond strength of single longitudinal bar in psi,
 - u_{cal} = bond strength contributed by surrounding concrete in psi,
 - u_{tr} = bond strength contributed by transverse (confining) reinforcement in psi,
 - C = smaller of clear concrete cover or one-half of clear spacing between splices in inches,
 - d_b = splice bar diameter in inches,
 - l_s = splice length in inches,
 - A_{tr} = area of transverse reinforcement, defined as total area of transverse reinforcement crossing the failure (splitting crack) plane divided by the number of splices in sq. in.,
 - f_{yt} = yield strength of transverse reinforcement in psi,
 - s = spacing of transverse reinforcement in inches, and
 - f'_c = compressive strength of concrete surrounding the splice in psi.

The upper limit of 3 in Eqn. (2-2) is based on the maximum effectiveness of confinement, afforded by the transverse reinforcement to the splice region. Equation (2-2)

is used in the current study to design retrofit schemes (presented in Appendix A) to supplement confinement in the splice region through additional transverse reinforcement.

Sugano [37] developed guidelines for improving confinement in the existing columns. An experimental study by Suleiman [38] focussed on the behavior of jacketed reinforced concrete columns subjected to combined axial load and bending. The reinforced concrete jackets were intended to improve the strength and ductility of the existing columns.

2.2.2 Direct Shear Transfer

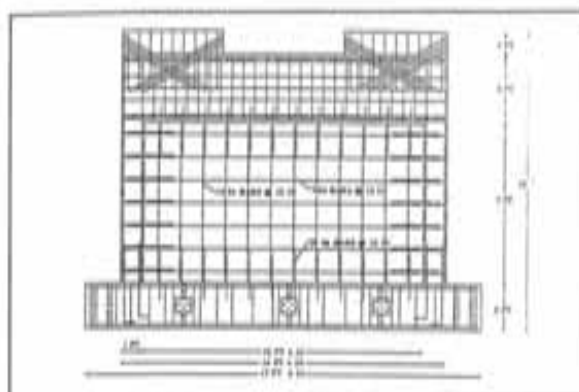
A comprehensive experimental study was conducted by Hofbeck [15] and Mattock [24, 25] at University of Washington at Seattle. In the study, shear transfer across planes in reinforced concrete was investigated in detail. Variables studied in the test program were: effect of precracking along the shear plane; effect of size, spacing, and yield strength of shear reinforcement across the shear plane; effect of concrete strength; contribution of dowel action to shear transfer strength; and influence of net compression across the shear plane. The contribution of shear reinforcement provided at an angle to the shear plane was also investigated. Eighty nine test specimens were constructed and the shear planes in all specimens were subjected to monotonic loading in direct shear until failure. Based on the study, design equations were developed to agree with the test data (Fig. 2.13).

Paulay [28, 29] conducted tests at the University of Canterbury, New Zealand to investigate shear transfer across concrete-to-concrete interfaces (Fig. 2.14). The test program consisted of eighty test specimens. Variables considered in the study were: amount of shear reinforcement across the interface; surface preparation techniques used typically to produce a rough and irregular interface; and contribution of dowel action and aggregate interlock to interface shear transfer strength. The PCI design handbook [31] provides specifications for designing concrete-to-concrete and concrete-to-steel interfaces for direct shear transfer. The recommendations are based on the shear-friction theory (explained in Art. 9.1) and are similar to the shear-friction provisions in ACI 318-89 [3]. Gambarova [12] developed models for the response of concrete-to-concrete and concrete-

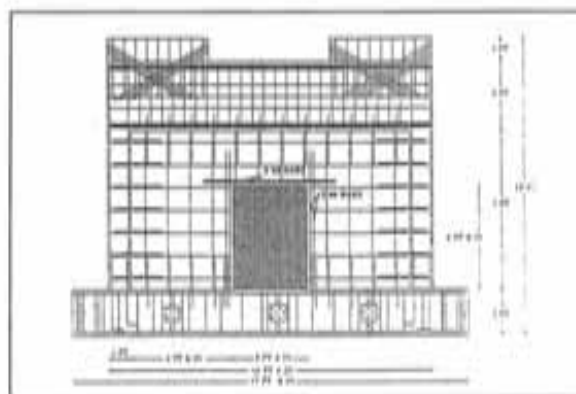
to-steel interfaces that can be used in finite element analysis of reinforced concrete structures.

Experimental studies by Anderson [5], Hanson [14], and Mast [23] focussed on investigating shear transfer across connections between precast and cast-in-place concrete. Birkeland [10] formulated design equations based on the test data obtained from these studies (Fig. 2.15). Kriz [21] investigated experimentally, the influence of steel reinforcement on the shear transfer strength of the interface between the columns and the corbels. Jimenez [18] and White [40] conducted experimental and analytical studies on shear transfer in cracked thick-walled reinforced concrete structures subjected to seismic forces. The contribution of dowels to shear transfer strength was investigated in detail by Vintzileou [39]. Design recommendations were proposed based on the experimental data. Experimental studies by Koseki [20] and Bakhoun [6] focussed on shear strength of joints in precast segmental bridges.

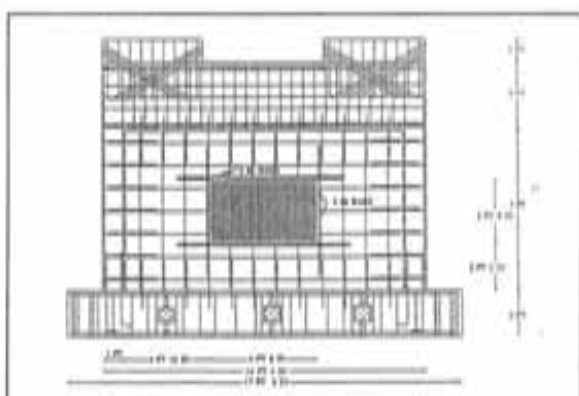
Altin [4] investigated experimentally the seismic behavior of reinforced concrete frames, strengthened by cast-in-place infill walls. The effect of various types of connections, between the frame and the wall, on the performance of retrofitted frame was considered in the study. Yamada [41, 42] investigated experimentally and analytically, the seismic behavior of reinforced concrete frames retrofitted with infill walls. The study included the effect of openings in the infill walls.



(a) Reinforcement layout, solid infill



(b) Reinforcement layout, infill with door



(c) Reinforcement layout, infill with window

Figure 2.1 Frame-wall specimens tested by Gaynor [13]

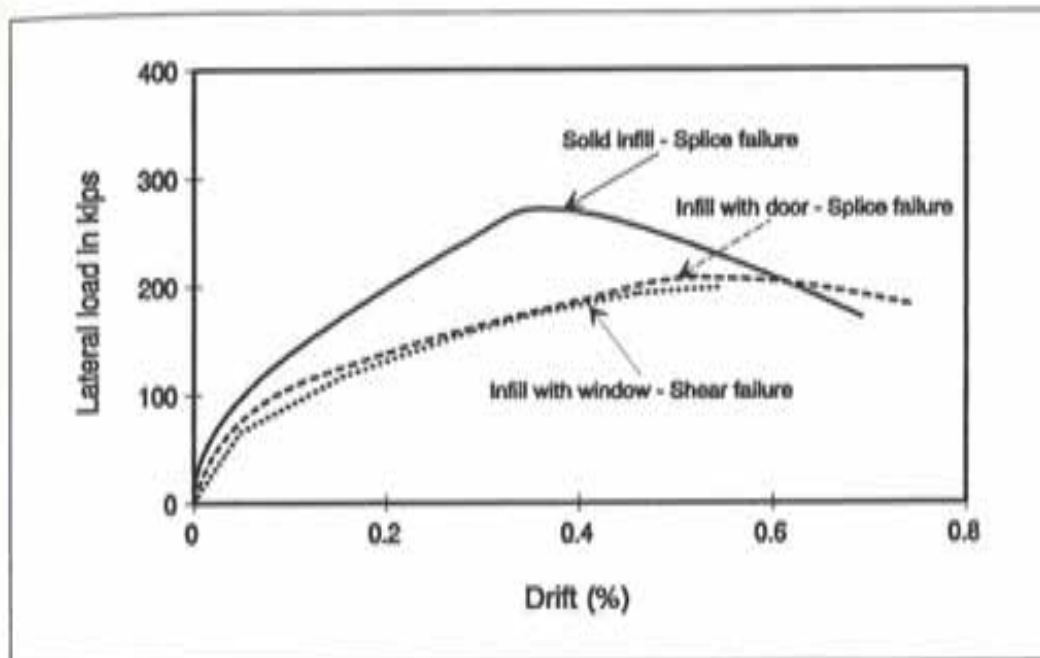


Figure 2.2 Performance of frames retrofitted by Gaynor [13] with shotcrete infill walls



Figure 2.3 Shotcrete wall separations and voids

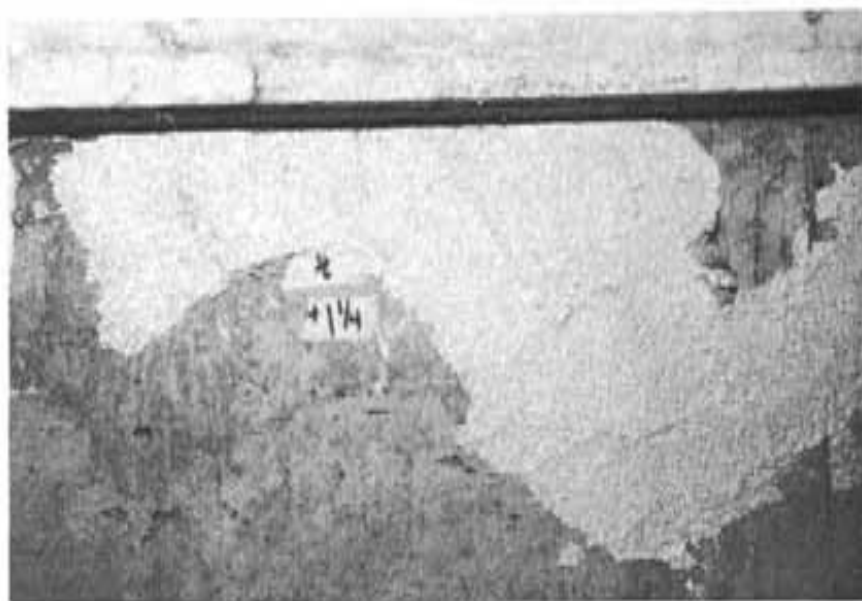


Figure 2.4 Finished epoxied interface (joint)

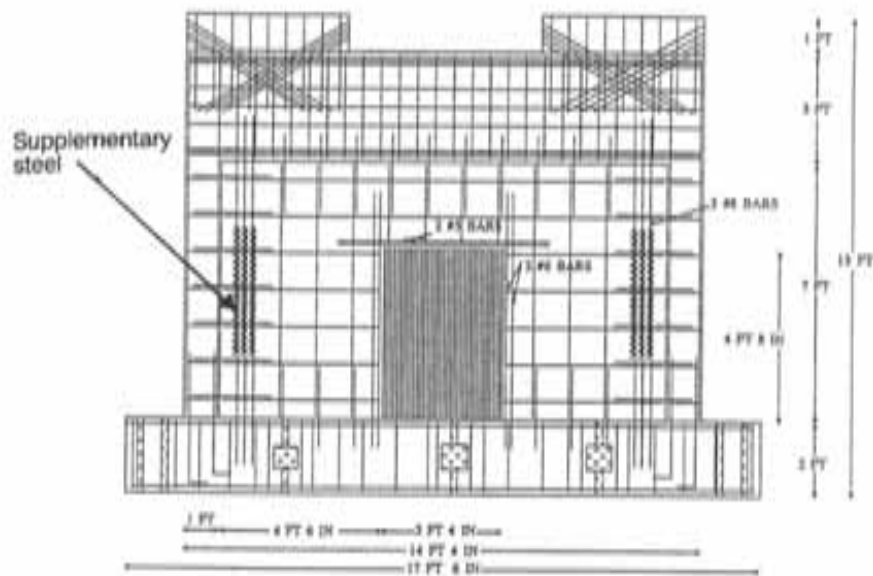


Figure 2.5 Reinforcement layout for test specimen retrofitted by Shah [33] with cast-in-place infill wall and supplementary tensile reinforcement in boundary element region

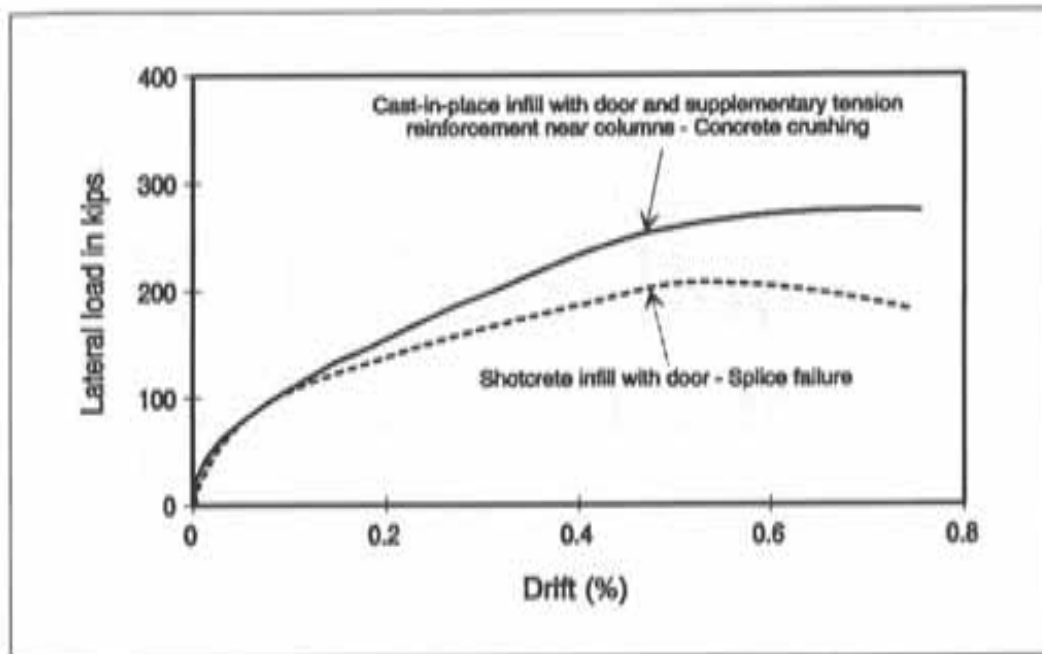


Figure 2.6 Performance of test specimens by Shah [33] and Gaynor [13]



Figure 2.7 Wall and encasing reinforcement for frame retrofitted by Jimenez [17]

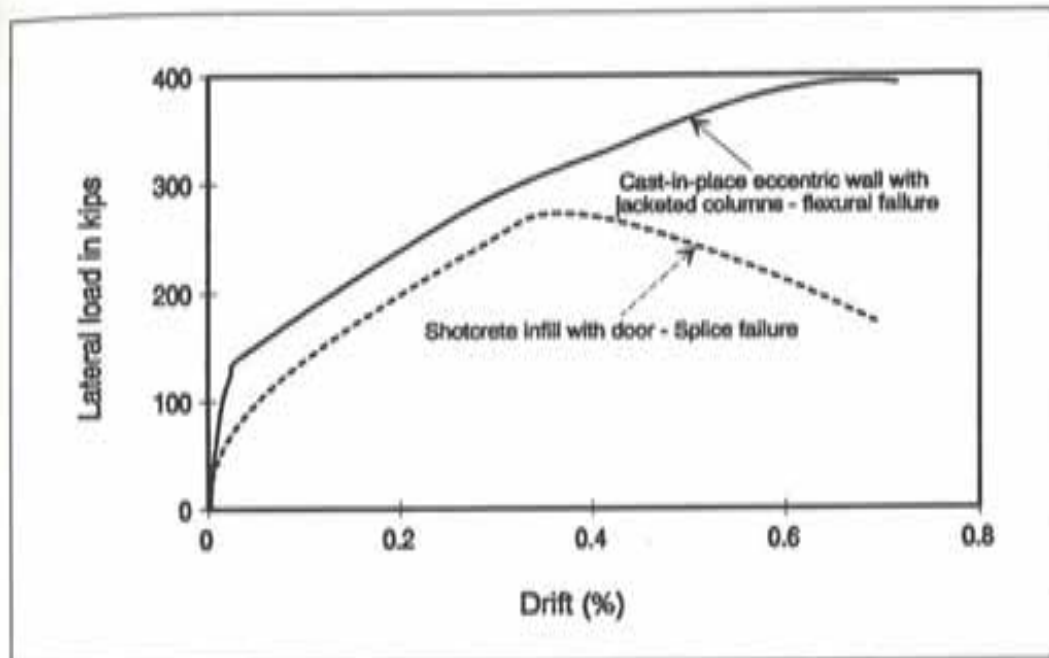


Figure 2.8 Performance of test specimens by Jimenez [17] and Gaynor [13]

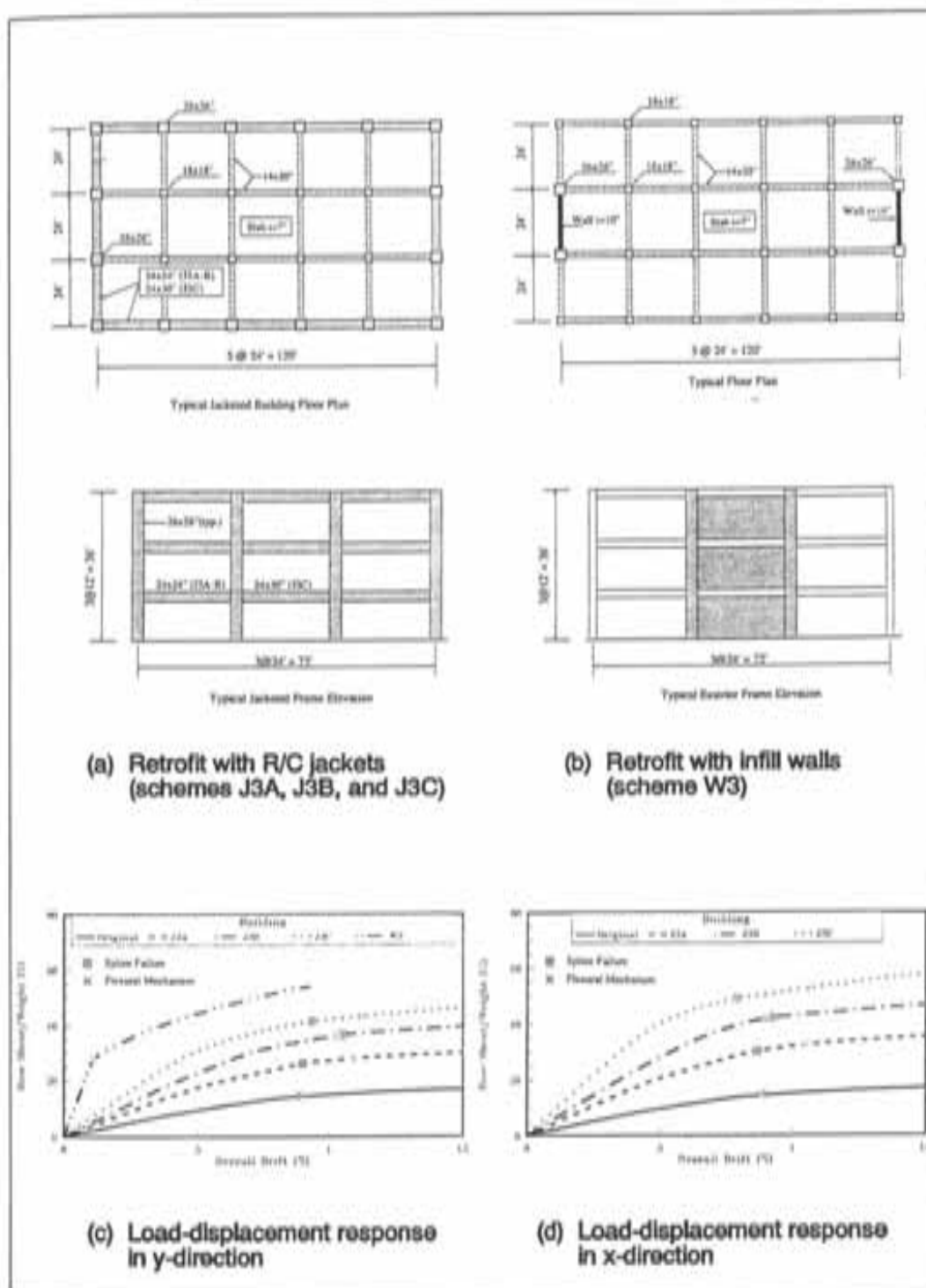


Figure 2.9 Retrofit schemes for low-rise building investigated analytically by Jordan [19]

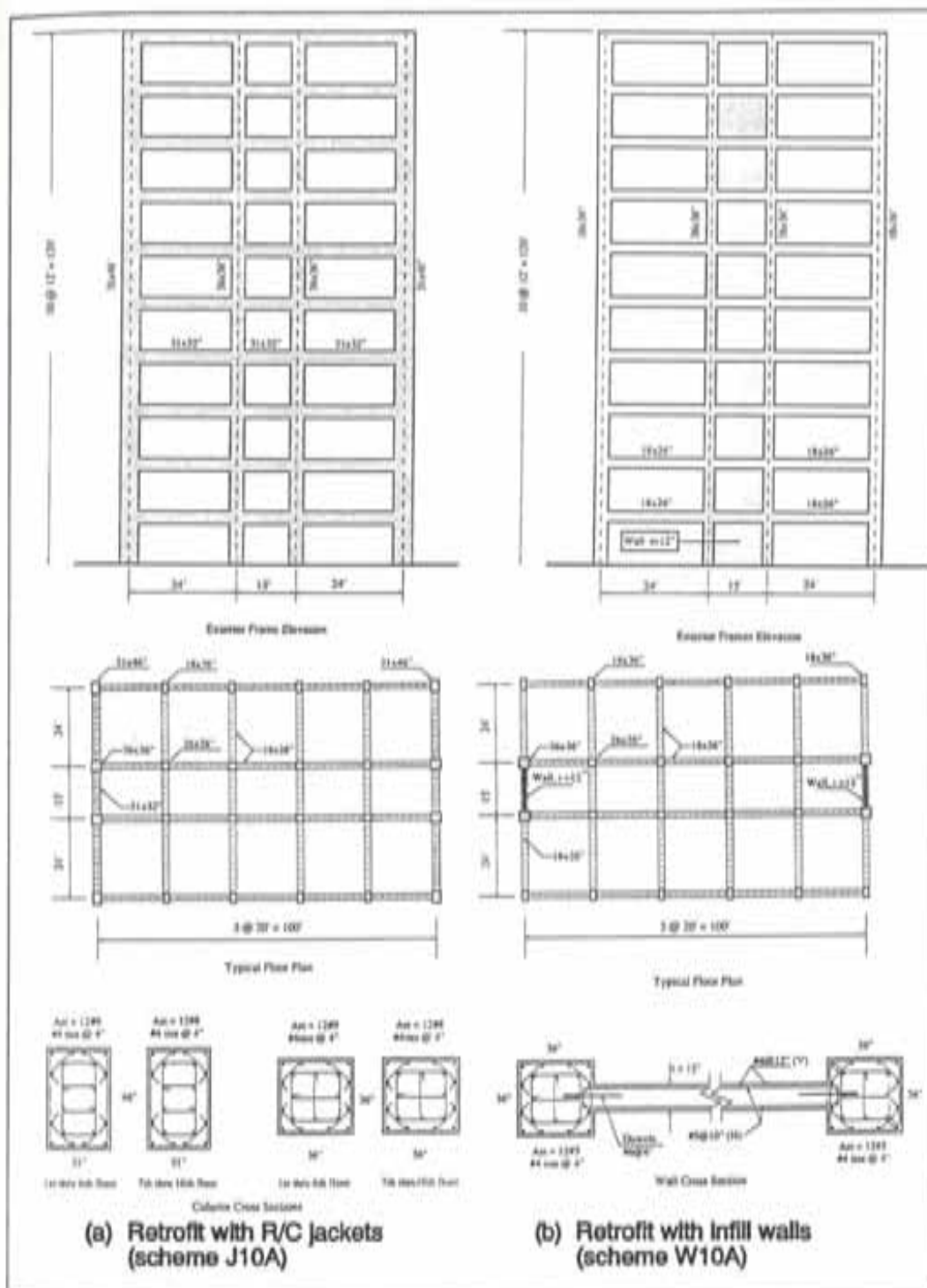


Figure 2.10 Retrofit schemes for medium-rise building investigated analytically by Jordan [19] contd.

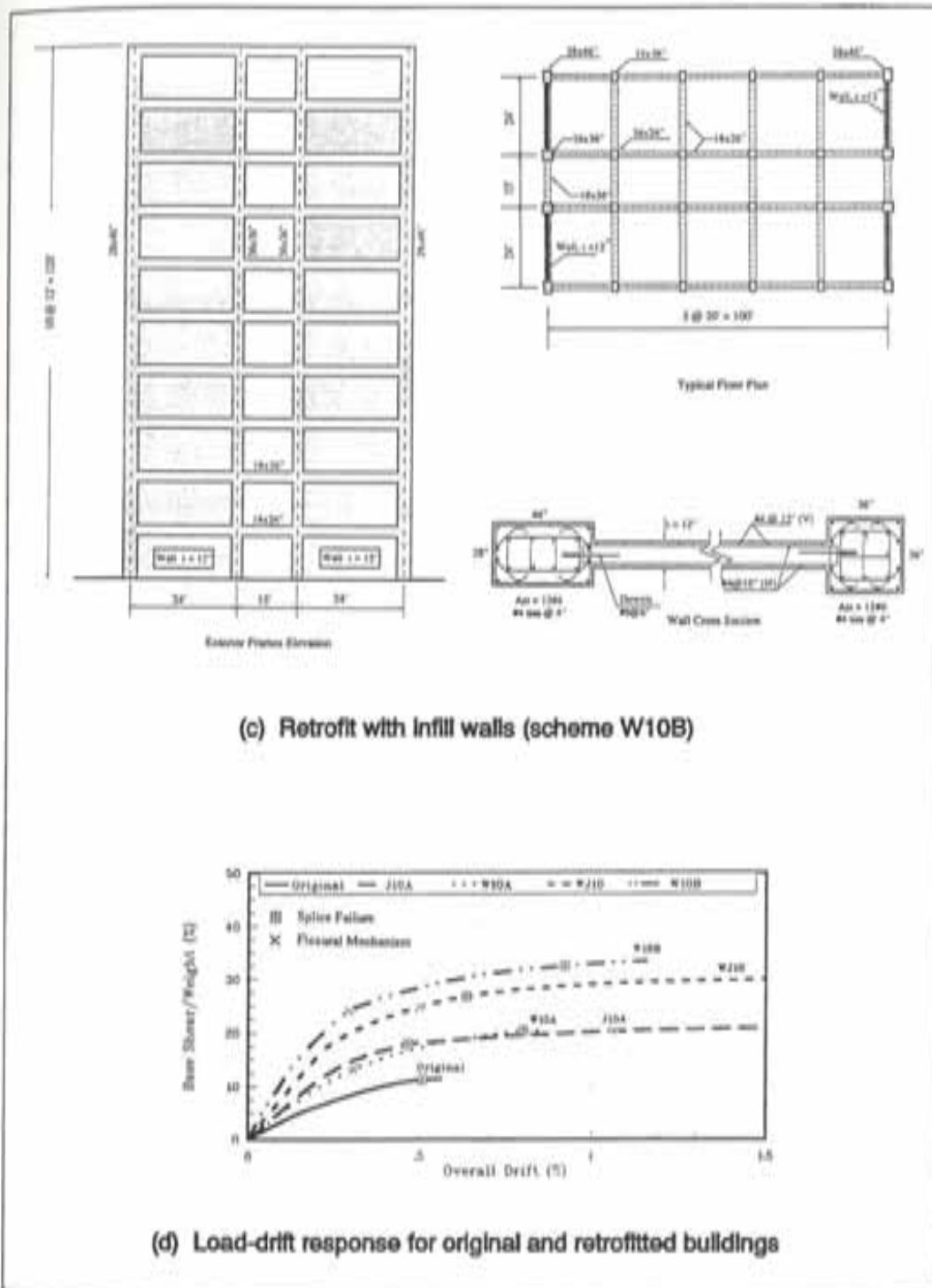
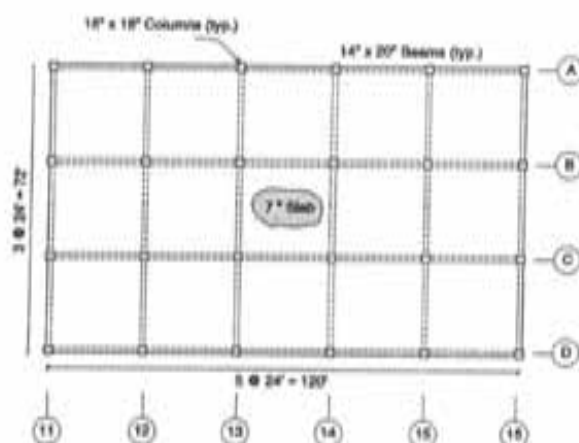
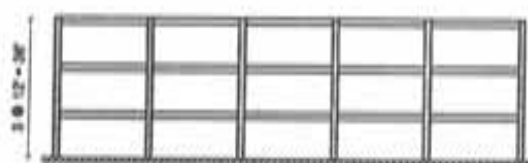


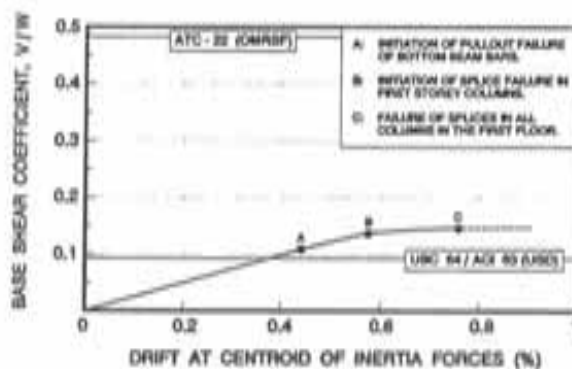
Figure 2.10 Retrofit schemes for medium-rise building investigated analytically by Jordan [19]



(a) Plan view of the three-story building



(b) Elevation in the longitudinal direction of the three-story building



(c) Response of the building in the longitudinal direction

Figure 2.11 Low-rise, unstrengthened building investigated analytically by Pincheira [30]

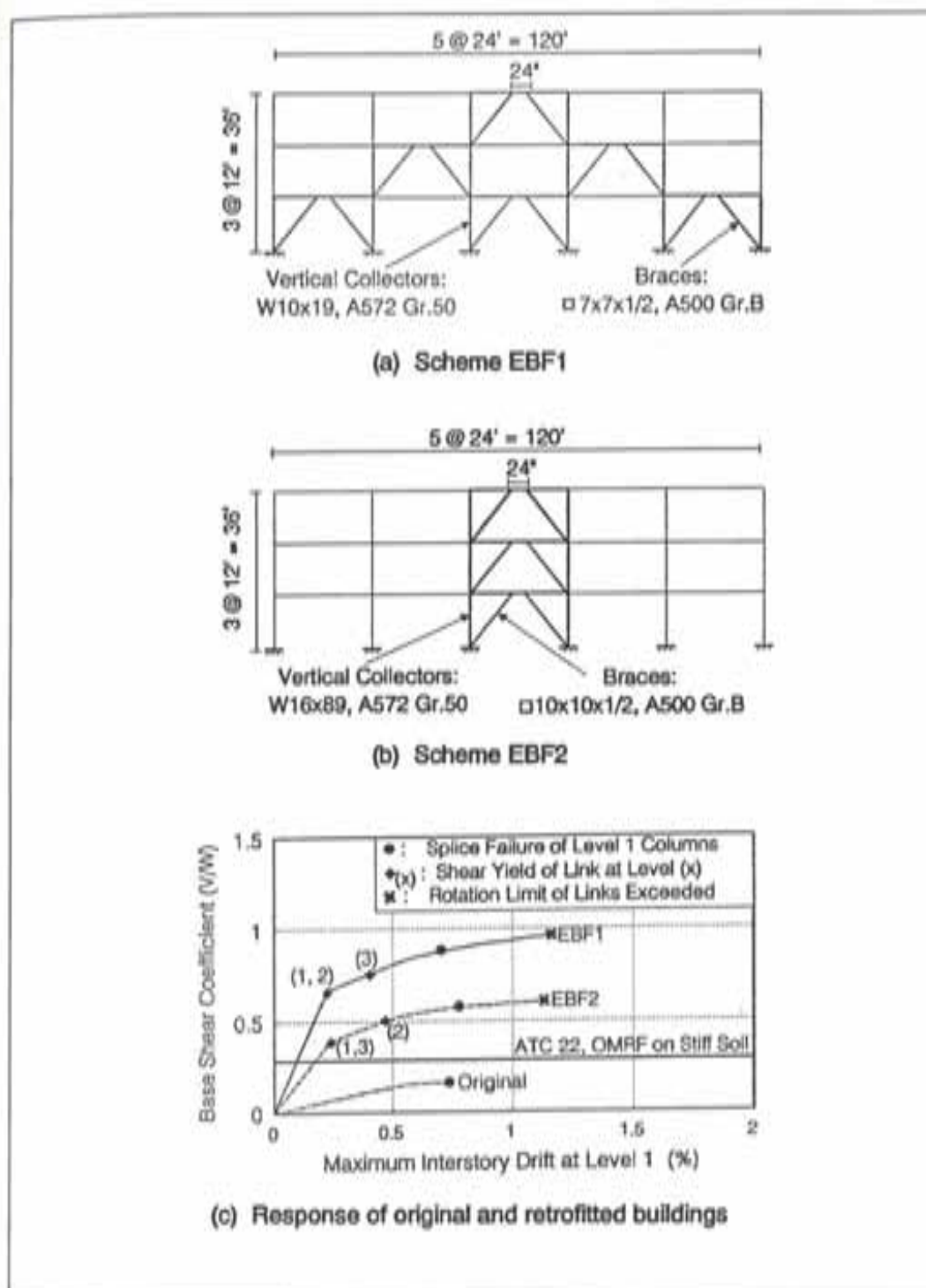
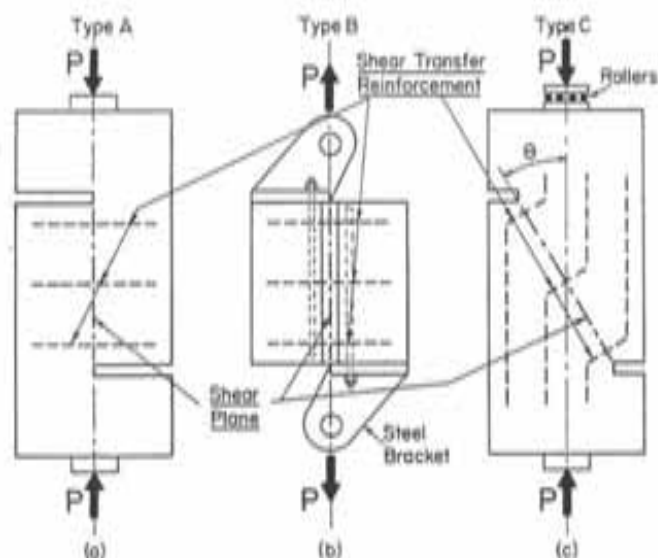
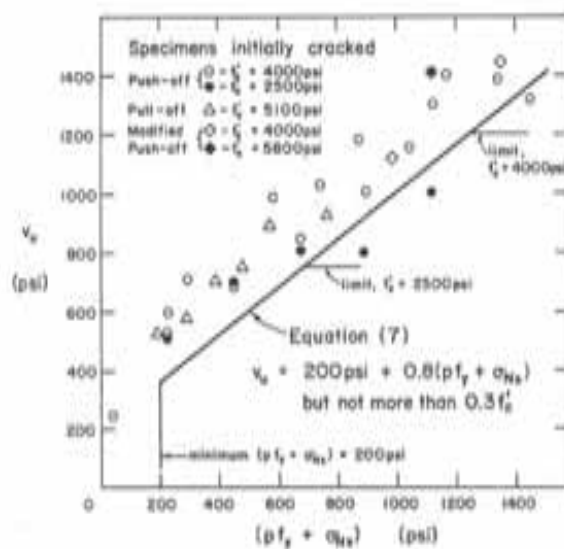


Figure 2.12 Eccentrically braced steel frames (EBF) for retrofit of low-rise buildings investigated analytically by Bouadi [11]

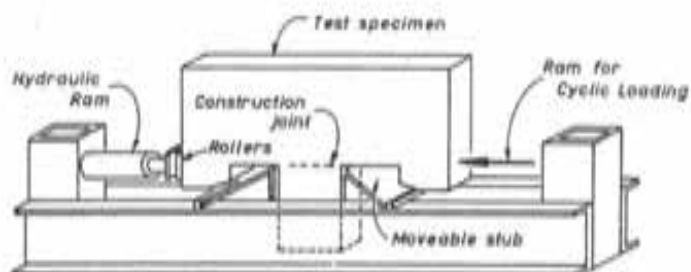


(i) Shear transfer test specimens: (a) push-off; (b) pull-off; and (c) modified push-off

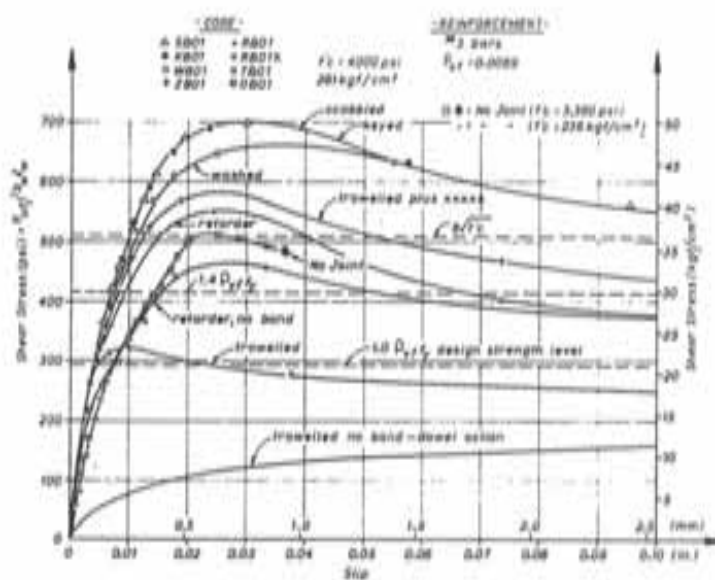


(ii) Design recommendations based on test data

Figure 2.13 Tests for direct shear transfer by Hofbeck [15] and Mattock [25]



(a) Test setup



(b) Load-slip response for test specimens with various surface preparations

Figure 2.14 Tests on direct shear transfer across concrete-to-concrete interfaces by Paulay [29]

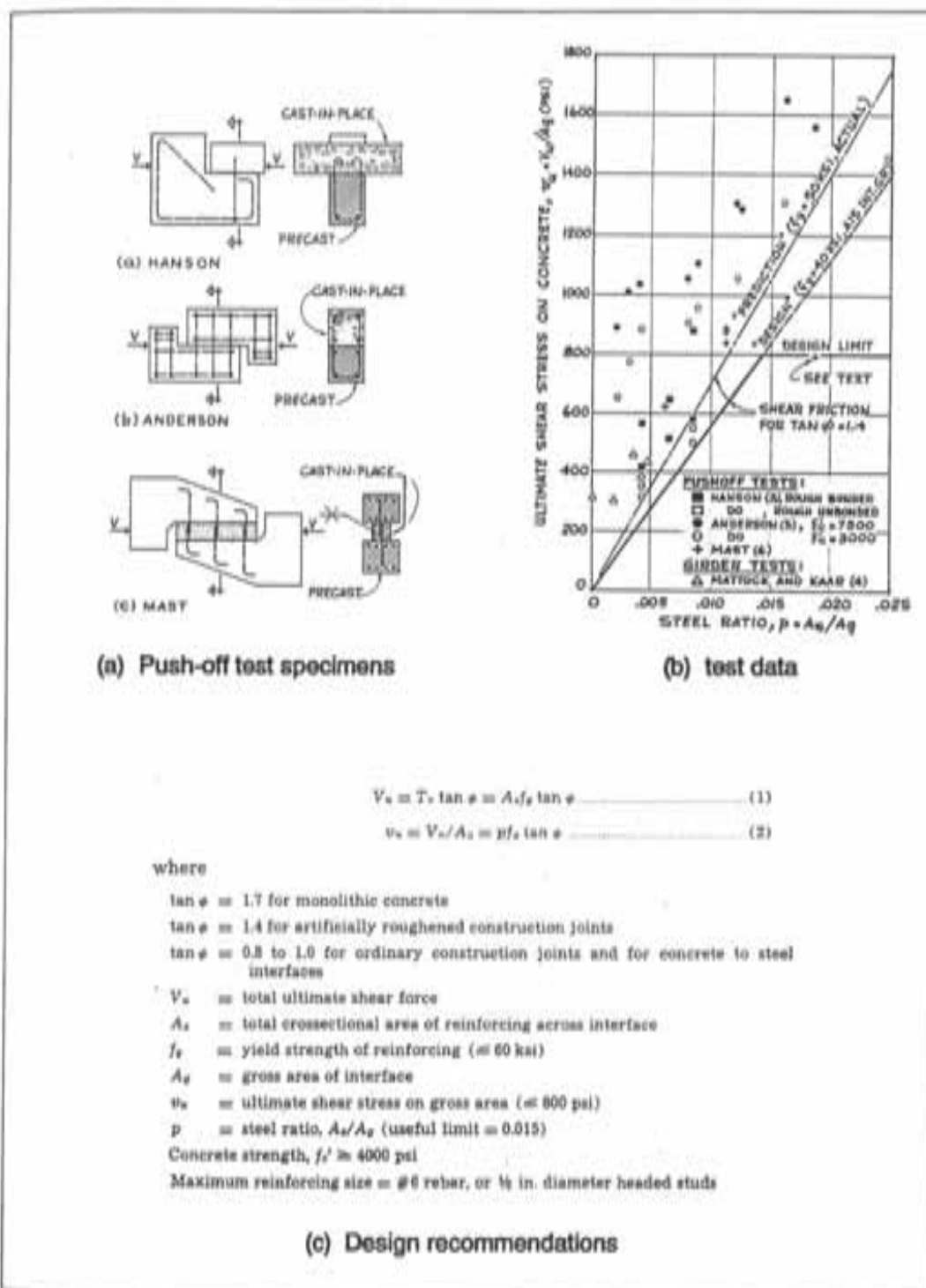


Figure 2.15 Design recommendations by Birkeland [10] based on direct shear tests by Anderson [5], Hanson [14], and Mast [23]

CHAPTER 3

RETROFITTING OF COLUMN SPLICES

EXPERIMENTAL PROGRAM

3.1 INTRODUCTION

The first phase of the experimental program focussed on (1) developing techniques that would improve the tensile strength and the deformation capacity (ductility) of short lap splices present in the columns, and (2) testing the performance of strengthened column specimens to verify the effectiveness of selected retrofit schemes. Retrofit schemes were selected based on ease of construction, minimal construction costs and minimum changes to column dimensions.

3.2 RETROFITTING TECHNIQUES

3.2.1 Retrofitting Methodology. Two approaches for retrofitting column lap splices were examined. The first consisted of supplementing confinement in the column splice region to improve bond along the spliced bars. The second involved making spliced bars continuous so that forces could be transferred directly without relying on surrounding concrete and confinement to develop bond between spliced bars.

3.2.2 Techniques for Supplementing Confinement in the Splice Region. Three different schemes were selected for improving confinement in the splice region: (1) addition of steel angles along the column corners over the splice region with steel straps connecting the angles, (2) addition of external steel reinforcing bar ties, and (3) placement of additional internal ties in the splice region. For the first two schemes, different grouting conditions (between external confining elements and existing concrete) were studied in order to determine the influence of grout on the effectiveness of external confinement.

3.2.3 Technique for Making Spliced Bars Continuous. Lapped bars were welded together to provide a direct load path for transfer of forces. Splices in the two column specimens strengthened using welded splices were constructed as non-contact splices (Fig. 3.1). This was done in order to simulate adverse field conditions where spliced bars are not in contact after construction is completed.

3.3 TEST SPECIMENS

3.3.1 Existing (Unstrengthened) Column Specimen. The prototype member selected for study was an 18 x 18 in. reinforced concrete column with 4 #9 longitudinal bars and #3 ties. Twelve test specimens were constructed. The test specimens were two-thirds scale models of the prototype column, and were designed and detailed to represent 1950's construction. Typical details of test specimens were a column compression splice length of 24 longitudinal bar diameters and tie spacing of 12 inches which conform to ACI 318-56 [1] and ACI 318-63 [2] provisions. Ties were fabricated with 90 degree hooks, typical of 1950's construction. A schematic of a typical specimen with existing (unstrengthened) lap splices is shown in Fig. 3.2. Splices were located at mid-height of the test specimens. The reinforcing cage for a column specimen with contact lap splices is shown in Fig. 3.3.

3.3.2 Retrofitted Column Specimens. One of the twelve column specimens was not strengthened to provide a bench mark. Splice regions in the other eleven specimens were retrofitted using the different schemes described earlier.

3.3.2.1 Nomenclature for Column Specimens. Test specimen notation was based on splice details, retrofit scheme selected, grouting details of strengthening elements, and specimen number when the same general retrofitting scheme is used. The column specimens and their notations are summarized in Table 3.1.

3.3.2.2 Column Specimens Retrofitted Using Steel Angles and Straps. Three specimens (U-SS6-UG-1, U-SS6-UG-2 and U-SS6-UG-3) were strengthened using steel angles (2 x 2 x 1/4 in.) and straps (12 x 1 x 1/4 in.). Column corners were chipped to permit a better fit of the steel angles to the column, and steel straps (spaced @ 6 in. c/c) were welded to the angles (Fig. 3.4). Care was taken to ensure that the angles fit tightly against existing concrete. Two more specimens (U-SS6-G-4 and U-SS6-G-5) were strengthened with similar details but with grout placed between the existing column and the steel angles and straps. The angles were fixed along the column corners with 1/4 in. spacers between the concrete and each steel angle, and then straps were welded to the angles. A dry-pack cementitious grout (non-shrink and non-corrosive grout mixed with a minimal amount of water) was placed and compacted in the gap between the existing column and steel elements (Fig. 3.5). Design details of the scheme are presented in Art. A.2 of Appendix A.

3.3.2.3 Column Specimens Retrofitted Using External Reinforcing Bar Ties. Three specimens (U-ES3-G-1, U-ES3-UG-2 and U-ES3-PG-3) were confined with external ties made of U-shaped #4 reinforcing bars. The ties were placed @ 3 in. c/c spacing and their overlapping legs were welded together (Fig. 3.6). Specimen U-ES3-UG-2 was left ungrouted (Fig. 3.7a). Ties in specimen U-ES3-G-1 were grouted with a very fluid mix forming a 1 in. cover over the existing concrete (Fig. 3.7b). The grout cover was cast by using a form around the column and a fluid cement grout. Specimen U-ES3-PG-3 was partially grouted; a dry-pack cementitious grout was applied by hand to fill the gap between the ties and the existing column and to cover the exposed ties (Fig. 3.7c). The partially-grouted scheme was intended to ensure that the external ties were in contact with the existing column. Design details for this scheme are presented in Art. A.3 of Appendix A.

3.3.2.4 Column Specimen Retrofitted Using Additional Internal Ties. Test specimen U-AT8-1 was provided with three additional #3 internal ties at 8 in. spacing after the existing concrete cover was removed at each tie location. The intent was to remove as little cover as possible. As a result, the tie spacing did not meet current specifications. The

ties consisted of U-shaped reinforcing bars with overlapping legs which were welded together (Fig. 3.8). The removed concrete cover was replaced with a non-shrink cement grout after the ties were placed. Design details for this retrofit scheme are presented in Art. A.4 of Appendix A.

3.3.2.5 Column Specimens Retrofitted with Welded Splices. In specimens S-WS-1 and S-WS-2, concrete cover along the column corners was removed over the splice region and the non-contact lap-spliced bars were welded together with a #3 reinforcing bar serving as a filler. The removed concrete cover was replaced by a non-shrink cement grout after the lap spliced bars were welded together. Specimen S-WS-2 was provided with a #3 tie near the end of the outer spliced bar (Fig. 3.9). This was done in order to restrain the outward thrust produced by eccentricity between the spliced bars. Design of this specimen was based on recommendations of Section 12.14.3.2 of ACI 318-89 [3] and "Structural Welding Code - Reinforcing Steel" (AWS D1.4) [36]. Design details are presented in Art. A.5 of Appendix A.

3.3.3 Characteristics of Materials

3.3.3.1 Concrete. Concrete was supplied by a local ready-mix plant. The 28-day design compressive strength was 3000 psi (typical of 1950's construction). It utilized 3/8 in. coarse aggregate (2/3 scale of 5/8 in. coarse aggregate used for the prototype column) and 5 in. slump. The compressive strength of concrete at different ages is listed in Table 3.2. All column specimens were tested at an age of 45 days or later.

3.3.3.2 Steel

(a) *Reinforcing bars.* Grade 60 reinforcing bars were used for all purposes due to the lack of availability of Grade 40 reinforcing steel which was used in 1950's

construction. The measured yield strength of reinforcing bars of all sizes ranged between 69 and 71 ksi.

(b) *Strengthening steel.* Grade A36 steel was used for steel angles and straps. The measured yield strength of steel angles and straps was 53 ksi.

3.3.3.3 Cement Grout. The cement grout, commercially known as, "SikaGrout 212" (manufactured by Sika Corporation, New Jersey) was used for all grouting procedures. It is a non-shrink and non-corrosive grout which can be mixed with varying quantities of water to obtain different levels of consistency (plastic to fluid states) depending on the purpose to be served.

3.3.3.4 Welds. Based on the recommendations of Section 12.14.3.2 of ACI 318-89 [3] and "Structural Welding Code - Reinforcing Steel" (AWS D1.4) [36], electrode type "AWS E9018-M" was used to weld lap splices of Grade 60 reinforcing bars.

3.4 TEST SETUP AND TESTING PROCEDURE

3.4.1 Test Setup. The test frame (Fig. 3.10) was designed to subject column specimens to alternating axial tensile and compressive forces. These are the primary forces experienced by boundary elements of a frame-infill wall system that is subjected to reversed cyclic lateral loads resulting from seismic action. Tension was applied to specimens through a 1.5 in. diameter rod embedded in each test specimen (Fig. 3.2). Specimens were subjected to axial tension and compression by activating the top ram (tension actuator) and the bottom ram (compression actuator) alternately.

3.4.2 Loading History. All test specimens were subjected to repeated cycles of load reversals. The load cycles consisted of a half cycle of tension load followed by a half

cycle of compression load of equal magnitude. The proposed loading pattern (Fig. 3.11) incorporated one cycle with a peak load of 60 K , followed by pairs of cycles with peak loads of 90 K, 120 K and 150 K each. This load history was modified slightly during the tests based on the observed behavior of test specimens.

3.4.3 Instrumentation. Two load cells, each placed under tension and compression actuators, monitored the applied load. This load was verified by a pressure transducer. Two displacement transducers were installed on opposite faces of the test specimen to measure axial elongation over the splice region (Fig. 3.12). Strain gages were mounted at critical locations in each specimen to measure steel strains.

3.4.4 Data Acquisition System. The data acquisition system consisted of an analog-to-digital converter, usually referred to as a "scanner." Load cells, pressure transducers, displacement transducers, and strain gages were monitored.

Table 3.1 Test specimen nomenclature

| Sl. No. | Splice details | Retrofit scheme selected | Grouting details | Scheme Index | Specimen index |
|---------|-----------------|--|------------------------|--------------|----------------|
| 1 | Contact (U) | Base splice (B) (unstrengthened) | --- | 1 | U-B-1 |
| 2 | U | Steel angles & straps @ 6 in. (SS6) | UngROUTed (UG) | 1 | U-SS6-UG-1 |
| 3 | U | SS6 | UG | 2 | U-SS6-UG-2 |
| 4 | U | SS6 | UG | 3 | U-SS6-UG-3 |
| 5 | U | SS6 | Grouted (G) | 4 | U-SS6-G-4 |
| 6 | U | SS6 | G | 5 | U-SS6-G-5 |
| 7 | U | External rebar ties @ 3 in. (ES3) | G | 1 | U-ES3-G-1 |
| 8 | U | ES3 | UG | 2 | U-ES3-UG-2 |
| 9 | U | ES3 | Partially grouted (PG) | 3 | U-ES3-PG-3 |
| 10 | U | Additional internal ties @ 8 in. (AT8) | --- | 1 | U-AT8-1 |
| 11 | Non-contact (S) | Welded splices (WS) | --- | 1 | S-WS-1 |
| 12 | S | WS with an additional tie | --- | 2 | S-WS-2 |

Table 3.2 Compressive strength of concrete at different ages

| Age (days) | Concrete cylinder strength in compression (psi) |
|------------|---|
| 7 | 2680 |
| 28 | 3510 |
| 45 | 3850 |
| 90 | 4010 |

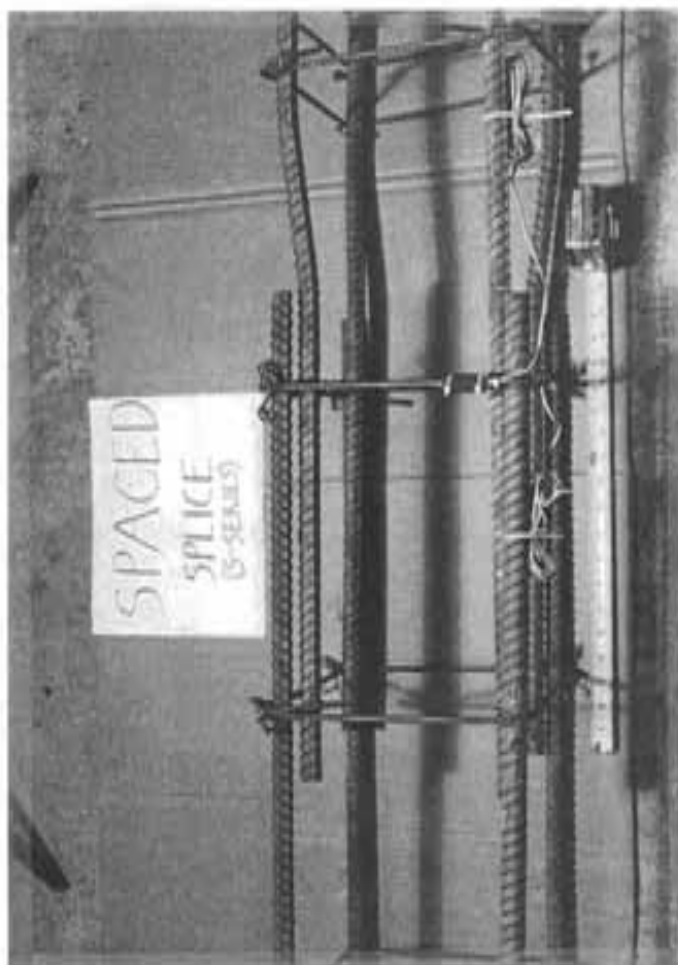


Figure 3.1 Example of non-contact lap splices

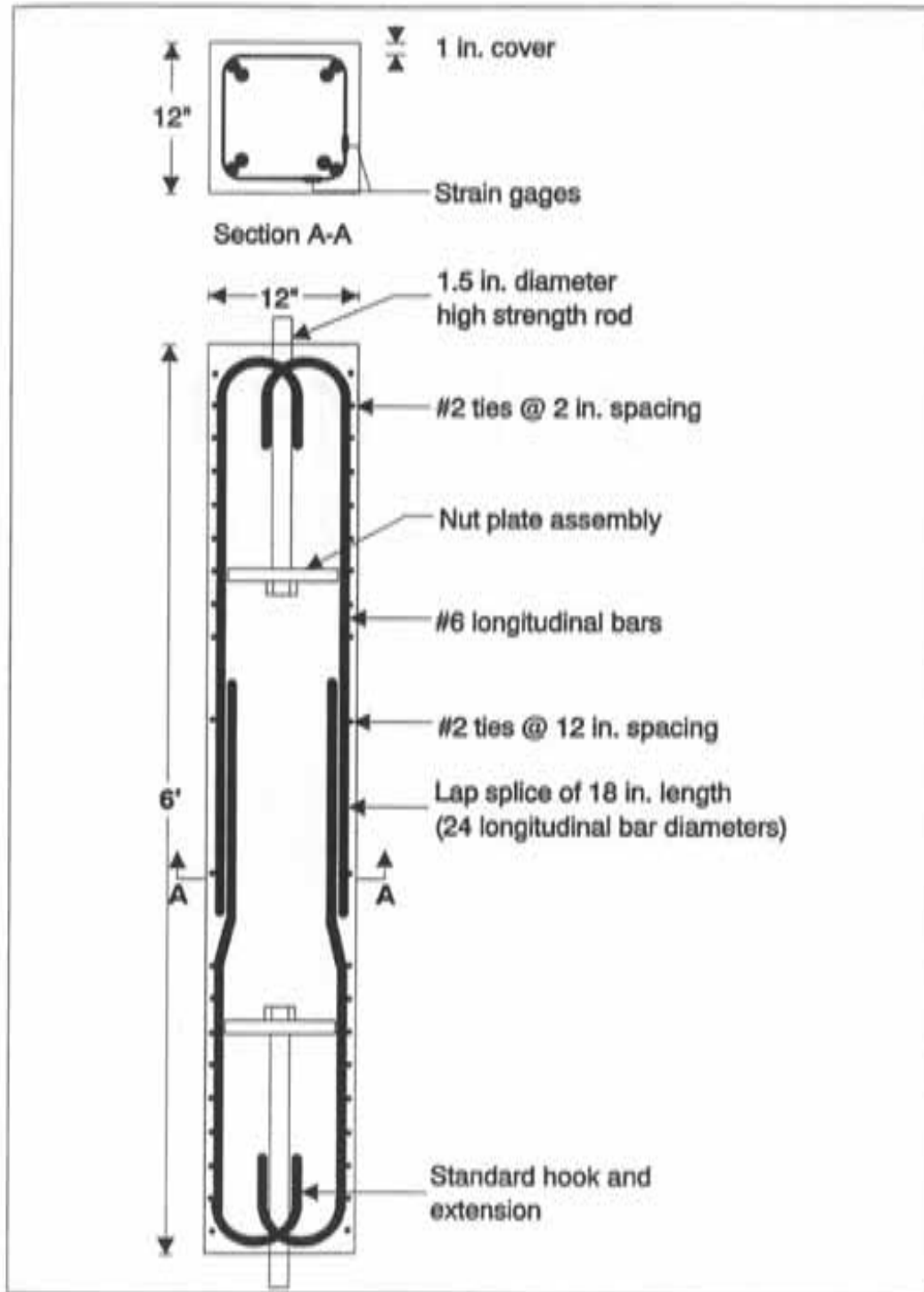


Figure 3.2 Test specimen with existing (unstrengthened) splice details



Figure 3.4 Welding of steel straps to angles

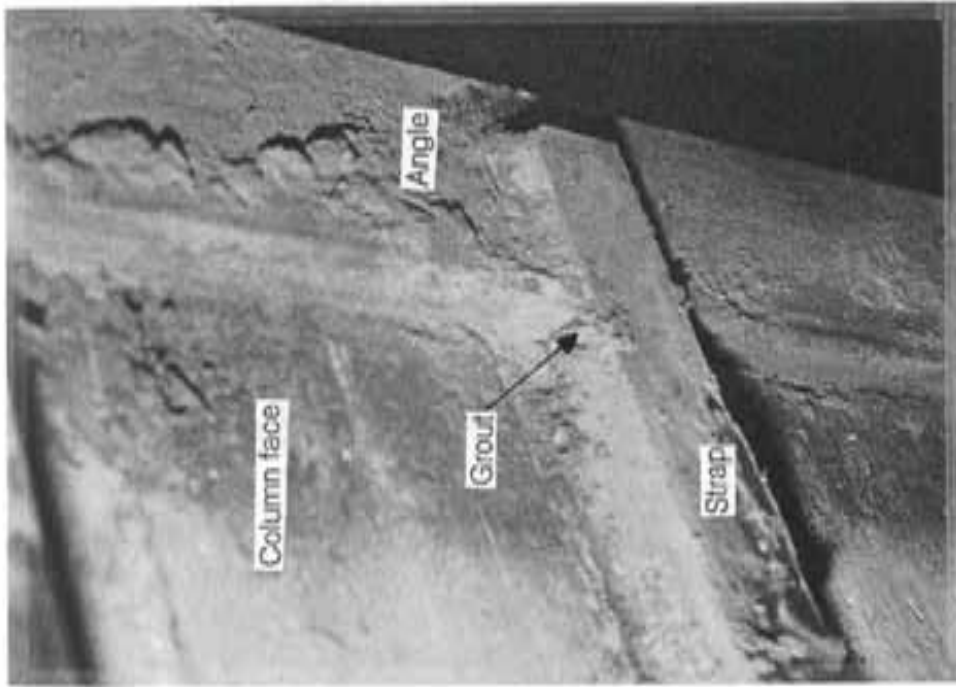


Figure 3.5 Cement grout between column face and steel elements (angles & straps)

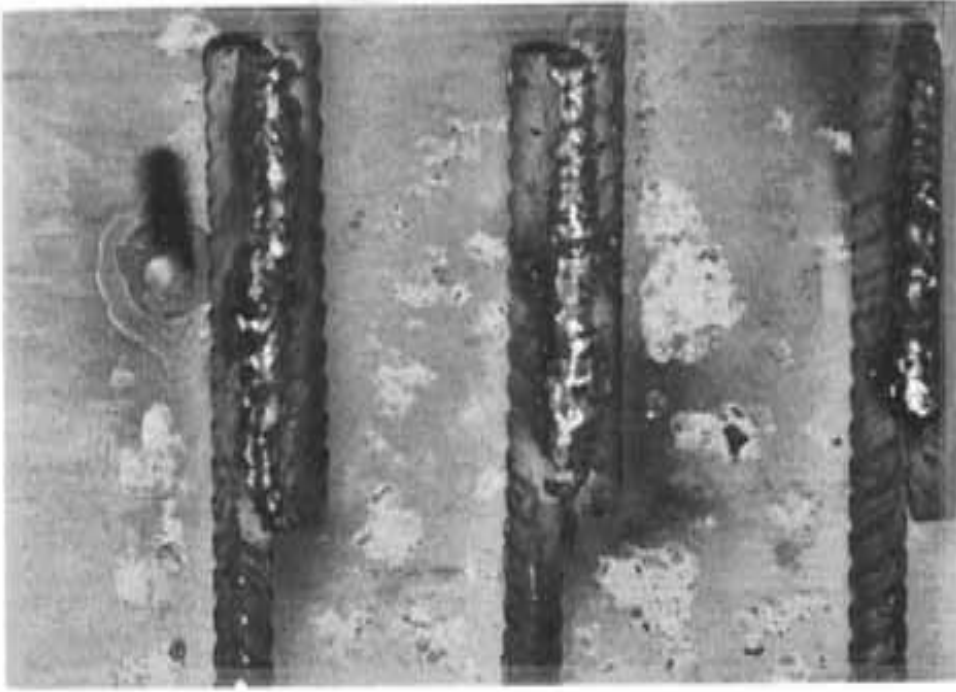


Figure 3.6 Welded external rebar ties

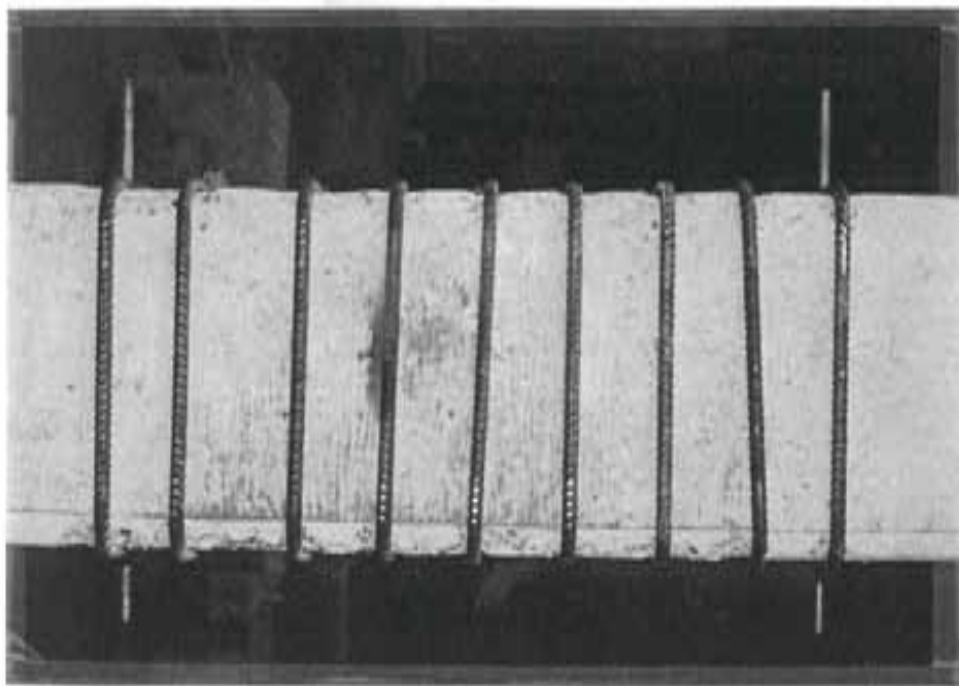


Figure 3.7a UngROUTED external rebar ties

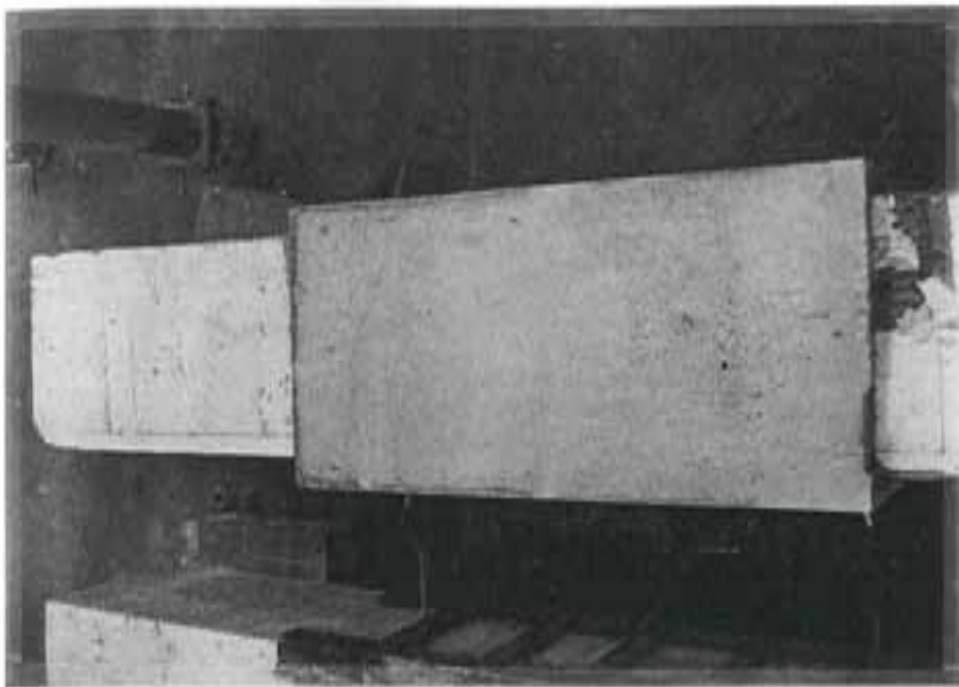


Figure 3.7b Grouted external rebar ties

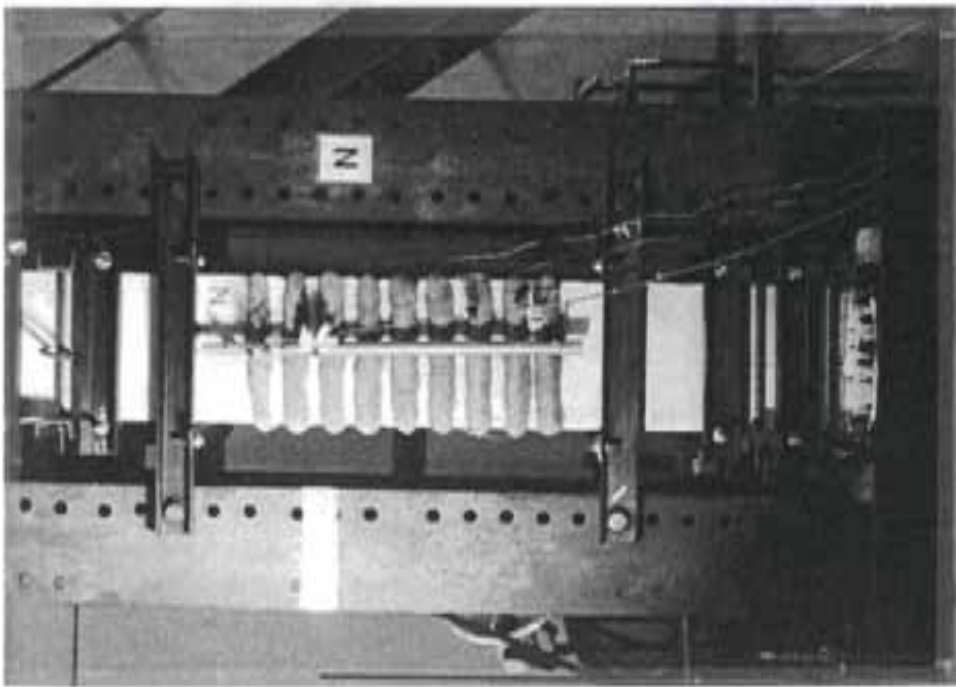


Figure 3.7c Partially-grouted external rebar ties

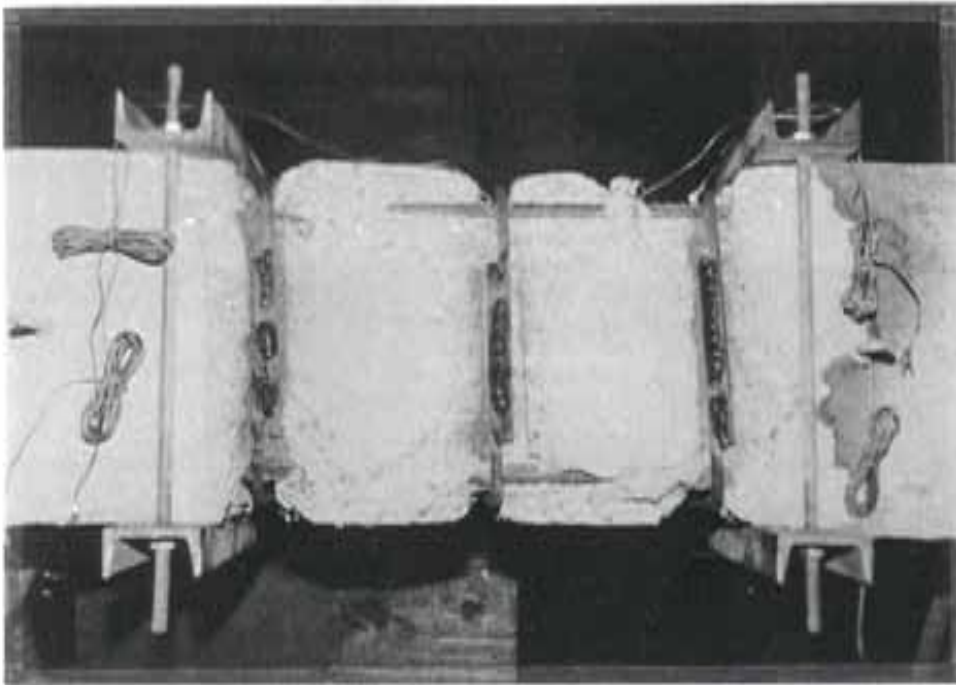


Figure 3.8 Additional internal ties

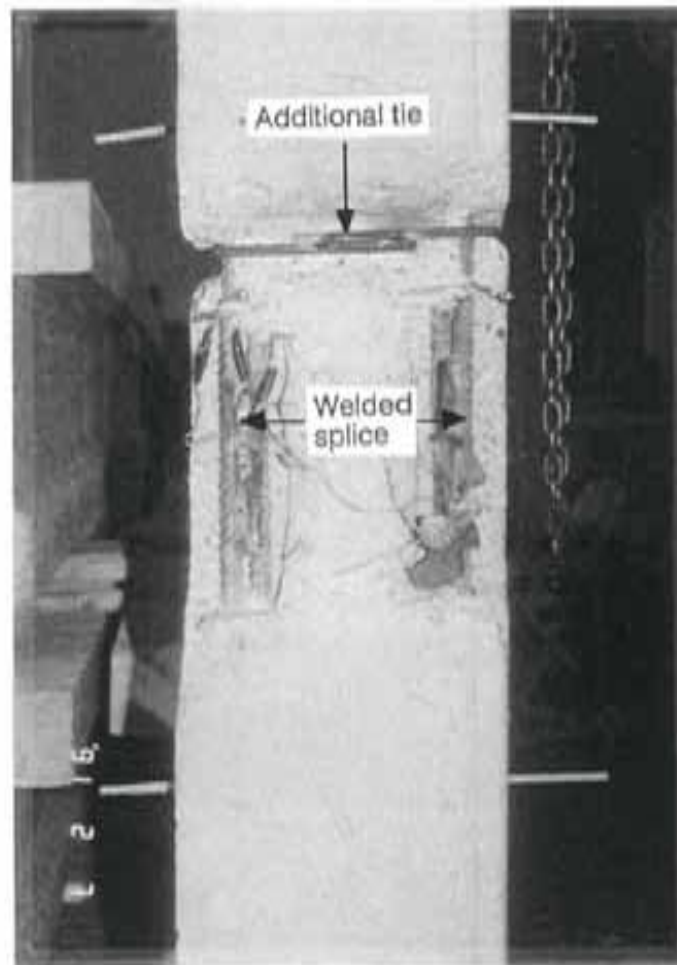


Figure 3.9 Welded splices with an additional tie

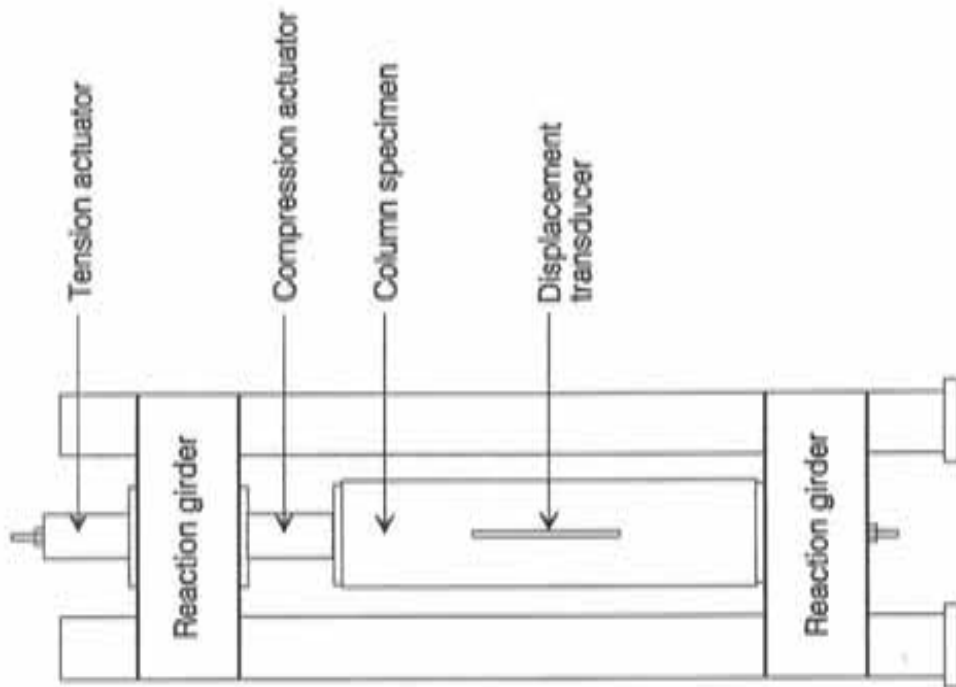
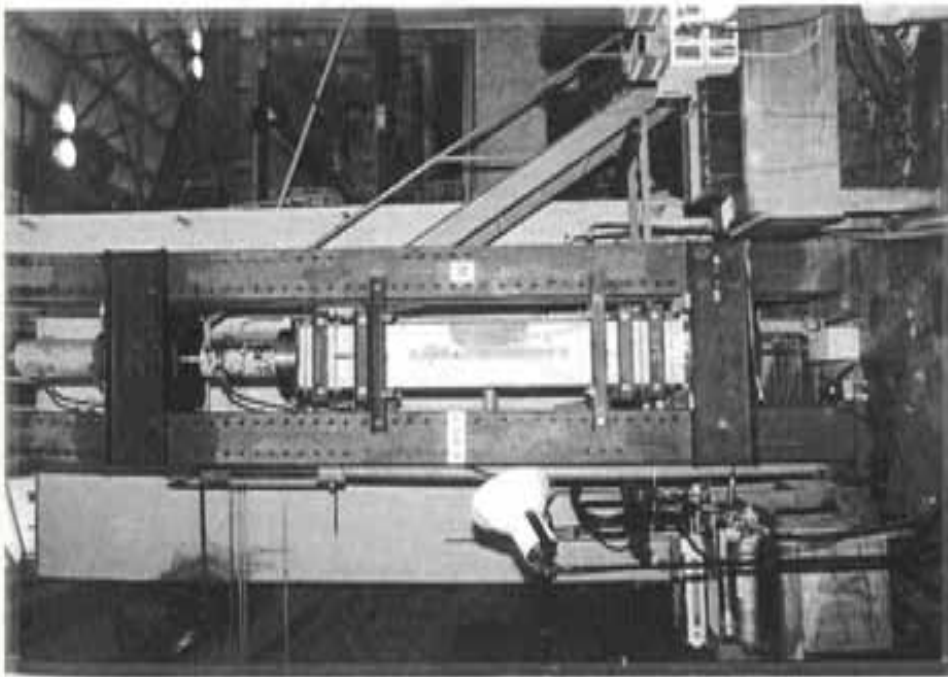


Figure 3.10 Test setup

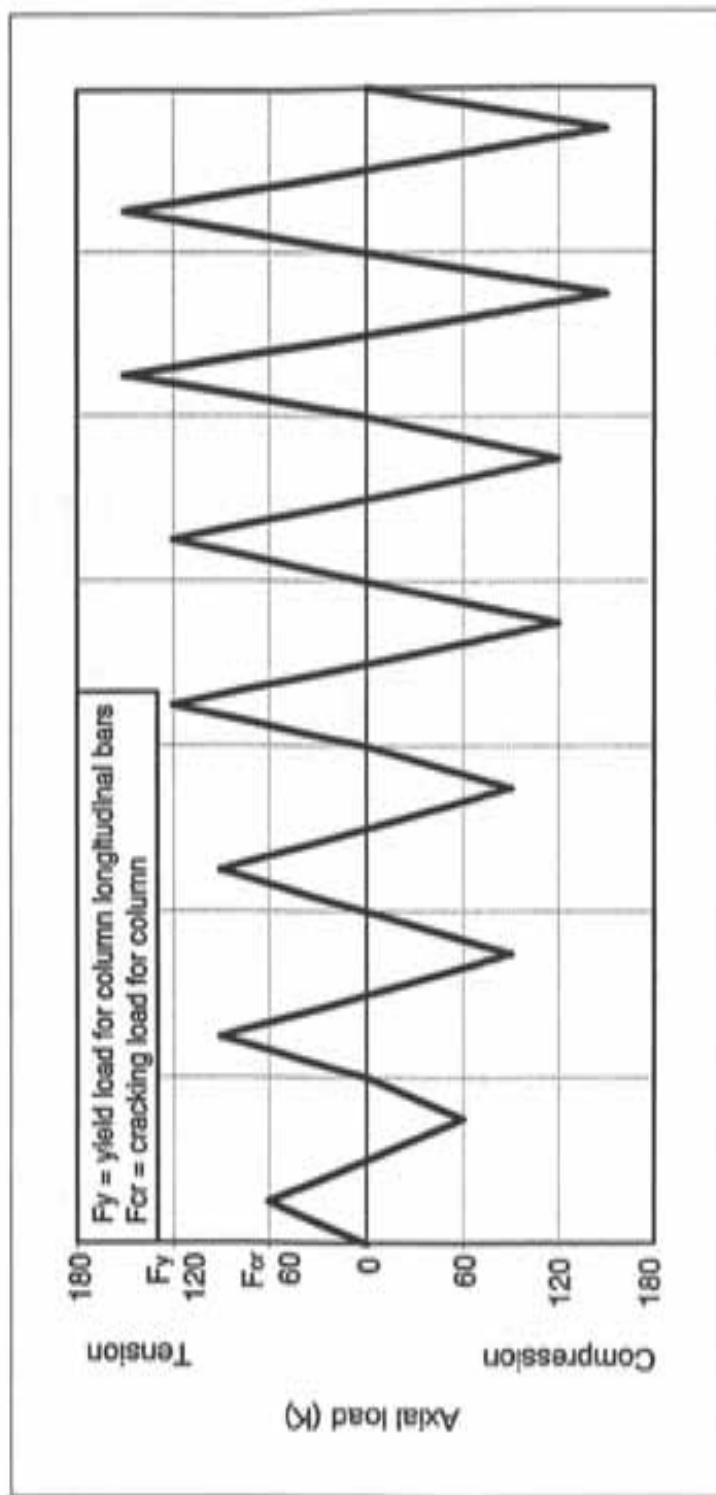


Figure 3.11 Typical loading history for the test specimens

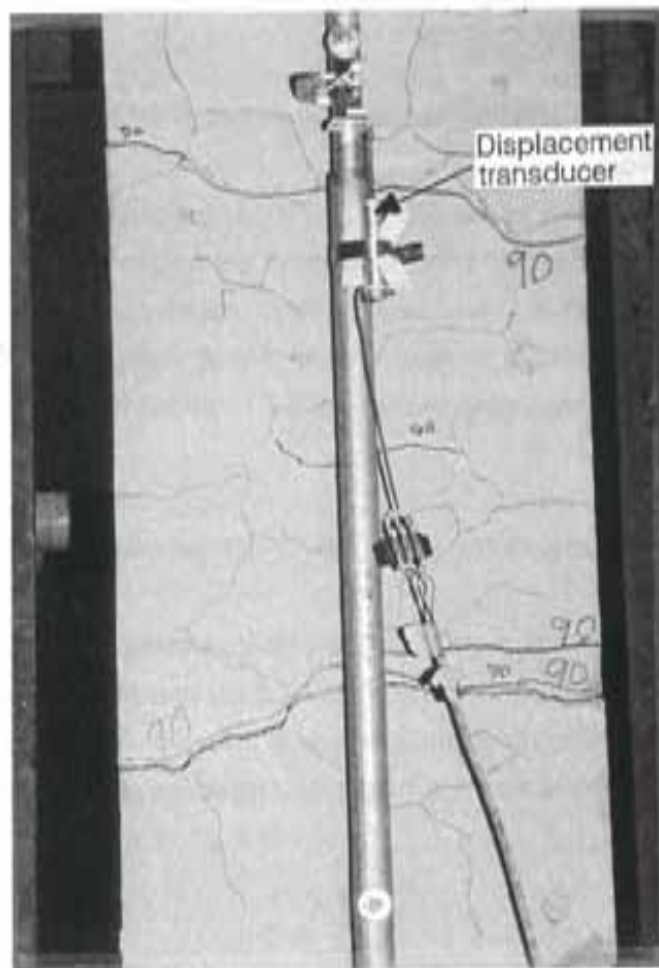


Figure 3.12 Measurement of axial deformation in splice region using a displacement transducer

CHAPTER 4

RETROFITTING OF COLUMN SPLICES

TEST RESULTS

4.1 EXISTING (UNSTRENGTHENED) COLUMN SPECIMEN

4.1.1 Column Specimen U-B-1. Splitting cracks initiated near the location of column ties in the splice region and progressed along the splices until a splitting tensile failure occurred during the third load cycle at a load level of 80 K (Fig. 4.1). The failure was brittle. A sketch of the crack pattern in the specimen at failure is shown in Fig. 4.2. Performance of column specimen U-B-1 and its load history are shown in Fig. 4.3.

4.2 COLUMN SPECIMENS RETROFITTED USING STEEL ANGLES AND STRAPS

4.2.1 Column Specimen U-SS6-UG-1. Cracks initiated near the ends of the splice region and between steel straps over the splice zone (Fig. 4.4). The test specimen failed during the third cycle at a load level of 80 K due to concrete splitting parallel to the splices. The failure zone in specimen U-SS6-UG-1 is shown in Fig. 4.5. The performance and load history are shown in Fig. 4.6.

4.2.2 Column Specimen U-SS6-UG-2. Behavior was different from that of specimen U-SS6-UG-1 in that the transverse splitting cracks which developed over the splice region did not progress as much along the splices as in the case of specimen U-SS6-UG-1 (Fig. 4.7). However, testing could not be continued beyond the third load cycle because hooks in one of the end connections began to fail at a load level of 120 K. The crack pattern in specimen U-SS6-UG-2 at end-connection failure is shown schematically in Fig. 4.7. The performance and load history for specimen U-SS6-UG-2 are shown in Fig. 4.8.

4.2.3 Column Specimen U-SS6-UG-3. Behavior was similar to that of specimen U-SS6-UG-2. Testing was discontinued during the third load cycle because of an end connection failure. The column specimen was subjected to a maximum load of 120 K. The performance and load history of specimen U-SS6-UG-3 are shown in Fig. 4.9.

Column ends in test specimens that followed were confined using steel channels and mild steel rods (Fig. 4.10). This was done in order to prevent end connection failures. Such failures would not occur in reality since the hooks (in end connections) would not exist in a prototype column.

4.2.4 Column Specimen U-SS6-G-4. Behavior of this specimen was satisfactory. The test specimen was subjected to six load cycles with load levels as high as 150 K. Column bars yielded outside the splice region and as a result large cracks were observed as shown in Fig. 4.11. No cracks were observed in the splice region until the final load stages. The splice zone did not show any sign of distress or failure during testing. The sketch of crack pattern for specimen U-SS6-G-4 at completion of testing is shown in Fig. 4.12. Performance and load history for the test specimen are illustrated in Fig. 4.13.

4.2.5 Column Specimen U-SS6-G-5. Behavior of specimen U-SS6-G-5 was similar to that of the companion specimen, U-SS6-G-4. The test specimen was subjected to seven load cycles with load levels as high as 140 K. No sign indicating imminent failure of splices was observed during the test. The performance and load history of specimen U-SS6-G-5 are shown in Fig. 4.14.

4.3 COLUMN SPECIMENS RETROFITTED USING EXTERNAL REINFORCING BAR TIES

4.3.1 Column Specimen U-ES3-G-1. The specimen continued to deform well past the point at which yielding of column bars was reached. Splitting cracks developed at early load stages followed by yielding of column bars in the splice region. The lap splices failed in tension during the eighth load cycle at a load level of 145 K (Fig. 4.15). The sketch

of crack pattern for specimen U-ES3-G-1 at failure is shown in Fig. 4.16. Performance and load history for the specimen are shown in Fig. 4.17.

4.3.2 Column Specimen U-ES3-UG-2. Specimen U-ES3-UG-2 performed no better than the unstrengthened specimen, U-B-1. Cracks initiated in the splice region at early load stages and the column splices failed in tension during the fourth load cycle at a load level of 90 K (Fig. 4.18). The sketch of crack pattern at failure is shown in Fig. 4.19. Performance and load history for the test specimen are illustrated in Fig. 4.20.

4.3.3 Column Specimen U-ES3-PG-3. Performance of U-ES3-PG-3 was closer to that of specimen U-ES3-G-1 than that of specimen U-ES3-UG-2. Cracks initiated near the ends of the splice region at early load stages followed by yielding of column bars in the splice region. Column splices failed in tension during the sixth load cycle at a load level of 135 K (Fig. 4.21). The sketch of crack pattern for specimen U-ES3-PG-3 at failure is shown in Fig. 4.22. Performance and load history for the specimen are shown in Fig. 4.23.

4.4 COLUMN SPECIMEN RETROFITTED USING ADDITIONAL INTERNAL TIES

4.4.1 Column Specimen U-AT8-1. The behavior of specimen U-AT8-1 was not satisfactory. Cracks developed in regions of newly added ties and at the ends of the splice region at early load stages (Fig. 4.24). Splices in the test specimen failed in tension during the fourth load cycle at a load level of 115 K (Fig. 4.25). Grout placed in the grooves appeared to adhere with the existing concrete cover (Fig. 4.26). Performance and load history for the test specimen are shown in Fig. 4.27.

4.5 COLUMN SPECIMENS RETROFITTED WITH WELDED SPLICES

4.5.1 Column Specimen S-WS-1. Specimen S-WS-1 reached load levels beyond the tensile yield capacity of the column bars. However, cracks developed near the ends of outer spliced bars at early load stages and progressed along the splice region (Fig. 4.28). The concrete cover along the column corners spalled due to the outward thrust produced by the eccentricity between the spliced bars (Fig. 4.29). The existing tie near the end of the outer spliced bars yielded in tension and the 90 degree hook opened at the onset of spalling of concrete (Fig. 4.30). Figure 4.31 shows the prying action of the outer spliced bar produced by the eccentricity between the spliced bars. The specimen was subjected to seven load cycles with load levels as high as 131 K. Behavior of the column specimen during its final stages was characterized by significant loss of member stiffness and energy absorbing capacity (Fig. 4.32). No visible distress could be observed in the welds. Performance and load history for the test specimen are shown in Fig. 4.32.

4.5.2 Column Specimen S-WS-2. The performance of specimen S-WS-2 was satisfactory. Not only did the column sustain yield capacity but it also maintained its stiffness and exhibited relatively stable hysteresis loops (Fig. 4.33). Cracks initiated near the end of the outer spliced bars as soon as the added tie reached yield in tension (Fig. 4.34). Also, the concrete cover over the offsets in spliced bars cracked (Fig. 4.35) and spalled (Fig. 4.36) due to the forces produced by the eccentricity in the bars. The column specimen was subjected to eight load cycles with load levels as high as 145 K. The sketch of crack pattern for specimen S-WS-2 is shown in Fig. 4.37.

A summary of test results for all test specimens is provided in Table 4.1.

Table 4.1 Summary of test results

| Specimen Index | Details of splice strengthening | Maximum load (K) | Fraction of actual tensile capacity ($f_y = 121$ K) | Failure mode |
|----------------|--------------------------------------|------------------|--|--|
| U-B-1 | unstrengthened | 80 | 0.66 | splice failure |
| U-SS6-UG-1 | steel angles & straps (ungROUTED) | 80 | 0.66 | splice failure |
| U-SS6-UG-2 | steel angles & straps (ungROUTED) | 120 | 0.99 | end connection failure |
| U-SS6-UG-3 | steel angles & straps (ungROUTED) | 120 | 0.99 | end connection failure |
| U-SS6-G-4 | steel angles & straps (gROUTED) | 150 | 1.24 | large deformations outside the splice region |
| U-SS6-G-5 | steel angles & straps (gROUTED) | 140 | 1.16 | large deformations outside the splice region |
| U-ES3-G-1 | external ties (gROUTED) | 145 | 1.20 | splice failure |
| U-ES3-UG-2 | external ties (ungROUTED) | 90 | 0.74 | splice failure |
| U-ES3-PG-3 | external ties (partially gROUTED) | 135 | 1.12 | splice failure |
| U-AT8-1 | additional internal ties | 115 | 0.95 | splice failure |
| S-WS-1 | welded splice | 131 | 1.08 | extensively damaged specimen |
| S-WS-2 | welded splice with an additional tie | 145 | 1.20 | yielding of additional tie |



Figure 4.1 Column specimen U-B-1 at failure

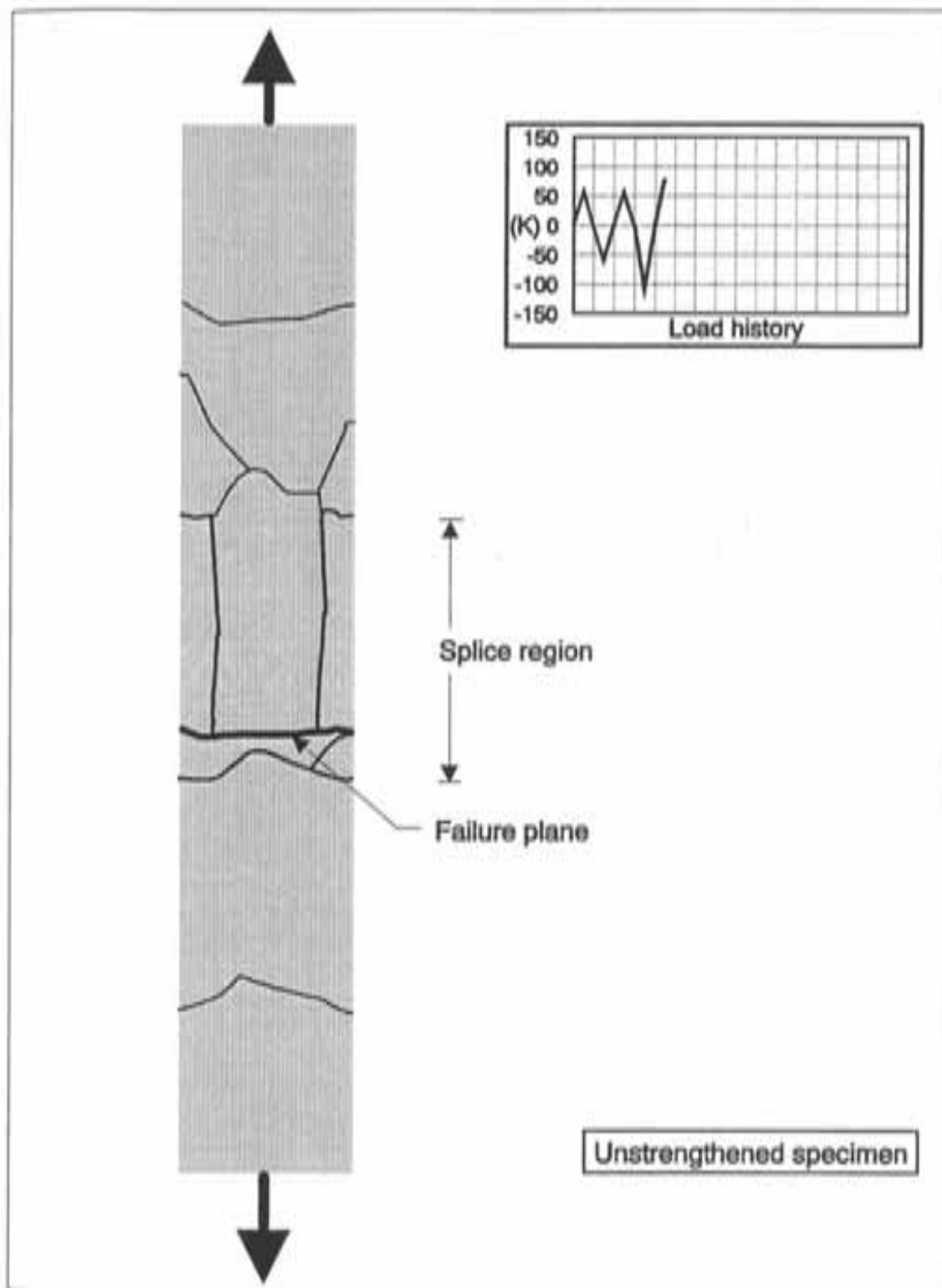


Figure 4.2 Crack pattern in specimen U-B-1 at failure

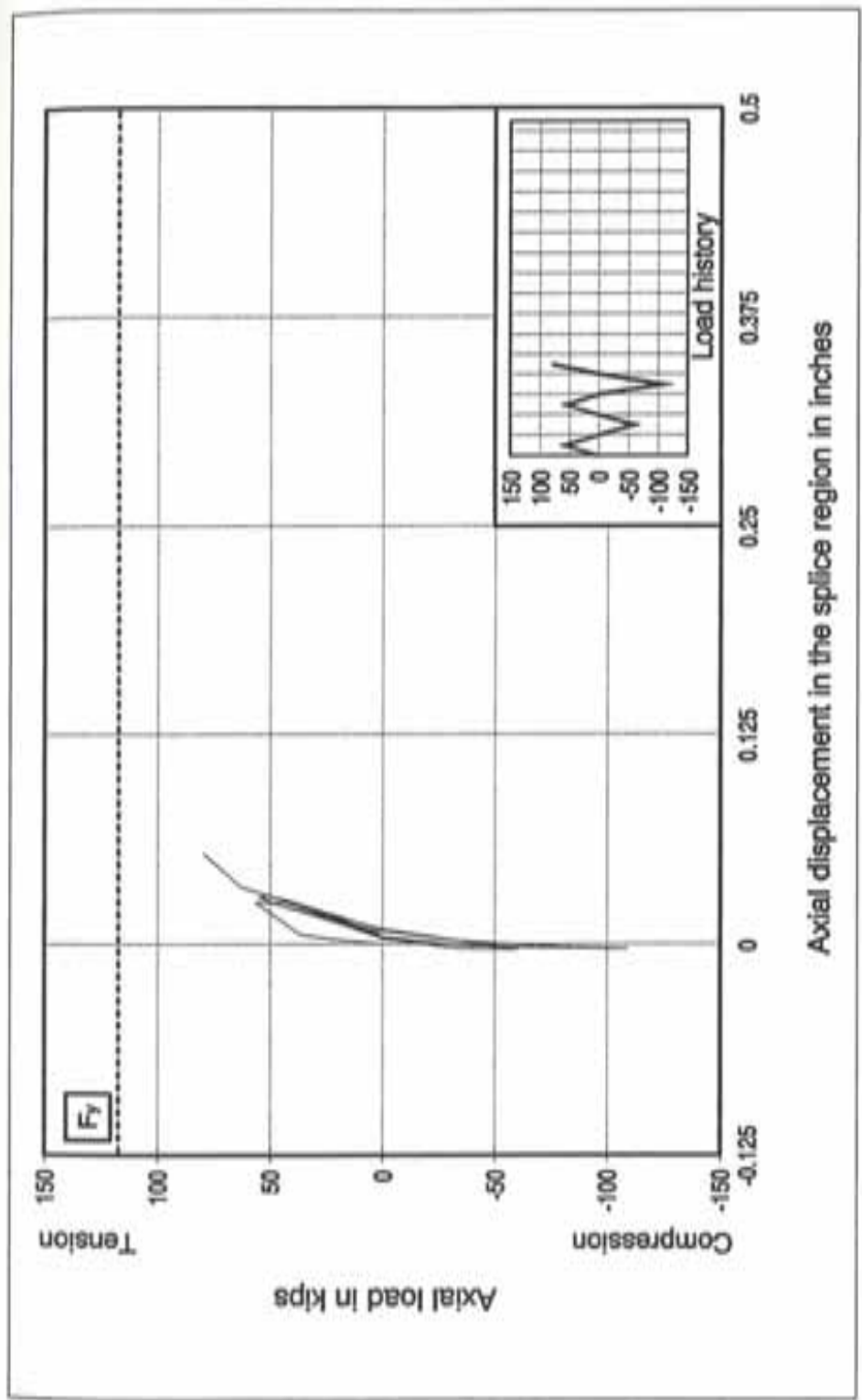


Figure 4.3 Performance of column specimen U-B-1

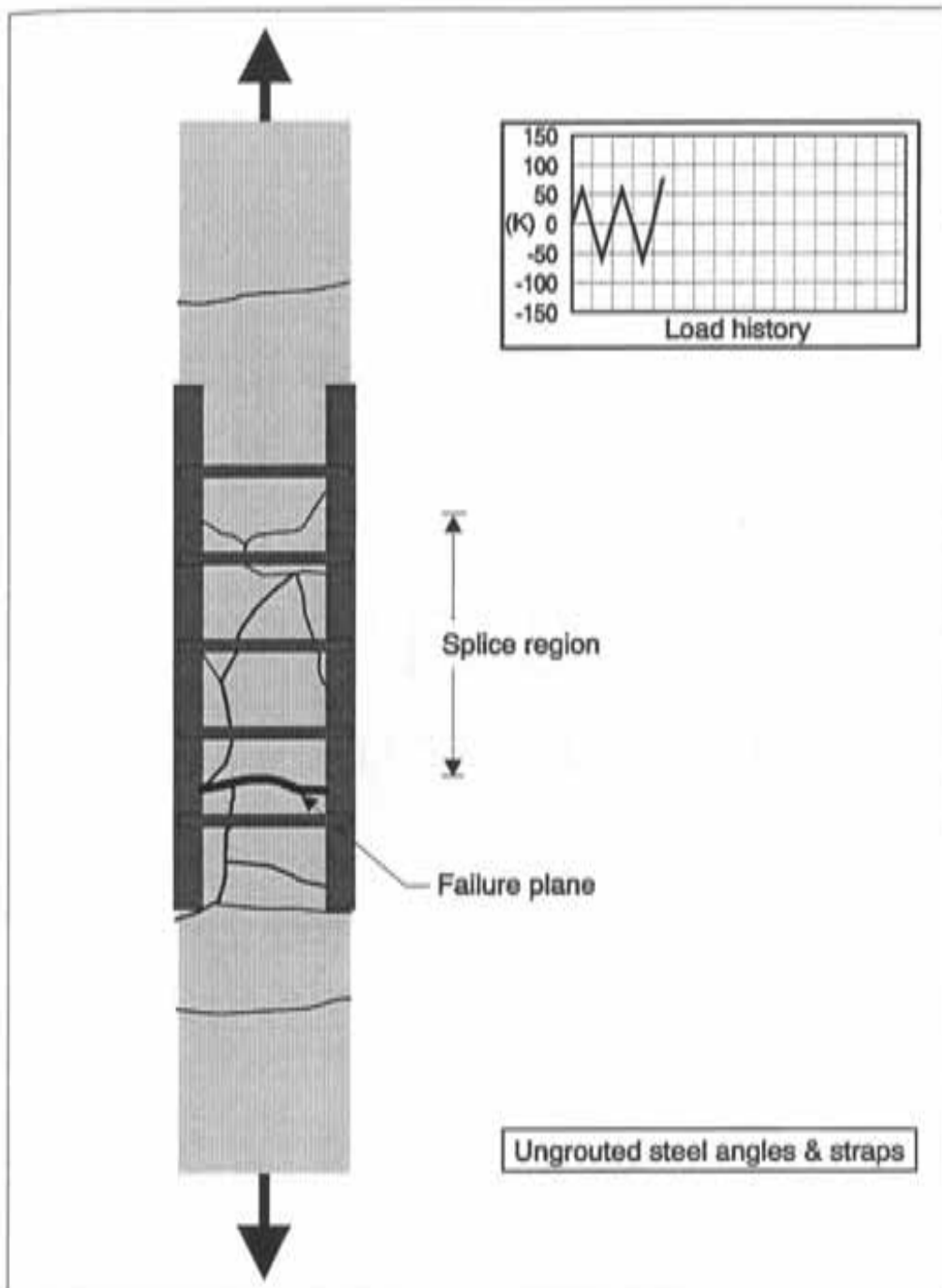


Figure 4.4 Crack pattern in specimen U-SS6-UG-1 at failure

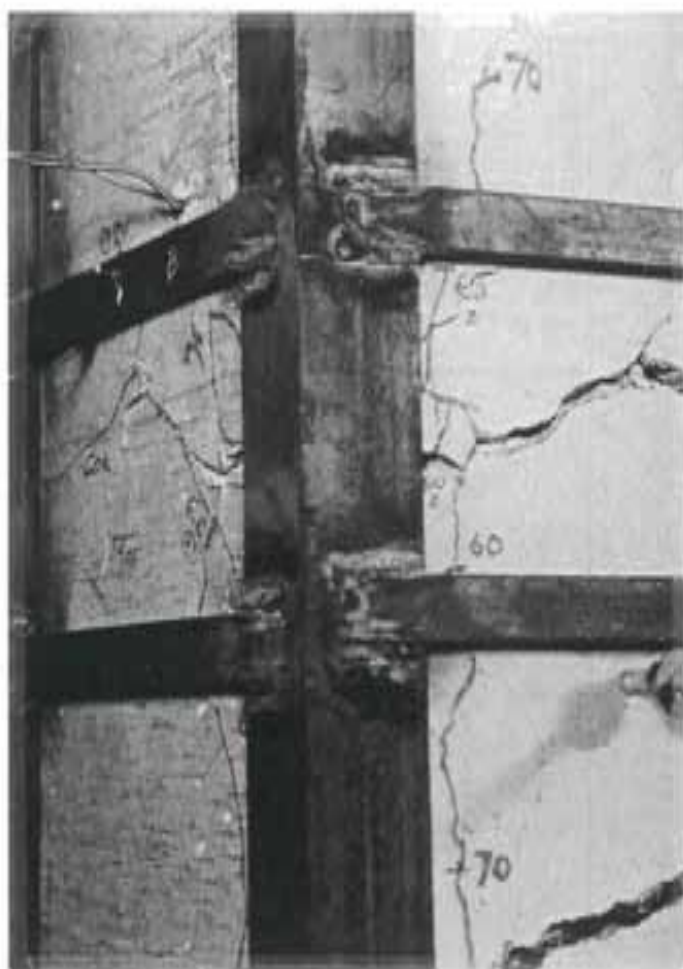


Figure 4.5 Column specimen U-SS6-UG-1 at failure

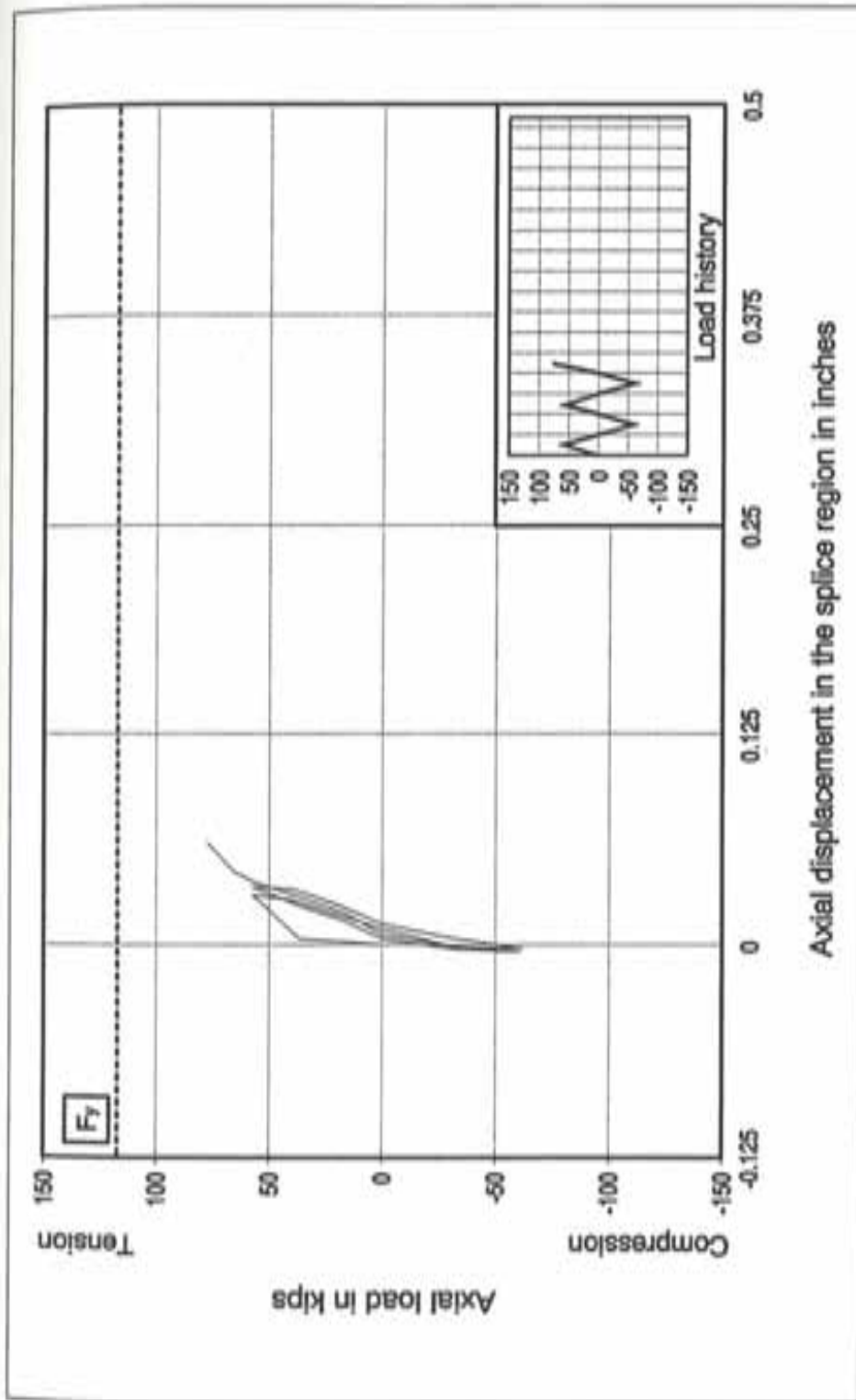


Figure 4.6 Performance of column specimen U-SS6-UG-1

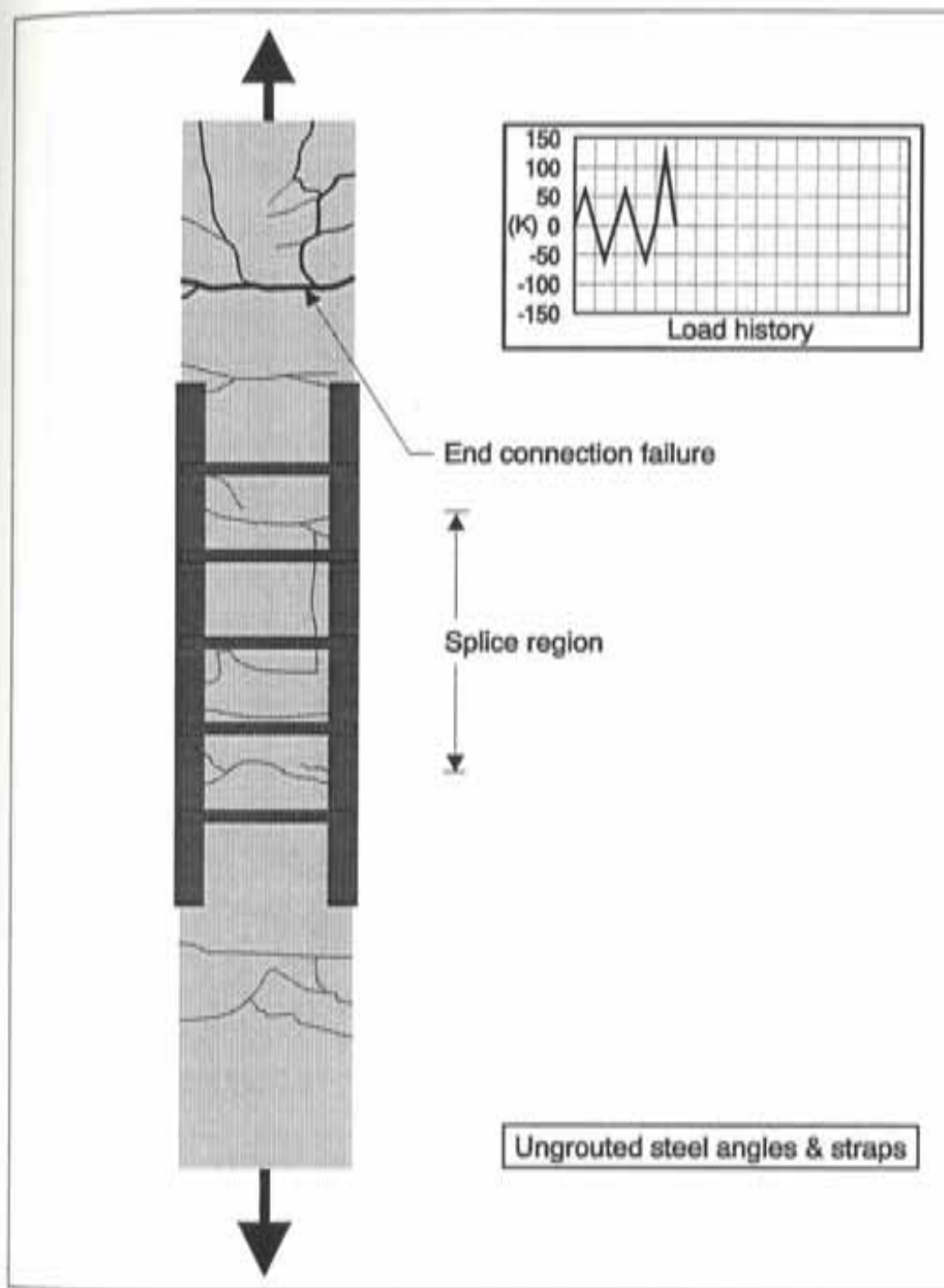


Figure 4.7 Crack pattern in specimen U-SS6-UG-2

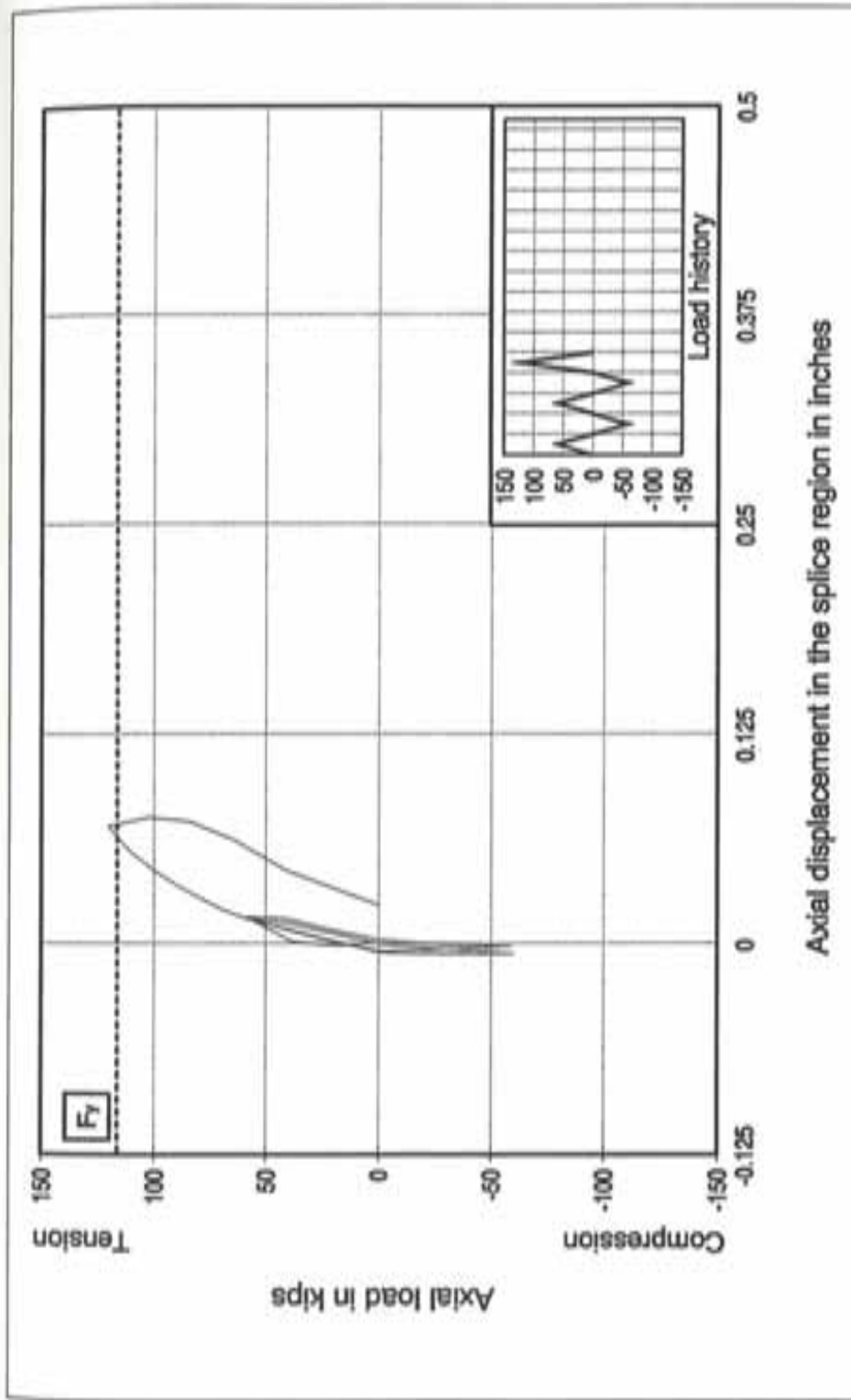


Figure 4.8 Performance of column specimen U-SS6-UG-2

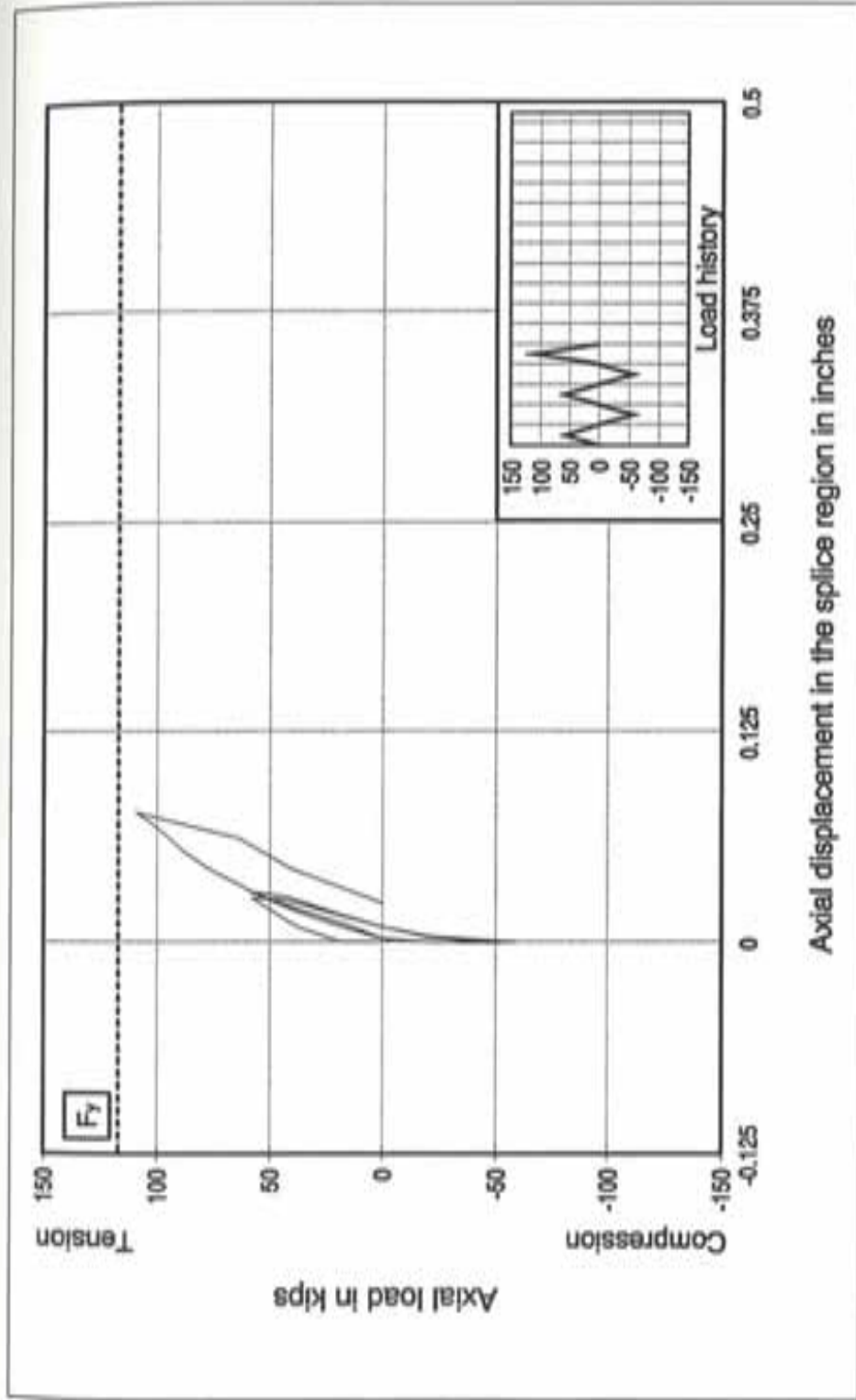


Figure 4.9 Performance of column specimen U-SS6-UG-3

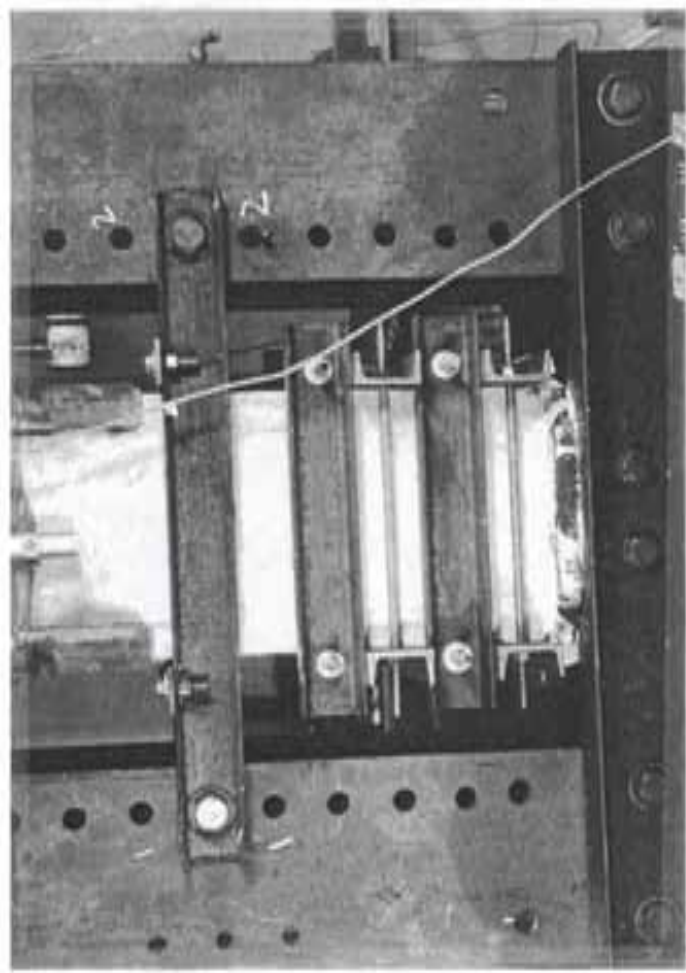


Figure 4.10 Confinement of column ends with steel channels and mild steel rods

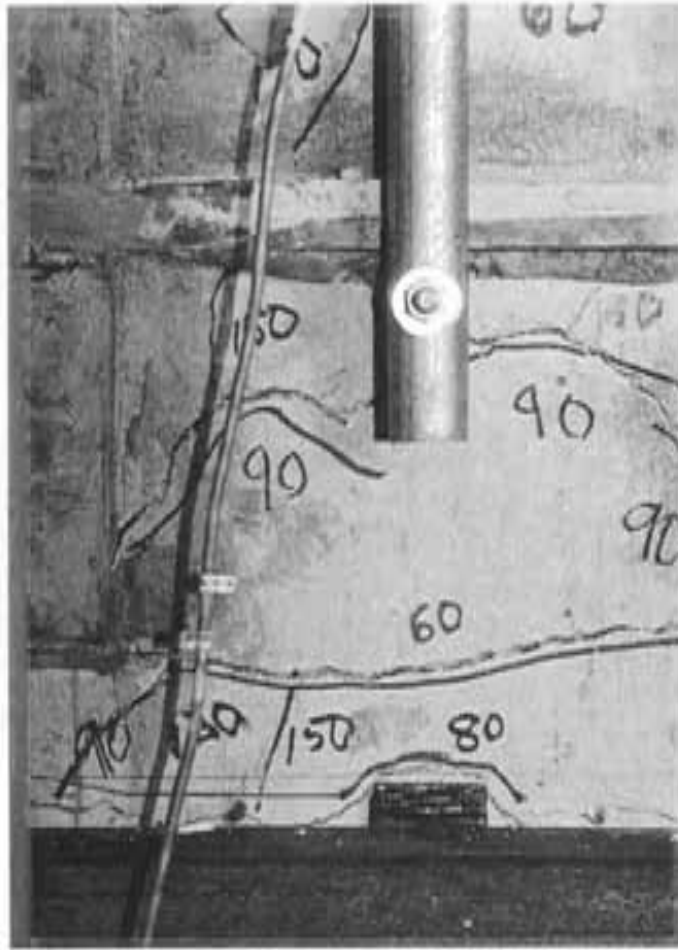


Figure 4.11 Large cracks outside the splice region demonstrating yielding of column reinforcing bars

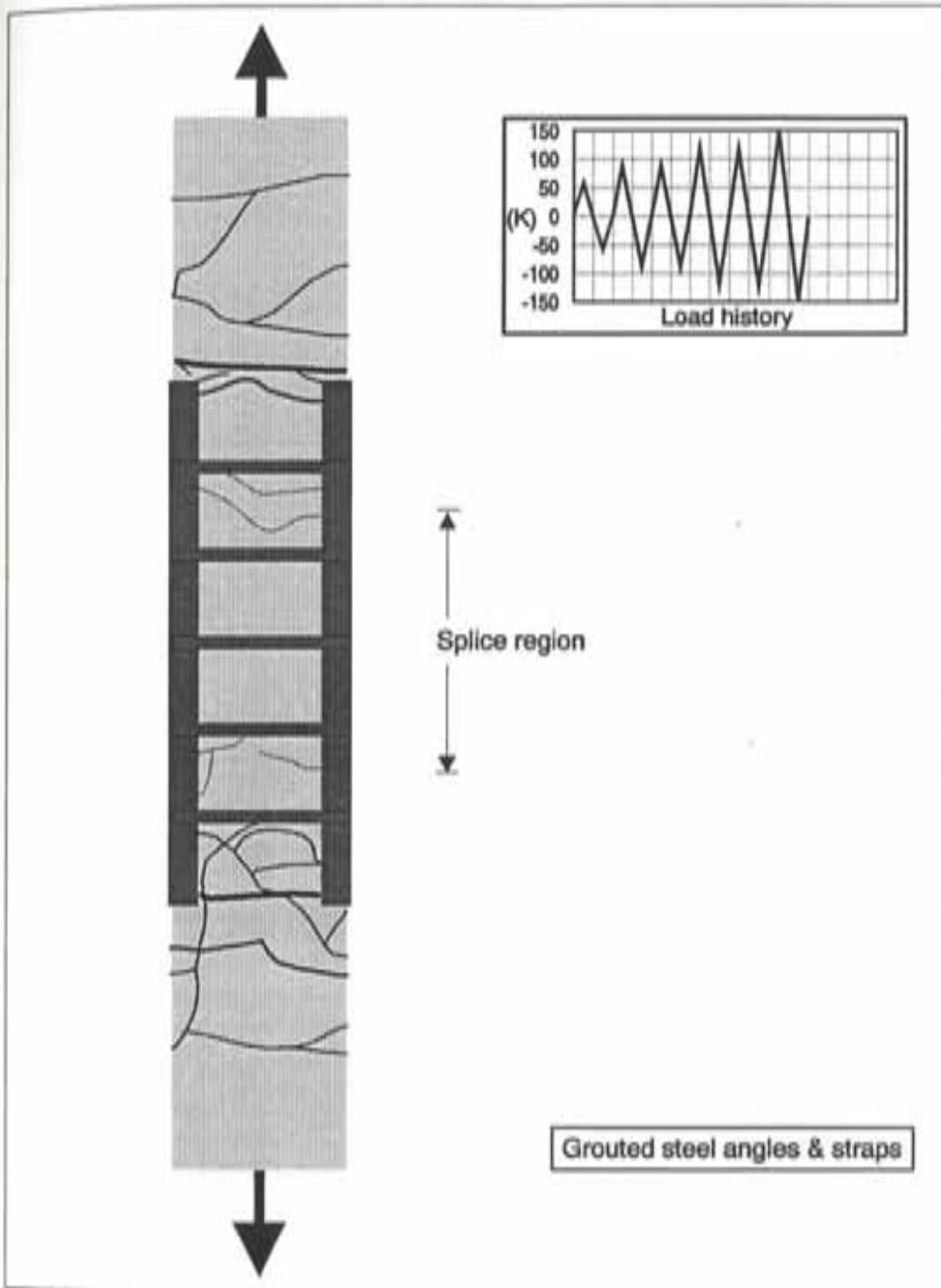


Figure 4.12 Crack pattern in specimen U-SS6-G-4

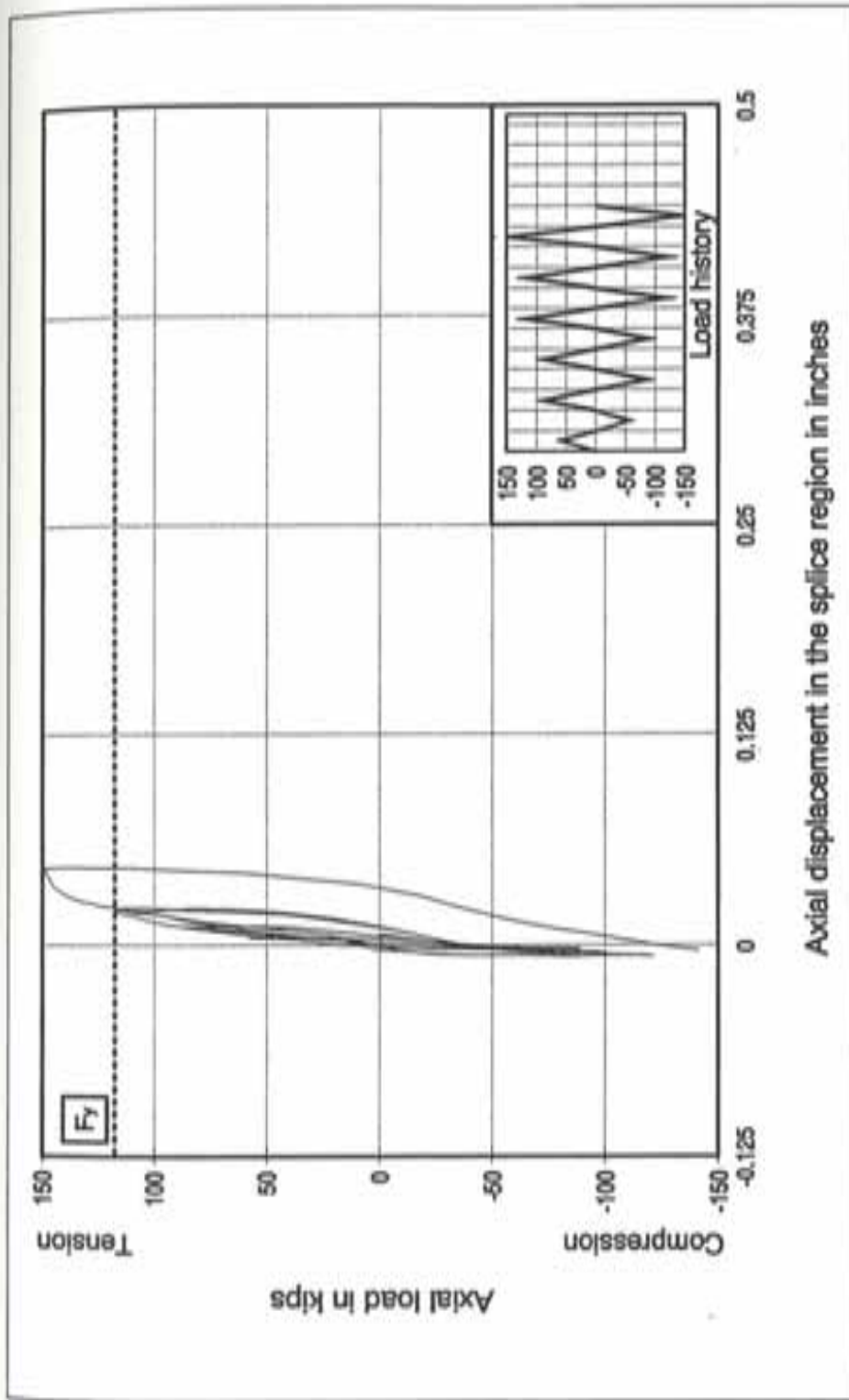


Figure 4.13 Performance of column specimen U-SS6-G-4

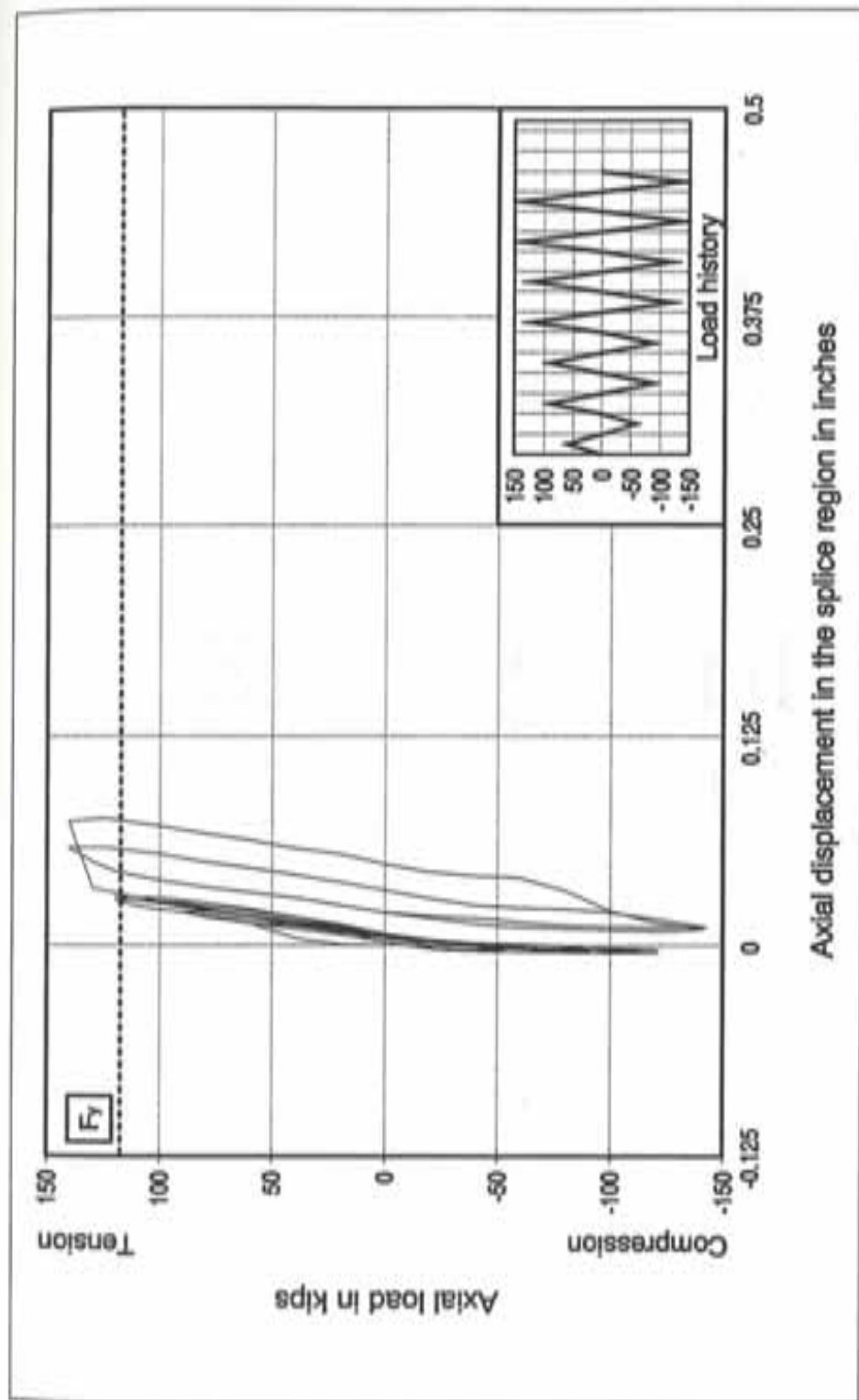


Figure 4.14 Performance of column specimen U-SS6-G-5

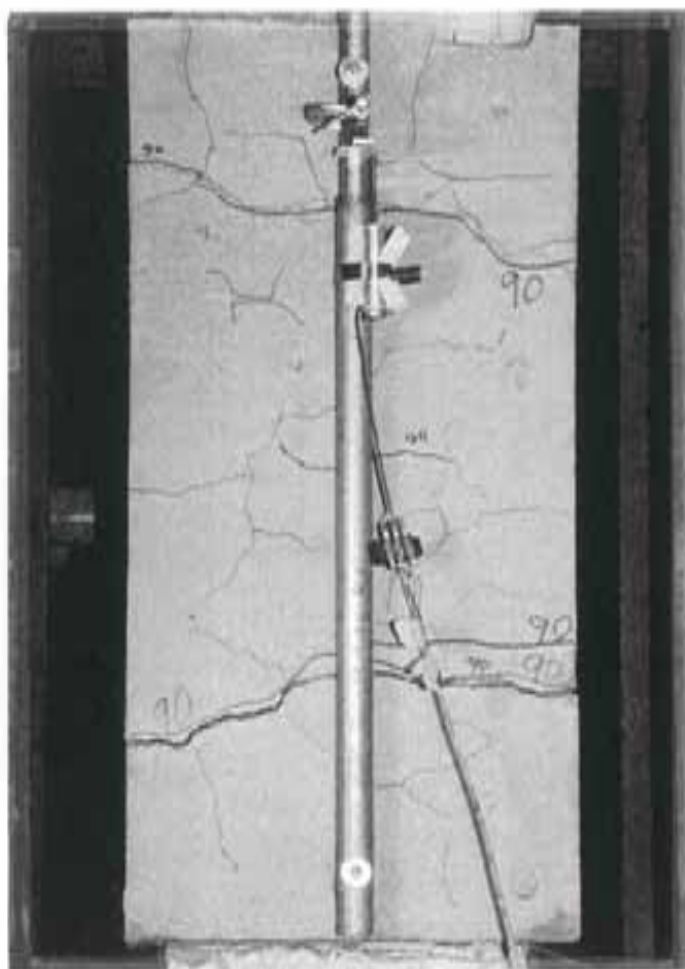


Figure 4.15 Column specimen U-ES3-G-1 at failure

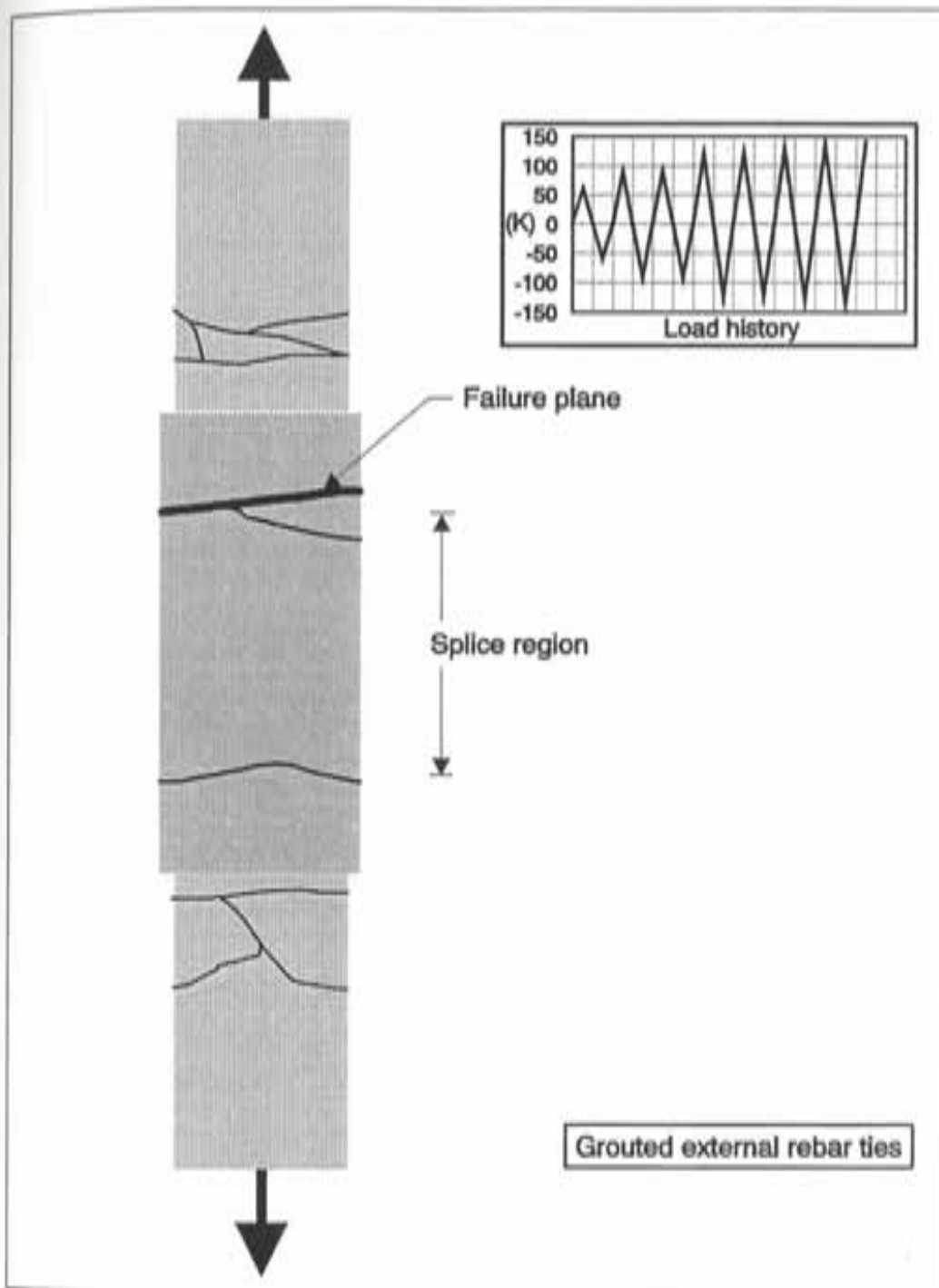


Figure 4.16 Crack pattern in specimen U-ES3-G-1 at failure

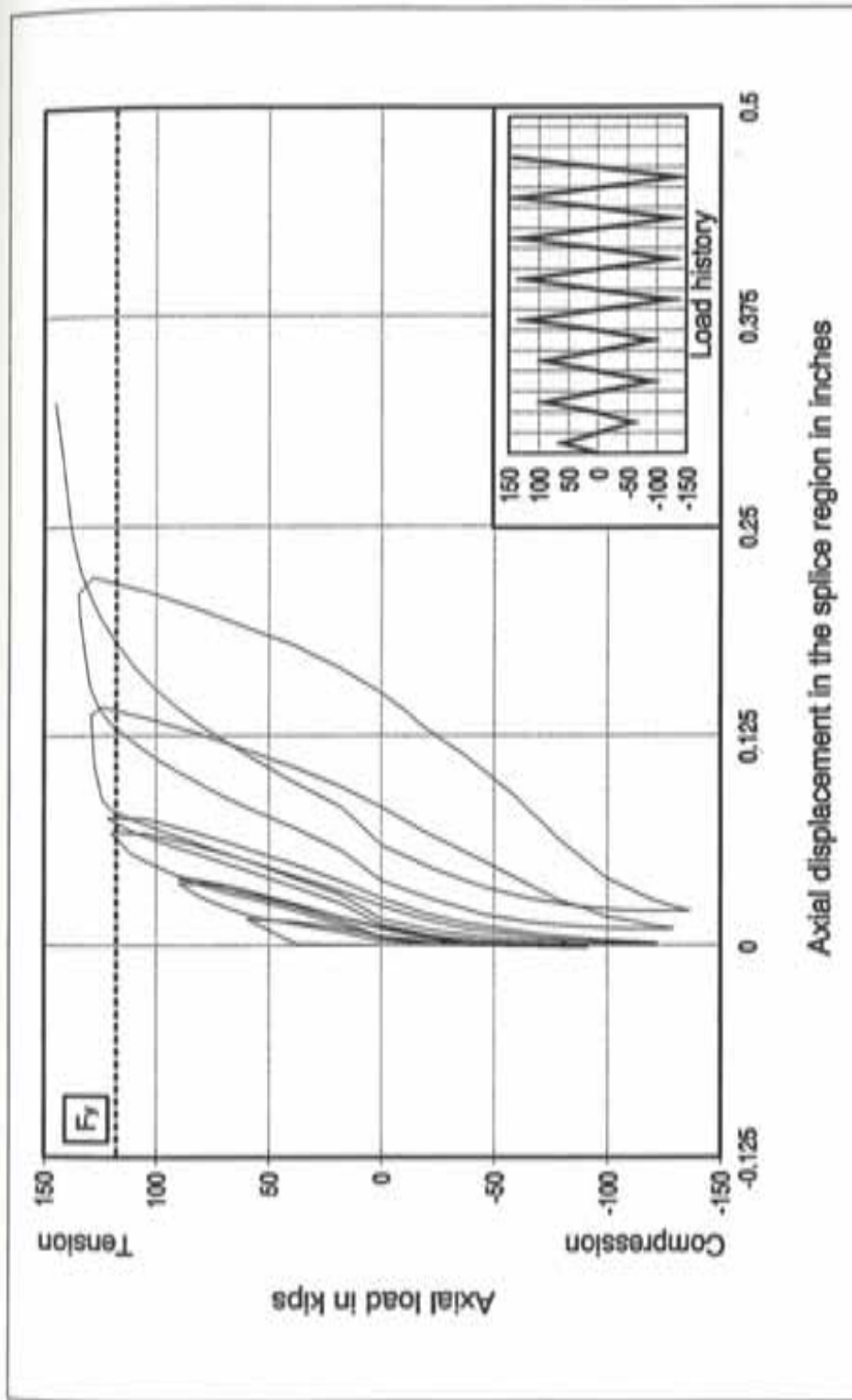


Figure 4.17 Performance of column specimen U-ES3-G-1

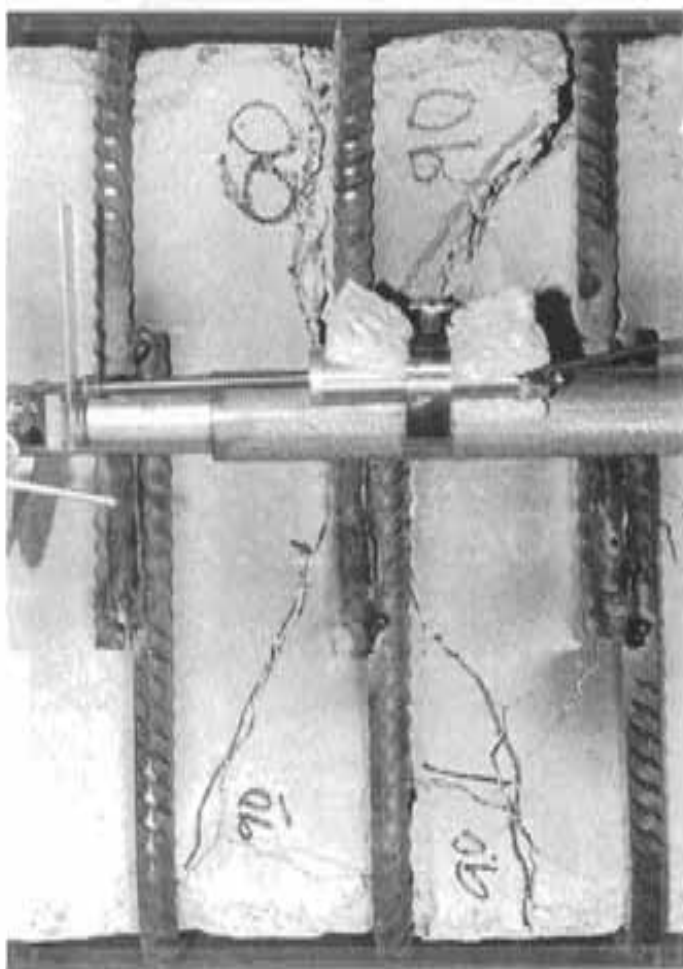


Figure 4.18 Column specimen U-ES3-UG-2 at failure

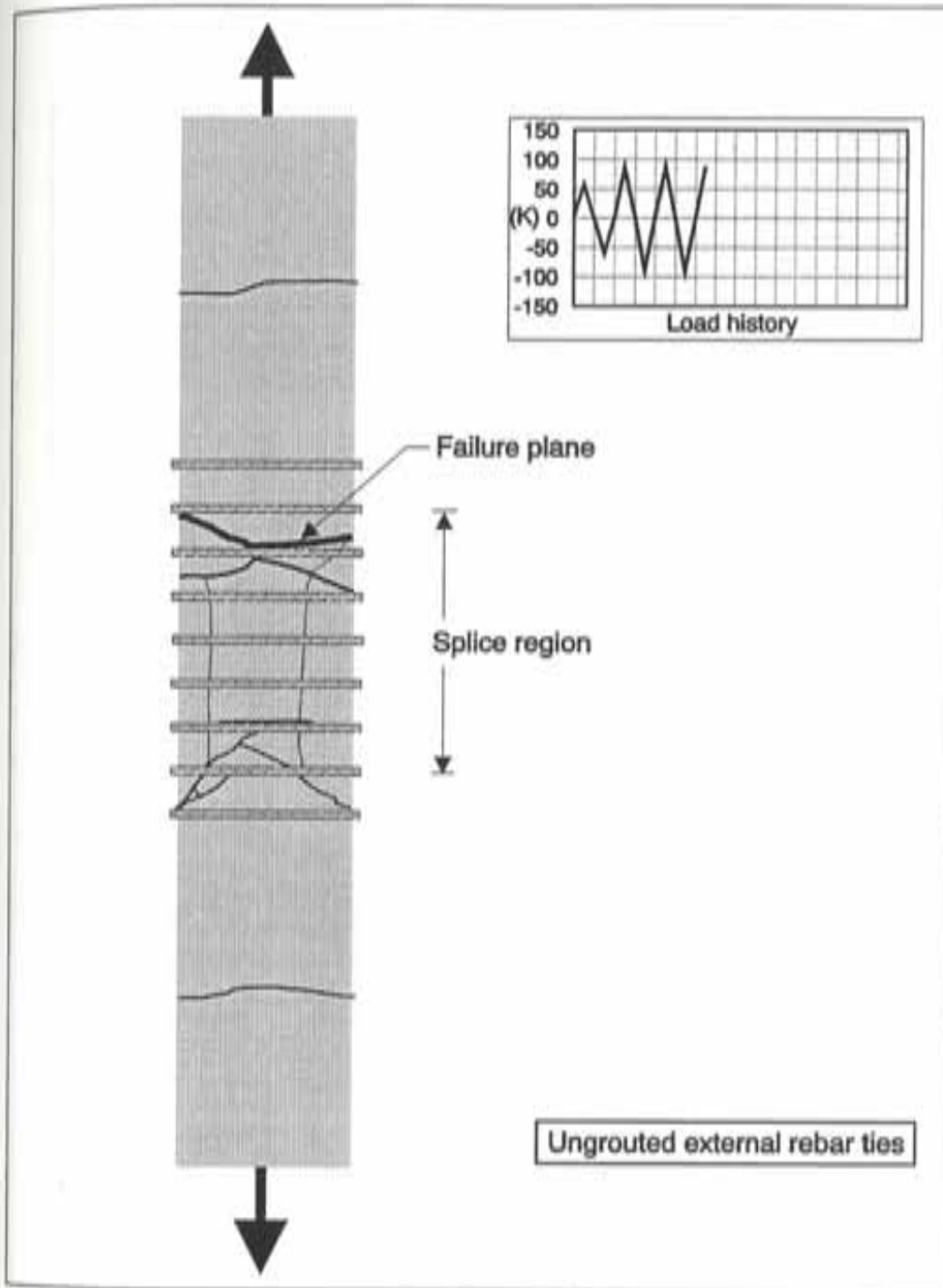


Figure 4.19 Crack pattern in specimen U-ES3-UG-2 at failure

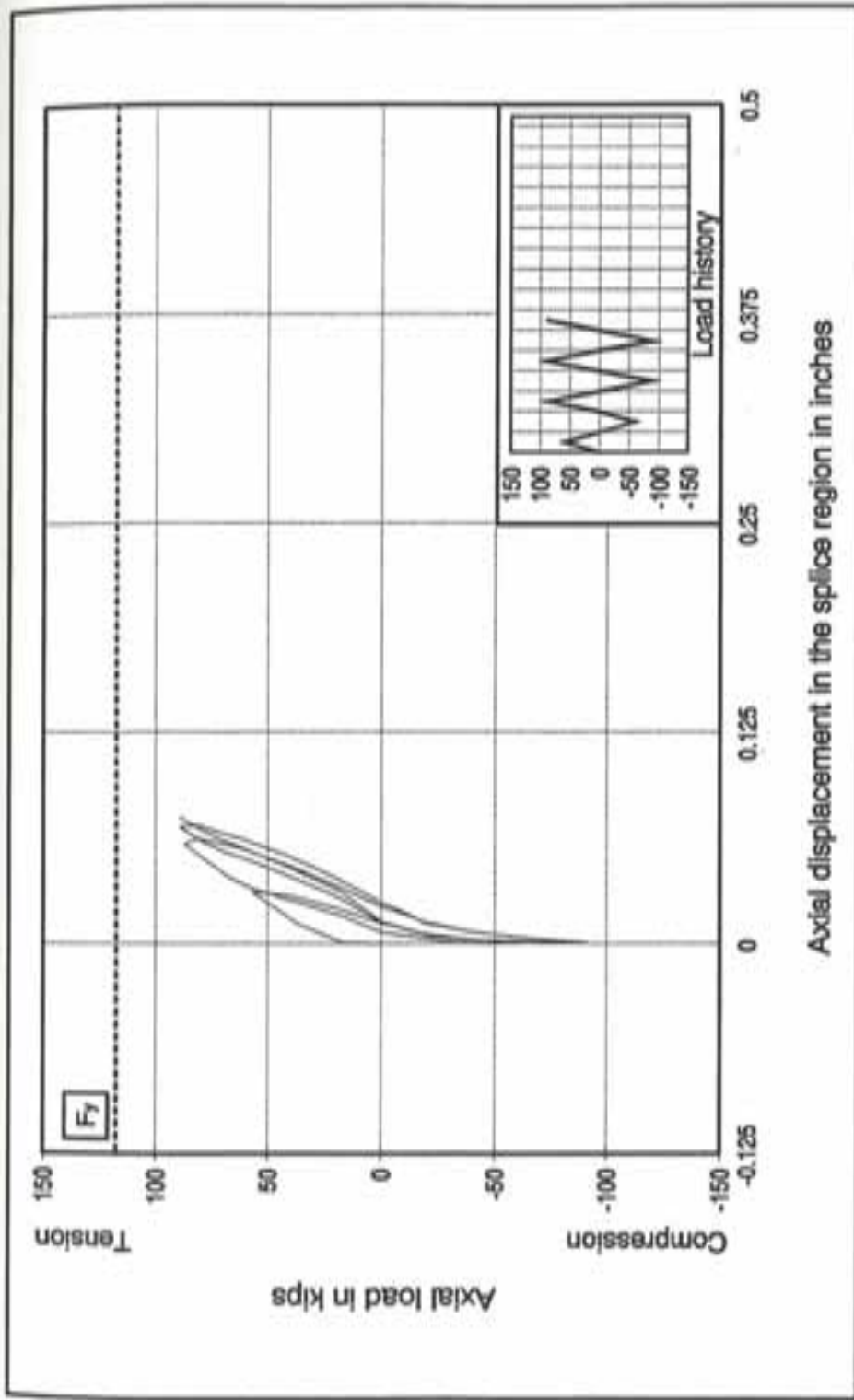


Figure 4.20 Performance of column specimen U-ES3-UG-2

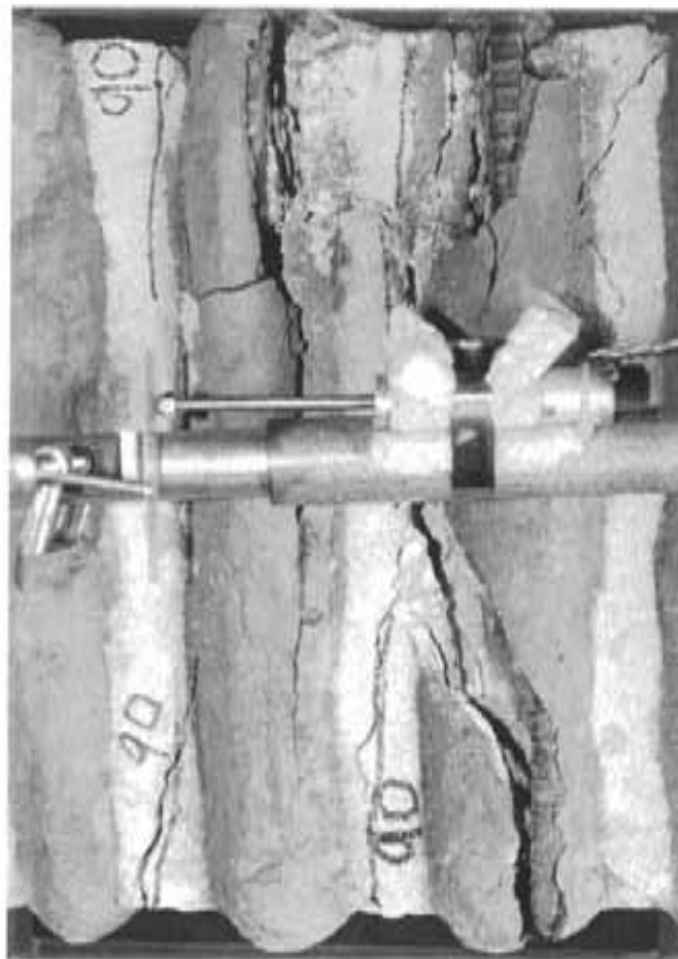


Figure 4.21 Column specimen U-ES3-PG-3 at failure

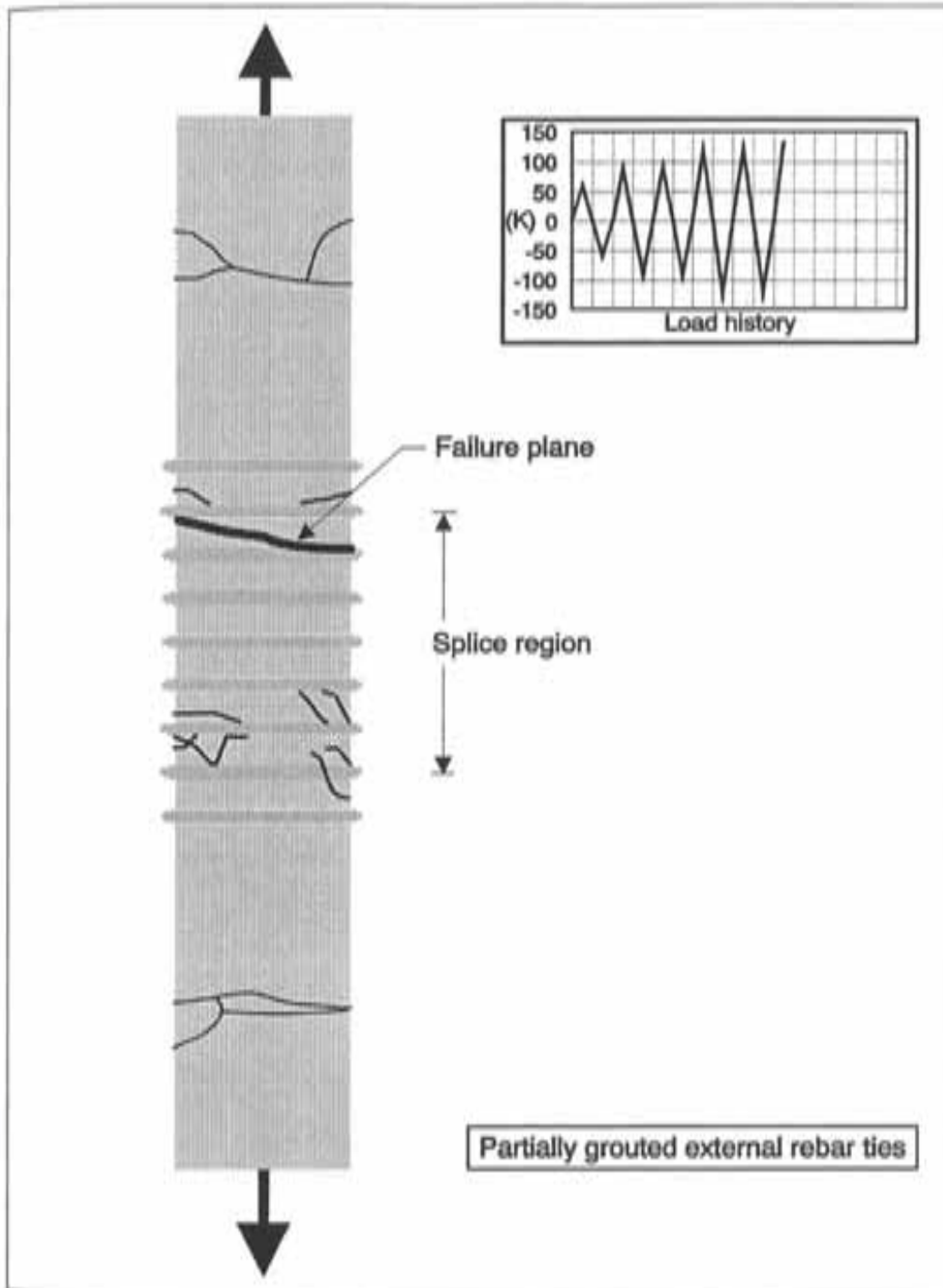


Figure 4.22 Crack pattern in specimen U-ES3-PG-3 at failure

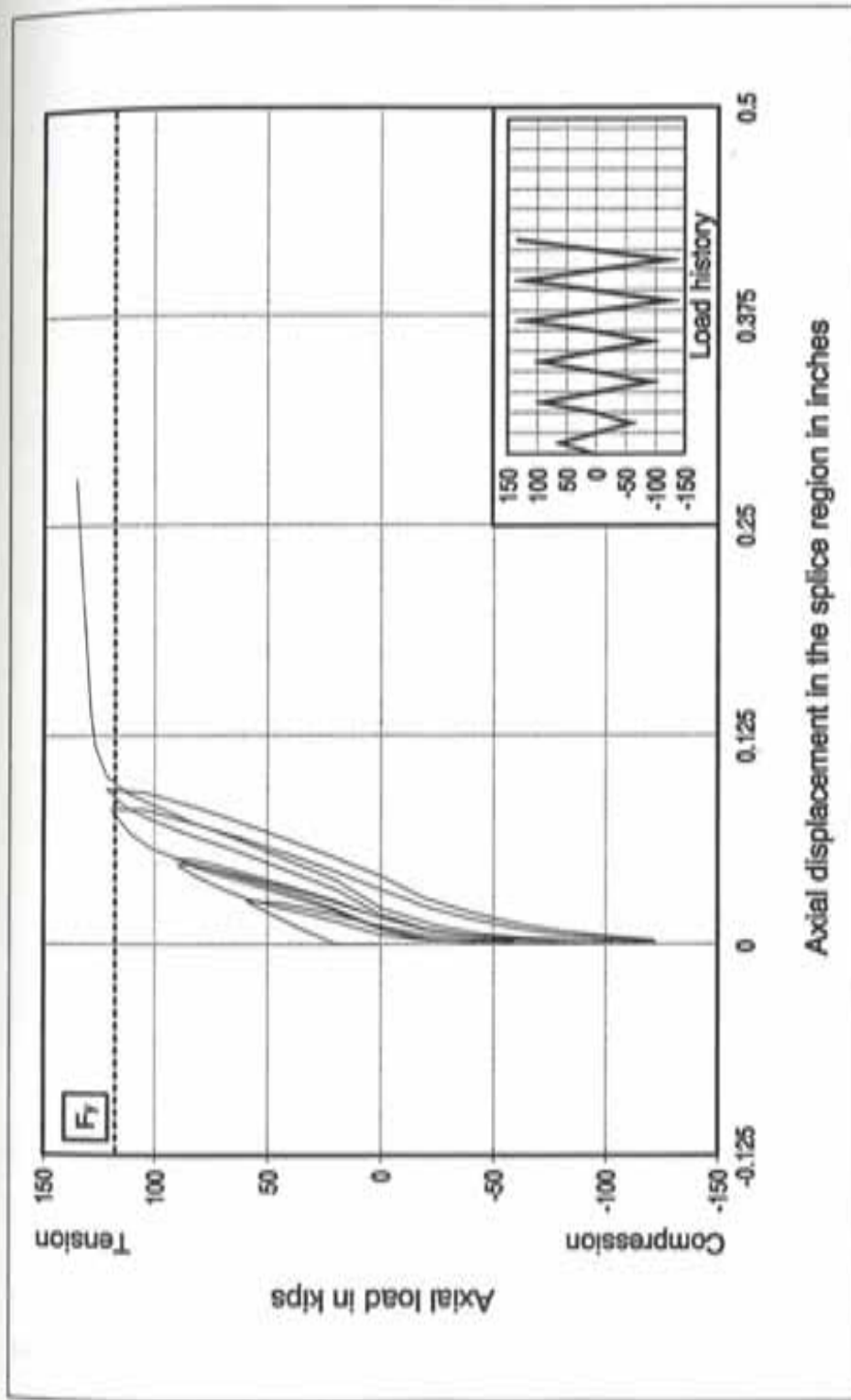


Figure 4.23 Performance of column specimen U-ES3-PG-3

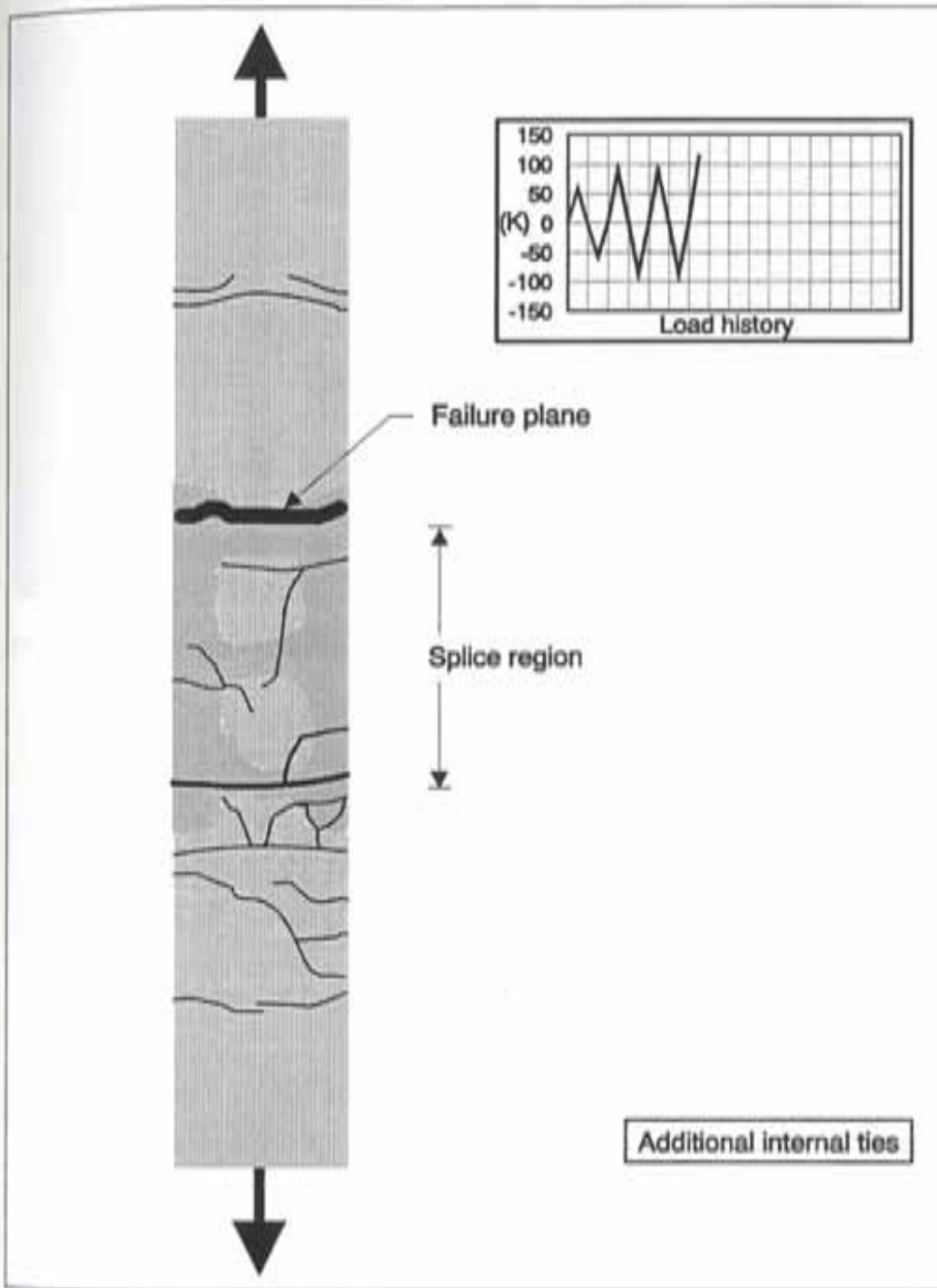


Figure 4.24 Crack pattern in specimen U-AT8-1 at failure

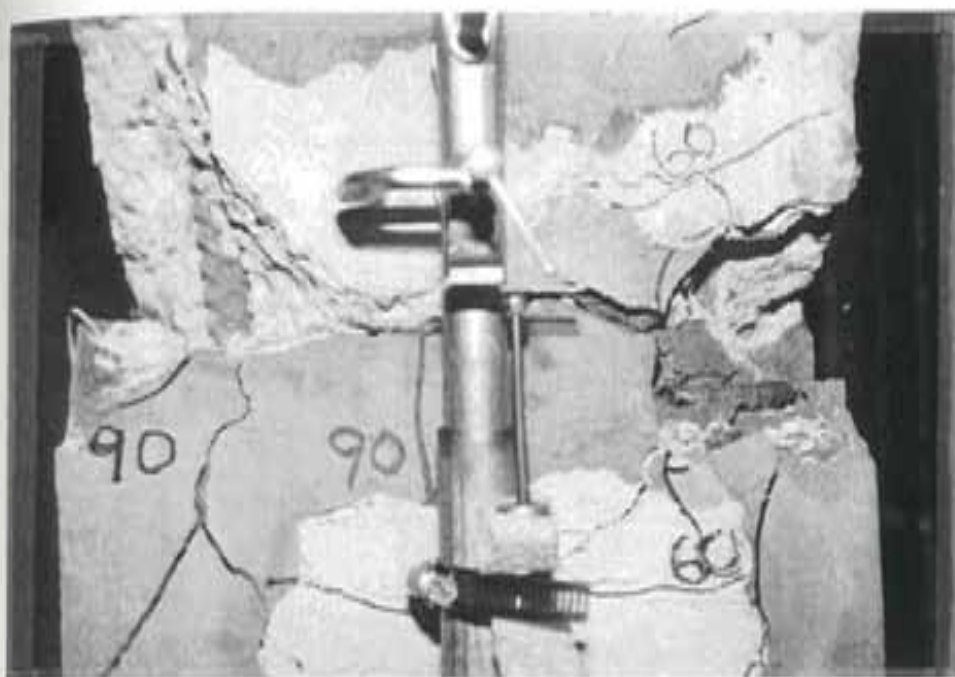


Figure 4.25 Column specimen U-AT8-1 at failure



Figure 4.26 Monolithic behavior between existing concrete and replacing cement grout in specimen U-AT8-1

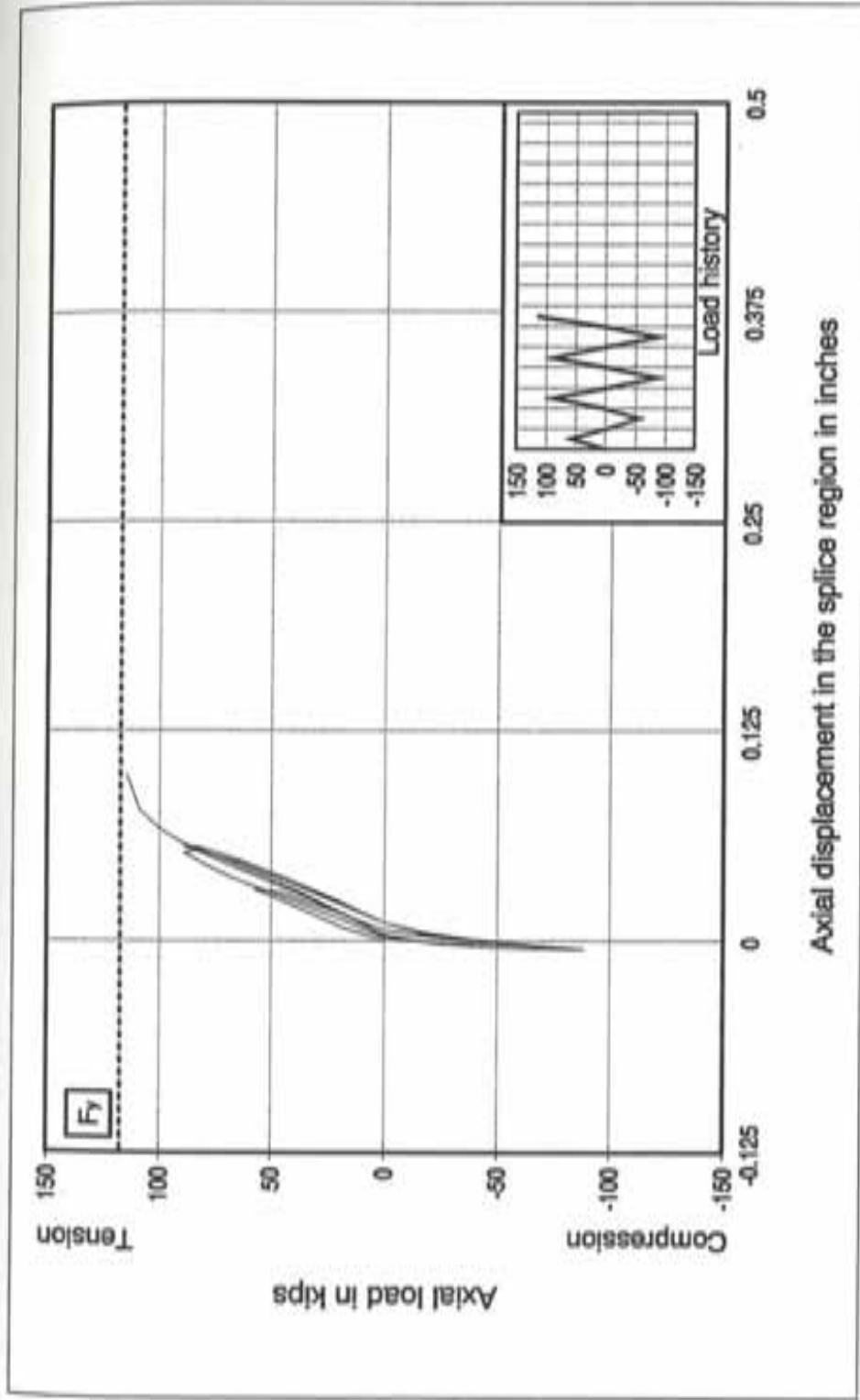


Figure 4.27 Performance of column specimen U-AT8-1

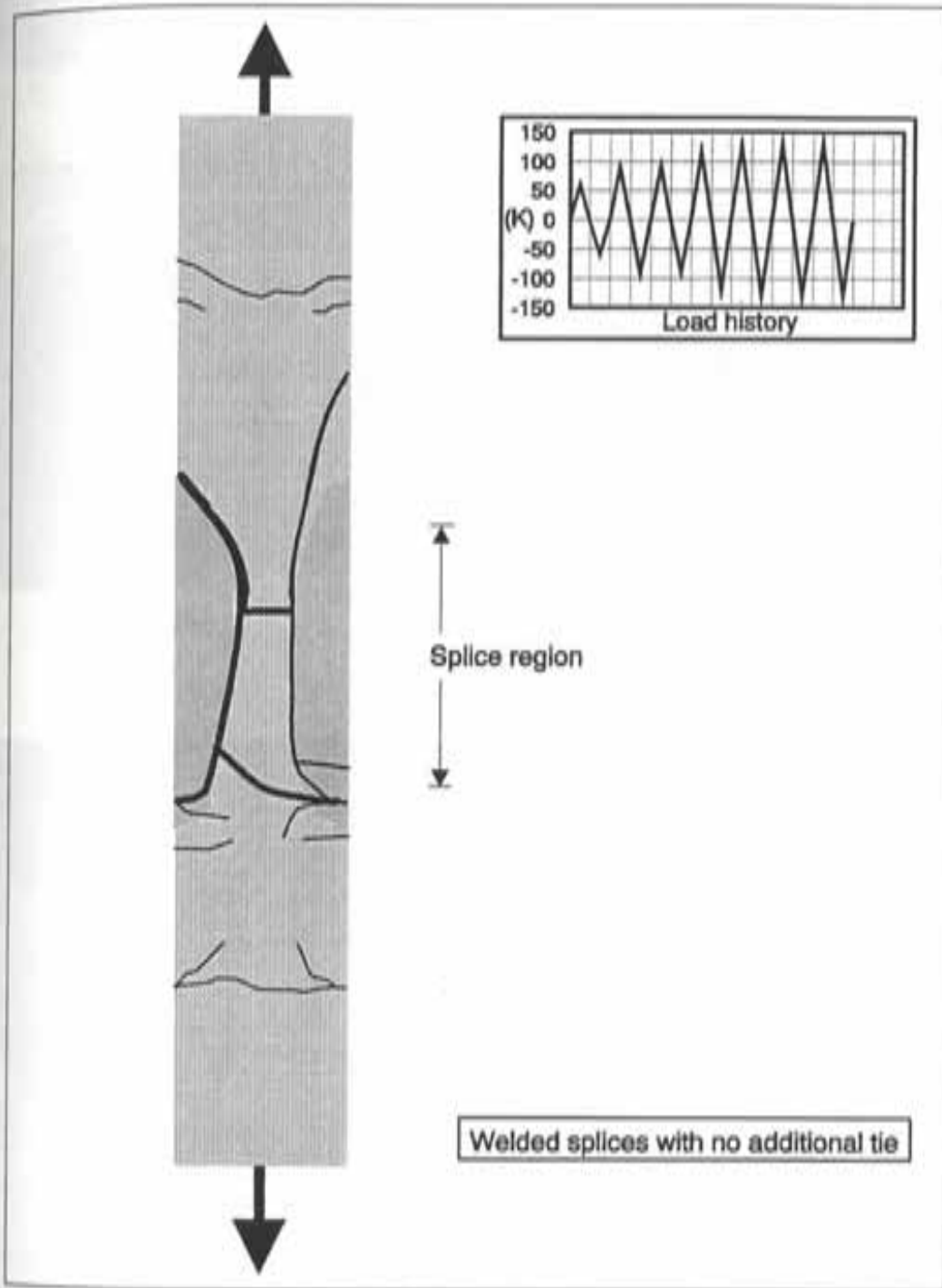


Figure 4.28 Crack pattern in specimen S-WS-1

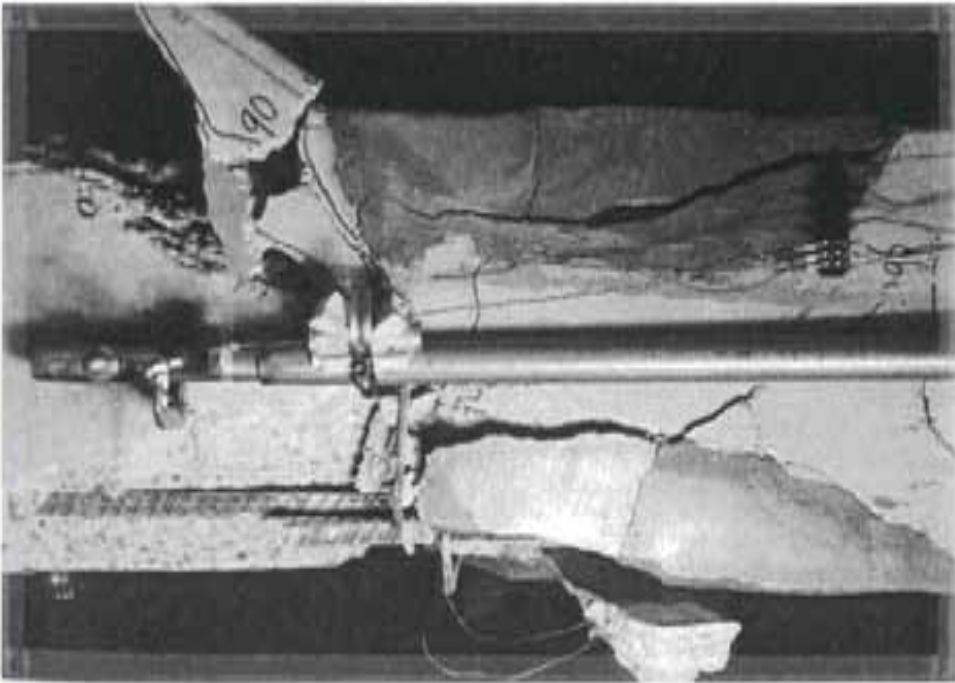


Figure 4.29 Spalling of concrete cover in specimen S-WS-1

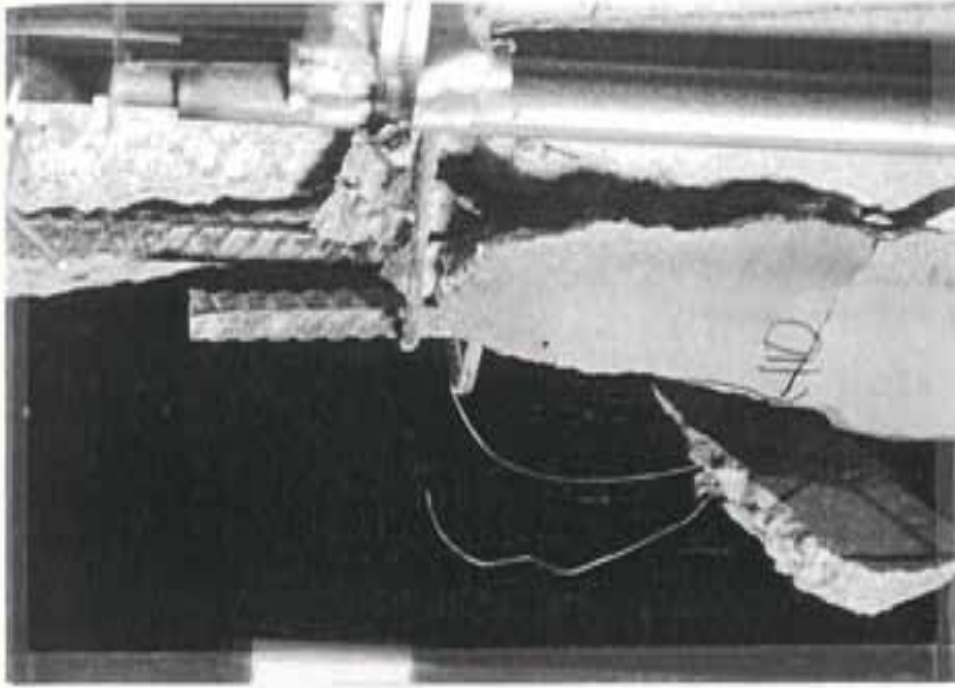


Figure 4.30 Opening of 90 degree hook in specimen S-WS-1

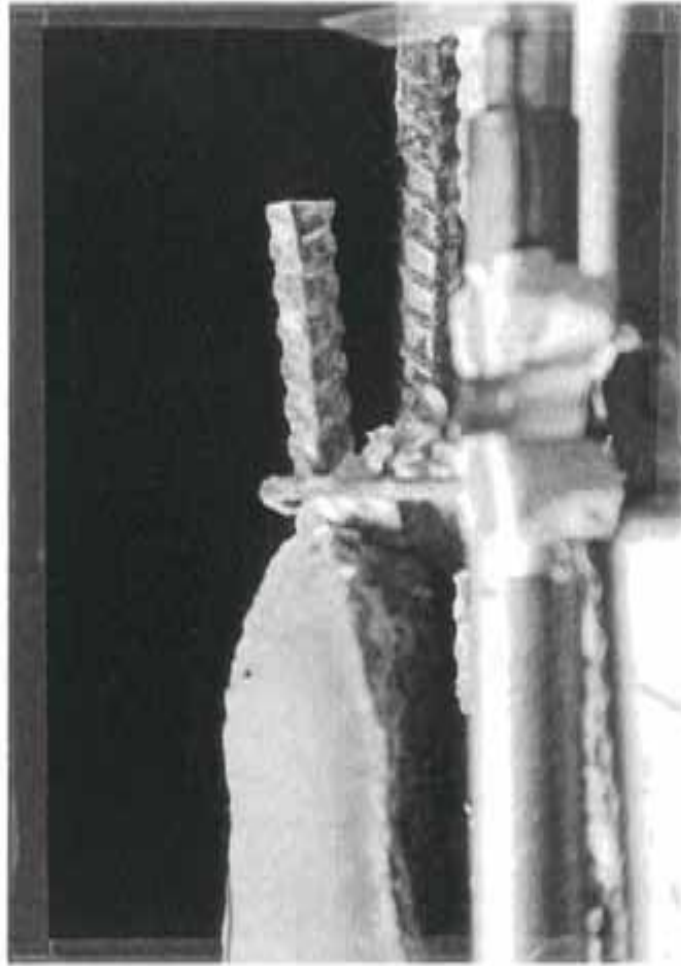


Figure 4.31 Prying action of outer spliced bar in specimen S-WS-1

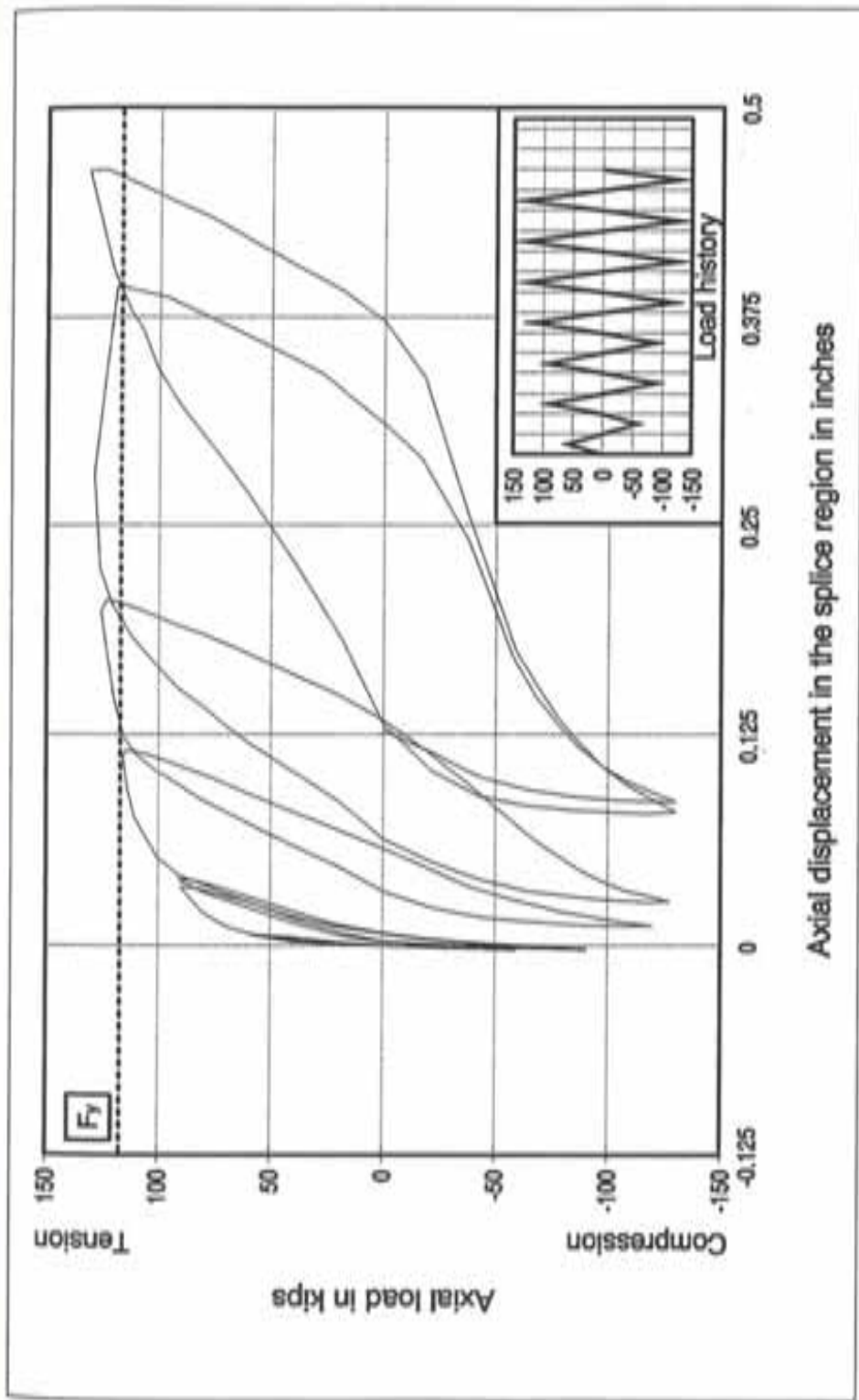


Figure 4.32 Performance of column specimen S-WS-1

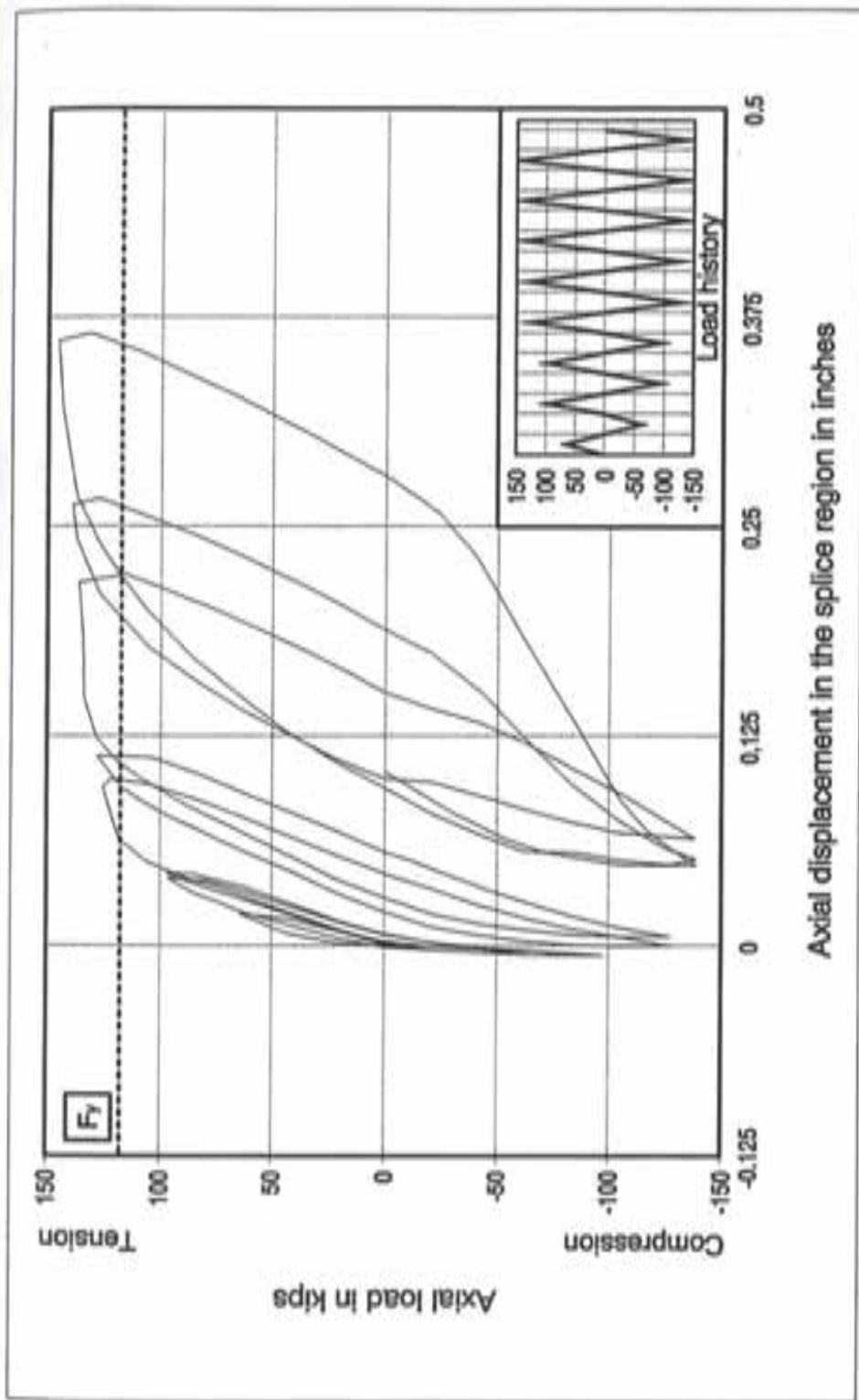


Figure 4.33 Performance of column specimen S-WS-2

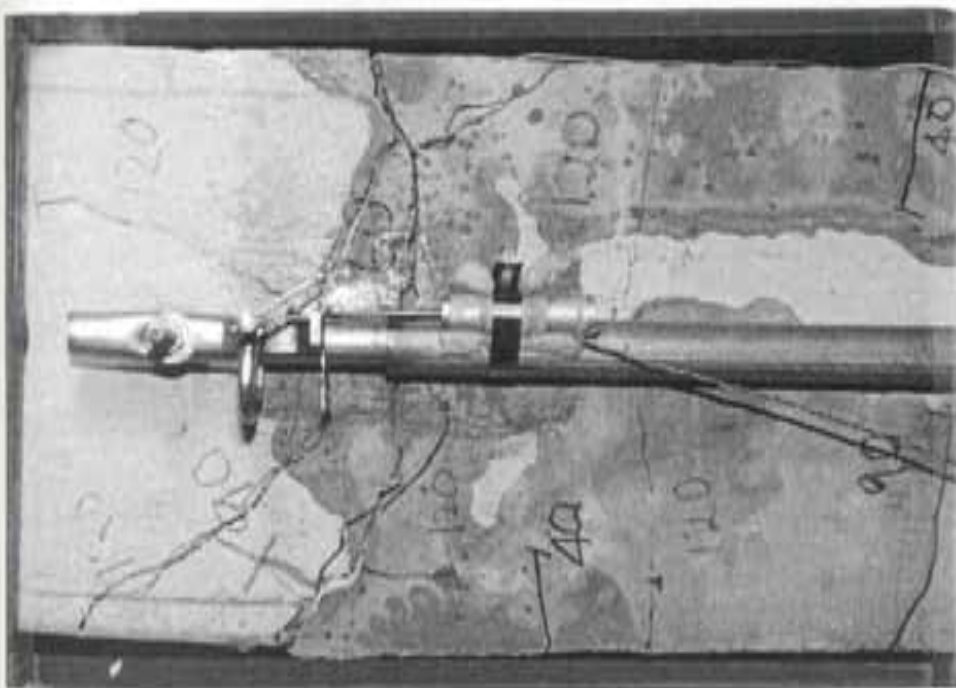


Figure 4.34 Development of cracks in specimen S-WS-2 upon yielding of additional tie

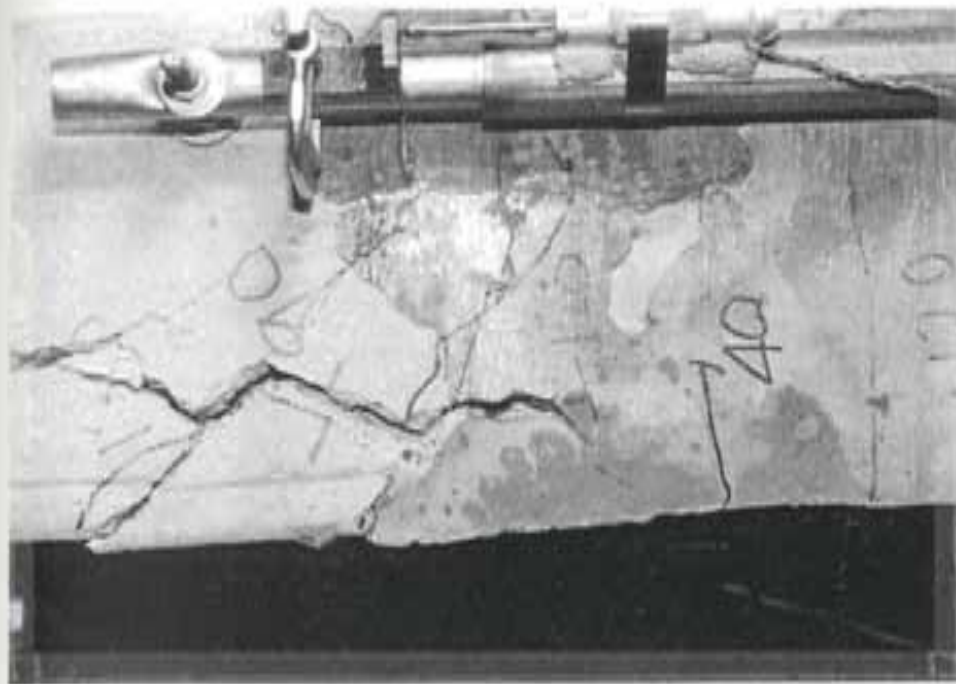


Figure 4.35 Cracks in specimen S-WS-2 developed by offset forces in spliced bars



Figure 4.36 Spalled cover in specimen S-WS-2 produced by offset forces in spliced bars

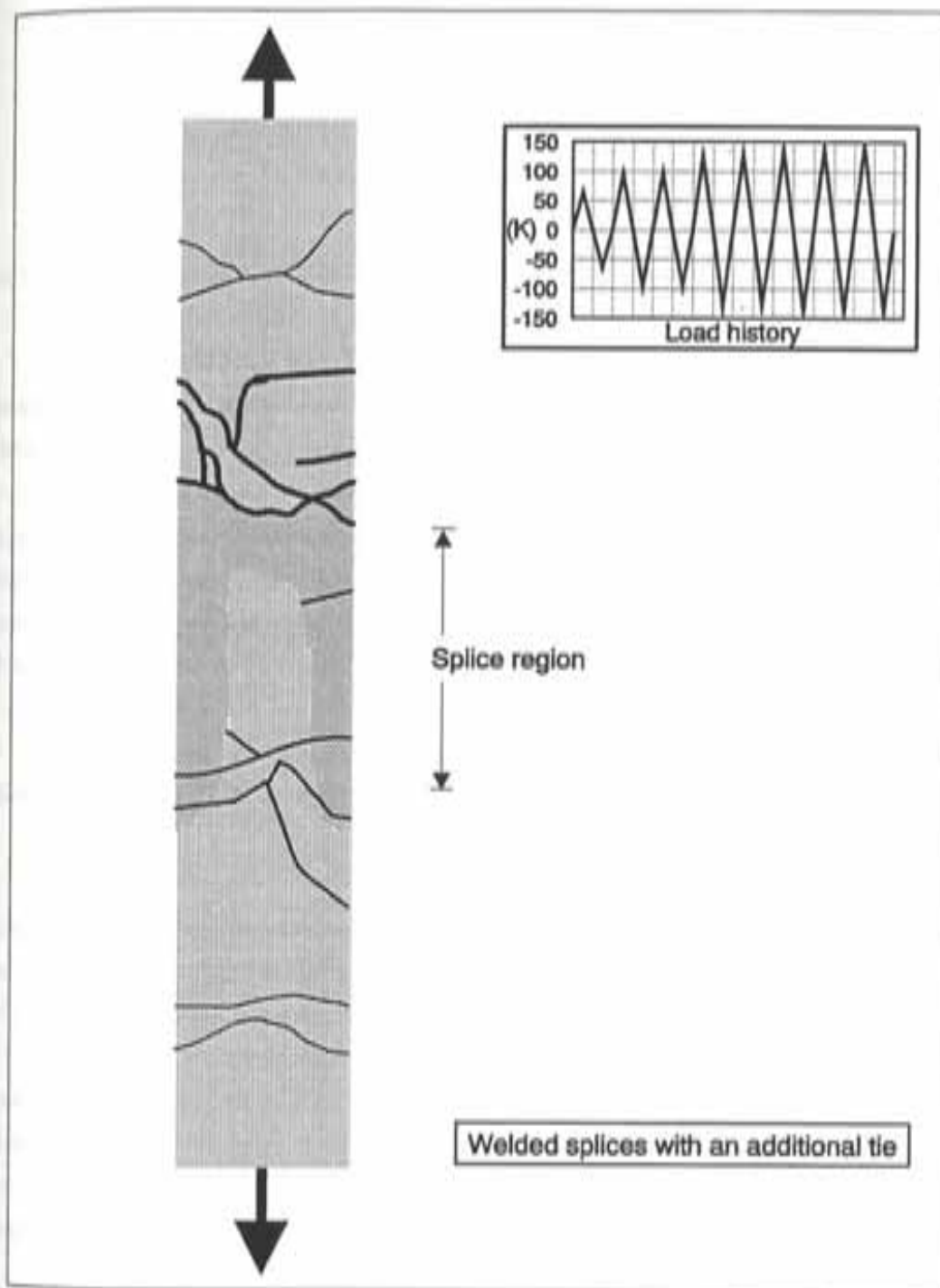


Figure 4.37 Crack pattern in specimen S-WS-2

CHAPTER 5

RETROFITTING OF COLUMN SPLICES

DISCUSSION OF TEST RESULTS AND THEIR IMPLICATIONS

SUMMARY, CONCLUSIONS AND RECOMMENDATIONS

5.1 EXISTING (UNSTRENGTHENED) COLUMN SPECIMEN

Splices in column specimen U-B-1 did not have adequate splitting resistance to enable the column bars to yield in tension. The lack of confinement in the splice region limited the splice strength and was not sufficient to prevent a brittle failure.

The radial outward forces produced by reinforcing bar lugs on the surrounding concrete could not be resisted by concrete cover alone. These forces have to be resisted by tension. For instance, more ties with closer spacing would have helped resist the radially acting splitting forces and delay failure in the splice region. This in turn would have improved the tensile strength and deformation (energy dissipation) capacity of the splices.

5.2 CONFINEMENT WITH STEEL ELEMENTS (ANGLES & STRAPS)

The "angles & straps" scheme improved the splice strength and column deformation capacity significantly. The scheme supplemented significant amount of confinement to the splice region against cover splitting. Most of the inelastic deformations took place outside the strengthened region making the scheme ideal for splice strengthening.

However, the different behavior of column specimens strengthened with ungrouted steel angles and straps indicated the necessity of grouting the steel elements to the existing concrete surface. The inherent difficulty in the use of ungrouted steel angles & straps lies in matching the new steel elements with an existing concrete surface. The steel elements must therefore be grouted in order to effectively confine the splice region.

Figure 5.1 shows the cyclic performance and envelopes of tension cycles for retrofitted column specimens with and without grout. It may be observed from Fig. 5.1b that grouting of externally confining steel elements resulted in significant improvement in splice

tensile strength and column energy dissipation capacity. Although it appears from Fig. 5.1b that the column specimen retrofitted with ungrouted steel angles and straps sustained larger deformations than the specimen strengthened with grouted steel elements, the fact is that the use of grouting forced yielding to take place outside the splice region (axial displacements were measured only over the splice region).

5.3 CONFINEMENT WITH EXTERNAL REINFORCING BAR TIES

External ties improved splice strength and column deformation capacity. Even though this approach supplemented confinement that was available in the existing splice region, the observed uniform distribution of inelastic deformations within and outside the strengthened region signified the absence of continuous resistance over the splice region against transverse splitting that was afforded by the grouted steel angles in the previous scheme.

Cyclic performance and envelopes of tension cycles for retrofitted specimens with different grouting conditions (grouted, ungrouted, and partially grouted) are shown in Fig. 5.2. The influence of grouting on the effectiveness of externally confining steel reinforcing bar ties is clearly shown. Ties must be well-grouted to effectively confine the splice region.

5.4 CONFINEMENT WITH ADDITIONAL INTERNAL TIES

Addition of internal ties alone to the splice region did not result in satisfactory improvement in the splice strength and column deformation capacity. The removal of concrete cover apparently caused microcracking of the concrete core and its replacement with non-shrink grout reduced the effectiveness of concrete cover. Even though the grout placed in grooves appeared to perform monolithically with the existing cover, it was still not effective in confining the splice zone and resisting splitting forces. The loss in splitting resistance was greater than the gain in confinement afforded by the added ties.

5.5 CONTINUITY USING WELDED SPLICES

Welded splices afforded an alternate load path for the transfer of forces between the lap-spliced bars. However, test results and observations indicated that the outward thrust produced by the prying action of the outer spliced bar (resulting from the eccentricity between spliced bars) must be controlled by adding ties internally near the end of the outer spliced bars.

Figure 5.3 shows the cyclic performance and envelopes of tension cycles for retrofitted column specimens with and without an additional tie. It may be observed from Fig. 5.3a that the addition of an internal tie near the outer spliced bar made the column splice zone stiffer and stronger than the specimen without an additional tie. Figure 5.3b indicates that the column specimen without an additional tie experienced large deformations with no increase in axial load during the final stages of loading.

Behavior of specimen S-WS-2 approached that of specimen S-WS-1 once the additional tie yielded. This indicated the need for providing stronger additional ties to resist the outward thrust without yielding.

5.6 SUMMARY AND CONCLUSIONS

The study focussed on (1) developing techniques to improve the tensile strength and the deformation capacity (ductility) of short lap splices present in the columns, and (2) testing the performance of strengthened column specimens to verify the effectiveness of selected retrofit schemes. Retrofit schemes were selected based on ease of construction, minimal construction costs, and minimum changes to column dimensions. The following conclusions are made based on the study:

- (1) Columns constructed with short lap splices designed for little or no flexure in combination with axial compression alone cannot develop large tensile forces or permit inelastic deformations when subjected to reversed cyclic loads resulting from seismic events. As a result, the benefit of strengthening non-ductile RCMRF using infill walls may be limited by the premature failure of splices in the existing columns.

(2) External reinforcement (steel elements or ties) around the splice region significantly improved confinement and splice tensile strength. The external reinforcement must be grouted in order to permit it to effectively confine the splice region.

(3) Addition of internal ties alone to the splice region was not an effective method for strengthening column splices because removal of concrete cover resulted in microcracking of the concrete core and reduction in effectiveness of concrete cover which reduced the splice strength more than the additional ties improved it.

(4) Providing continuity in the splice region by welding the longitudinal bars enabled the columns to yield in tension under reversed cyclic loads. However, it was necessary to add ties internally (by removing the concrete cover) to restrain the outward thrust produced by the eccentricity between spliced bars.

5.7 RECOMMENDATIONS BASED ON TEST RESULTS

5.7.1 Pros and Cons of Schemes Investigated and Final Choice. In Fig. 5.4, the behavior of column splice zones exhibiting the best performance for each of the different strengthening schemes, is compared with that of the splice region in the unstrengthened (existing) specimen. It must be borne in mind that the plots show only the displacements that were sustained within the splice region. They do not, therefore, give an account of the total deformation capacity of the column specimens. For example, the specimen with grouted angles and straps yielded outside of the splice region and the instrumentation was used to measure deformations in the splice region only.

Grouted "angles and straps" scheme offers an ideal retrofit for column splices based on performance. The scheme provides continuous resistance over the splice region against cover splitting. As a result, the deformations are concentrated outside the splice region. The scheme therefore keeps the splice zone intact even though significant energy is dissipated by the column. However, external confining steel elements must be grouted in order to ensure the effectiveness of the scheme. Grouting of angles and straps may be labor intensive. Difficulty of construction may therefore make the scheme less attractive. Also,

aesthetics of columns retrofitted using angles and straps and limitations on changes to column dimensions must be taken into consideration.

"External ties" scheme significantly improves confinement in the splice region provided that the ties are grouted adequately to the existing concrete surface. This approach offers resistance against cover splitting thereby improving the splice tensile behavior in terms of its strength and ductility. However, the scheme fails to offer continuous resistance against transverse splitting that was provided by steel angles in the previous scheme. The scheme is easier to construct and is cost-effective so long as there are no limitations on changes to column dimensions. Aesthetics of the scheme must again be considered in the choice of a final scheme.

Addition of internal ties to the splice region is not a reliable retrofit scheme. While improving confinement in the splice region, the scheme aggravates transverse splitting through microcracking of the concrete core and reduces the effectiveness of concrete cover. Any scheme that would damage the concrete core and reduce the effectiveness of concrete cover must be eliminated from consideration as an alternate, unless the existing load path (bond strength between spliced bars and surrounding concrete) is changed by the selected scheme.

"Welded splices" may be considered a suitable scheme in situations where any changes to column dimensions must be avoided. Quality control of the welding must be maintained in order to allow this approach to perform properly. Also, additional ties must be provided internally over the splice region to control the outward thrust produced by eccentricity between spliced bars.

The final choice of a retrofit scheme for column lap splices should be based on desired performance level, ease and feasibility of construction, limitations on changes to column dimensions, construction costs, and aesthetics.

5.7.2 Recommended Features for Additional Confinement Schemes. Figure 5.5 shows the force transfer mechanism in lap-spliced bars and the forces initiating transverse splitting of concrete cover. While Fig. 5.5a depicts the forces on reinforcing bars at a splice, Fig. 5.5b illustrates forces induced by the reinforcing bar lugs on the surrounding concrete at a splice.

Forces induced by reinforcing bar lugs normal to the reinforcing bar axis will initiate cover splitting along the splice region unless there is adequate transverse reinforcement to resist these tensile forces (Fig. 5.5c). The transverse reinforcement so provided to control cover splitting must be distributed at smaller spacings for effective confinement of the splice region. Test results show that the steel angles and straps offered more resistance against cover splitting than external reinforcing bar ties. This is because the steel angles provided continuous support over the splice region while the external reinforcing bar ties were distributed at 3 in. c/c spacing. Distribution of transverse reinforcement at closer spacings demands that the supplementary confining reinforcement be provided externally rather than internally. This is due to the fact that provision of transverse reinforcement at smaller spacings internally would result in, as verified by tests, extensive damage to the existing concrete core and less effective concrete cover. The supplementary transverse reinforcement should therefore be provided externally over the splice region. However, the externally confining elements must be well-integrated with the existing concrete surface by using a suitable scheme such as grouting to ensure the effectiveness of external confinement. This was demonstrated by current tests.

5.7.3 Offsets in Spliced Bars. Offsets in reinforcing bars are widely used in column lap splices. Their use helps to limit variations in column dimensions (unless demanded by structural requirements) in tall buildings and facilitates reuse of forms resulting in considerable savings in construction costs. However, equilibrium of forces at the offset requires that the horizontal force component be resisted by a suitable material. Figure 5.6 shows the forces produced by offsets in lap spliced bars. Zone A becomes critical when the column is subjected to axial compression. It has to be provided with an adequate amount of transverse reinforcement to sustain the outward horizontal force component since the resulting outward thrust cannot be resisted by concrete cover alone. Likewise, when the column is under axial tension zone B needs ties to sustain the outward thrust resulting from column bar forces at offsets.

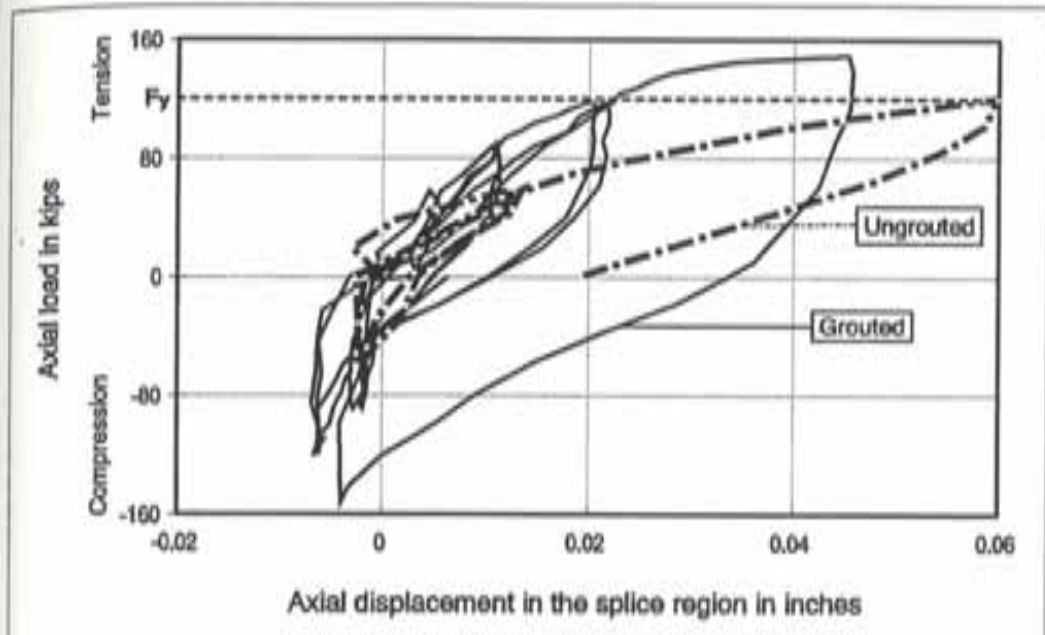
5.8 SUGGESTIONS FOR FURTHER RESEARCH

The short lap splices in test specimens investigated during the current phase of experimental study were located at column corners, hereafter referred to as the "corner splices." There are situations where columns with larger dimensions have lap splices located along the column faces, hereafter referred to as the "middle splices."

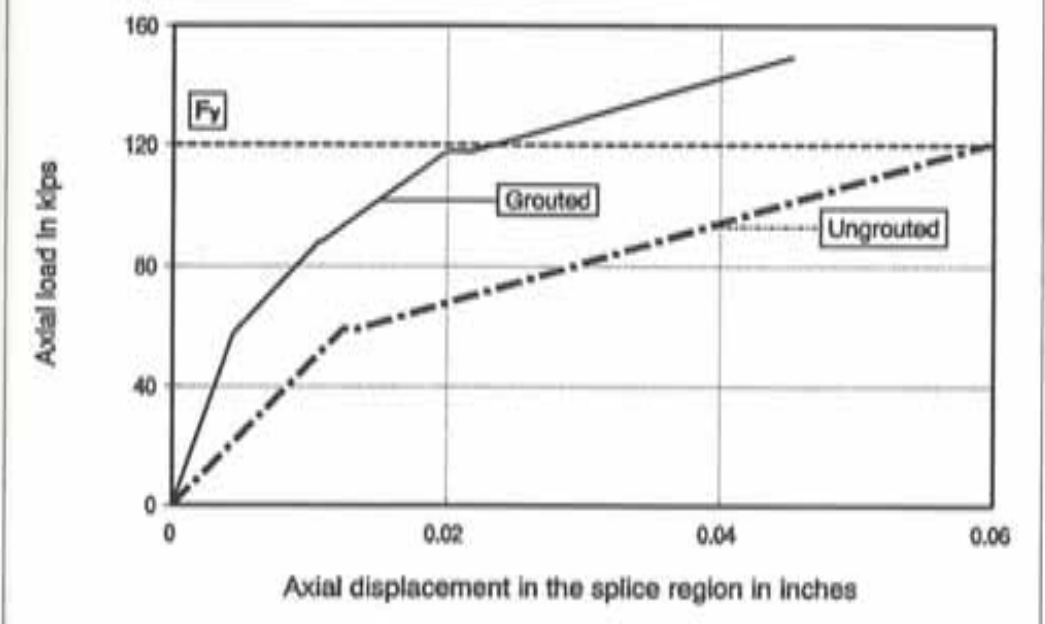
Retrofit schemes selected for current study to supplement confinement in the splice region may not provide as much confinement to the middle splices as they did to the corner splices. Because, the externally confining steel elements are more rigid at column corners than along column faces. Retrofit of middle splices is of special concern when they are located along the longer faces of large, rectangular columns.

Welding of lap spliced bars to provide continuity in load path may not be a feasible retrofit solution for middle splices due to access limitations.

It is therefore essential to explore techniques for retrofitting middle splices and verify these techniques experimentally.

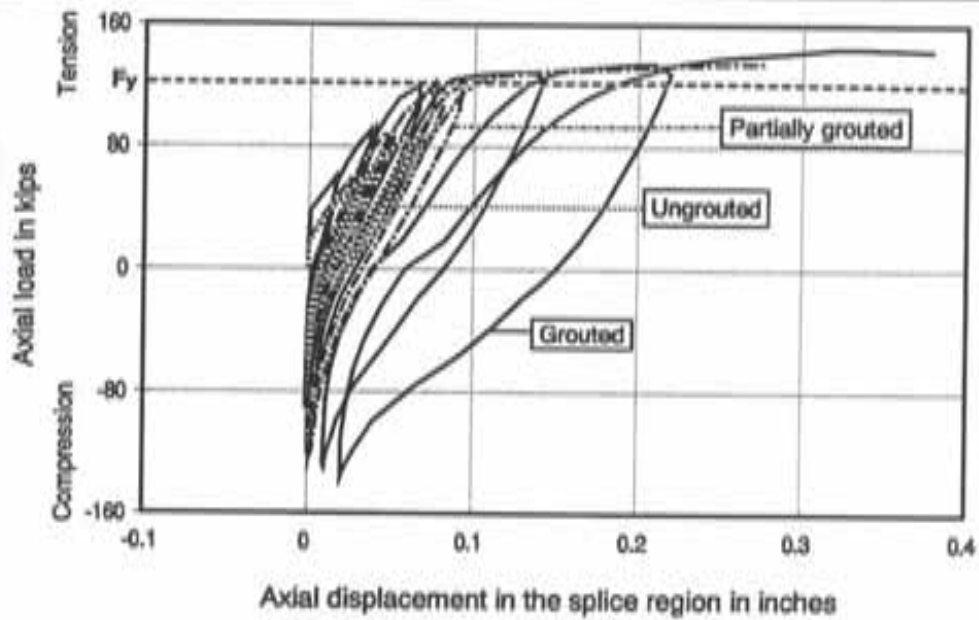


(a) Load vs displacement in the splice region

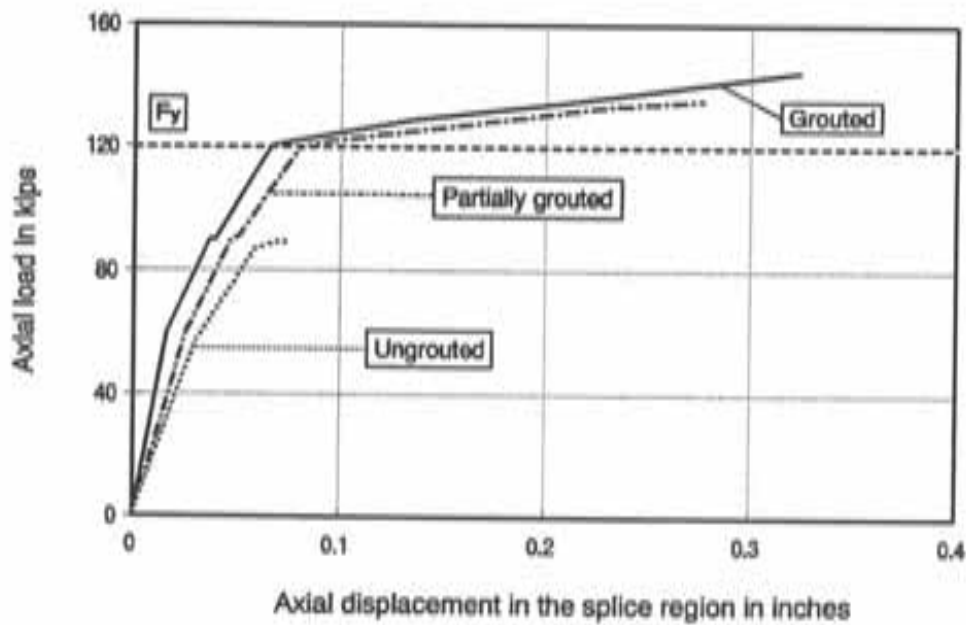


(b) Envelopes of tension cycles

Figure 5.1 Measured responses of specimens strengthened with steel angles and straps

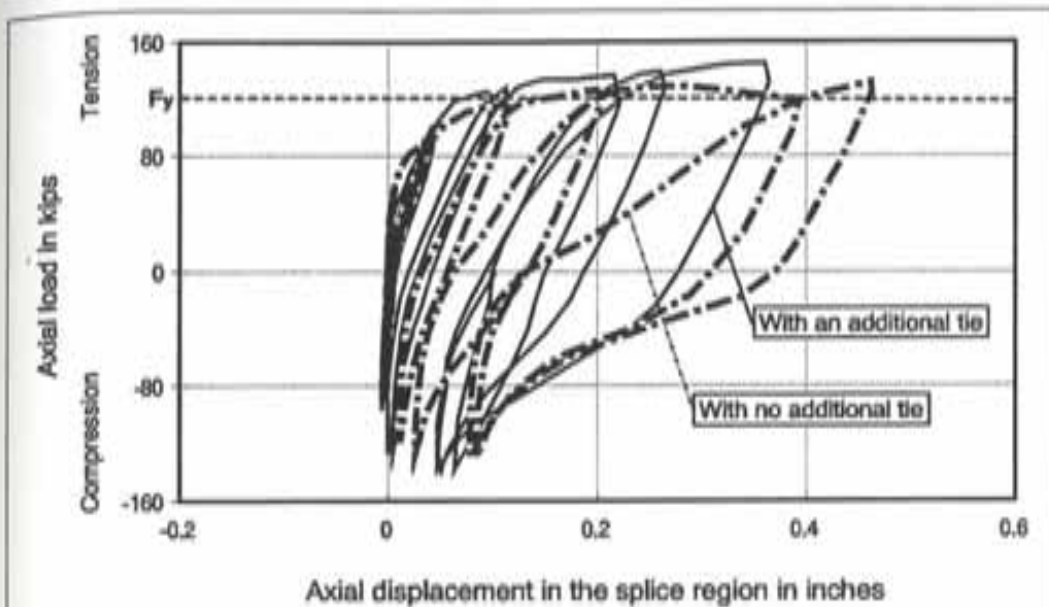


(a) Load vs displacement in the splice region

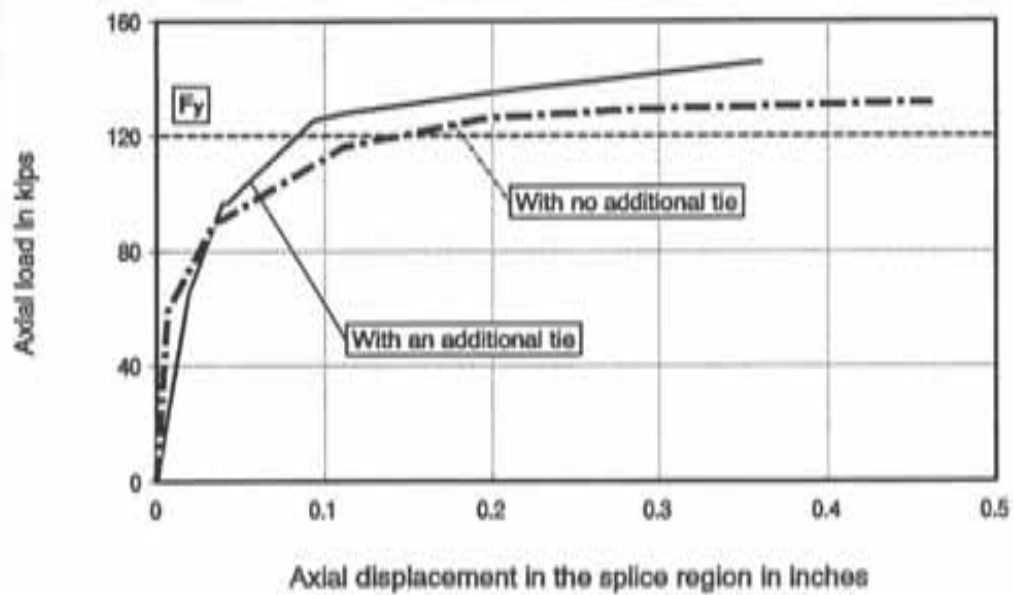


(b) Envelopes of tension cycles

Figure 5.2 Measured responses of specimens strengthened with external rebar ties



(a) Load vs displacement in the splice region



(b) Envelopes of tension cycles

Figure 5.3 Measured responses of specimens strengthened with welded splices

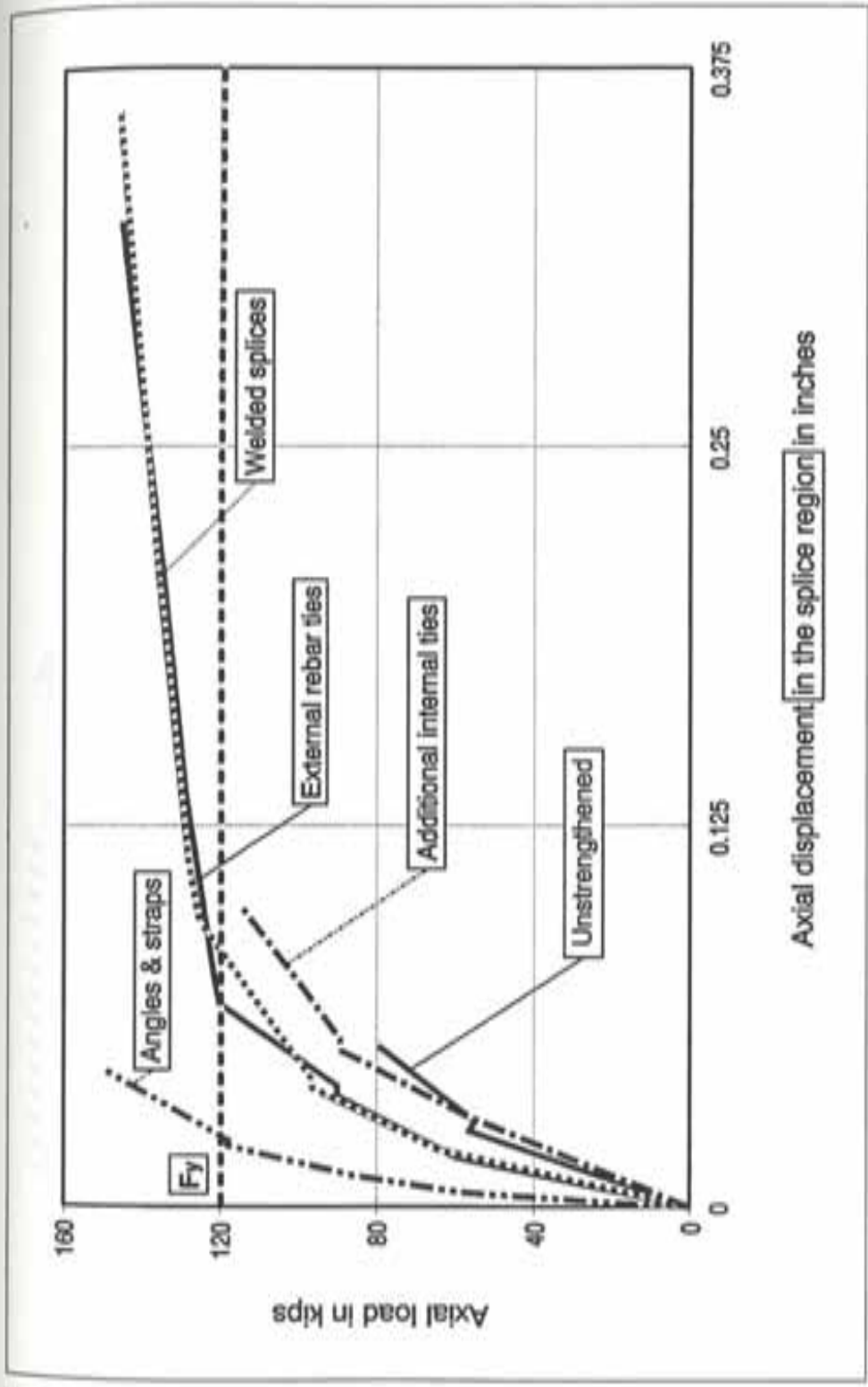


Figure 5.4 Performance of unstrengthened specimen vs retrofitted specimens

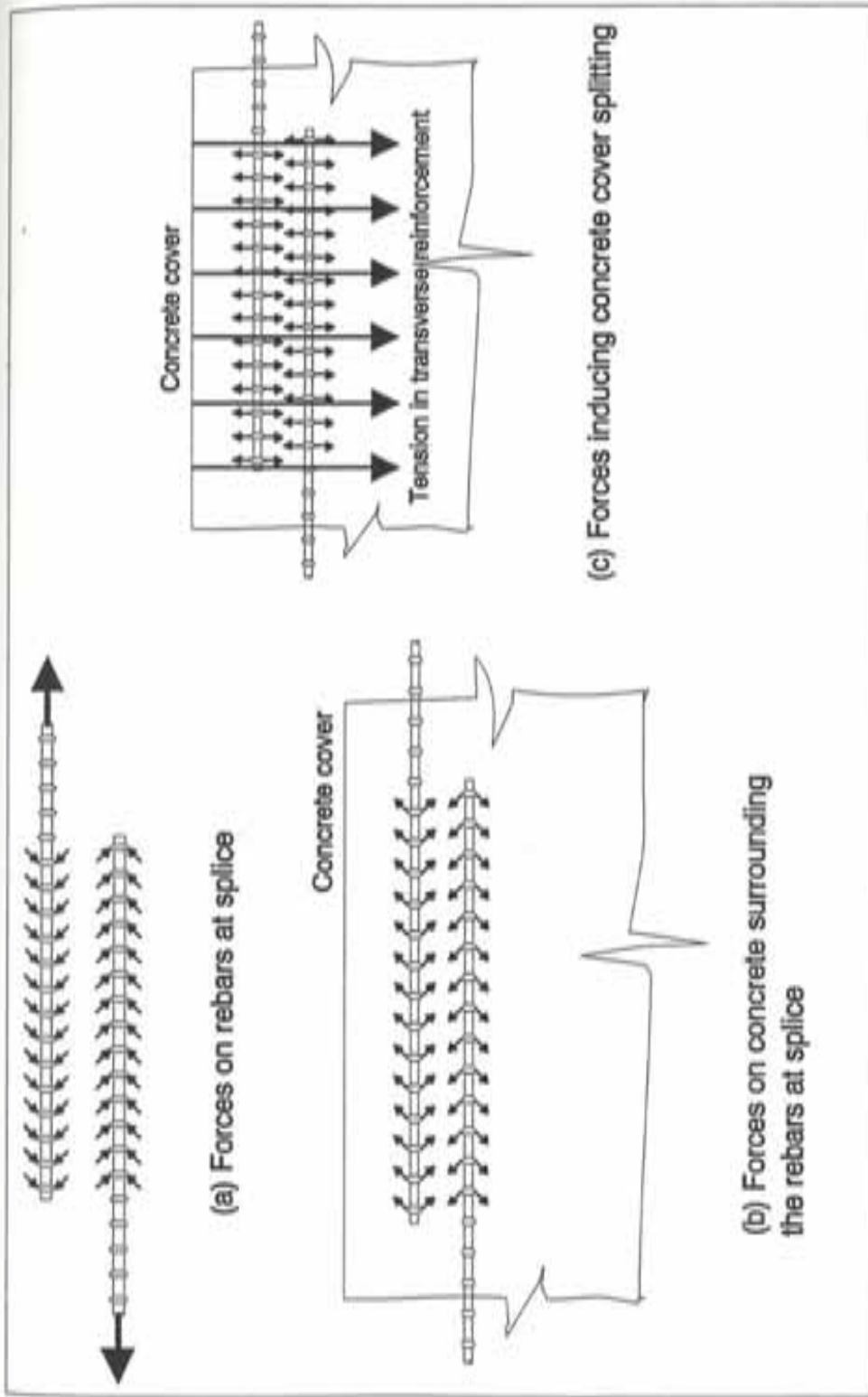


Figure 5.5 Force transfer mechanism in lap spliced bars and forces initiating cover splitting

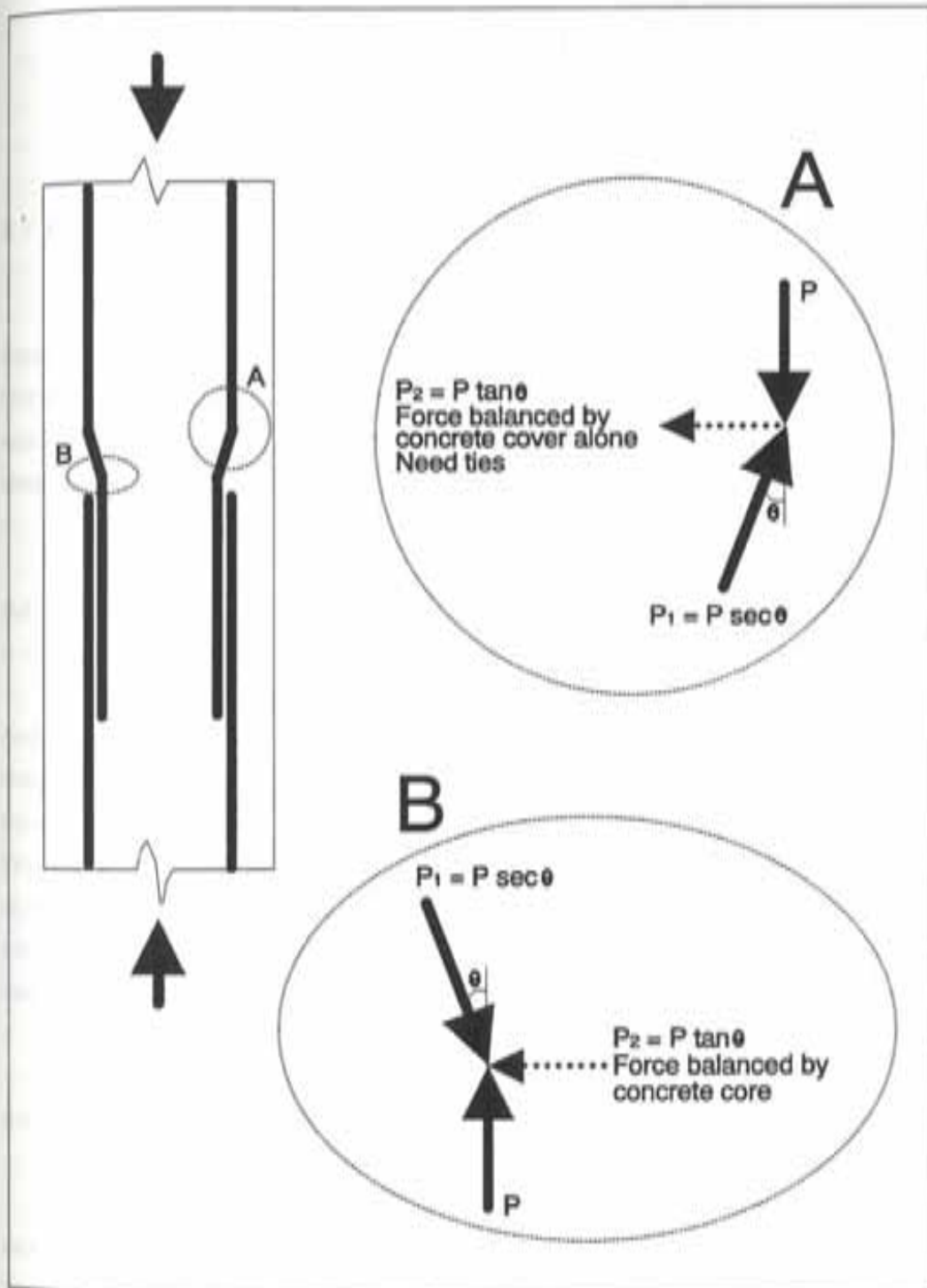


Figure 5.6 Forces produced by offsets in lap spliced bars

CHAPTER 6

SHEAR TRANSFER ACROSS FRAME-WALL INTERFACES EXPERIMENTAL PROGRAM

6.1 INTRODUCTION

The second phase of the experimental program focussed on investigating shear transfer mechanisms across frame-wall interfaces. The investigation involved constructing test specimens that represented segments from a frame-wall interface, subjecting the specimens to different load patterns, and making design recommendations for interface shear transfer.

6.2 TEST VARIABLES

Variables investigated in the test program included: shear loading pattern (reversed cyclic vs monotonic), compressive stress level across the specimen interface, number of dowels across the specimen interface, concrete strength in the test specimen segment representing the existing structure, and the construction procedure for the specimen interface. For some specimens, concrete was cast directly against the roughened surface of the existing frame segment (typical in the construction of bottom and side frame-wall interfaces, Fig. 6.1). For other specimens, a suitable cementitious dry-pack material was used to fill the gap at the top of the infill wall where it is difficult to cast concrete (Fig. 6.1).

6.3 TEST SPECIMENS AND MATERIALS

Seventeen test specimens were constructed. Each test specimen was designed to represent a portion of the frame-wall interface. Reinforcement details in the frame and wall segments were similar in all specimens. Test specimen details are shown in Fig. 6.2. Note that the cross section was reduced at the frame-wall interface. This was done due to the

limitations in the capacity of actuators available at the laboratory. Figure 6.3 shows the existing frame (beam or column) reinforcement cage inside a wooden form. Frame segments were cast in the vertical position (Fig. 6.4). The surface of each existing frame segment where a wall element was later attached was sandblasted to produce a rough surface (Fig. 6.5). Six inch deep holes (8 bar diameters) were drilled in frame segments (Fig. 6.6) and were cleaned using stiff brushes and a vacuum cleaner. The sandblasted interface was cleaned using a metal wire brush and vacuum cleaner. Dowels (#6 bars) were set into holes using a quick-setting epoxy gel.

Wall reinforcement cages were either tied to the dowels (Fig. 6.7) or supported by chairs in the absence of dowels (Fig. 6.8). Wall segments were cast in place as shown in Fig. 6.9. For the two specimens designed to represent the top frame-wall interface, a 1.5 in. gap was left between the frame and wall segments (Fig. 6.10). Wall segments for the two specimens were cast in the overhead position (inverted from what is shown in Fig. 6.10) and the frame elements with dowels were lowered into position from above so that the dowels were embedded in the wall segment. This was done to simulate prototype construction of top frame-wall interface where the wall would be cast in the overhead position. The gap between the frame and wall segments was later dry-packed with a non-shrink, non-metallic cement grout. Test specimens were cured in the laboratory environment for 28-days. A completed specimen is shown in Fig. 6.11. Test specimen details are summarized in Table 6.1.

Frame segments were cast from two concrete mixes having different 28-day compressive strengths. Mix B had a 28-day compressive strength of 3500 psi (typical of construction in the 1950s and 60s), and Mix A had a very low compressive strength of 1750 psi, representative of an even earlier vintage concrete. Measured 28-day compressive strengths for wall segments were 6000 psi for Mix B and 5100 psi for Mix A. Maximum coarse aggregate size was three-quarters of an inch. Grade 60 reinforcing bars were used for both frame and wall segments. The measured yield strength of #6 dowels used as shear connectors across the interface was 69 ksi. The epoxy gel was manufactured by HILTI corporation, USA. Non-shrink, non-metallic cement grout (28-day nominal compressive strength = 9000 psi), commercially known as MASTERFLOW 928, was supplied by Master Builders, USA.

6.4 TEST SETUP AND TESTING PROCEDURE

The test setup shown in Fig. 6.12 was designed to subject the interface to either reversed cyclic or monotonic loading in direct shear. The wall segment in each test specimen along with the rigid loading head could be pushed in either direction using one of the two 400-kip capacity actuators connected to the test frame ends. The frame segment of each test specimen was clamped in the test frame. External compressive stress was applied on the interface by a self-equilibrating vertical loading system which consisted of two steel tubes beneath the frame element, two built-up girders made up of channel sections above the wall element, four high-strength rods that connected the top and bottom steel sections, and four 60-kip actuators that applied load to the four rods. Loads applied to each test specimen are shown schematically in Fig. 6.13.

Test specimens were subjected to either reversed cyclic or monotonic loading in direct shear. Loading histories for specimens subjected to load reversals, consisted of cycles of increasing load or displacement magnitude. Cycles were load-controlled until the test specimen reached peak shear capacity, and were displacement-controlled thereafter. Cyclic load histories are shown in Fig. 6.14 and were modified slightly depending on actual behavior of test specimens. Load history for specimen B9, which was subjected to cyclic compressive stress, was established based on the performance of specimen B5, which was subjected to constant compressive stress. A linear relationship was assumed between applied interface shear and normal compressive stress to establish the cyclic compressive stress history for specimen B9, as shown in Fig. 6.15. Applied shear and normal compressive load were monitored using pressure transducers and pressure gages. Interface slip and uplift were measured with displacement transducers at multiple locations, as denoted in Fig. 6.16 by prefixes HD (horizontal) and VD (vertical).

Table 6.1 Summary of test program

| Specimen Index | Frame f'_c (psi) | Wall f'_c (psi) | Number of dowels | Compressive stress across specimen interface | | | Shear loading type | Load history and remarks |
|----------------|--------------------|-------------------|------------------|--|----------------|--------------------|--------------------|--------------------------|
| | | | | magnitude (psi) | x frame f'_c | constant or cyclic | | |
| A2 | 1750 | 5100 | 3 #6 | 0 | --- | --- | reversed cyclic | LH1 (Fig. 6.14a) |
| A3 | 1750 | 5100 | 3 #6 | 0 | --- | --- | monotonic | LH1 (Fig. 6.14a) |
| A4 | 1750 | 5100 | 6 #6 | 0 | --- | --- | reversed cyclic | LH1 (Fig. 6.14a) |
| A5 | 1750 | 5100 | none | 1000 | 0.57 | constant | monotonic | LH2 (Fig. 6.14b) |
| A6 | 1750 | 5100 | 3 #6 | 1000 | 0.57 | constant | reversed cyclic | LH2 (Fig. 6.14b) |
| A7 | 1750 | 5100 | 6 #6 | 1000 | 0.57 | constant | rev. cyclic | LH2 (Fig. 6.14b) |
| A8 | 1750 | 5100 | none | 1000 | 0.57 | constant | rev. cyclic | LH2 (Fig. 6.14b) |

Note: Specimen A1 was used as a trial specimen

cont'd.

Table 6.1 Summary of test program (contd.)

| Specimen index | Frame f'_c (psi) | Wall f'_c (psi) | Number of dowels | Compressive stress across specimen interface | | | Shear loading type | Load history and remarks |
|----------------|--------------------|-------------------|------------------|--|----------------|--------------------|--------------------|--------------------------|
| | | | | magnitude (psi) | x frame f'_c | constant or cyclic | | |
| B1 | 3500 | 6000 | 3 #6 | 0 | --- | --- | rev. cyclic | LH1 (Fig. 6.14a) |
| B2 | 3500 | 6000 | 6 #6 | 0 | --- | --- | rev. cyclic | LH1 (Fig. 6.14a) |
| B3 | 3500 | 6000 | none | 1000 | 0.29 | constant | rev. cyclic | LH2 (Fig. 6.14b) |
| B4 | 3500 | 6000 | none | 1500 | 0.43 | constant | rev. cyclic | LH2 (Fig. 6.14b) |
| B5 | 3500 | 6000 | 3 #6 | 1000 | 0.29 | constant | rev. cyclic | LH2 (Fig. 6.14b) |
| B6 | 3500 | 6000 | 6 #6 | 1000 | 0.29 | constant | rev. cyclic | LH2 (Fig. 6.14b) |
| B7 | 3500 | 6000 | 3 #6 | 0 | --- | --- | rev. cyclic | LH1, grouted interface |
| B8 | 3500 | 6000 | 3 #6 | 1000 | 0.29 | constant | rev. cyclic | LH2, grouted interface |
| B9 | 3500 | 6000 | 3 #6 | 1000 | 0.29 | cyclic | rev. cyclic | LH3 (Fig. 6.15) |
| B10 | 3500 | 6000 | 3 #6 | 350 | 0.1 | constant | rev. cyclic | LH2 (Fig. 6.14b) |

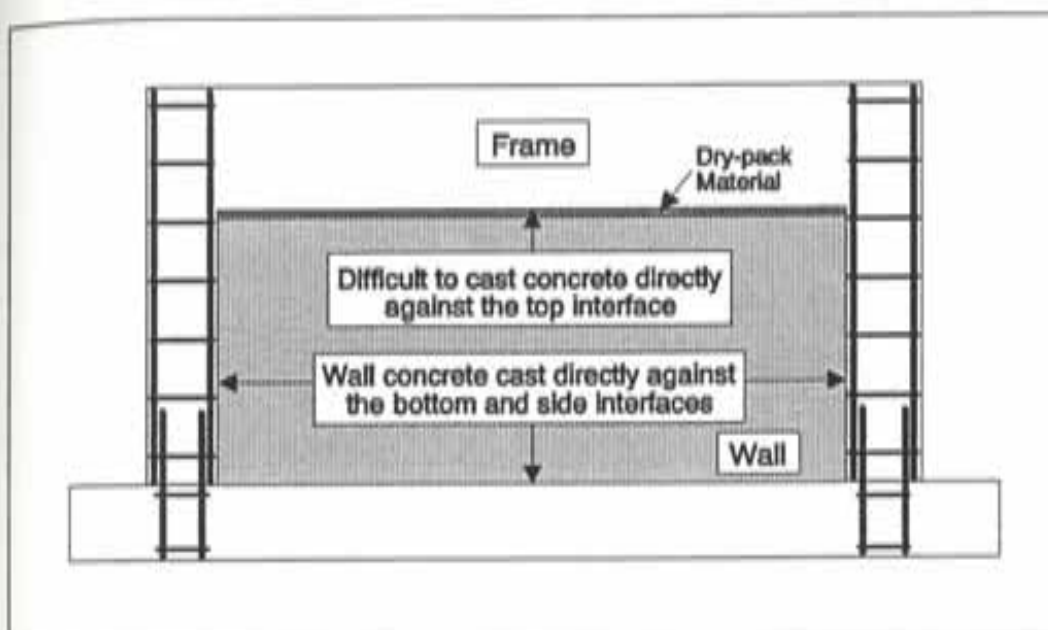


Figure 6.1 Frame-wall interfaces

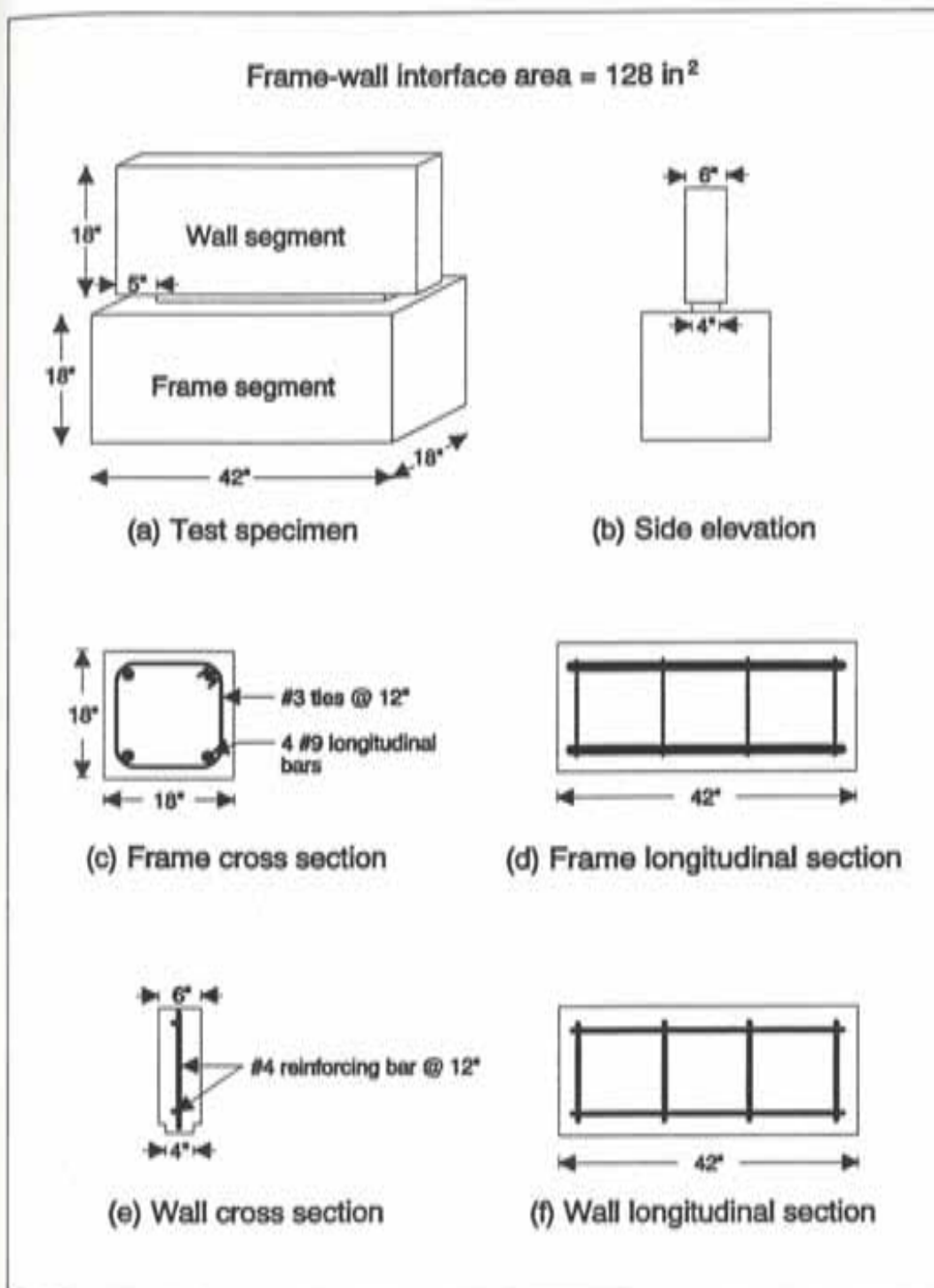


Figure 6.2 Test specimen details

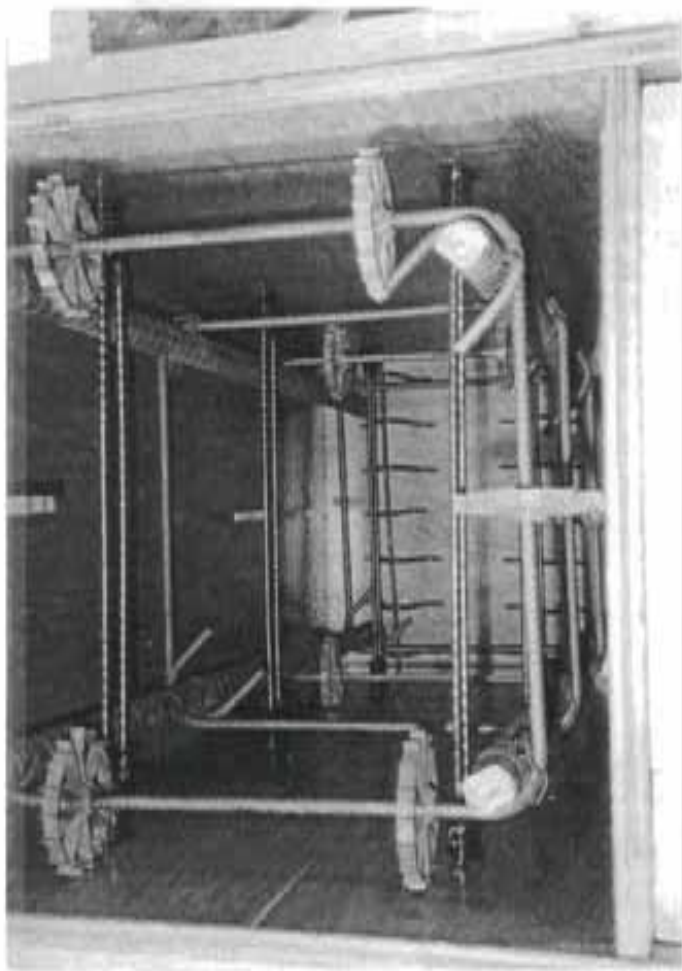


Figure 6.3 Frame reinforcement cage inside wooden form



Figure 6.4 Casting of frame segments

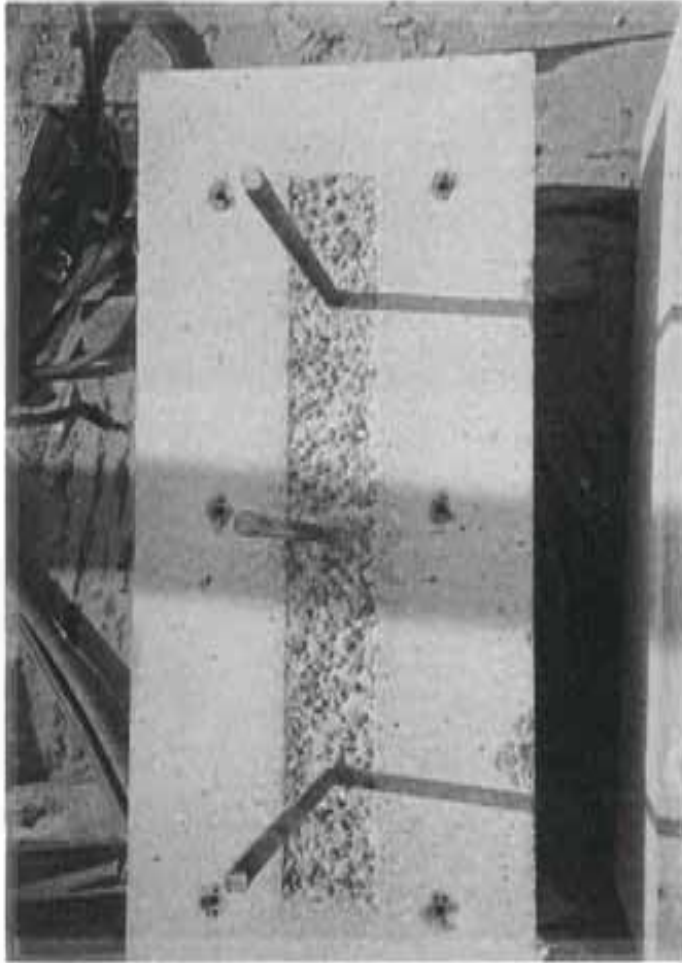


Figure 6.5 Sandblasted frame-wall interface



Figure 6.6 Drilling of holes in frame segments for placement of dowels

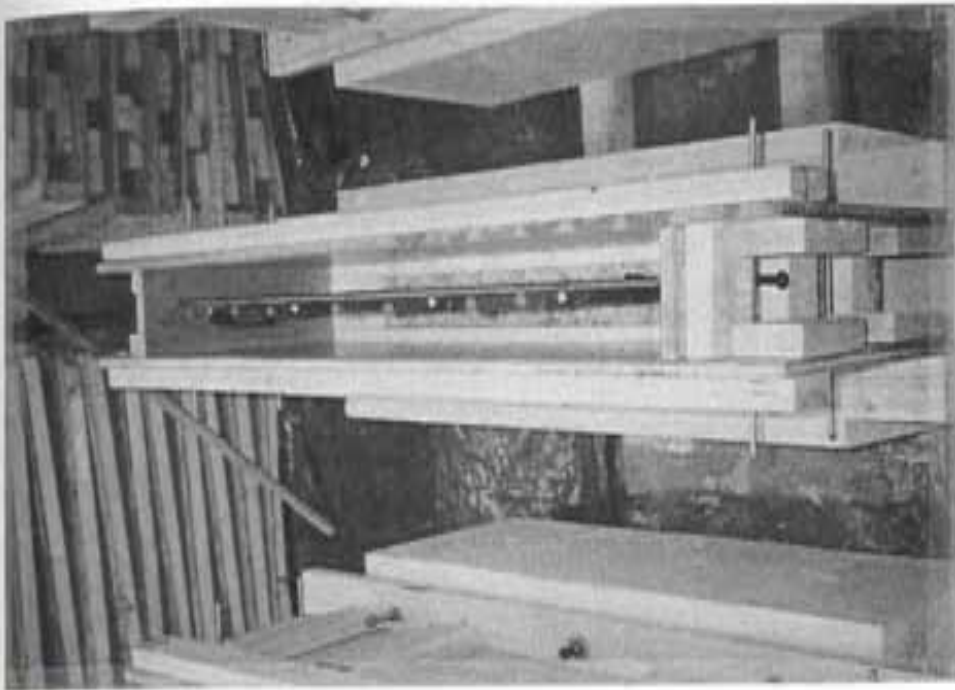


Figure 6.7 Wall reinforcement cage tied to dowels

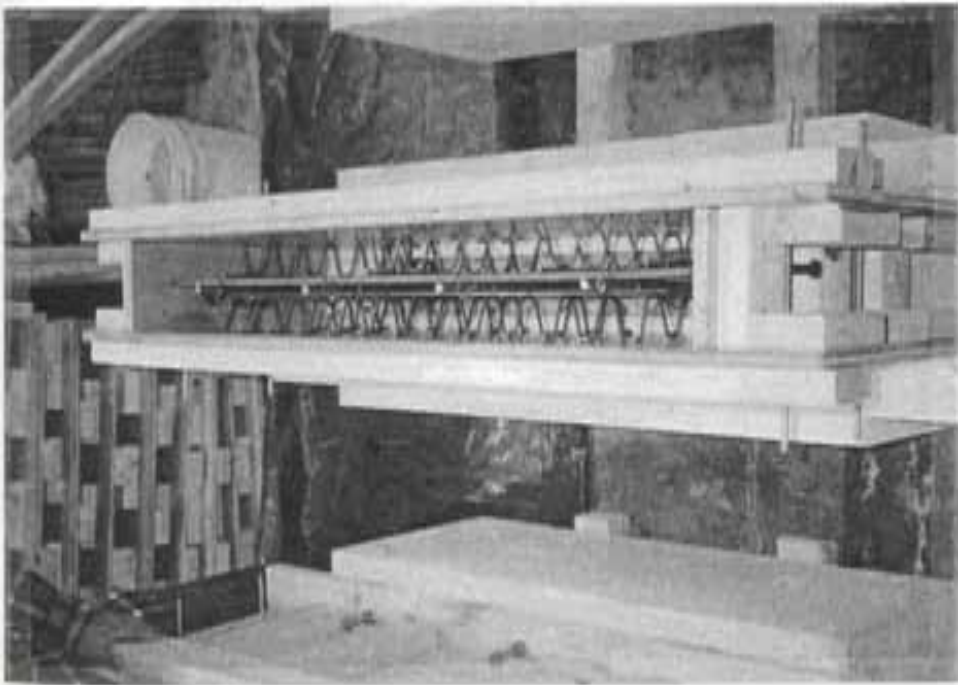


Figure 6.8 Wall reinforcement cage supported by chairs



Figure 6.9 Casting of wall segments

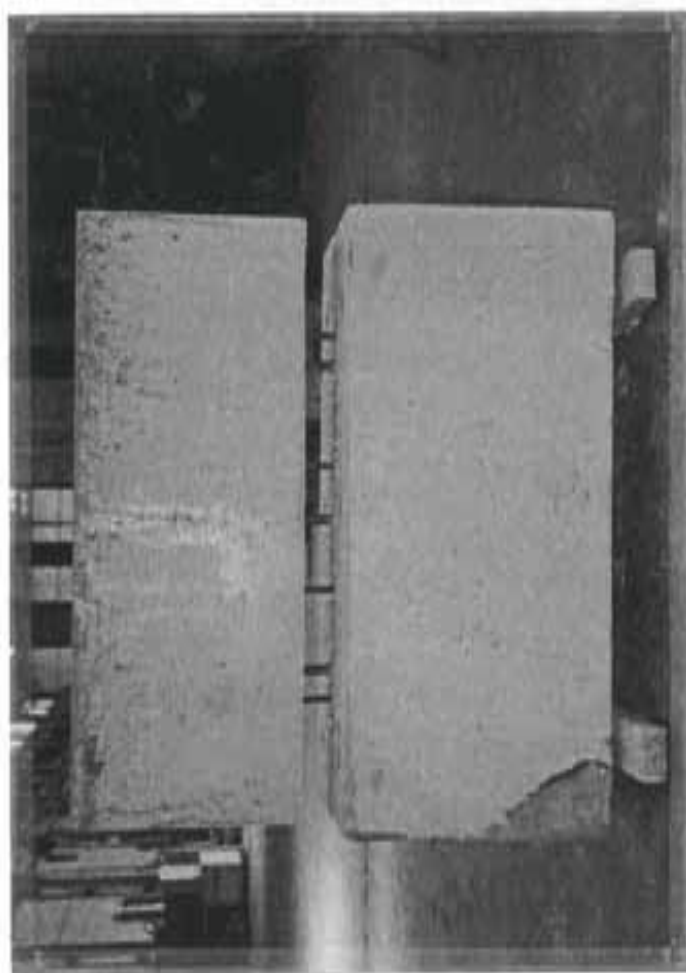


Figure 6.10 Gap in top frame-wall connection after casting frame and wall segments



Figure 6.11 Completed test specimen

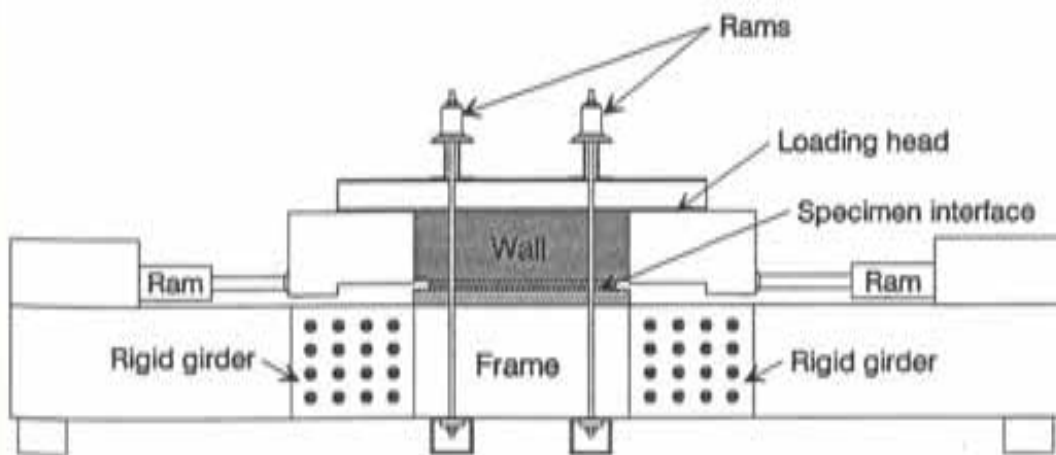
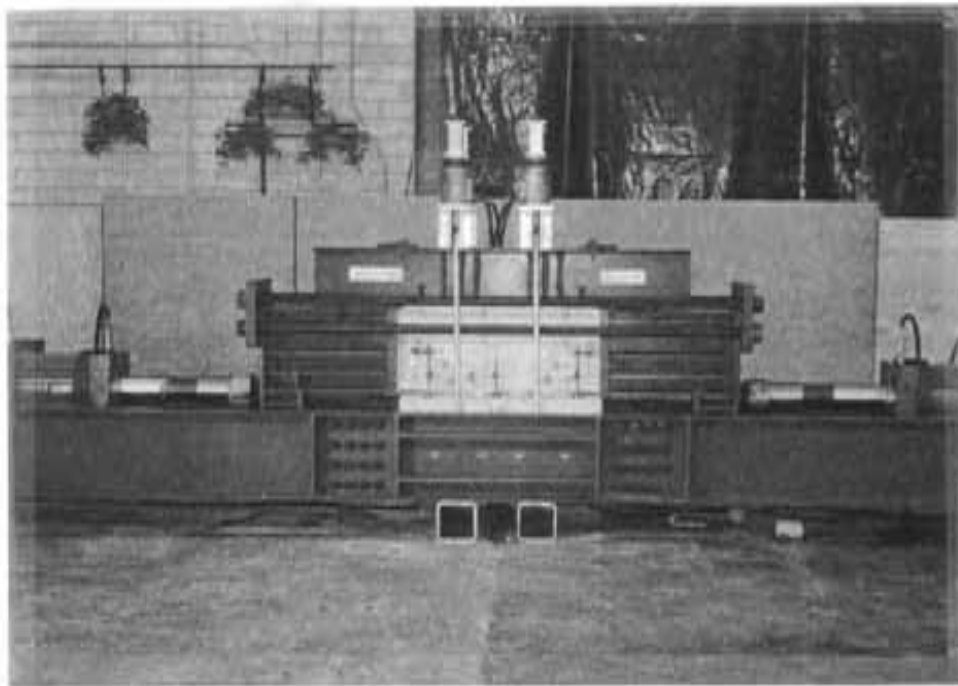


Figure 6.12 Test setup

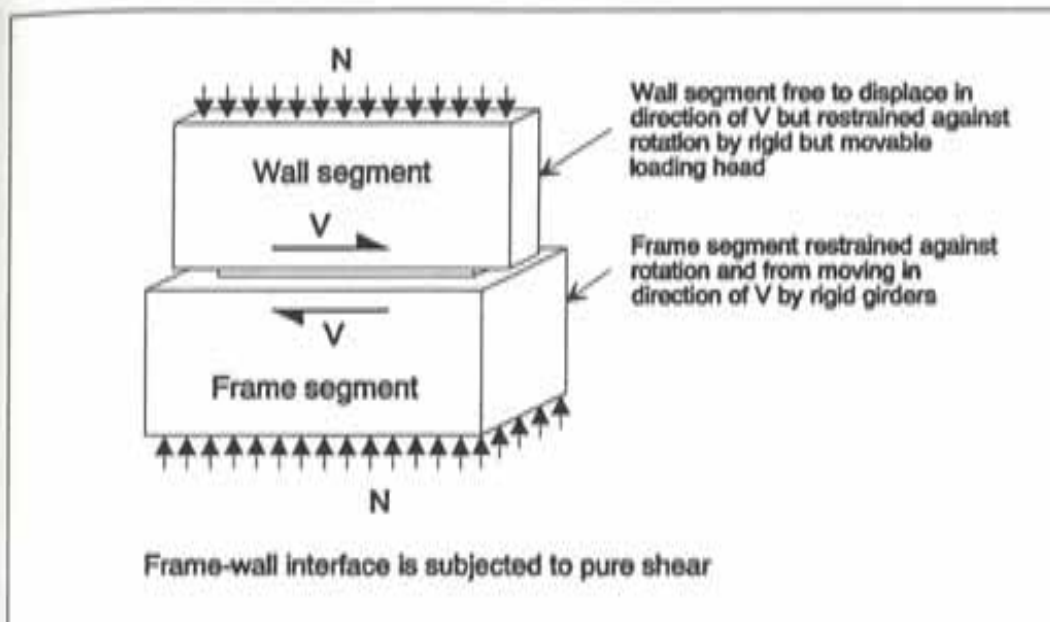


Figure 6.13 Schematic of loads applied on each test specimen

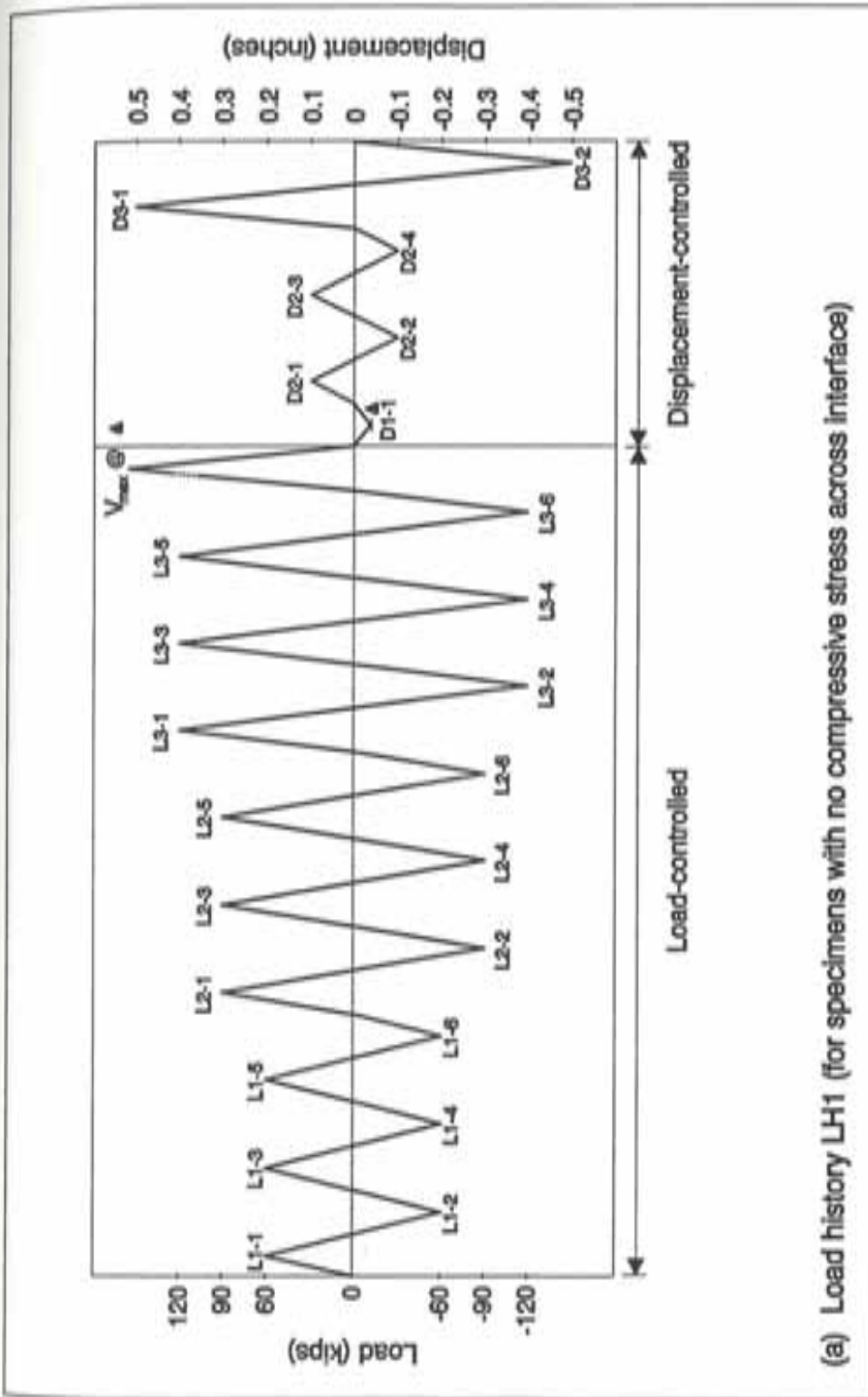


Figure 6.14 Load histories for test specimens (contd.)

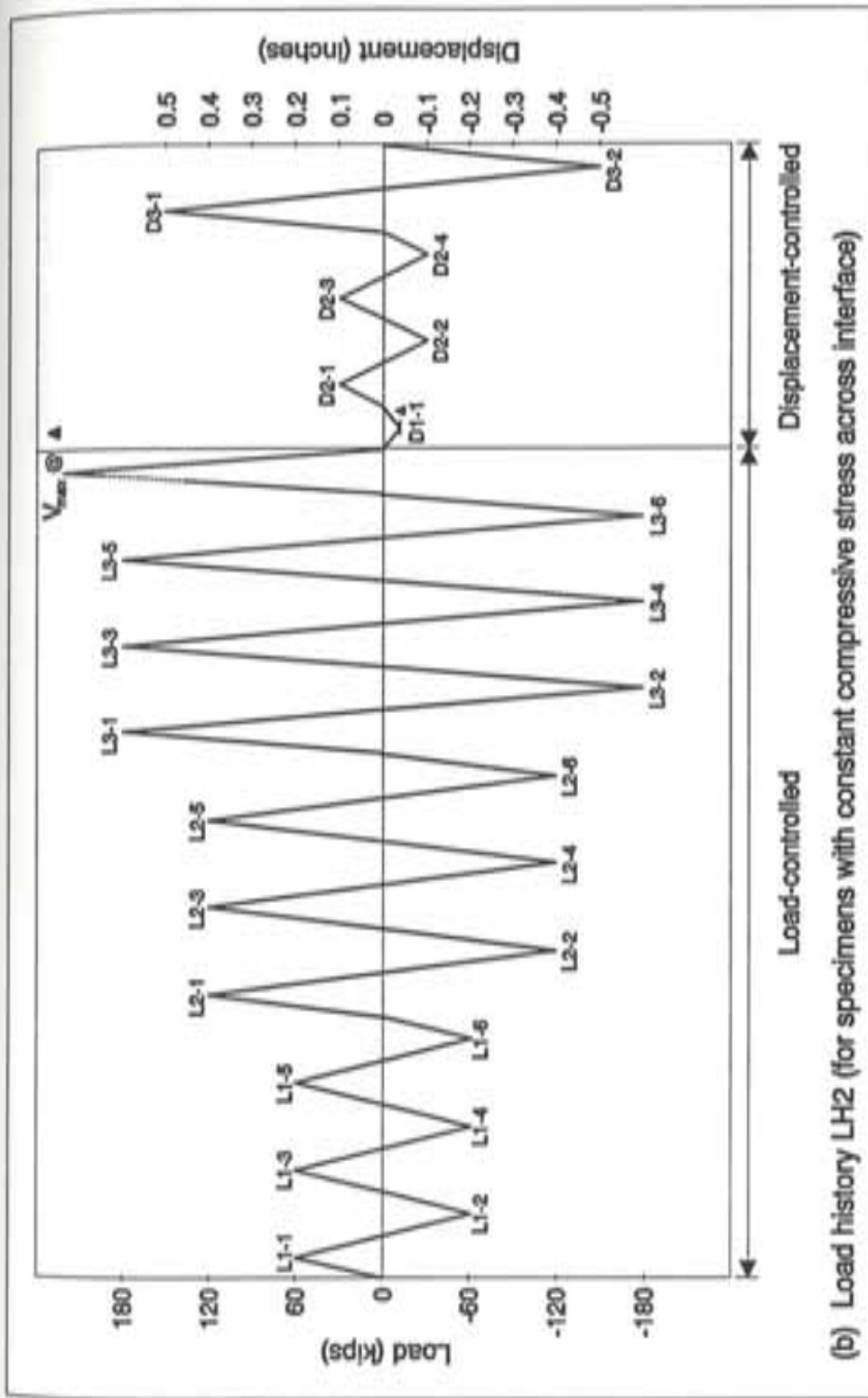


Figure 6.14 Load histories for test specimens

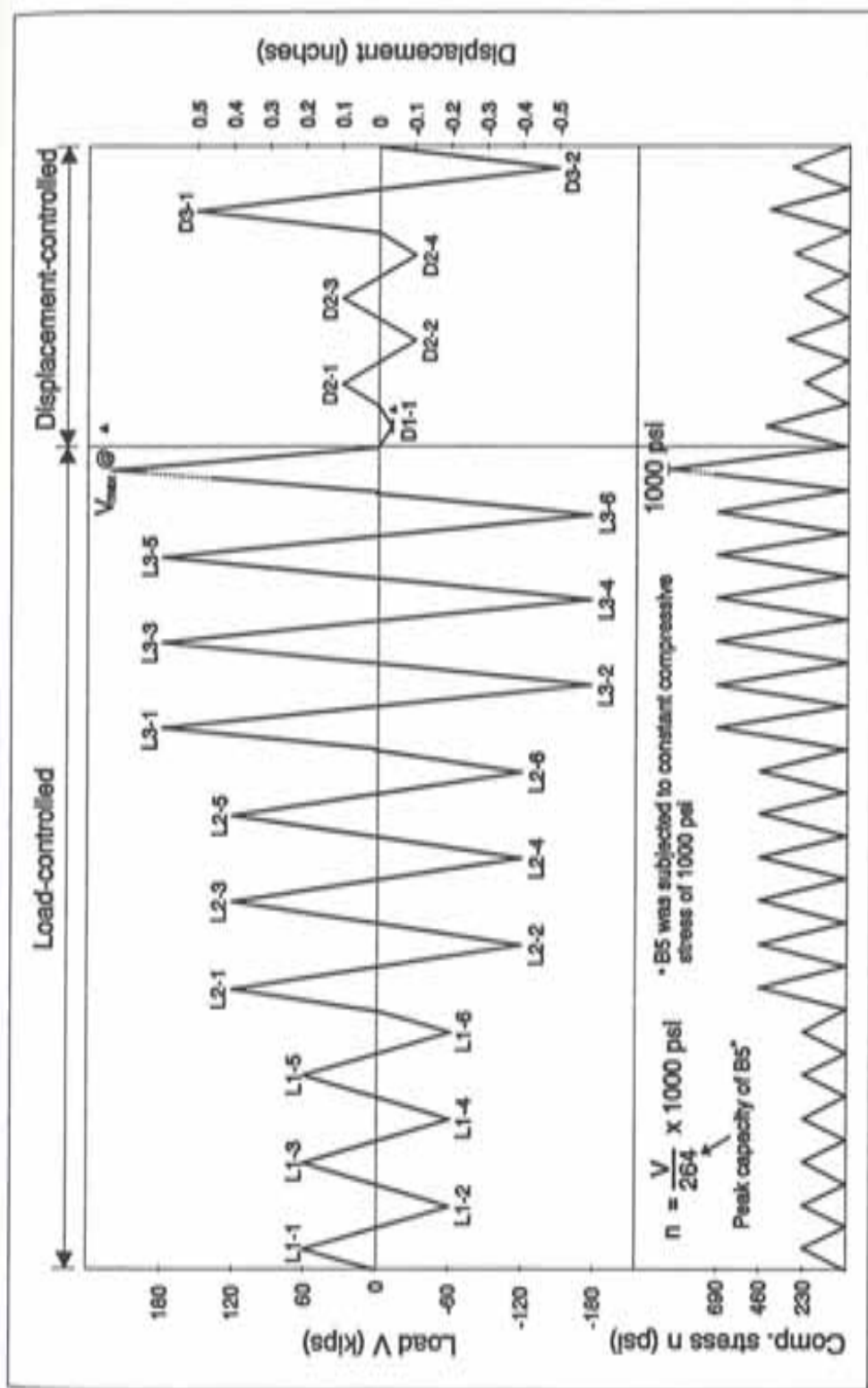


Figure 6.15 Load history LH3 for test specimen B9 (cyclic compressive stress)

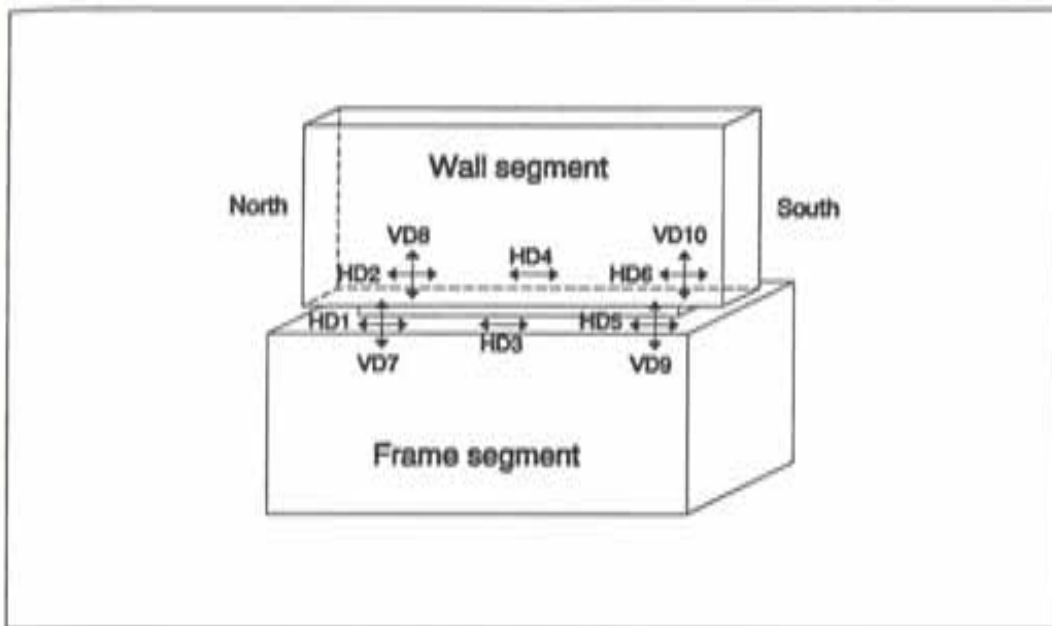


Figure 6.16 Displacement transducer locations

CHAPTER 7

SHEAR TRANSFER ACROSS FRAME-WALL INTERFACES TEST RESULTS - MEASUREMENTS AND SPECIMEN BEHAVIORS

7.1 INTRODUCTION

The current chapter presents measurements taken during interface shear transfer tests and uses these measurements to establish overall behavior of test specimens, including failure modes. Peak shear strength, corresponding slip measurement, and failure mode for each test specimen are summarized in Table 7.1.

7.2 LOAD AND DEFORMATION MEASUREMENTS

7.2.1 Shear Stresses. Shear stresses transferred across the specimen interface were obtained by dividing measured shear loads by the interface area. All test specimens had the same interface area of 128 in^2 (32 in. by 4 in.).

7.2.2 Interface Slips. Relative displacements between the frame and wall elements in the direction of applied shear (interface slip) were measured at six locations (on both sides of the ends and middle of each specimen) as shown in Fig. 6.16.

Shear stresses are plotted against measured interface slip values for both sides (east and west) of specimen A2 in Fig. 7.1. The average of the east and west values at each end and the middle of the specimen are also plotted in Fig. 7.1. Note that the difference in slip values measured on east and west sides of the interface was insignificant. For consistency, the average of slip values measured on both sides (east and west) of the interface are reported for remaining specimens. Figure 7.2 presents shear stresses versus measured interface slip at the middle and ends of specimen A2. There was no significant difference between the slip measured at the ends and the middle of the interface. Slip measured at the middle of the interface could therefore be considered representative of all interface slips. The shear stress vs slip relationship for all test specimens was established

using the average of slip values measured at the middle of the interface (at locations HD3 and HD4 in Fig. 6.16). For all purposes hereafter, the average slip calculated at the middle of the interface is referred to as the "interface slip." Shear stress vs interface slip relationships for all test specimens are provided in Appendix B.

7.2.3 Interface Uplifts. Displacements measured across the frame-wall interface and perpendicular to the direction of applied shear (interface uplift) provided information on the formation of horizontal cracks and their progression during testing. Uplift was measured at four locations (on both sides of the test specimen at each end) as shown in Fig. 6.16.

Figure 7.3 presents the shear stress versus interface uplift response on both sides (east and west) of specimen A2 in addition to the average response at each end of the frame-wall interface. Because displacement transducers measuring uplift on the east and west sides of the specimen interface (displacement transducer pairs VD7 and VD8, and VD9 and VD10 in Fig. 6.16) were equi-distant from sides of the interface, an average of measured uplift was considered representative of actual interface uplift. For all purposes hereafter, the average of uplift measured on both sides (east and west) of the interface is referred to as "interface uplift." Shear stress vs interface uplift relationships for all test specimens are provided in Appendix B.

7.3 BEHAVIOR OF TEST SPECIMENS

The behavior of test specimens was studied and compared in terms of the peak shear strength, peak-to-peak shear stiffness, and residual shear capacity (post-failure capacity) which are illustrated in Fig. 7.4. Peak shear strength was defined as the maximum strength possessed by a test specimen. Peak-to-peak shear stiffness was taken as the slope of the straight line connecting the peak positive and negative response for the shear stress vs slip cycle with a maximum interface slip response of approximately 0.1 inch. Residual shear capacity was defined as the resistance maintained by a test specimen after failure.

The overall behavior of test specimens was influenced by such factors as the loading pattern (reversed cyclic vs monotonic), level of compressive stress across specimen

interface, number of dowels across the specimen interface, strength of concrete in the portion of test specimen representing the existing structure, and procedure used for construction of the specimen interface. Not only did many of these factors affect specimen peak shear strength but they also influenced peak-to-peak shear stiffness and residual shear capacity. Peak shear strength of test specimens was controlled by the following failure modes which were established based on instrument measurements and visual observations:

7.3.1 Pull Out Failure of Dowels. Anchorage or pull out failure of embedded dowels occurs when tension in dowels exceeds anchorage capacity. Shear strength of an interface is initially provided by adhesion between the existing frame material and new concrete in the wall. When shear exceeds the adhesive bond a crack forms and the wall begins to slide along the crack. However, irregularities in the cracked surface force the wall and existing frame to separate as sliding occurs. Separation is resisted by tensile forces in dowels that cross the interface. Tension in the dowels results in a compressive clamping force across the interface and improved shear capacity.

Figure 7.5 demonstrates that pull out failure of dowels (provided as shear reinforcement across the interface) controlled the peak shear strength of specimen B1. Strength of specimen B1 dropped abruptly when pull out of dowels occurred as denoted by the symbol x in Fig. 7.5a and b. Dowel pull out could also be established visually because a wide crack (0.05 in.) appeared along the specimen interface (Fig. 7.6) at the same time an abrupt drop in measured shear resistance was observed. Because dowels continued to pull out with increasing slip levels, the loss in residual tension in dowels resulted in strength and stiffness reduction in the specimen during successive load cycles.

7.3.2 Aggregate Interlock Failure. Aggregate interlock is a combination of friction between surfaces on each side of a crack and resistance against shearing off of protrusions on these surfaces. Aggregate interlock failure is caused by shearing off these protrusions along the cracked interface.

Figure 7.7 illustrates the behavior of specimen B3 which was consistent with aggregate interlock failure. External compression was the only clamping force across the interface because no reinforcement was provided across the interface. Failure was

characterized by an abrupt and significant drop in measured shear strength (Fig. 7.7a) and crushed concrete around the failed interface (Fig. 7.8). No formation of cracks could be observed along the interface through measured uplifts (Fig. 7.7b) or visual observations until the test specimen reached its peak shear strength. An uncracked interface until failure and crushed concrete around the interface immediately after failure supported the argument that peak shear strength of specimen B3 was controlled by aggregate interlock failure.

7.3.3 Failure Due to Disintegration of Concrete or Grout Around the Dowels.

This type of failure may control shear capacity when disintegration of concrete (usually in the element having lower strength) or dry-packed grout (used for construction of interface in the top frame-wall connection) occurs around the dowels. Such a failure may be considered undesirable but must be anticipated in repair and retrofit schemes where concrete in existing structural elements is low in strength or grout is not of high quality.

Figure 7.9 demonstrates the behavior of a specimen (A4) which was limited by disintegration of concrete (in the frame segment) around the dowels. Compressive strength of concrete in the frame segment of specimen A4 was only 1750 psi. A reduction in measured shear capacity was observed at failure as denoted by x in Fig. 7.9a. However, the observed reduction was neither abrupt nor significant. No increase in measured crack width was noticed upon failure of specimen A4 (Fig. 7.9b). Figure 7.9a shows that peak strengths of the loading cycle in which the test specimen failed (denoted by x and x') were similar. Examination of Fig. 7.5a indicates that the maximum strength in the negative direction (denoted by x') for specimen B1 (failed due to pull out of dowels) was significantly less than the peak strength in the positive direction (denoted by x). These observations helped in reaching the conclusion that peak shear strength of specimen A4 was controlled by disintegration of concrete (in the frame segment) around the dowels and not by pull out failure of dowels. It may, however, be observed from Figs. 7.9a and 9b that dowels began to pull out with increasing slip levels and, as a result, shear strength and stiffness of specimen A4 were significantly reduced during successive inelastic cycles.

The failure mechanism for specimen B8 (whose interface was dry-packed using a cementitious grout) was established based on the load-displacement behavior shown in Fig. 7.10. Strength of the test specimen increased with increasing slip levels up to 0.16 in. of

horizontal slip but began to drop when measured uplift was still negative (denoted by x in Fig. 7.10b). No deterioration of grout was observed visually around the specimen interface. Measured negative uplift (that means grout in the interface crushed and compressed under normal load) and absence of external damage to grout supported the argument that peak shear strength of specimen B8 was controlled by disintegration of grout around the dowels.

Table 7.1 Summary of test results

| Specimen Index | Interface details | | Performance of test specimen | | | Failure mode |
|----------------|-------------------|--------------------------|------------------------------|-------------------------|---------------------------|--|
| | No. of dowels | Compressive stress (psi) | Peak shear strength (kips) | Peak shear stress (psi) | Slip @ peak strength (in) | |
| A2 | 3 #6 | 0 | 76 | 593 | 0.015 | Disintegration of frame concrete around dowels followed by pull out of dowels @ larger slip levels |
| A3* | 3 #6 | 0 | 76 | 593 | 0.011 | |
| A4 | 6 #6 | 0 | 90 | 703 | 0.011 | |
| A5* | none | 1000 | 204 | 1593 | 0.014 | |
| A6 | 3 #6 | 1000 | 182 | 1421 | 0.011 | |
| A7 | 6 #6 | 1000 | 213 | 1664 | 0.036 | |
| A8 | none | 1000 | 201 | 1570 | 0.015 | |

+ Indicates monotonic loading

contd.

Table 7.1 Summary of test results (contd.)

| Specimen index | Interface details | | Performance of test specimen | | | Failure mode |
|----------------|-------------------|--------------------------|------------------------------|-------------------------|---------------------------|---|
| | No. of dowels | Compressive stress (psi) | Peak shear strength (kips) | Peak shear stress (psi) | Slip @ peak strength (in) | |
| B1 | 3 #6 | 0 | 113 | 882 | 0.011 | Pull out failure of dowels |
| B2 | 6 #6 | 0 | 130 | 1015 | 0.019 | * |
| B3 | none | 1000 | 254 | 1984 | 0.015 | Failure of aggregate interlock |
| B4 | none | 1500 | 291 | 2273 | 0.02 | * |
| B5 | 3 #6 | 1000 | 264 | 2062 | 0.021 | * |
| B6 | 6 #6 | 1000 | 274 | 2140 | 0.014 | * |
| B7** | 3 #6 | 0 | 52 | 406 | 0.07 | Pull out failure of dowels |
| B8** | 3 #6 | 1000 | 102 | 796 | 0.16 | Extensive slip due to inadequate resistance by dry-packed grout |
| B9 | 3 #6 | 1000 (cyclic) | 254 | 1984 | 0.02 | Failure of aggregate interlock |
| B10 | 3 #6 | 350 | 167 | 1304 | 0.016 | Pull out failure of dowels |

** Indicates grouted (dry-packed) interface

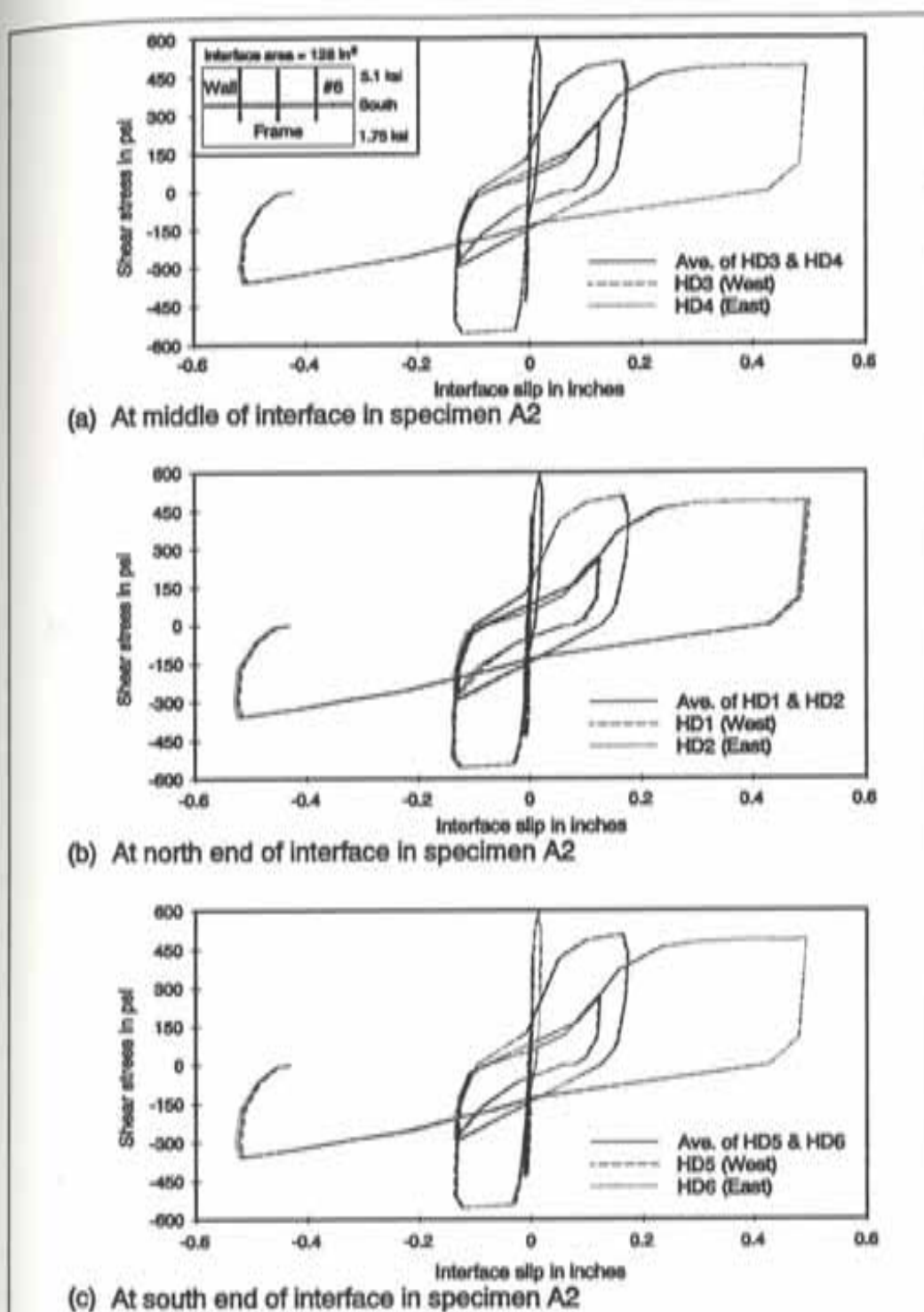


Figure 7.1 Interface slip for both sides (east and west) of interface

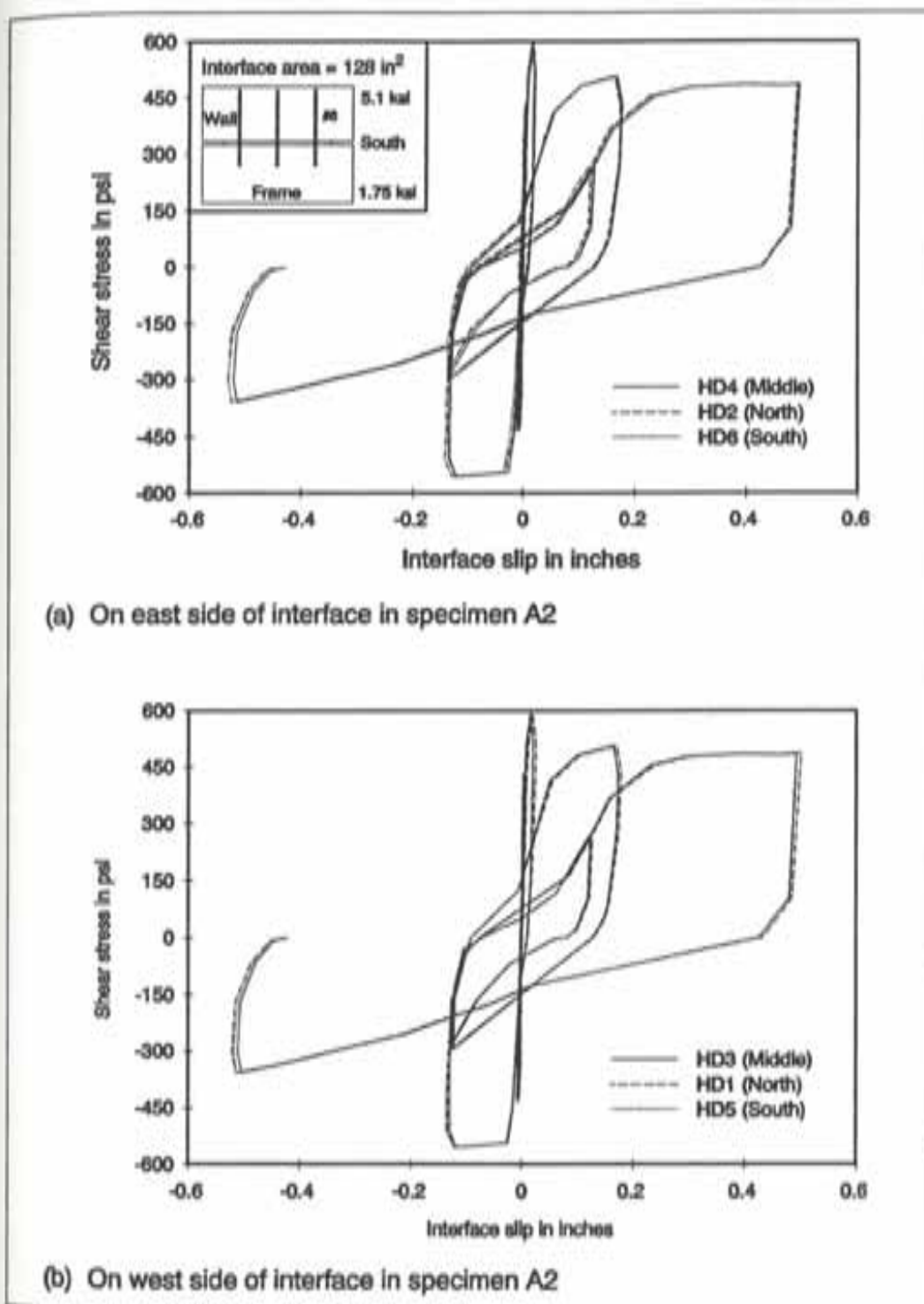


Figure 7.2 Interface slip at locations along interface

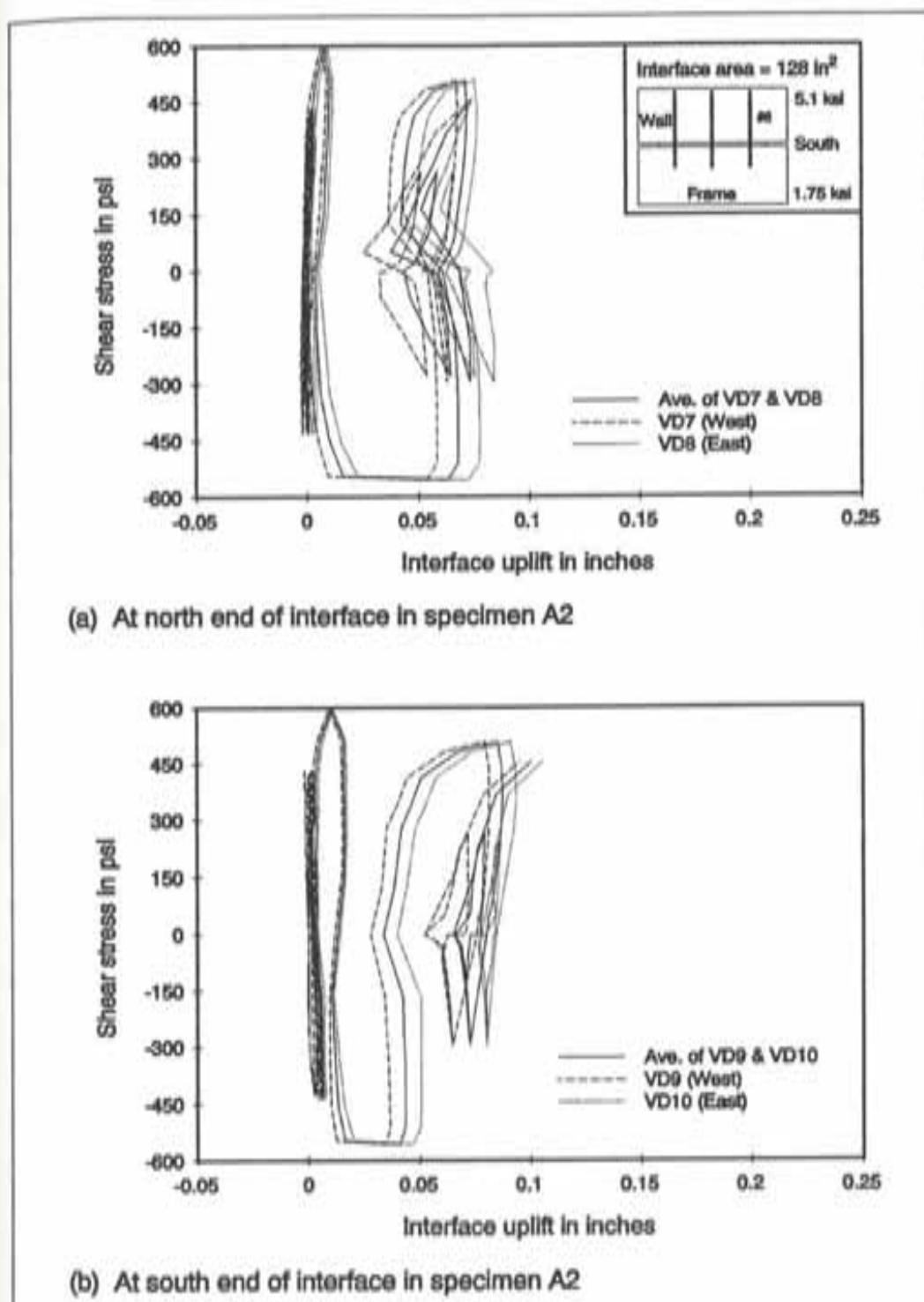


Figure 7.3 Interface uplift for both sides (east and west) of interface

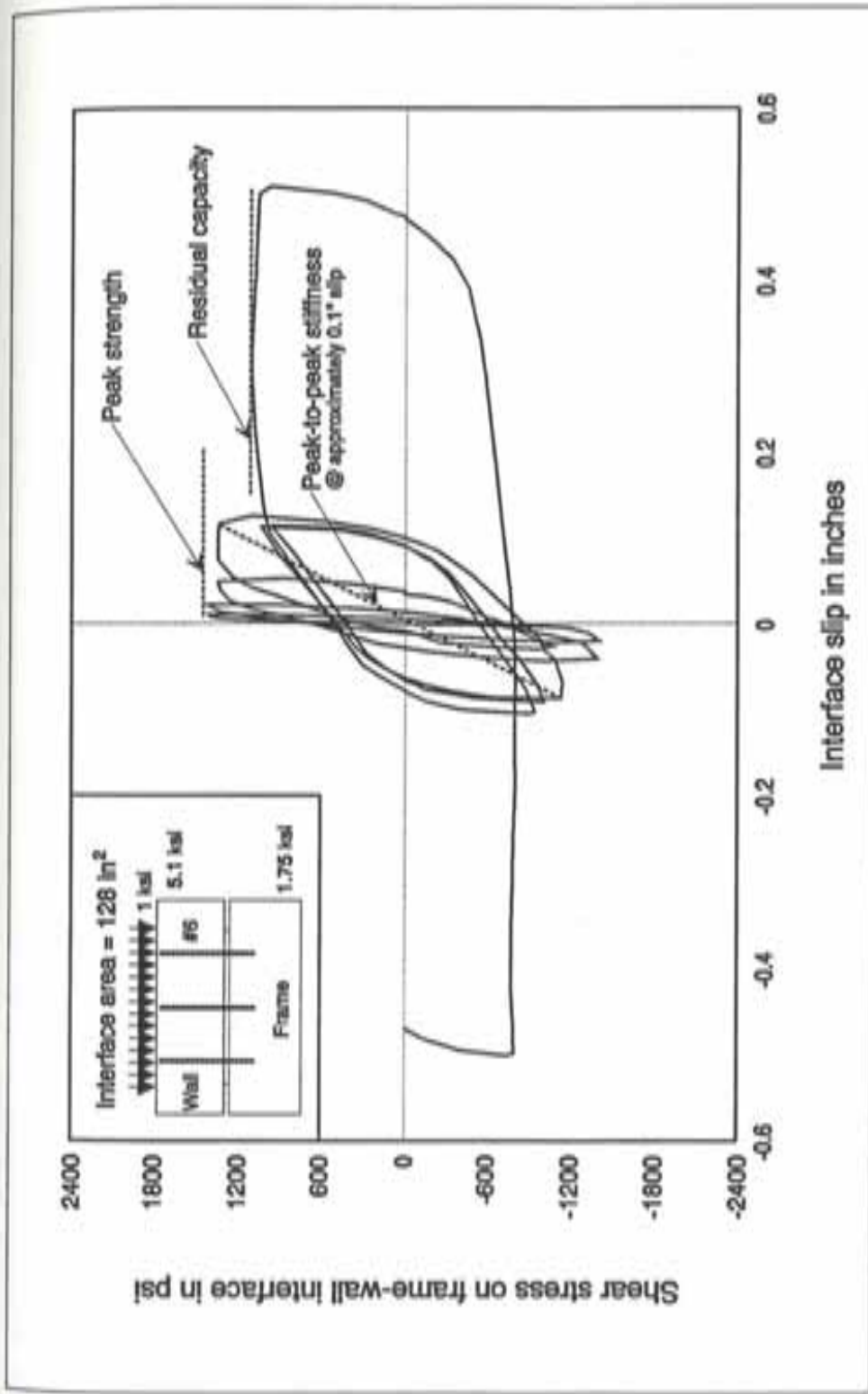
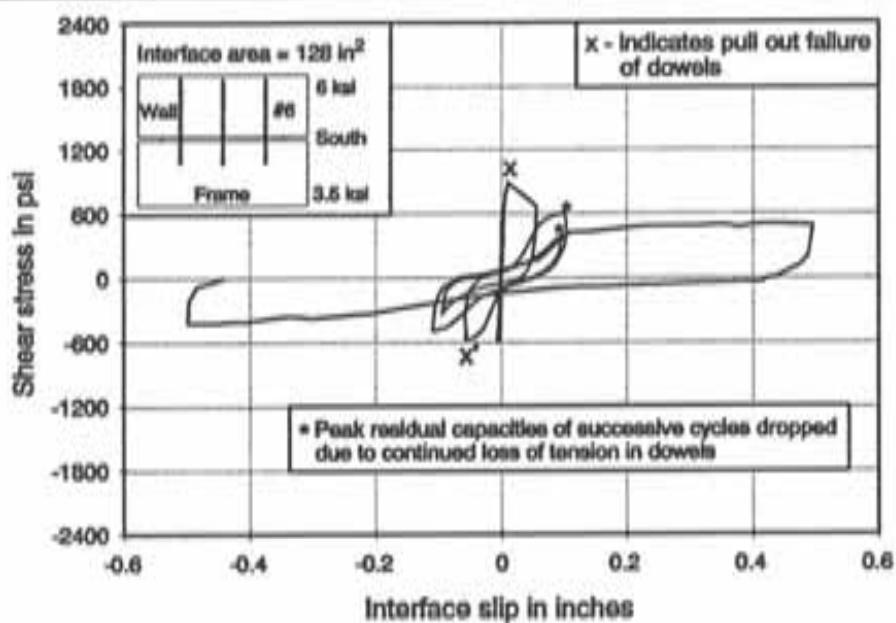
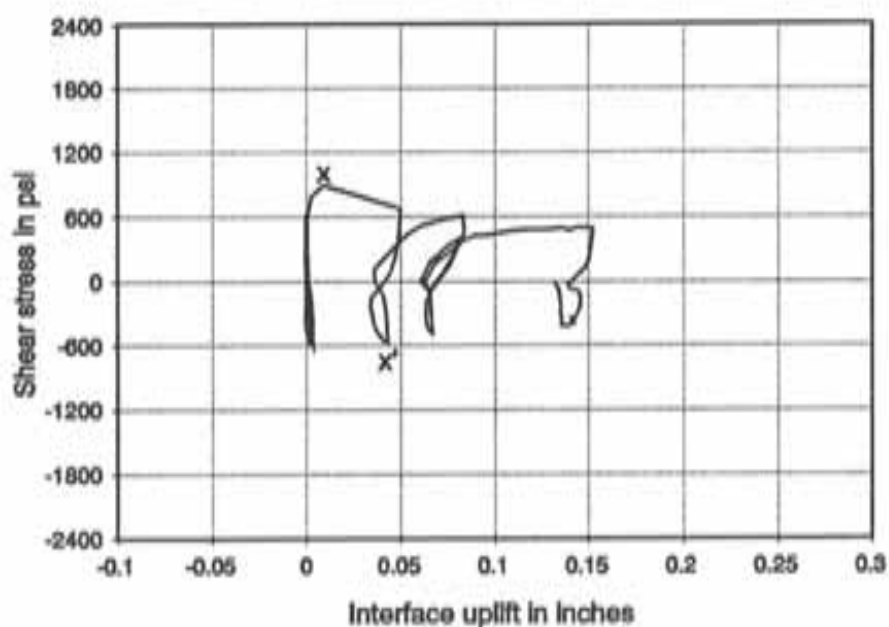


Figure 7.4 Performance of shear specimen A6



(a) Shear stress vs slip relationship for specimen B1



(b) Shear stress vs uplift relationship for specimen B1

Figure 7.5 Peak strength of specimen B1 controlled by pull out failure of dowels

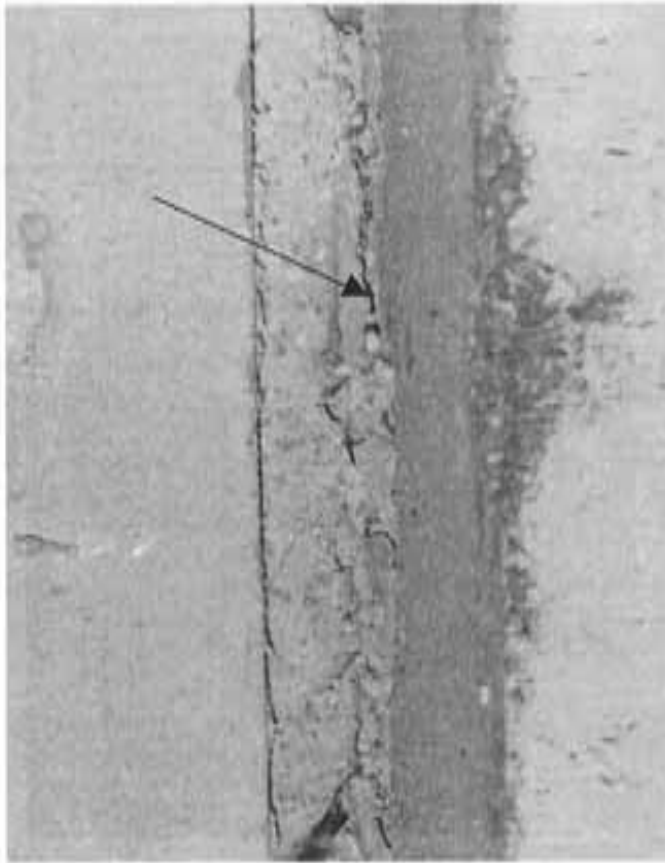
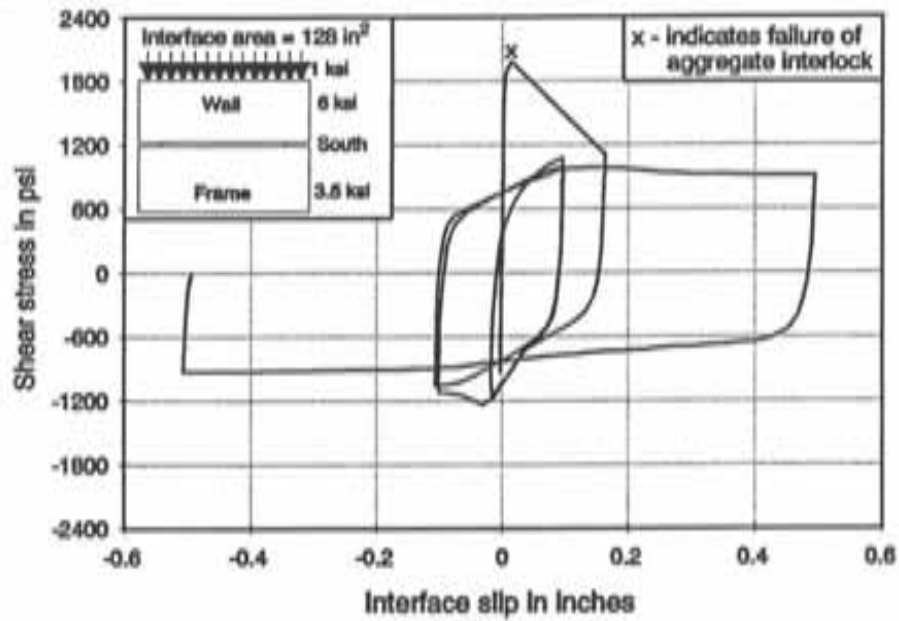
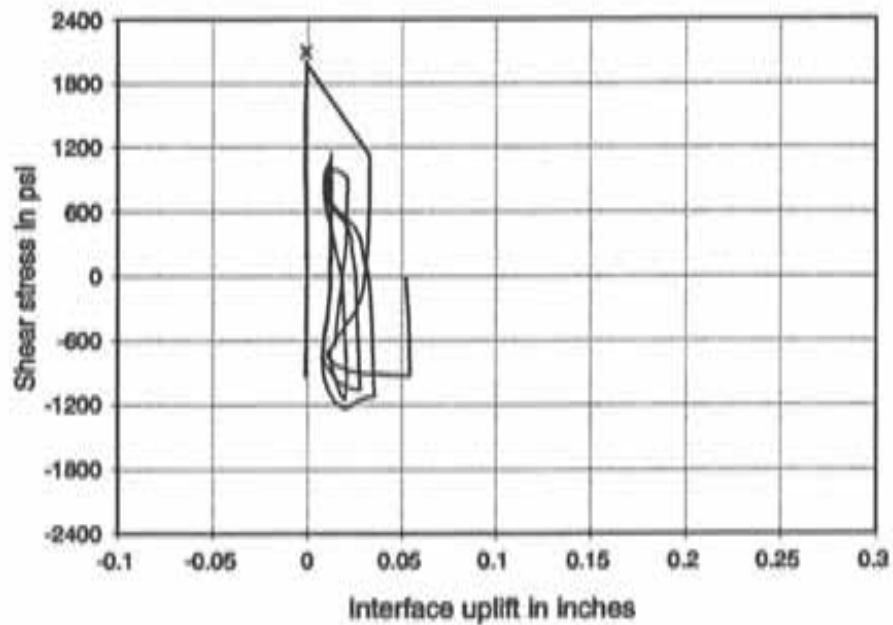


Figure 7.6 Appearance of interface upon pull out failure of dowels



(a) Shear stress vs slip relationship for specimen B3



(b) Shear stress vs uplift relationship for specimen B3

Figure 7.7 Peak strength of specimen B3 controlled by aggregate interlock failure

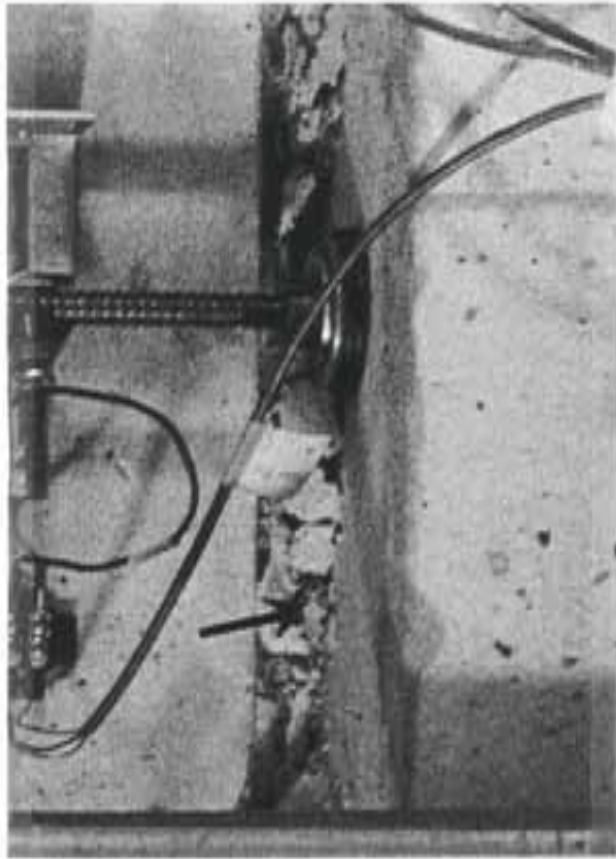
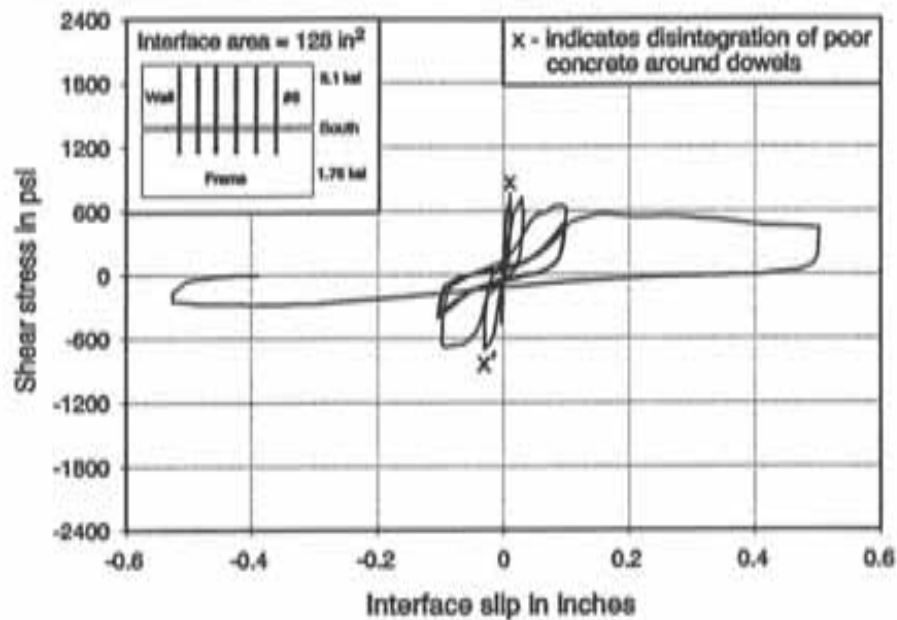
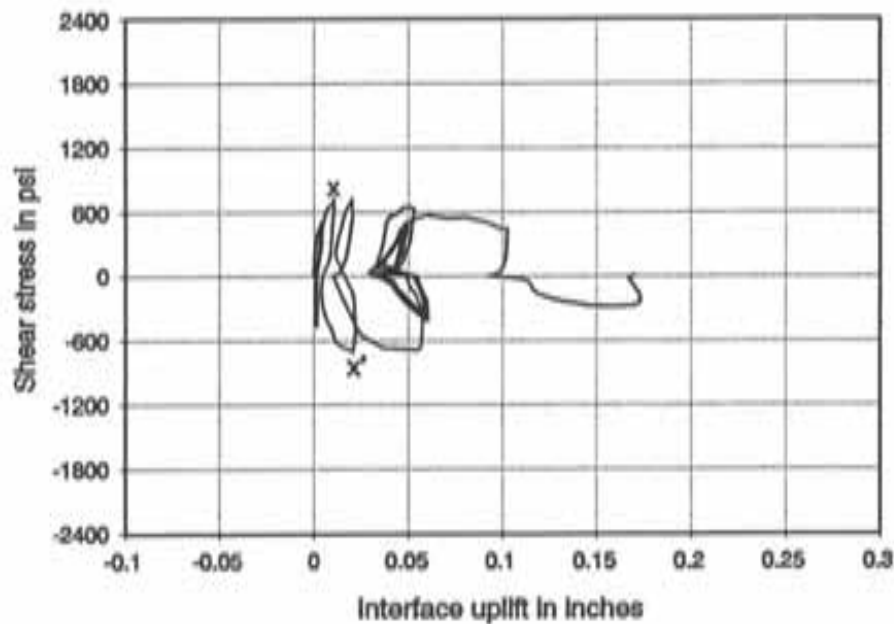


Figure 7.8 Appearance of interface upon failure of aggregate interlock

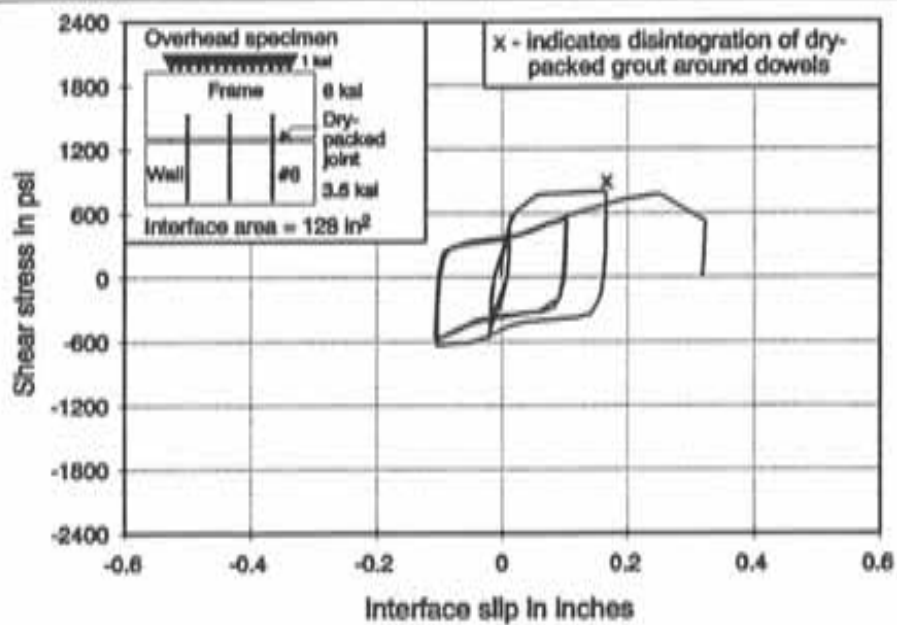


(a) Shear stress vs slip relationship for specimen A4

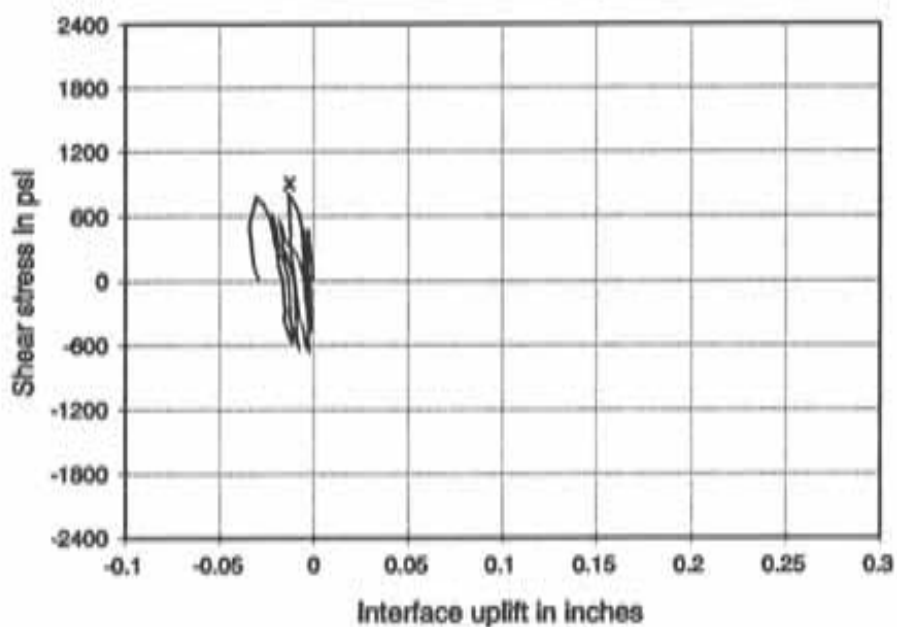


(b) Shear stress vs uplift relationship for specimen A4

Figure 7.9 Peak strength of specimen A4 controlled by disintegration of low-strength concrete around dowels



(a) Shear stress vs slip relationship for specimen B8



(b) Shear stress vs uplift relationship for specimen B8

Figure 7.10 Peak strength of specimen B8 controlled by disintegration of dry-packed grout around dowels

CHAPTER 8

SHEAR TRANSFER ACROSS FRAME-WALL INTERFACES DISCUSSION OF TEST RESULTS AND THEIR IMPLICATIONS, SUMMARY, CONCLUSIONS AND RECOMMENDATIONS

8.1 INTRODUCTION

The effects of the variables investigated on the overall behavior of test specimens are compared using the test results. Variables investigated were shear loading pattern (reversed cyclic vs monotonic), compressive stress across specimen interface, number of dowels across the specimen interface, strength of concrete in segment of test specimen representing the existing structure, and procedure used for construction of the specimen interface. Practical implications of the test results are discussed. Discussions also include the interaction of different variables studied in the test program. Data from selected tests will be presented here to describe typical response. However, data from all tests are included in Appendix B.

8.2 DISCUSSION OF TEST RESULTS AND IMPLICATIONS

8.2.1 Influence of Loading Pattern in Shear

Performance of specimen A2 (subjected to reversed cyclic loading) is compared with that of specimen A3 (subjected to monotonic loading) in Fig. 8.1. The cyclically-loaded test specimen had the same peak shear strength as the monotonically-loaded test specimen but at a slightly larger slip level (0.015 in. vs 0.011 in.). The shear stress vs slip plot for specimen A3 formed an envelope for the hysteresis loops of specimen A2.

The behavior of specimen A8 (subjected to reversed cyclic loading) is compared with that of specimen A5 (subjected to monotonic loading) in Figure 8.2. Interface in both test specimens had constant compressive stress. Peak shear strengths of both test

specimens and corresponding slip levels were identical. Peak points in the hysteresis loops of specimen A8 did not reach the envelope represented by the shear stress vs slip plot of specimen A5. The shear capacity of specimen A8 was 35% less than that of specimen A5 at a slip level of 0.1". The reduced strength during inelastic cycles can be attributed to the damage that occurred during reversed cycling of specimen A8.

Discussion: Peak shear strengths and corresponding slip levels were identical for cyclically-loaded and monotonically-loaded test specimens whether or not the specimen interface was subjected to external compression. Residual shear capacities of cyclically-loaded and monotonically-loaded test specimens were however similar for test specimens with no compression across the interface and were different for test specimens with compression across the interface.

For the cyclically-loaded test specimen that had no external compression across the interface (specimen A2), separation of the interface occurred when dowels across the interface began to pull out after failure of the test specimen (Figs. B.2, and 3 in Appendix B). With external compression across the interface, separation of the interface was less than that with no compression across the interface (Fig. B.20, and 21 in Appendix B). The loss in aggregate interlock due to inelastic cyclic reversals in direct shear was therefore more severe for the test specimen that had external compression across the interface (specimen A8) and consequently its residual shear capacity was not as much as that of the companion specimen which was loaded monotonically (specimen A5).

8.2.2 Influence of External Compression Across Specimen Interface

8.2.2.1 Level of Compression. Figures 8.3, 4, and 5 show the performance of test specimens under different levels of compressive stress; Fig. 8.3 includes test specimens with dowels across the interface, Fig. 8.4 includes test specimens with no dowels across the interface, and Fig. 8.5 includes test specimens with frame segments having low-strength concrete ($f'_c = 1750$ psi). Note that the presence of external compressive stress across the interface of test specimens improved their performance. The higher the level of compression, the better were the peak shear strength, peak-to-peak shear stiffness, and

residual shear capacity of test specimens. Figure 8.6 shows that the residual shear capacity did not increase exactly in the same proportion as the peak shear strength for higher levels of compressive stress. The deterioration of aggregate interlock (at failure) may have become more and more extensive with the increase in level of compression and as a result the residual shear capacity decreased. Residual strengths of test specimens even at slip levels as large as 0.2 in. were about the same or more than the magnitude of permanent net compression across the shear plane (Figs. 8.3a, 4a, and 5a).

8.2.2.2 Pattern of Compression (Constant vs Cyclic). The effect of different patterns of compressive stress across the interface on the performance of test specimens is shown in Fig. 8.7. Specimens B5 (constant level of compression) and B9 (cyclic pattern of compression shown in Fig. 8.15) were characterized by identical behaviors until they reached their peak shear strengths (Fig. 8.7c). However the inelastic behaviors of both specimens differed significantly. Residual shear capacity of specimen B9, particularly at smaller slip levels, was significantly less than that of specimen B5. Such a drastic drop in residual shear capacity may be attributed to the cyclic pattern of external compression since the shear capacity was dependent of the external compression. The role of dowels present across the interface of specimen B9 became significant after the specimen's failure. Because, the dowels pulled out due to anchorage failure (Figs. B.47 and 48 in Appendix B).

Discussion: Test results show that the behavior of "new concrete - to - existing concrete" connections is influenced significantly by the level of external compression that existed across the interface. The higher the level of compression across the interface, the better were peak shear strength, peak-to-peak shear stiffness, and residual shear capacity of test specimens. Improvement in residual shear capacity, however, depended on the pattern of such compression (whether it was constant or cyclic) and was affected (reduced) significantly when the pattern was cyclic.

In a frame-wall system, the benefit of external compression can be considered in design of frame-wall connections by estimating the seismic lateral loads that are expected to act on the frame-wall system and by determining the geometric properties of the frame-wall system such as its aspect ratio. The magnitude of external compression that results across the interface from seismic forces is a function of the strut angle (formed in the infilled

wall) which in turn is governed by the frame-wall aspect ratio. It must, however, be remembered that compression across a frame-wall interface resulting from seismic loads is cyclic. Cyclic compression as established by behavior of specimen B9 reduced the residual shear capacity significantly. Better residual shear capacity of frame-wall connections must be achieved since frame-wall connections that have failed in a major earthquake may be subjected to other earthquakes and/or aftershocks before the connections can be repaired. Also, the possibility of a pre-existing potential crack along the shear planes caused by factors unrelated to shear such as tension forces caused by restrained shrinkage, temperature deformations, accidental damage, etc must be taken into consideration. The presence of pre-existing cracks along the shear plane whose overall behavior in shear may be inelastic can affect the shear strength and stiffness of connections. Caution must therefore be exercised in considering the benefit of cyclic compression.

8.2.3 Influence of Dowels Across the Specimen Interface

Performance of specimen B1 (3 #6 dowels) is compared with that of specimen B2 (6 #6 dowels) in Fig. 8.8. Peak shear strength of specimen B2 was 15 percent higher than that of specimen B1. Peak-to-peak shear stiffness of specimen B2 was also better than that of specimen B1 (Fig. 8.8b). Residual shear capacities of both test specimens dropped significantly (Figs. 8.8a and 8b) because peak shear strengths were limited by pull out failure of dowels.

The performance of specimen B5 (3 #6 dowels) is compared with that of specimen B6 (6 #6 dowels) in Fig. 8.9. Both test specimens had external compression across the interface. Peak shear strengths and peak-to-peak shear stiffnesses of both test specimens were identical (Fig. 8.9b). Uplifts measured across the interface remained negative (Figs. B.35, 36, 38, and 39 in Appendix B) until the test specimens reached their peak shear strengths. Measured identical peak shear strengths and negative uplifts until failure indicated that the dowels present across the interface did not contribute to the peak shear strengths significantly. Residual shear capacity of specimen B6 at larger slip levels was however slightly higher than that of specimen B5 (Fig. 8.9a) since specimen B6 had 6 #6 dowels

instead of 3 #6 dowels in specimen B5. Peak shear strength of both test specimens was controlled by failure of aggregate interlock which resulted in a significant drop (more than 40 percent) in residual shear capacity.

Discussion. The influence of different number of dowels across the interface on overall performance (peak shear strength, peak-to-peak shear stiffness, and residual shear capacity) of test specimens depended on whether or not there was compressive stress across the interface. In the absence of compressive stress, more dowels improved the peak shear strength, peak-to-peak shear stiffness, and residual shear capacity of test specimens. Whereas, dowels in test specimens with external compression across the interface did not contribute to peak shear strength. The contribution of dowels to residual shear capacity through pure dowel action was minimal even at larger slip levels. Because, specimen B6 with 6 #6 dowels across the interface had residual shear strength only slightly higher than that of specimen B5 which had 3 #6 dowels across the interface. The pull out of dowels at failure of specimen B9 (which was subjected to cyclic compression as shown in Fig. 6.15) verified the importance of their presence when the external compression is cyclic and showed the necessity of anchoring the dowels adequately to avoid premature pull out failures (Figs. B.46, 47, and 48 in Appendix B).

Frame-wall connections subjected to seismic lateral loads can be designed in two different ways; (1) by accounting for the compression that would result from seismic forces across the interface and by neglecting the presence of dowels, or (2) by accounting for the presence of dowels across the interface and by neglecting the benefit of compressive stress. Benefit by both, i.e. presence of dowels and external compression, should not be combined because both cannot be mobilized at the same time. Test results indicate that shear capacities (peak strength and residual capacity) of test specimens with constant compressive stress across the interface were much better than those of test specimens with only dowels across the interface. However, in view of the cyclic nature of compressive stresses, which would reduce the residual shear capacity significantly and would also affect the shear strength and stiffness of interfaces that are already cracked due to factors unrelated to shear, connections should be designed conservatively based on the influence of dowels. Also, dowels provided across the interface must be anchored (if possible) to yield in tension (since design equations on estimation of connection shear capacity are

usually based on the nominal tensile yield strength of dowels) or more dowels should be provided to account for premature pull out failure of dowels.

8.2.4 Influence of Strength of Concrete in the Frame Segment

Performance of specimen A2 (frame $f'_c = 1750$ psi) is compared with that of specimen B1 (frame $f'_c = 3500$ psi) in Fig. 8.10. Peak shear strength of specimen B1 was about 50 percent higher than that of specimen A2. Peak shear strengths of both test specimens were controlled by different failure modes; while peak shear strength of specimen A2 was controlled by disintegration of concrete around dowels (which pulled out at larger slip levels as shown in Figs. B.2 and 3 in Appendix B) in the frame segment, peak shear strength of specimen B1 was controlled by pull out failure of dowels. Simple pull out tests (refer to Appendix C) conducted on frame segments of two different strengths showed that the average pull out strength of dowels embedded in frame segments of lower strength concrete ($f'_c = 1750$ psi) was about 13 percent less than that of dowels embedded in frame segments of higher strength concrete ($f'_c = 3500$ psi). Lower peak shear strength of specimen A2 (about 33 percent less than that of specimen B1) can be attributed to the different failure mode (since disintegration of lower strength concrete in the frame segment of specimen A2 preceded pull out failure of dowels which controlled the peak shear strength of specimen B1) and the weaker aggregate interlock (due to lower strength concrete in the frame segment). As evidenced in Fig. 8.10b, the peak-to-peak stiffness of specimen B1 was better than that of specimen A2 due to the stronger aggregate interlock. Residual shear capacity of specimen B1 was better than that of specimen A2 at smaller slip levels and was almost similar at larger slip levels (slips > 0.2 in.). Pull out of dowels at larger slip levels caused separation of the interface in the frame and wall segments thereby resulting in loss of aggregate interlock and identical residual shear capacities.

In Fig. 8.11, the performance of specimen A6 (frame $f'_c = 1750$ psi) is compared with that of specimen B5 (frame $f'_c = 3500$ psi). Both test specimens had external compression across the interface. Peak shear strength of specimen B5 was about 45 percent higher than that of specimen A6. The peak shear strengths of both test specimens were controlled by failure of aggregate interlock which was apparently stronger in specimen

B5. Measured negative uplifts until or even after failure of specimens A6 and B5 (Figs. B.14, 15, 35, and 36 in Appendix B) indicated that dowels across the interface did not contribute to peak shear strengths of test specimens. Peak-to-peak shear stiffness of specimen B5 was better than that of specimen A6 (Fig. 8.11b). Residual shear capacities of both test specimens did not differ significantly (Figs. 8.11a).

Discussion. The strength of concrete in the frame segments influenced the performance of test specimens whether or not there was compressive stress across the interface. The higher the strength of concrete in the frame segment, the better were peak shear strength and peak-to-peak shear stiffness of test specimens. While peak shear strengths of test specimens that had no external compression across the interface were controlled by disintegration of frame concrete around dowels or dowel pull out, peak shear strengths of test specimens that had external compression across the interface were controlled by failure of aggregate interlock.

Frame-wall shear connections with relatively weaker frame elements (having low-concrete strength) must be provided with more dowels since their shear strength may be governed by disintegration of frame concrete around the dowels.

8.2.5 Influence of Procedures Used for Interface Construction

Performance of specimen B1 (concrete was cast directly against the sandblasted interface of the frame segment) is compared with that of specimen B7 (gap between frame and wall segments was dry-packed with cementitious grout) in Fig. 8.12. Peak shear strength of specimen B7 was about 54 percent less than that of specimen B1. Interface in specimen B7 slipped extensively (about seven times the slip level corresponding to peak strength of specimen B1) before reaching its peak strength (Fig. 8.12b). The dry-packed grout in specimen B7 was apparently not as strong as the concrete in the interface of specimen B1. The strength of the grouted interface in specimen B7 was also impaired by the absence of coarse aggregate that provided interlock in the interface of specimen B1. Dowel action was the major contributor to shear strength of grouted interface in specimen

B7. Peak shear strengths of both test specimens were limited by pull out failure of dowels. Peak-to-peak shear stiffness of specimen B7 was less than that of specimen B1 (Fig. 8.12b).

In Fig. 8.13, the performance of specimen B5 (concrete was cast directly against the sandblasted interface of frame segment) is compared with that of specimen B8 (gap between frame and wall segments was dry-packed with cementitious grout). Both test specimens had external compression across the interface. Peak shear strength of specimen B8 was about 60 percent less than that of specimen B5. Slip levels corresponding to peak strengths of specimens B8 and B5 had a ratio of about 8 (Fig. 8.13a). Absence of aggregate interlock and presence of dry-packed grout in the interface reduced the shear strength and stiffness of specimen B8. Dowel action was the major contributor to shear strength of grouted interface in specimen B8. While peak shear strength of specimen B5 was controlled by failure of aggregate interlock, the peak shear strength of specimen B8 was limited by disintegration of dry-packed grout around the dowels.

Discussion. Strength and stiffness of grouted (dry-packed) interfaces were much less than those of interfaces constructed by casting concrete directly against the sandblasted surface of frame segments. Absence of aggregate interlock and presence of dry-pack material in the interface resulted in significant reduction in strengths and stiffnesses of grouted interfaces. Dowel action was the major contributor to shear strength of grouted interfaces. It must be remembered that slip levels at which specimens with grouted interfaces developed their peak shear strengths may not be within the useful slip levels that would typically occur in a frame-wall interface. Tests conducted by Gaynor [13] and Shah [33] showed that measured maximum slips (frame-wall interface displacements) were in the order of 0.01 to 0.06 inches.

Grouting of frame-wall interface (typically the top frame-wall interface) must be avoided as far as possible. Suitable methods that would enable this interface type to be constructed to enable aggregate interlock and better confinement must be explored and resorted to.

8.3 SUMMARY, CONCLUSIONS AND RECOMMENDATIONS

The study focussed on investigating shear transfer mechanisms across frame-wall interfaces. The investigation involved constructing test specimens that would represent a portion of a frame-wall interface, subjecting the specimens to different load patterns, and making recommendations based on the test results. The performance of the test specimens was evaluated using three major criteria; shear strength, shear stiffness, and residual shear capacity (post-failure capacity). The following conclusions were arrived at based on the test results:

(1) Peak shear strengths and corresponding slip levels were similar for cyclically-loaded (reversed cyclic) and monotonically-loaded test specimens whether or not the specimen interface was subjected to external compression.

Residual shear capacities of cyclically-loaded and monotonically-loaded test specimens were however similar for test specimens with no compression across the interface and were different for test specimens with compression across the interface. Test specimen subjected to reversed cyclic loading with compression across the interface possessed less residual capacity due to the increased loss in aggregate interlock that occurred during cyclic reversals.

(2) Presence of external compression across interfaces improved the performance of test specimens significantly. The higher the level of compression, the better were peak shear strength, peak-to-peak shear stiffness, and residual shear capacity. However, residual shear capacity was reduced significantly when external compression was cyclic.

The benefit of cyclic compression, which reduces the residual shear capacity significantly and also affects the shear strength of interfaces that are already cracked due to factors unrelated to shear, that results across frame-wall interfaces from seismic forces shall be neglected conservatively and an adequate number of dowels shall be provided across the interface so as to transfer design shear forces effectively. The number of dowels shall be determined based on the shear-friction provisions as proposed by ACI 318-89 [3].

Even though the role of dowels was insignificant (under the presence of external compression across the interface) until the test specimens reached the peak shear strength,

their contribution (under cyclic compression) to residual shear capacity through dowel tension verified the importance of their presence.

(3) The influence of the number of dowels across the interface on the overall performance (peak shear strength, peak-to-peak shear stiffness, and residual shear capacity) of test specimens depended on whether or not there was external compression across the interface. In the absence of external compression, more dowels improved the peak shear strength, peak-to-peak shear stiffness, and residual shear capacity of test specimens.

The contribution of dowel action to peak shear strength was minimal (whether or not the interface was subjected to external compression) because test specimens reached the peak shear capacity at relatively smaller slip levels.

Dowels provided across the interface must be anchored to yield in tension (if possible) or more dowels should be provided to account for premature pull out failures.

(4) Strength of concrete in segment of test specimen representing the existing structure (frame) influenced the performance of test specimens whether or not there was external compression across the interface. The higher the strength of concrete in the frame segment, the better were the shear strength and stiffness of test specimens.

Frame-wall shear connections with relatively weaker frames (having low-strength concrete) must be provided with more dowels since their strength may be governed by disintegration of frame concrete around the dowels.

(5) Strength and stiffness of grouted (dry-packed) interfaces were much less than that of interfaces constructed by casting concrete directly against the sandblasted surface of frame segments. Absence of aggregate interlock and presence of dry-packed grout in the interface resulted in significant reduction in shear strength and stiffness of grouted interfaces. The slip levels at which specimens with grouted interfaces developed peak shear strength were not within the useful slip levels that would typically occur in a frame-wall interface.

Grouting of a frame-wall interface (typically the top frame-wall interface) must be avoided as far as possible. Suitable methods that would enable such an interface to be

constructed enabling aggregate interlock and better confinement must be explored and resorted to. In cases where the infill walls are shotcreted, the separations and voids near the bottom of the beam can be patched up using epoxy injection (Figs. 2.3 & 4). For cast-in-place walls, top frame-wall joint construction will depend on feasibility of construction. The walls can also be cast eccentrically with the frame as shown in Fig. 2.7.

8.4 SUGGESTIONS FOR FURTHER RESEARCH

(1) Effect of direct tensile stresses acting transverse to the shear plane. The current study focussed on investigating the influence of direct compressive stresses acting transverse to the shear plane. Pattern of external compression applied across the shear plane was either of constant magnitude or cyclic nature.

Shear planes such as frame-wall interfaces are usually subjected to reversed cyclic transverse stresses (compressive and tensile stresses) under the action of seismic forces. It may therefore be of interest to study the influence of such reversed cyclic transverse stresses (acting across the shear plane) on direct shear transfer capacity. If some of tensile capacity is already utilized by "tension" across interface, "rest" may be available for shear transfer.

(2) Effect of pre-existing cracks formed by factors unrelated to shear. Test results from the current study showed that the post-failure capacity of the shear plane was reduced significantly when external compression acting across the shear plane was cyclic.

It is considered that the presence of pre-existing potential cracks along a shear plane caused by factors unrelated to shear such as restrained shrinkage, temperature deformations, accidental damage, etc may influence the shear strength and stiffness of shear planes significantly, especially when the compression resulting across the shear plane will be of cyclic nature. Since the compression resulting across shear planes from seismic forces is of cyclic nature, a study on the effect of these pre-existing cracks on shear strength and stiffness of shear planes will be of use and interest.

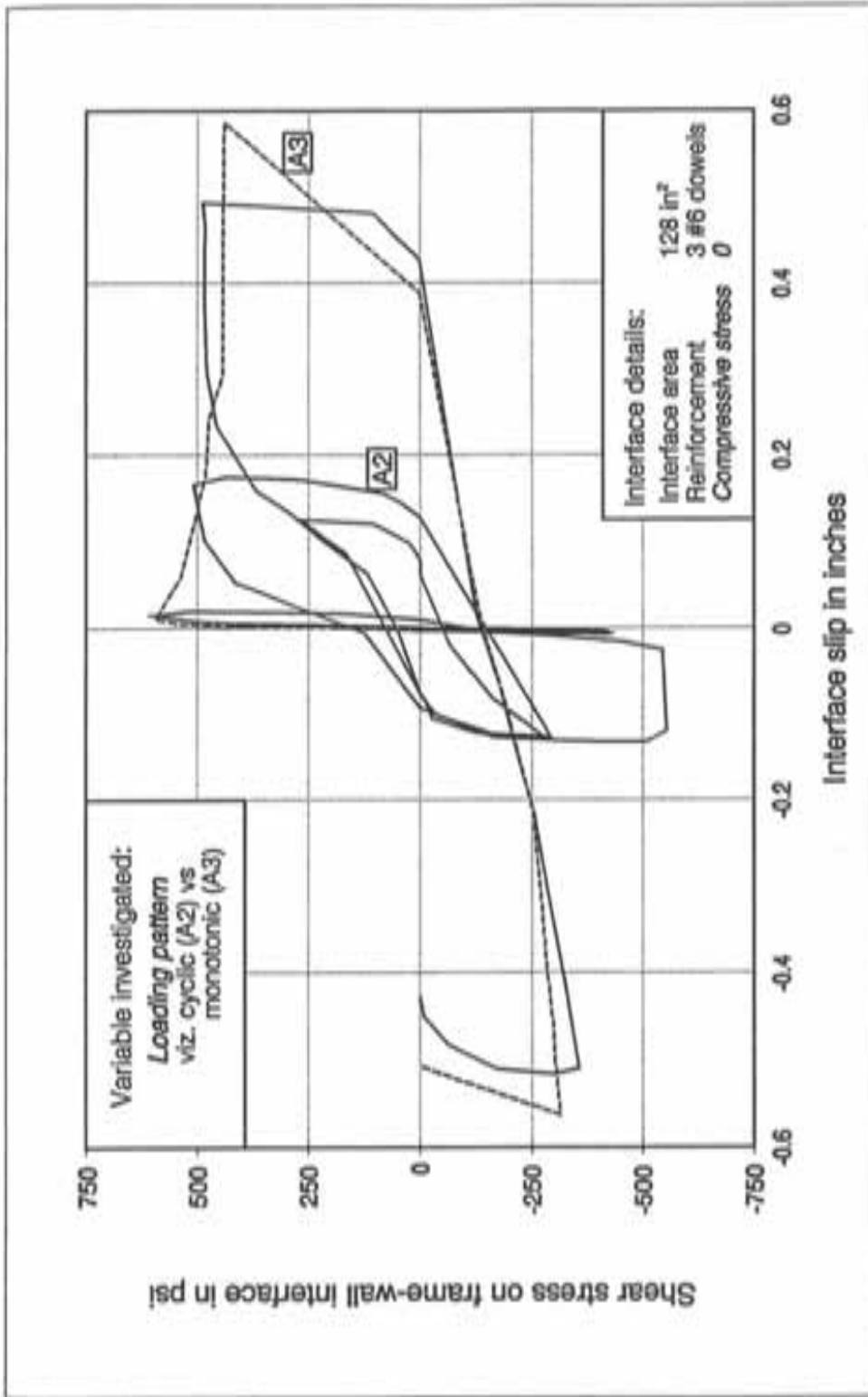


Figure 8.1 Performance of test specimens without compressive stress for different loading patterns

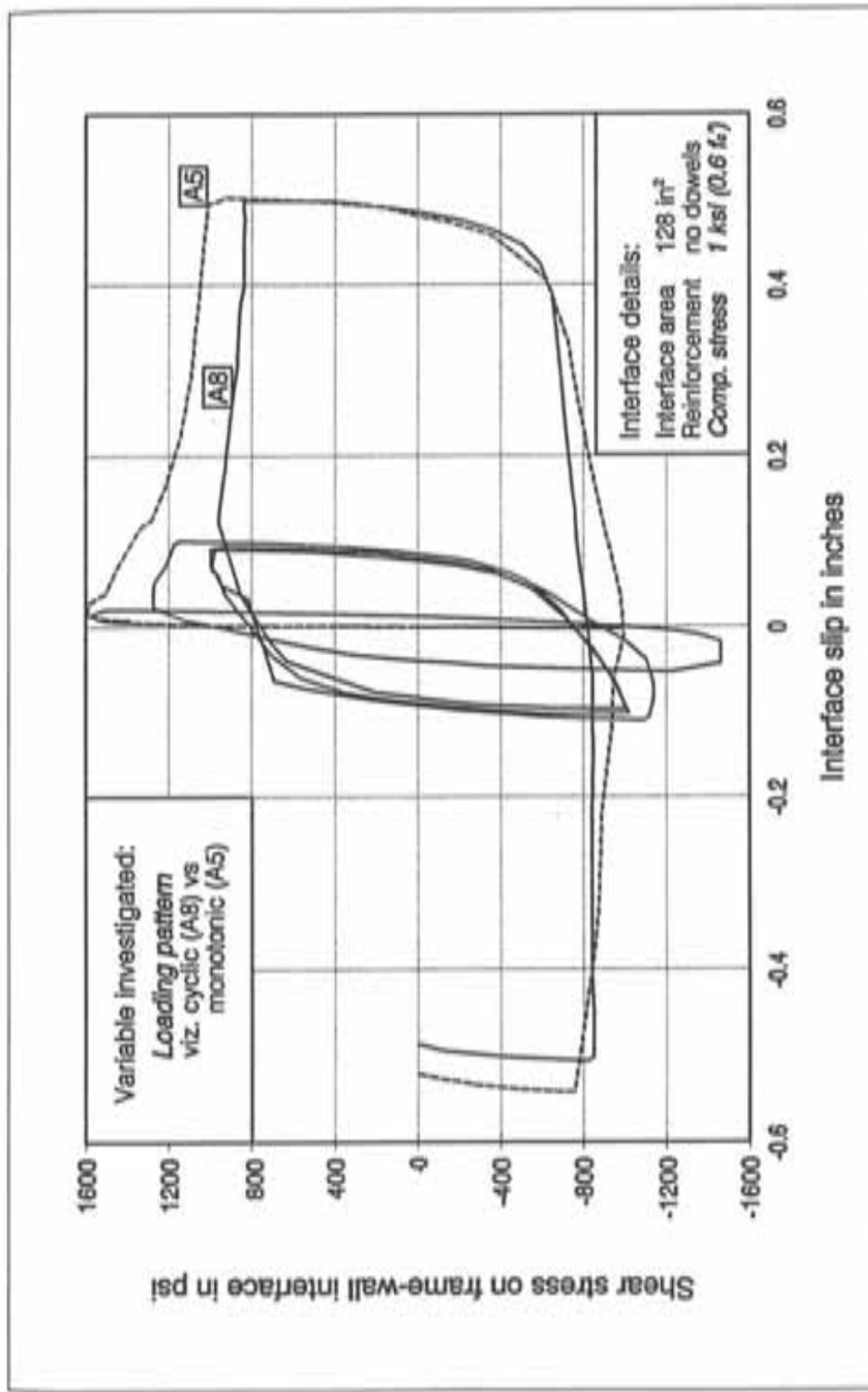


Figure 8.2 Performance of test specimens with compressive stress for different loading patterns

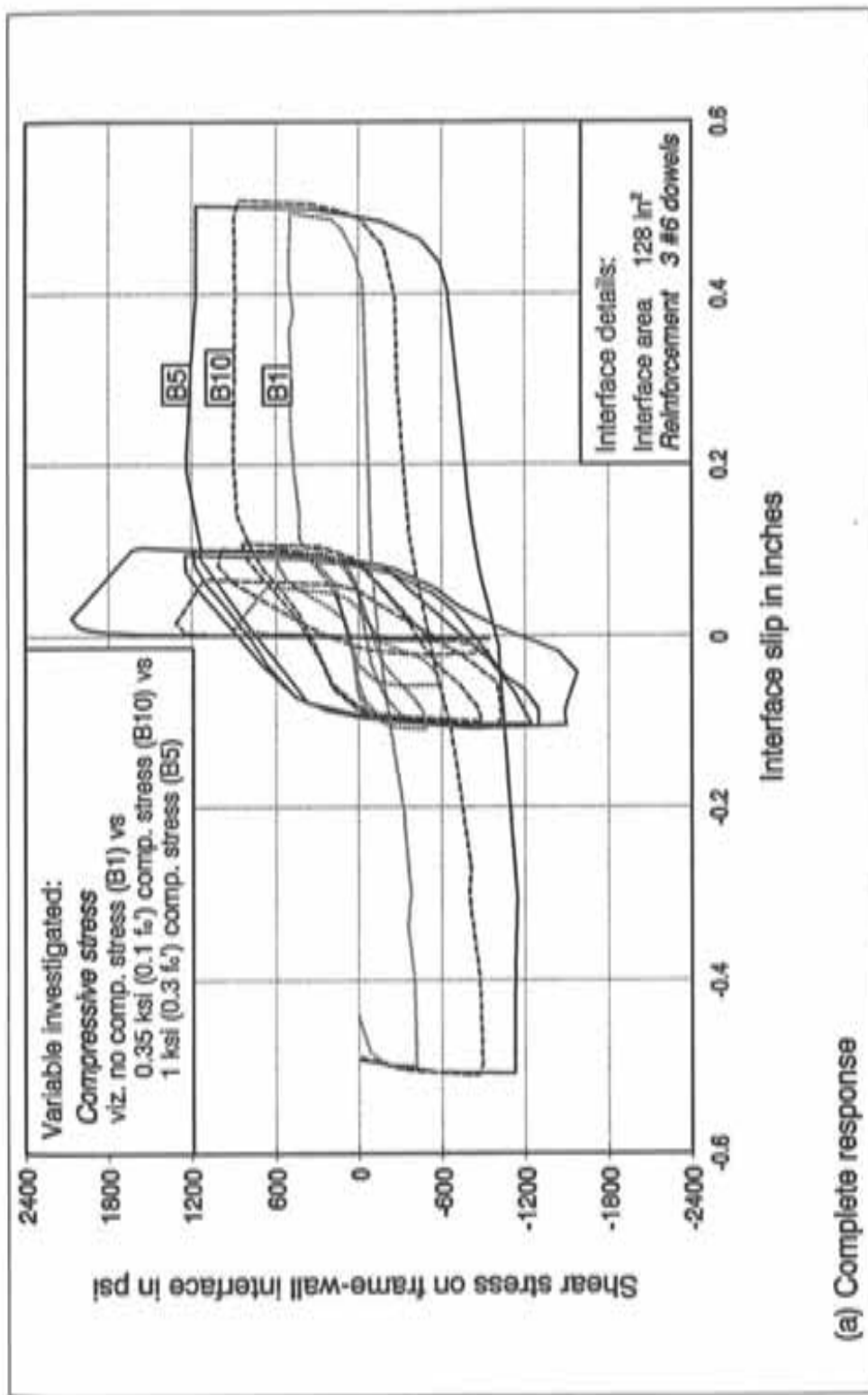


Figure 8.3 Performance of test specimens with dowels for different levels of compressive stress (contd.)

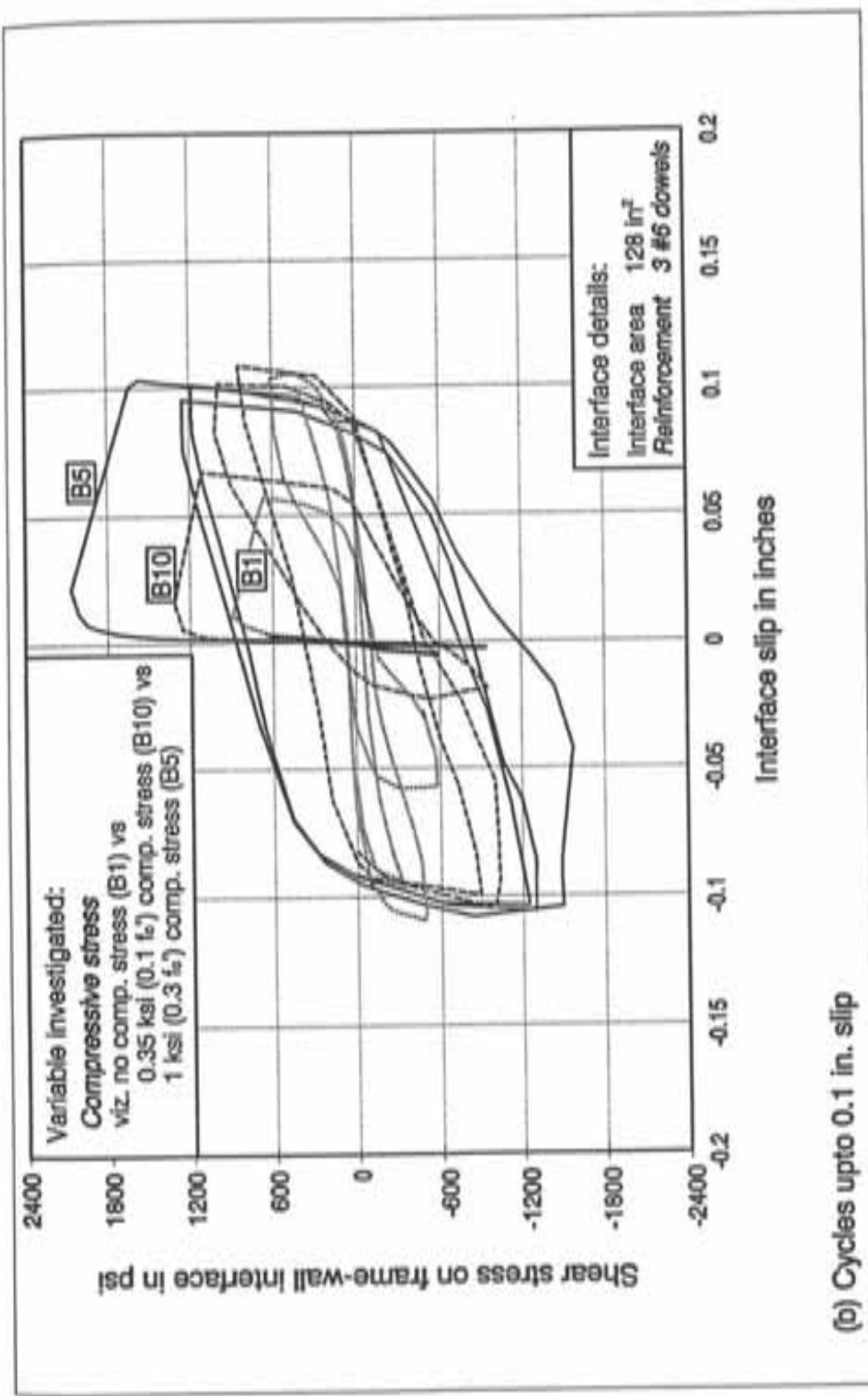
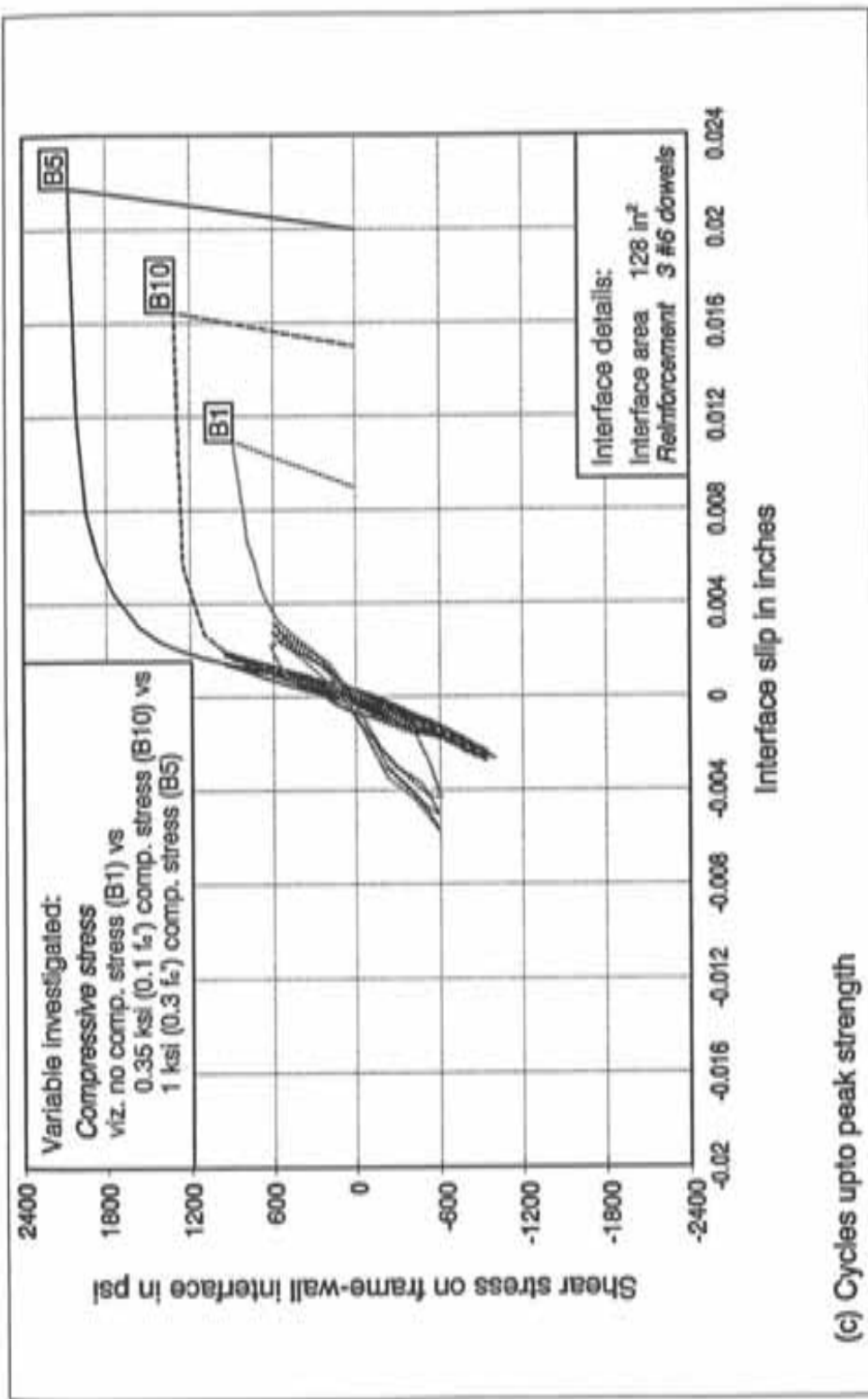


Figure 8.3 Performance of test specimens with dowels for different levels of compressive stress (contd.)



(c) Cycles upto peak strength

Figure 8.3 Performance of test specimens with dowels for different levels of compressive stress

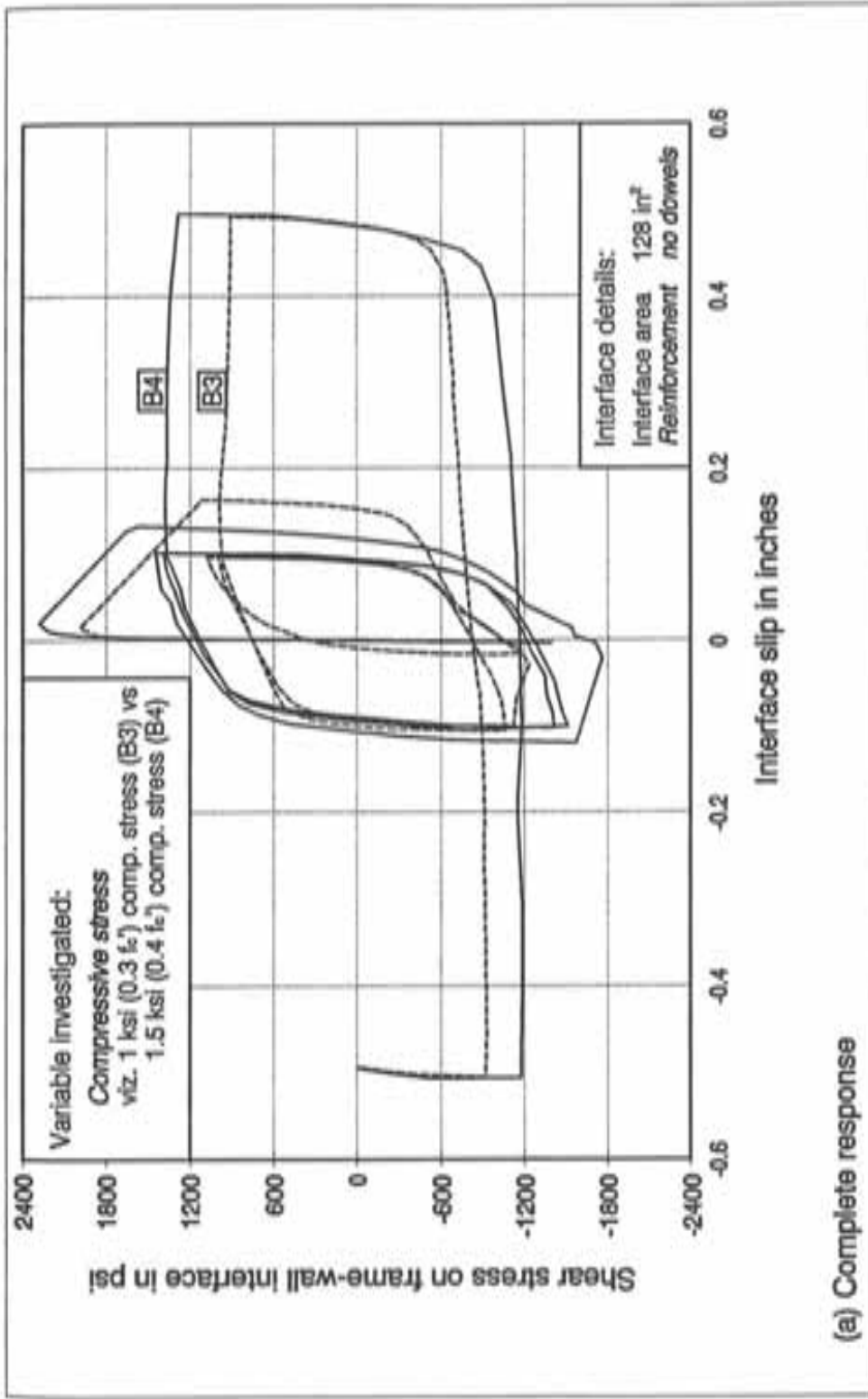


Figure 8.4 Performance of test specimens without dowels for different levels of compressive stress (contd.)

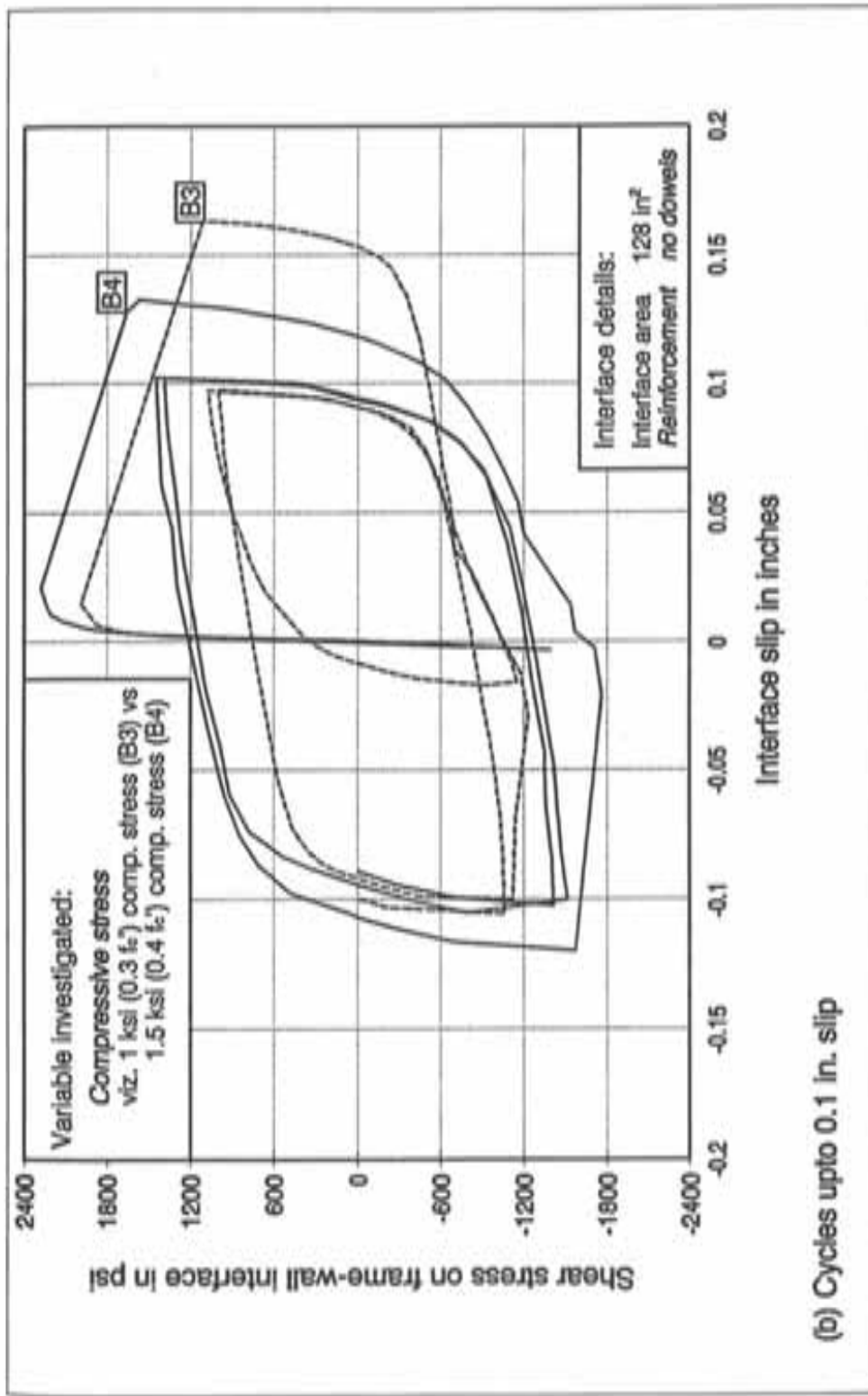


Figure 8.4 Performance of test specimens without dowels for different levels of compressive stress (contd.)

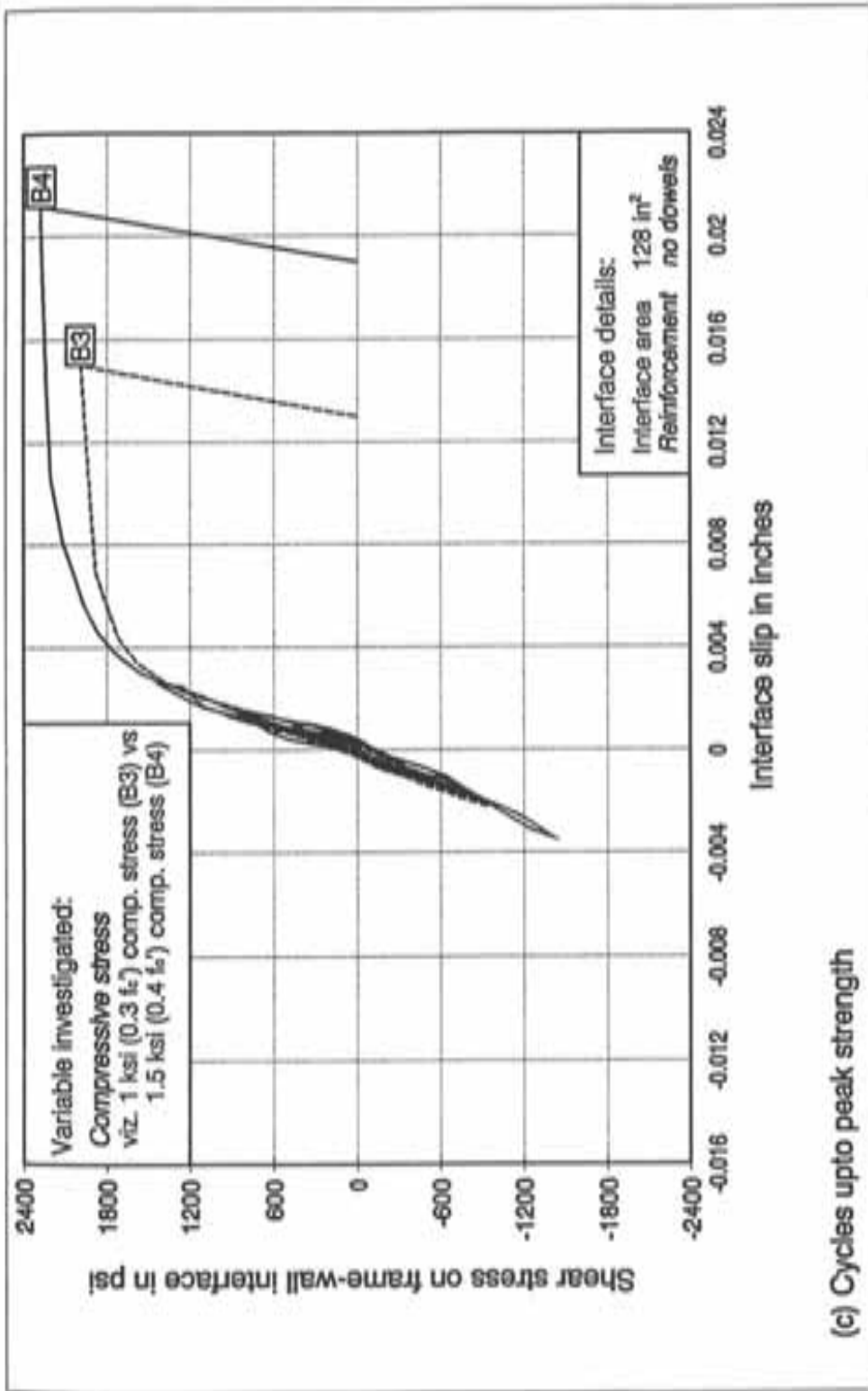


Figure 8.4 Performance of test specimens without dowels for different levels of compressive stress

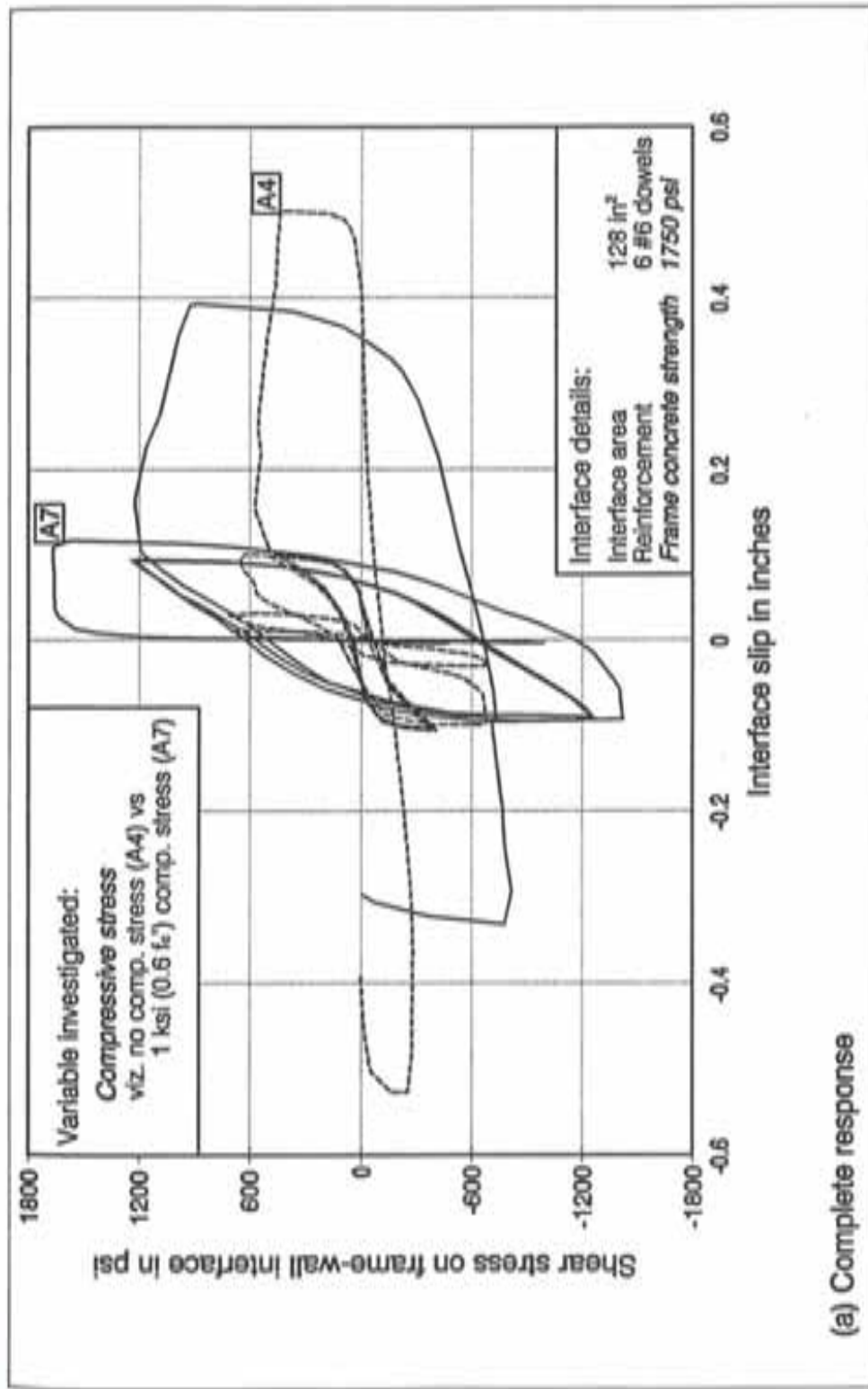


Figure 8.5 Performance of test specimens with lower frame strength for different levels of compressive stress (contd.)

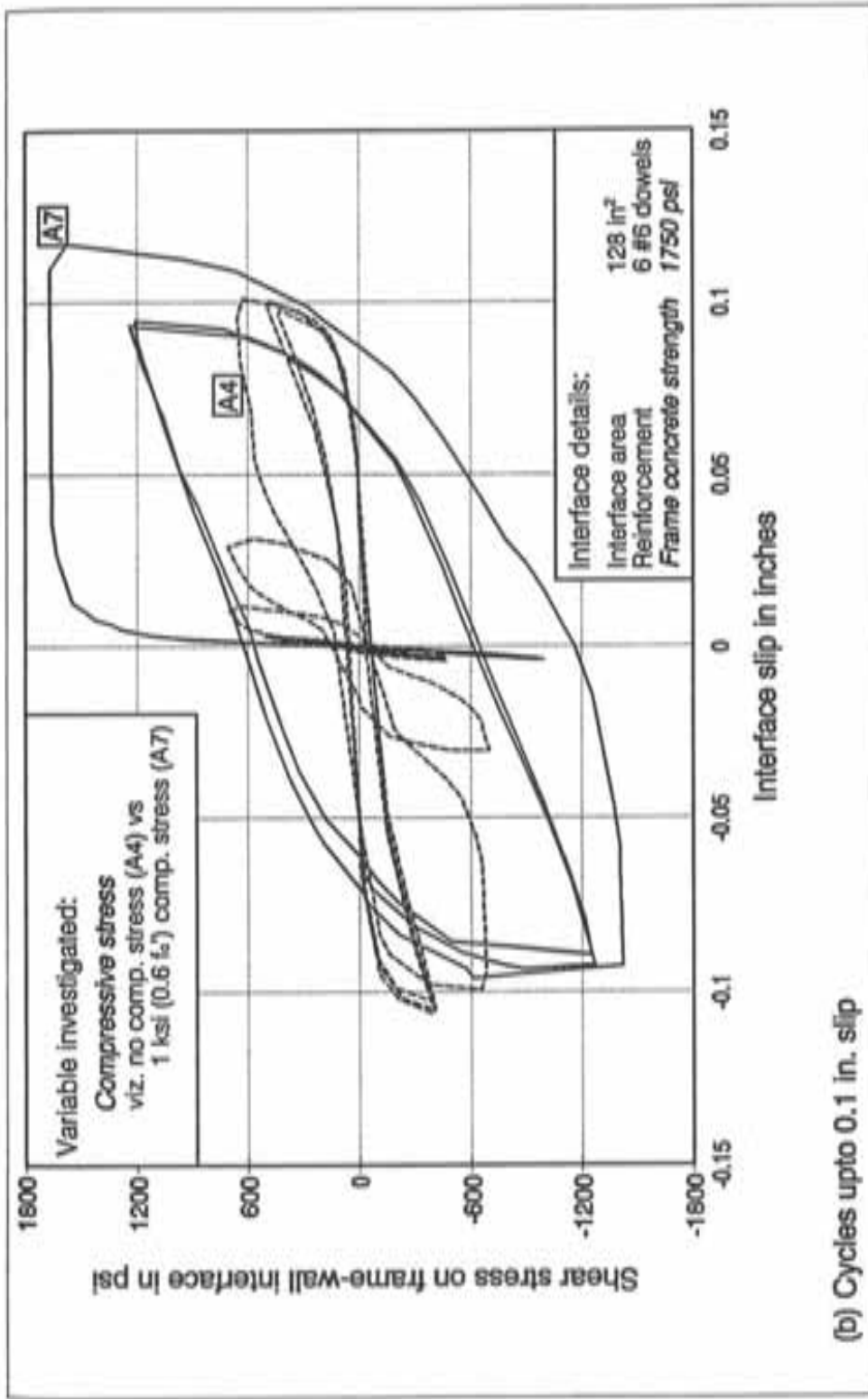
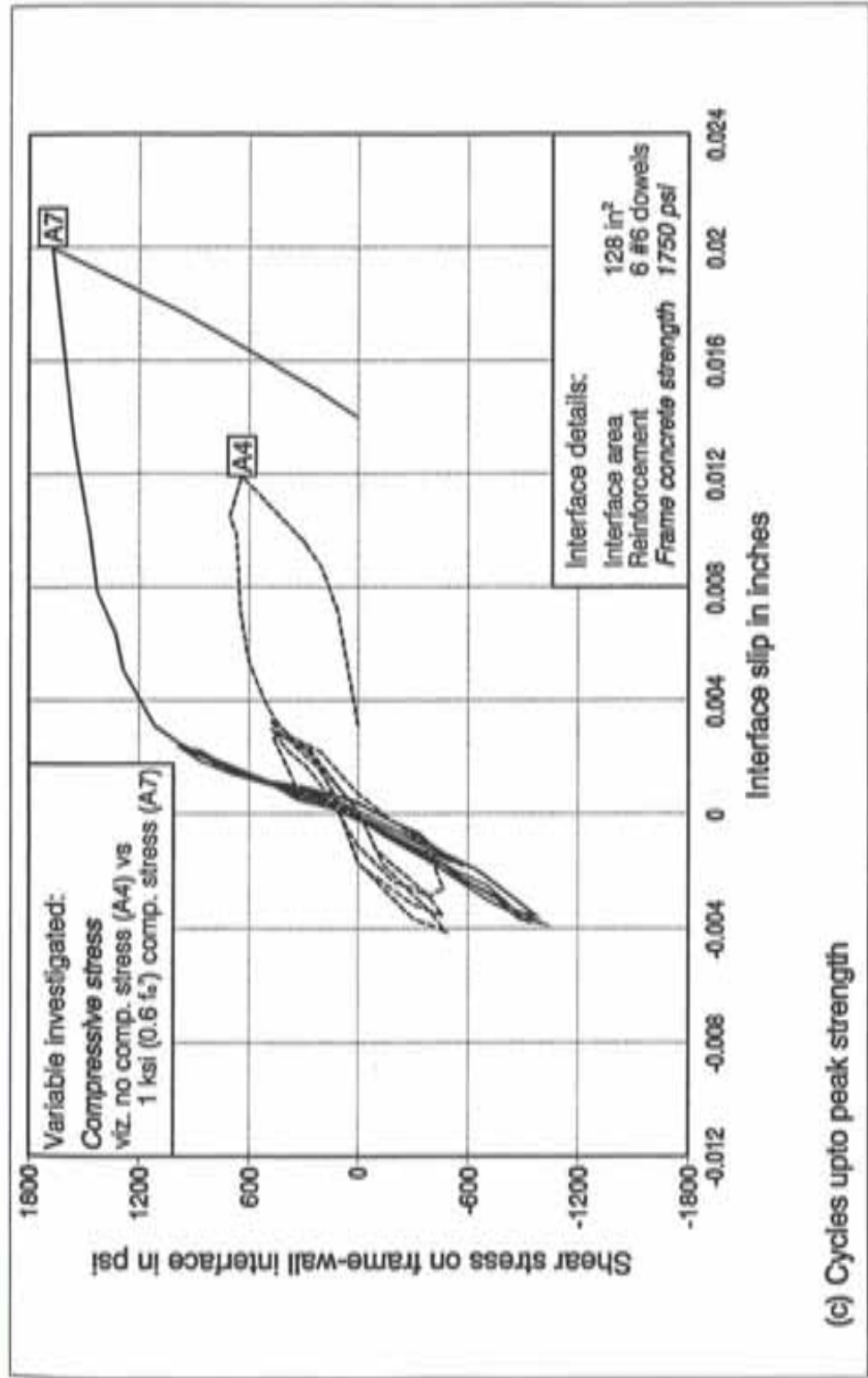


Figure 8.5 Performance of test specimens with lower frame strength for different levels of compressive stress (contd.)



(c) Cycles upto peak strength

Figure 8.5 Performance of test specimens with lower frame strength for different levels of compressive stress

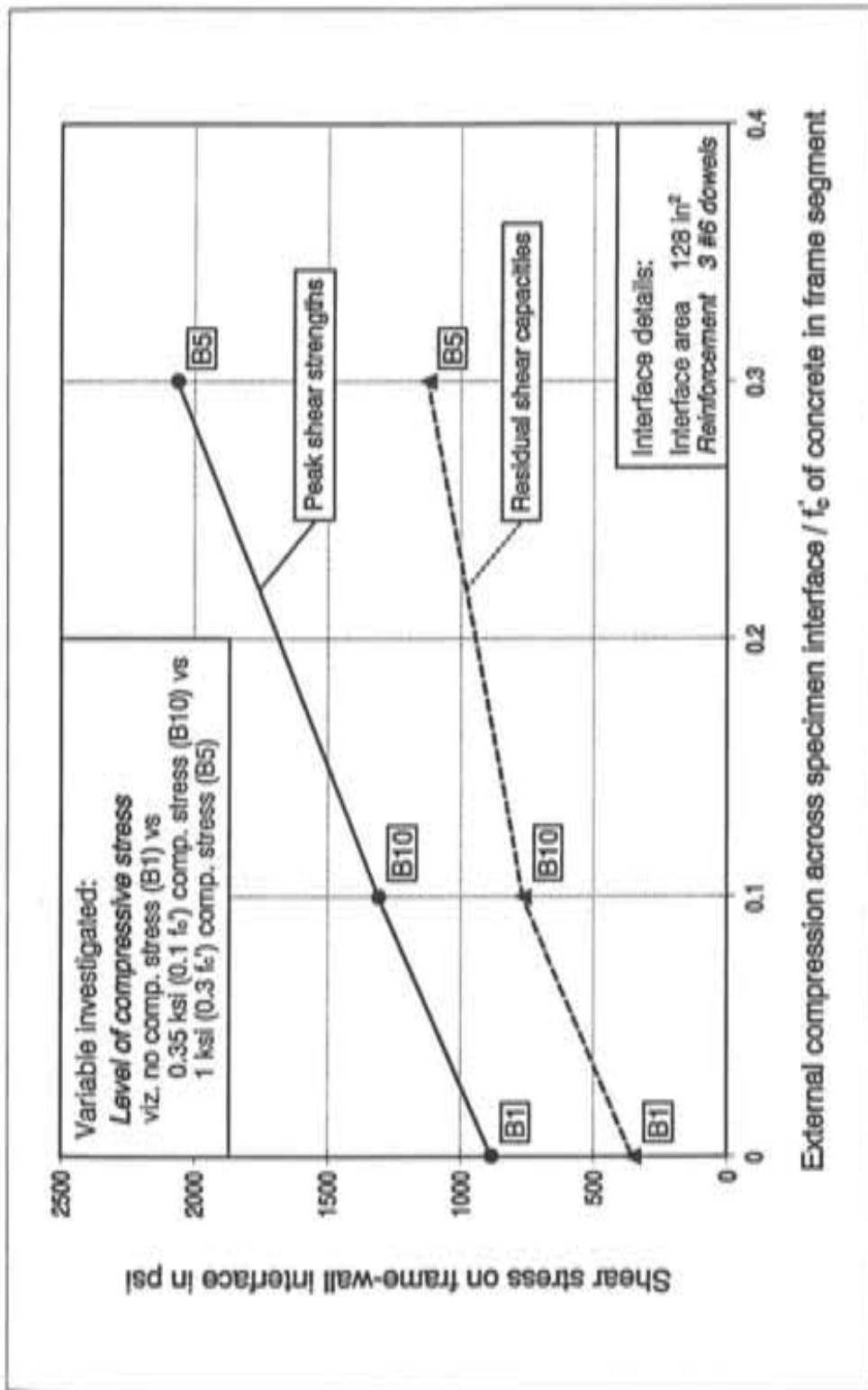


Figure 8.6 Peak strengths and residual capacities of test specimens for different levels of compressive stress

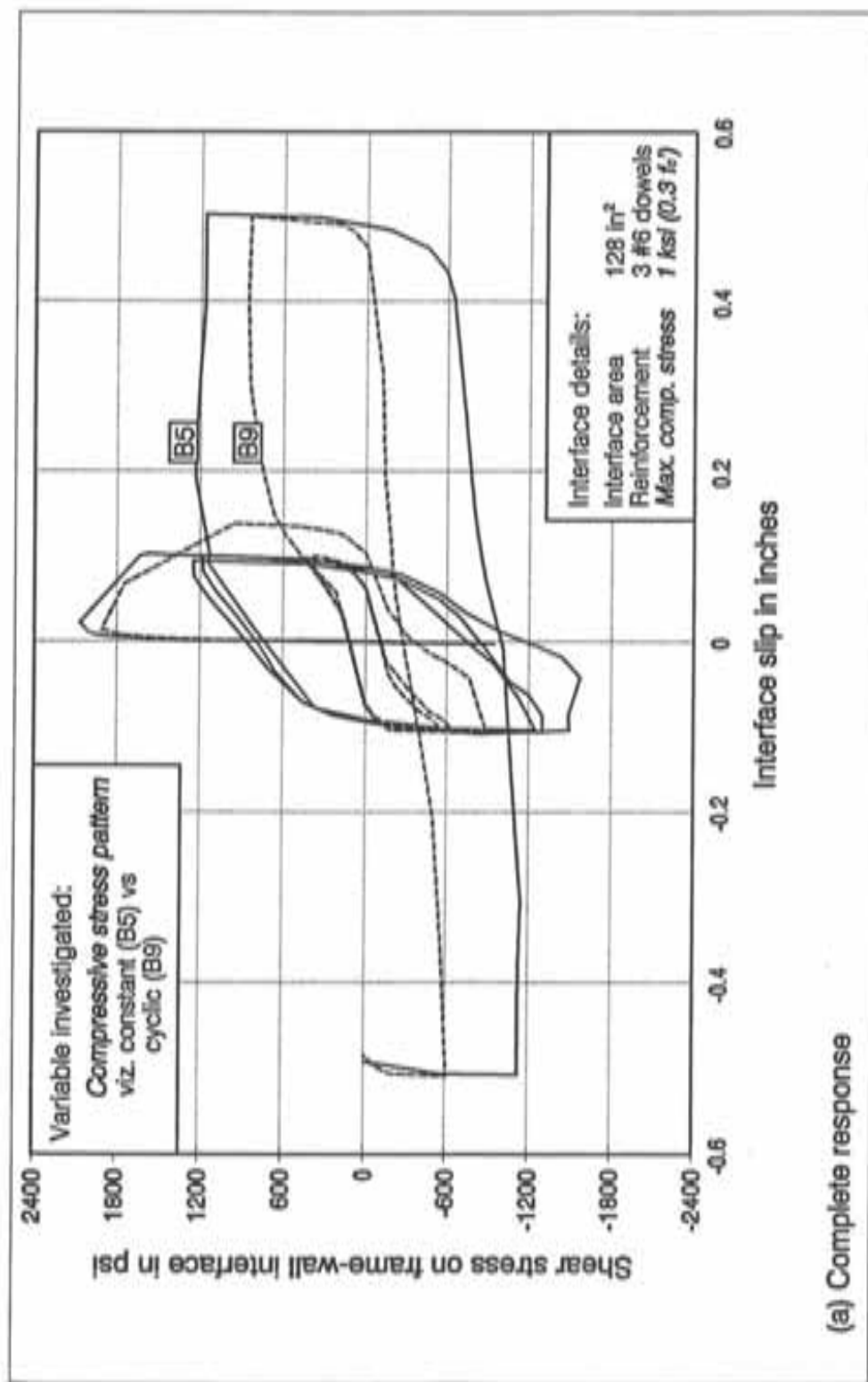


Figure 8.7 Performance of test specimens with different patterns of compressive stress (contd.)

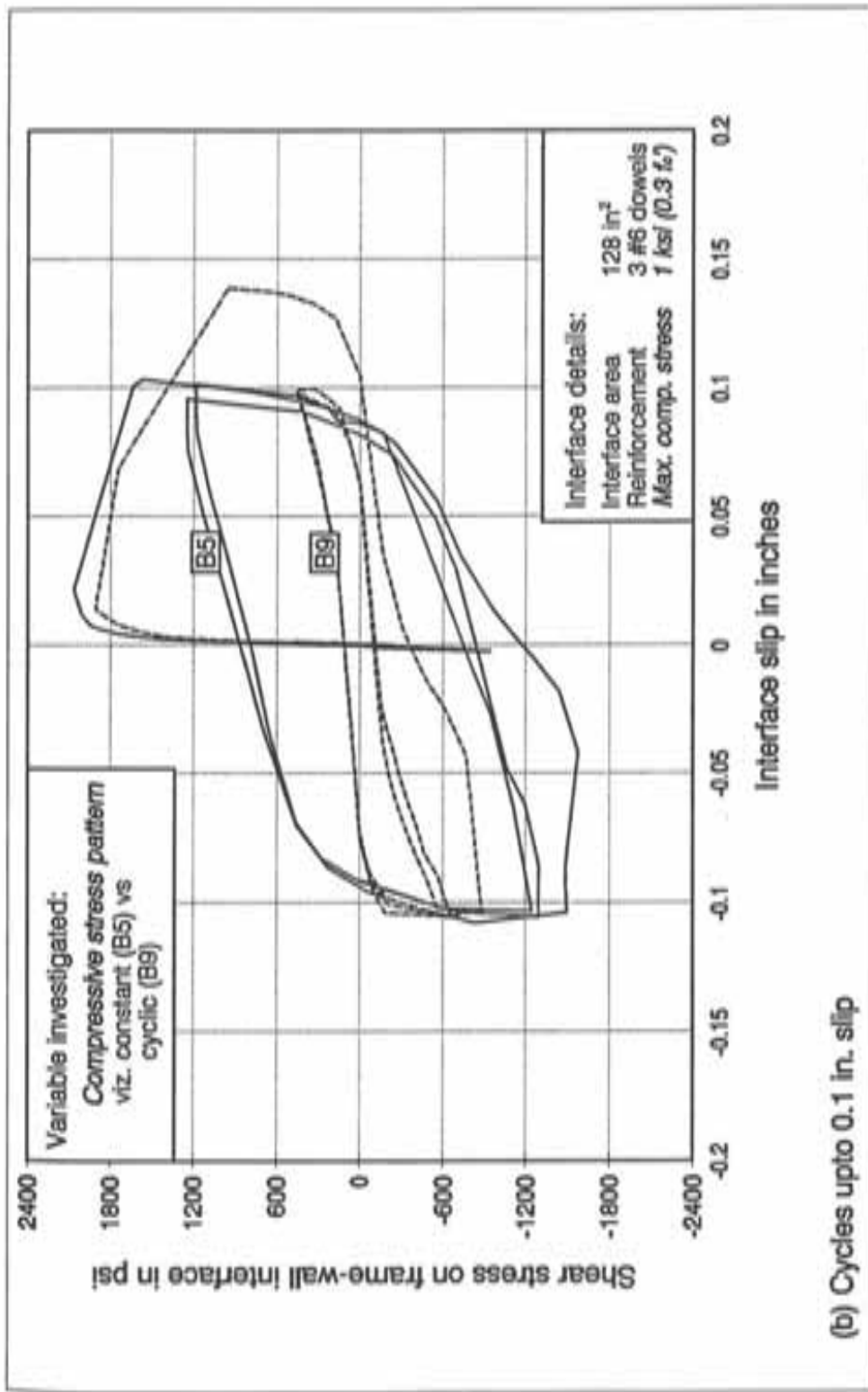


Figure 8.7 Performance of test specimens with different patterns of compressive stress (contd.)

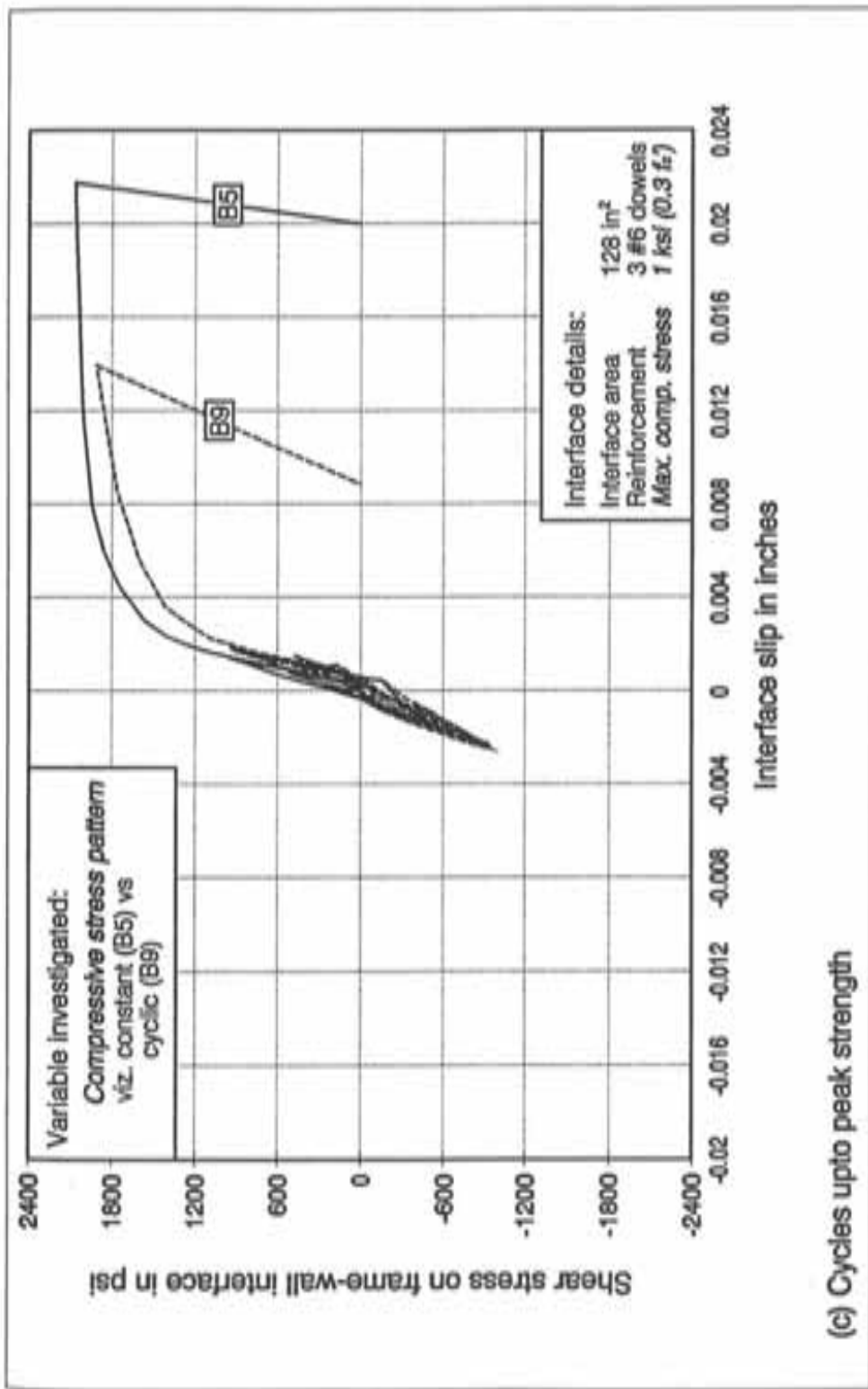
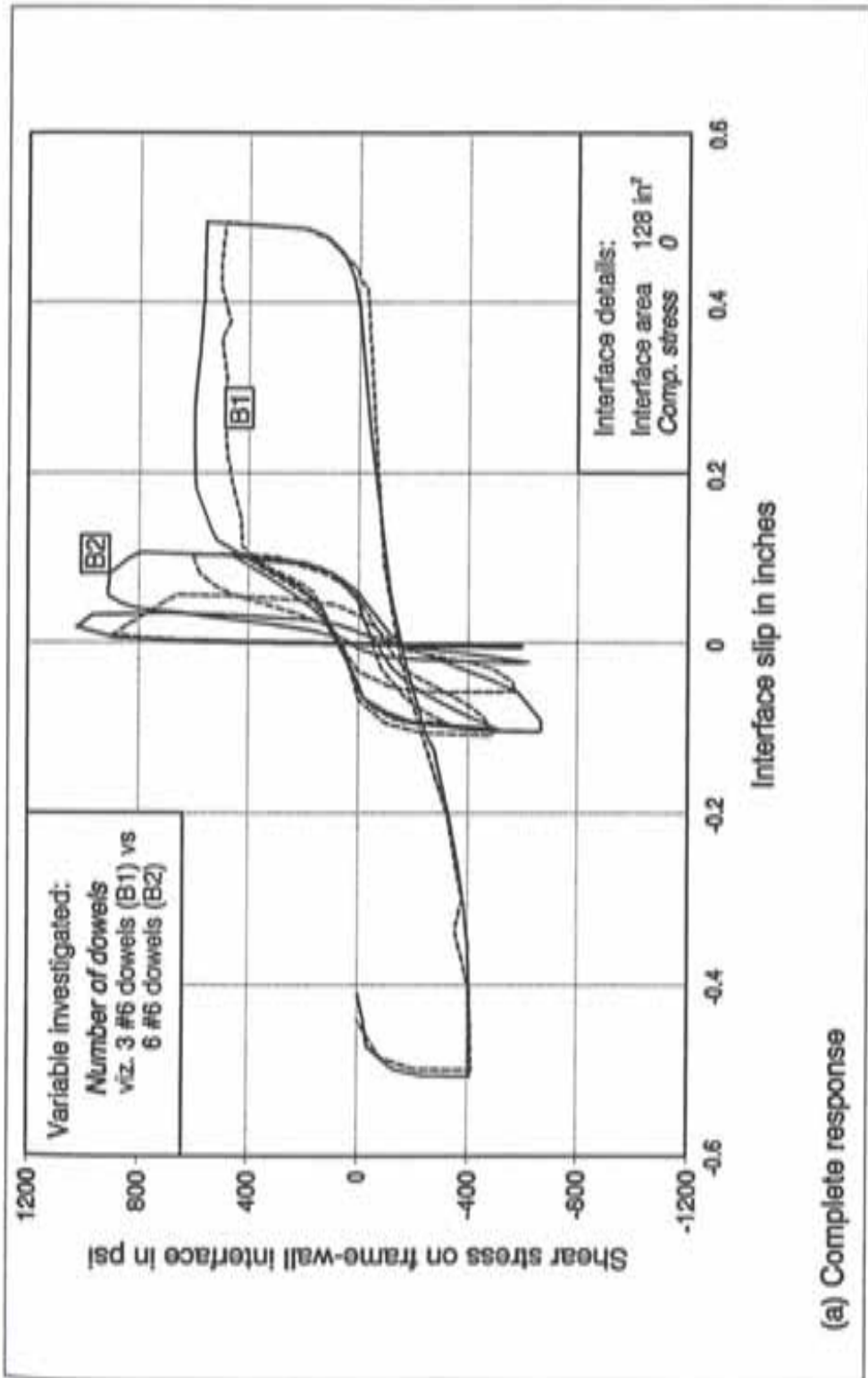


Figure 8.7 Performance of test specimens with different patterns of compressive stress



(a) Complete response

Figure 8.8 Performance of test specimens without compressive stress for different number of dowels (contd.)

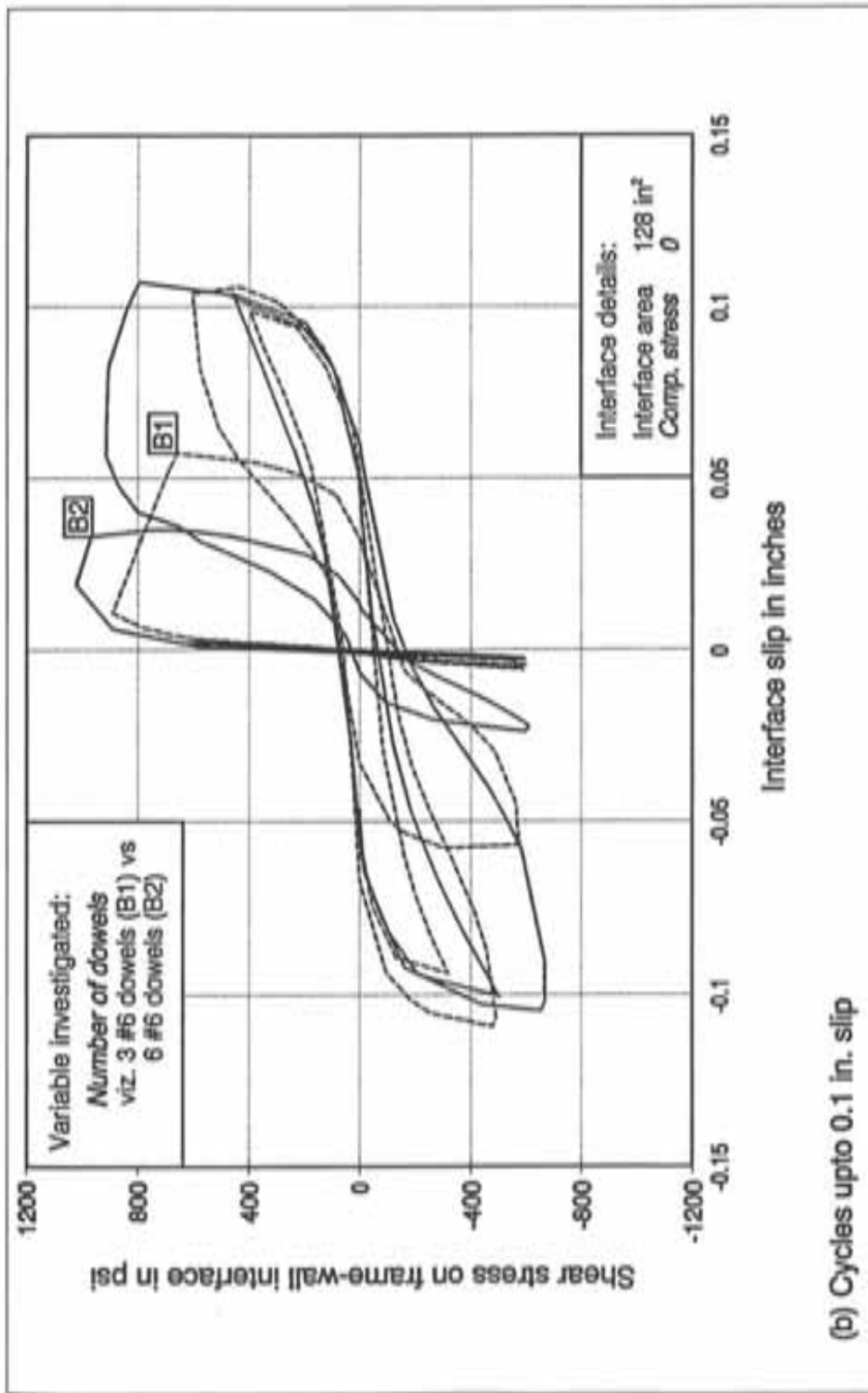


Figure 8.8 Performance of test specimens without compressive stress for different number of dowels (contd.)

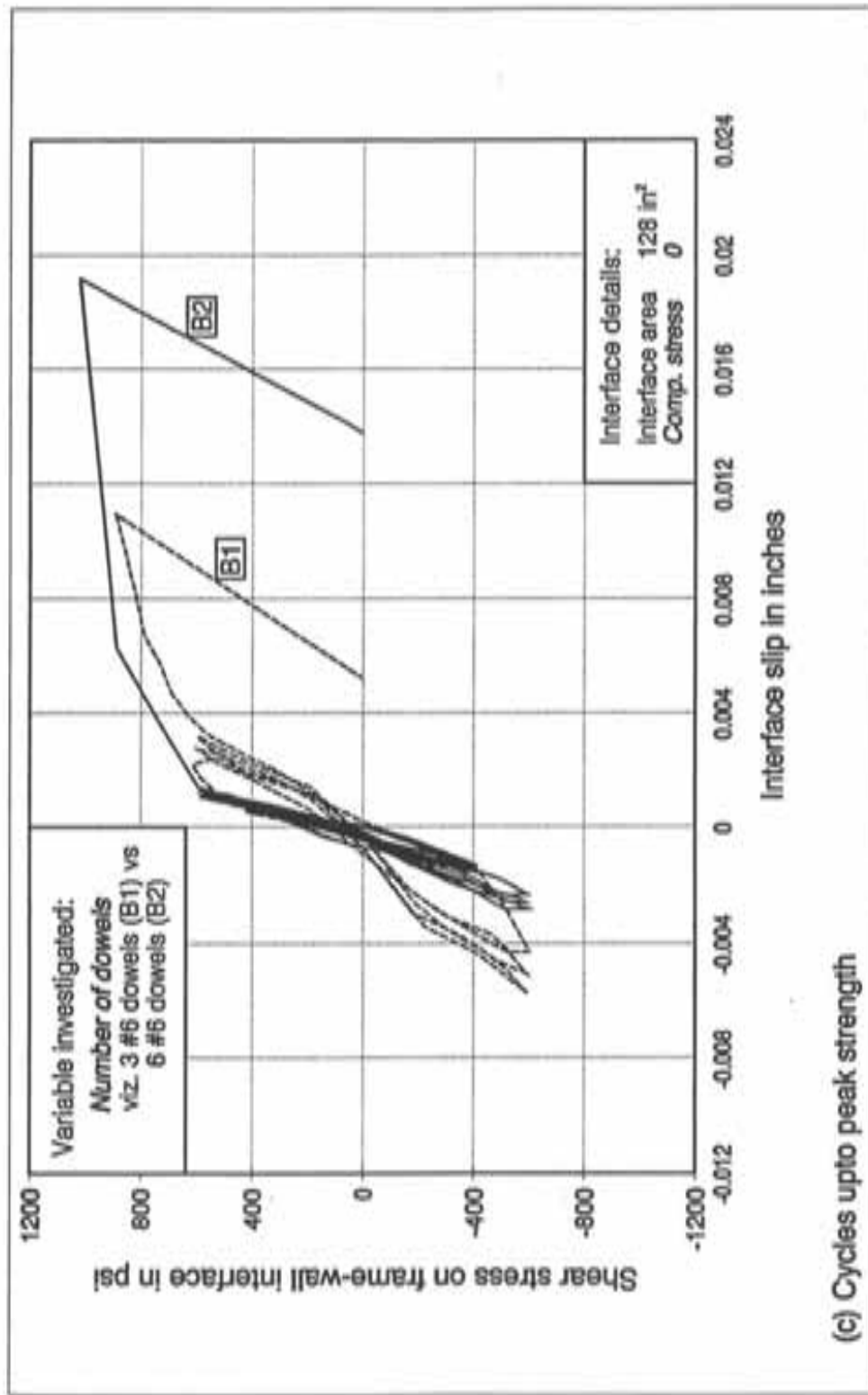


Figure 8.8 Performance of test specimens without compressive stress for different number of dowels

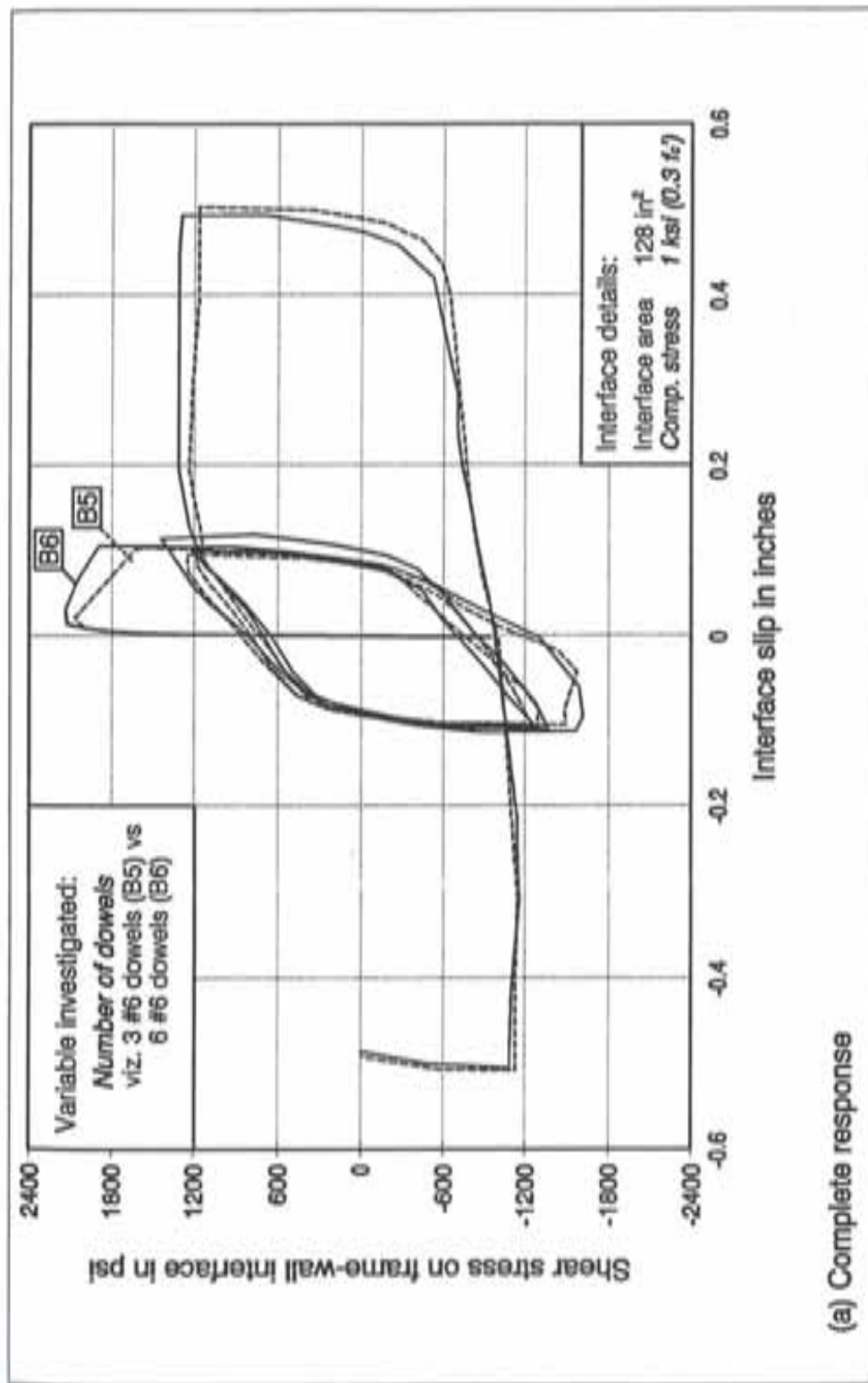


Figure 8.9 Performance of test specimens with compressive stress for different number of dowels (contd.)

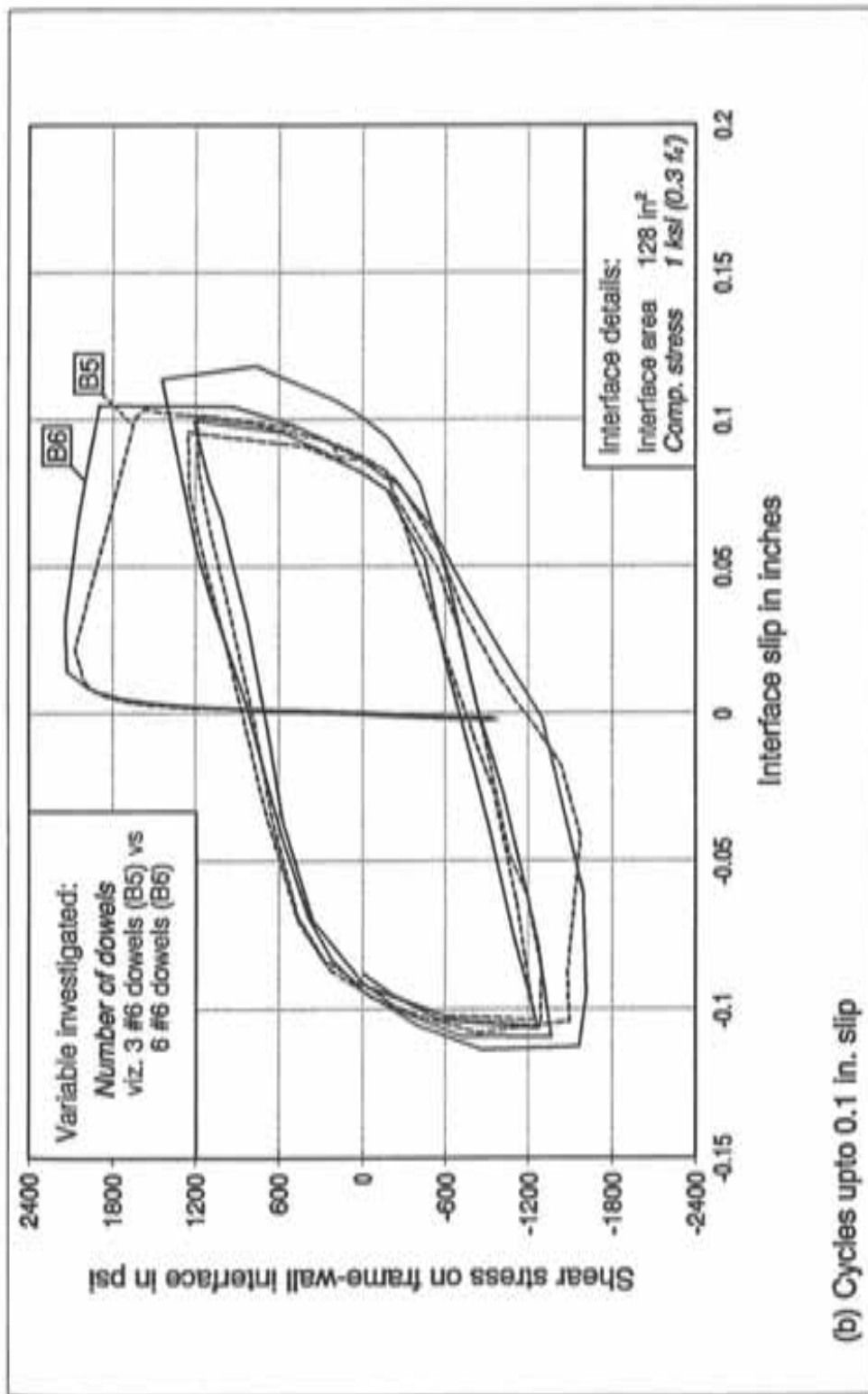


Figure 8.9 Performance of test specimens with compressive stress for different number of dowels (contd.)

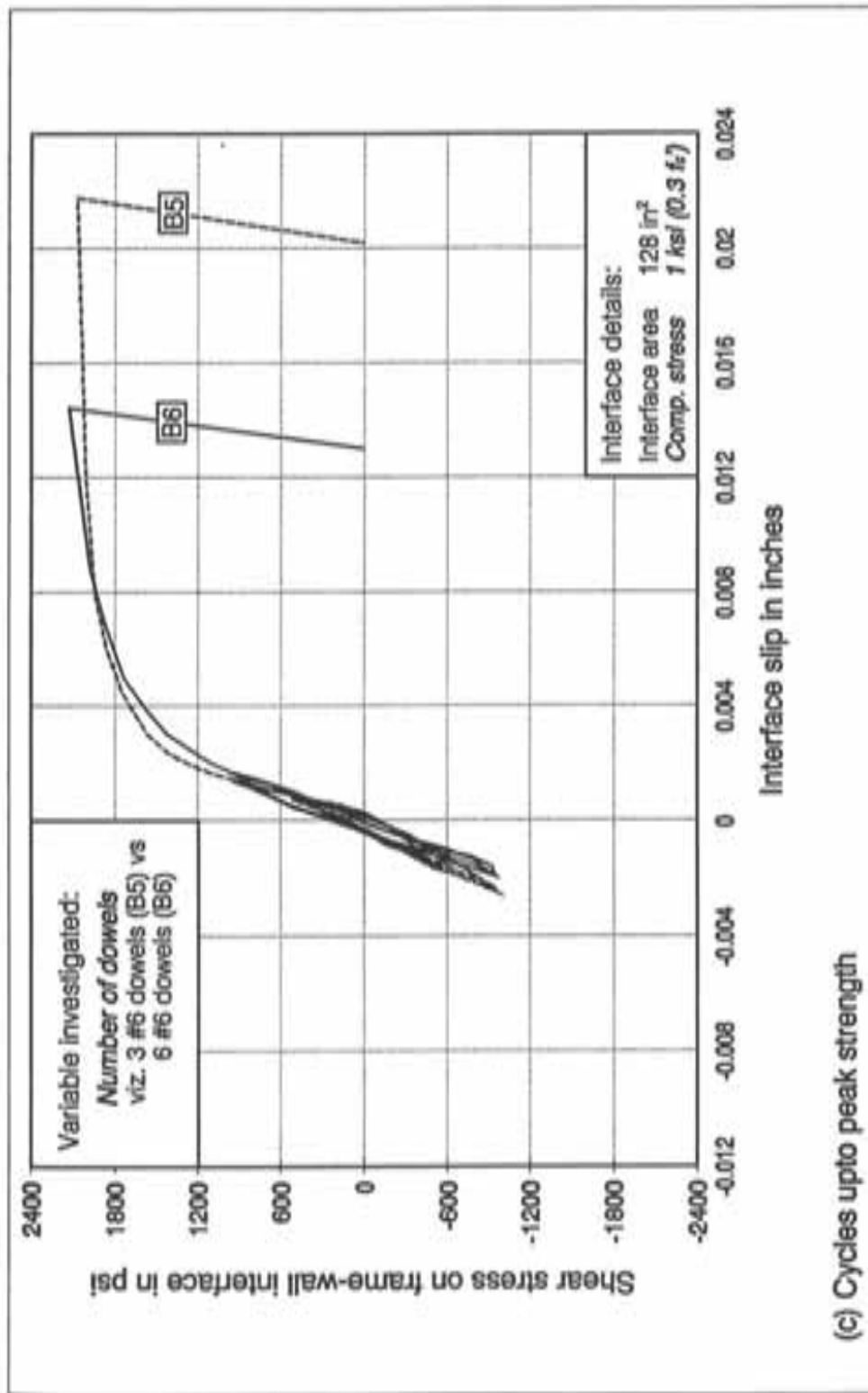
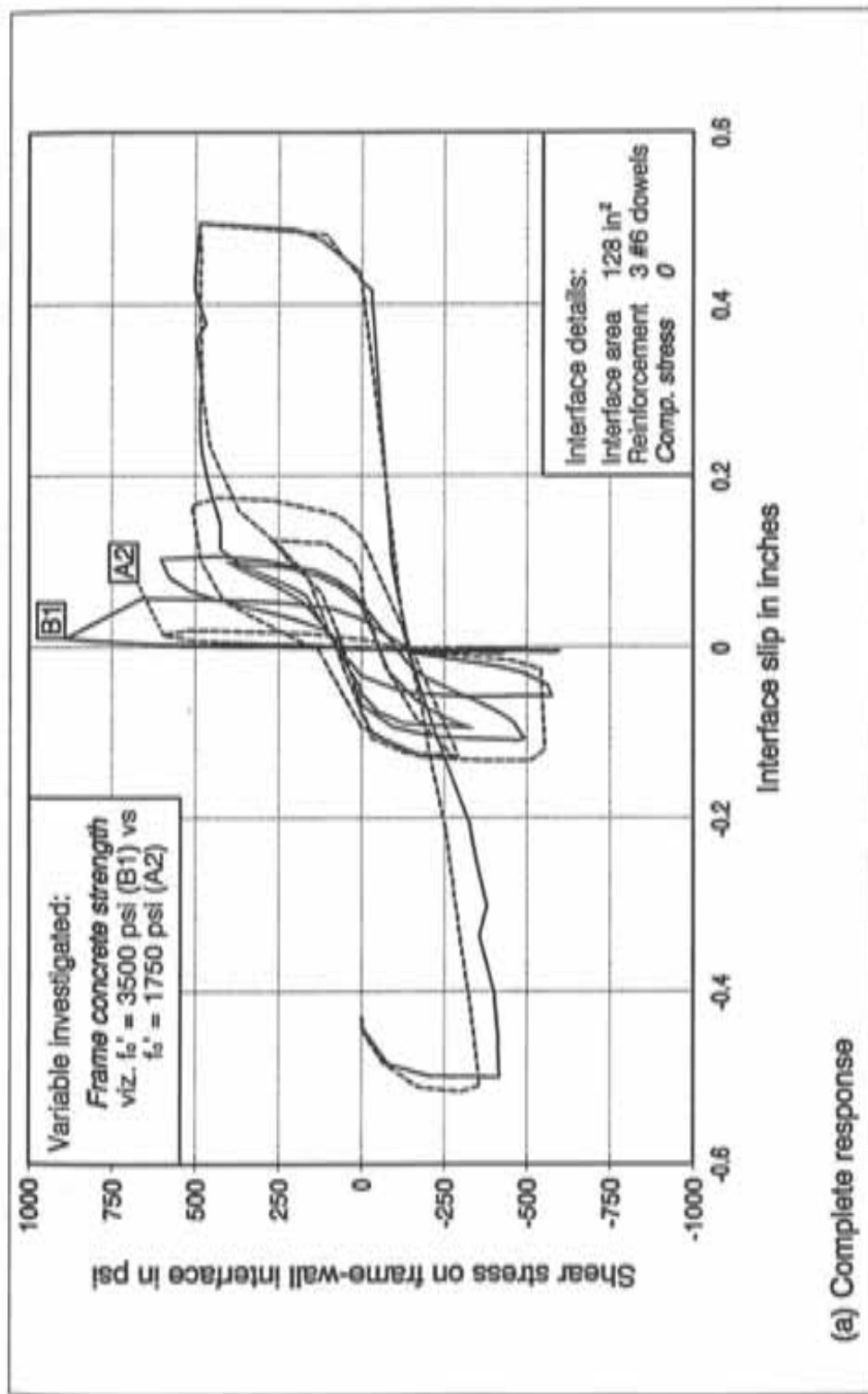


Figure 8.9 Performance of test specimens with compressive stress for different number of dowels



(a) Complete response

Figure 8.10 Performance of test specimens without compressive stress for different frame strengths (contd.)

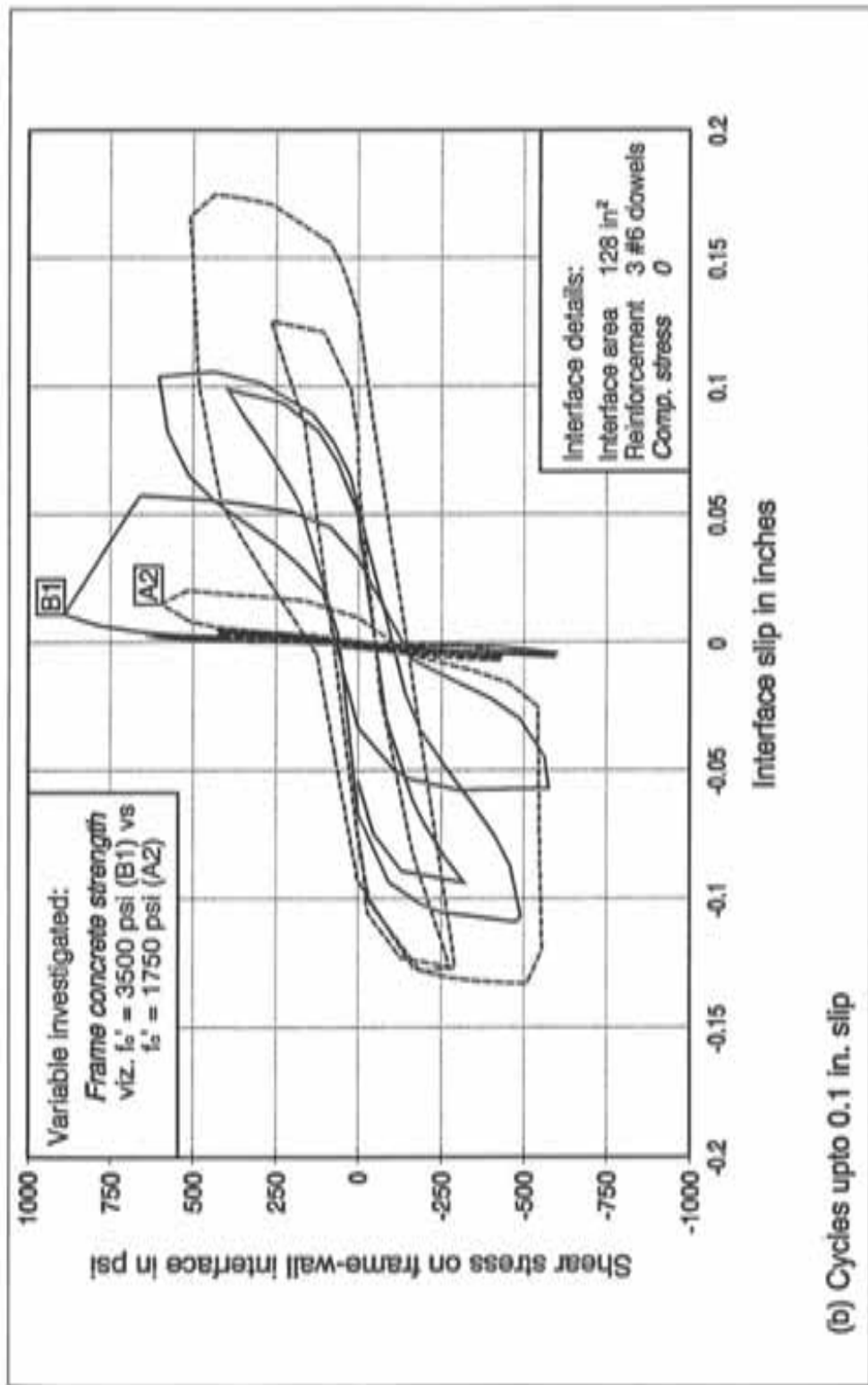


Figure 8.10 Performance of test specimens without compressive stress for different frame strengths (contd.)

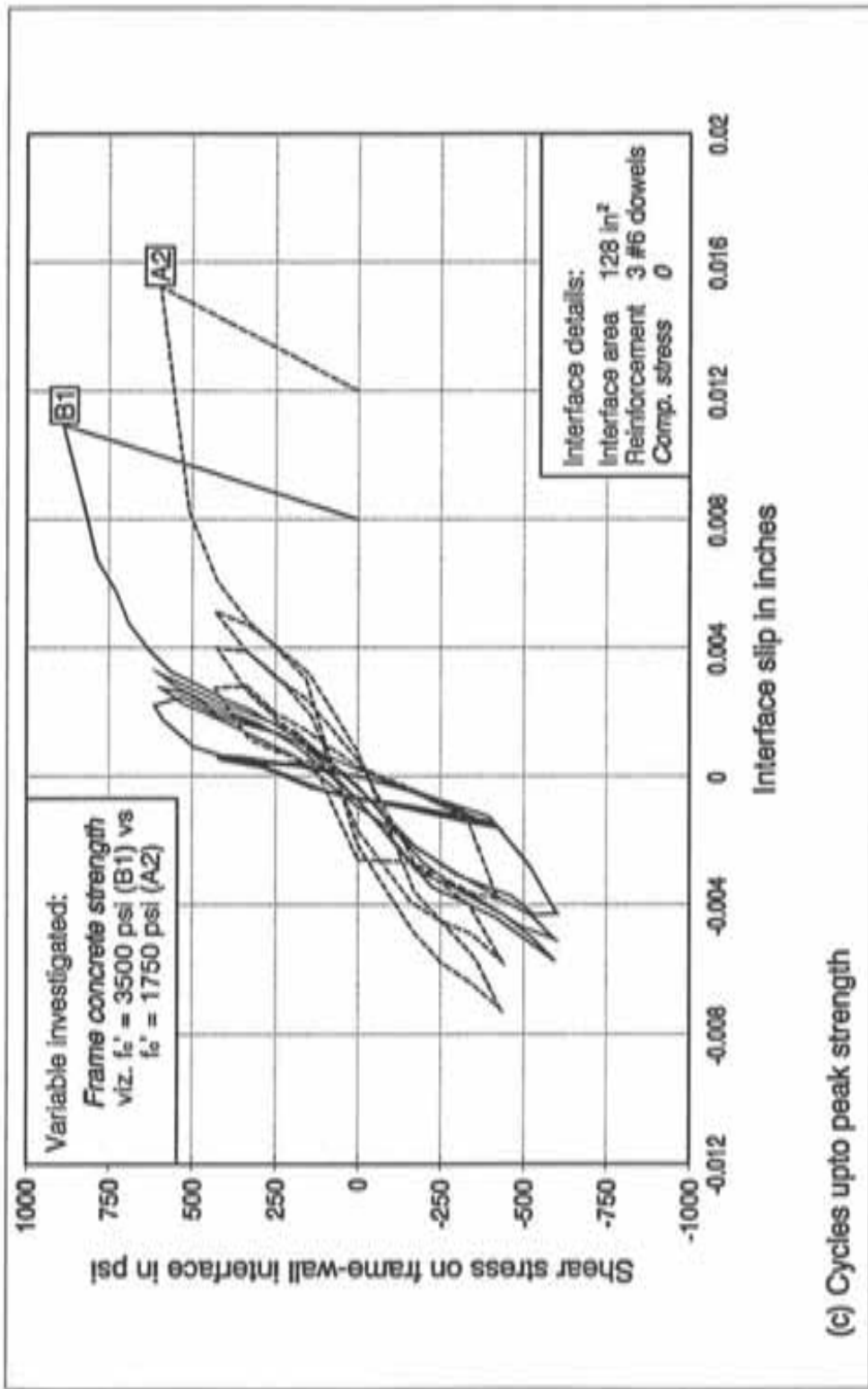


Figure 8.10 Performance of test specimens without compressive stress for different frame strengths

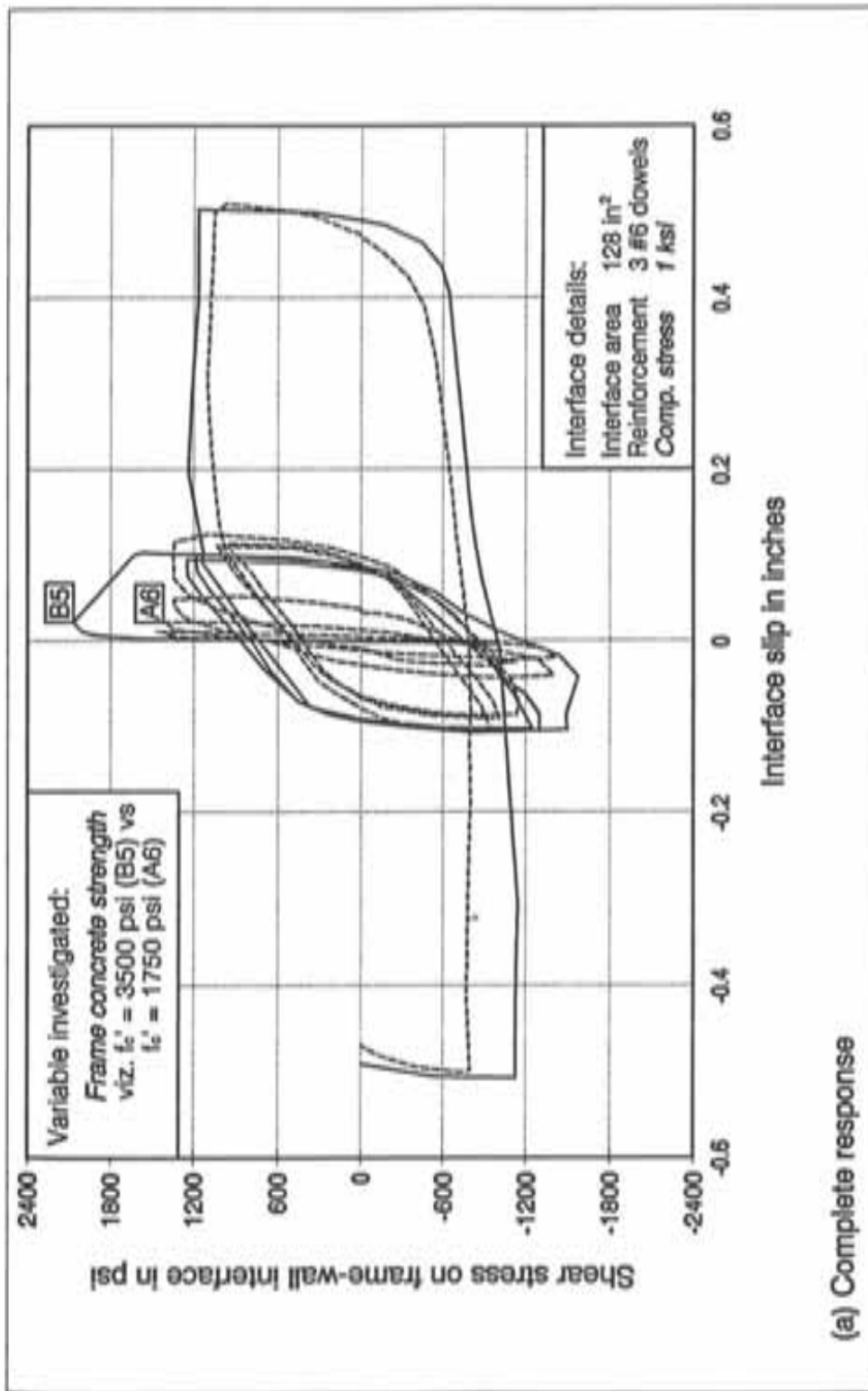


Figure 8.11 Performance of test specimens with compressive stress for different frame strengths (contd.)

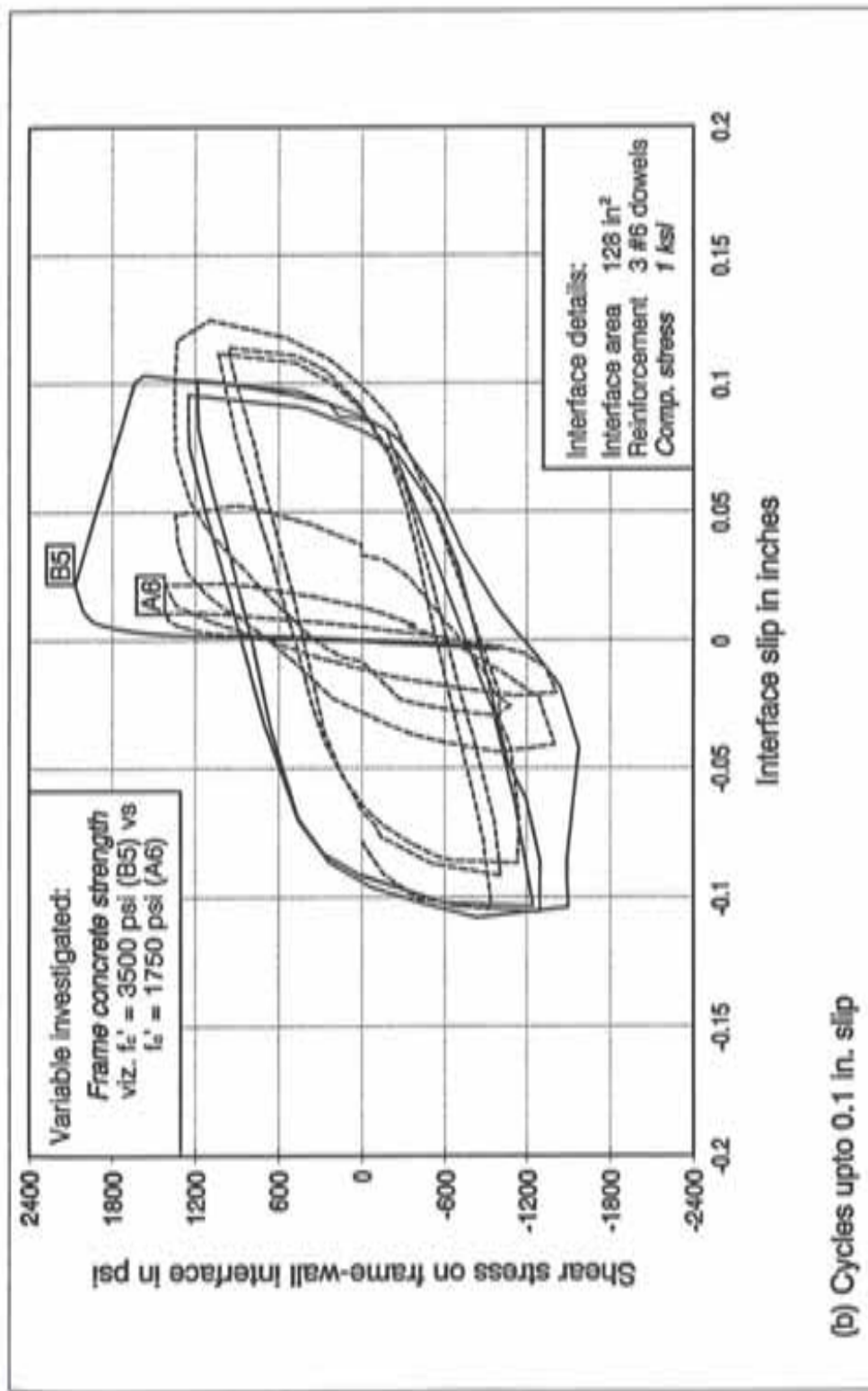


Figure 8.11 Performance of test specimens with compressive stress for different frame strengths (contd.)

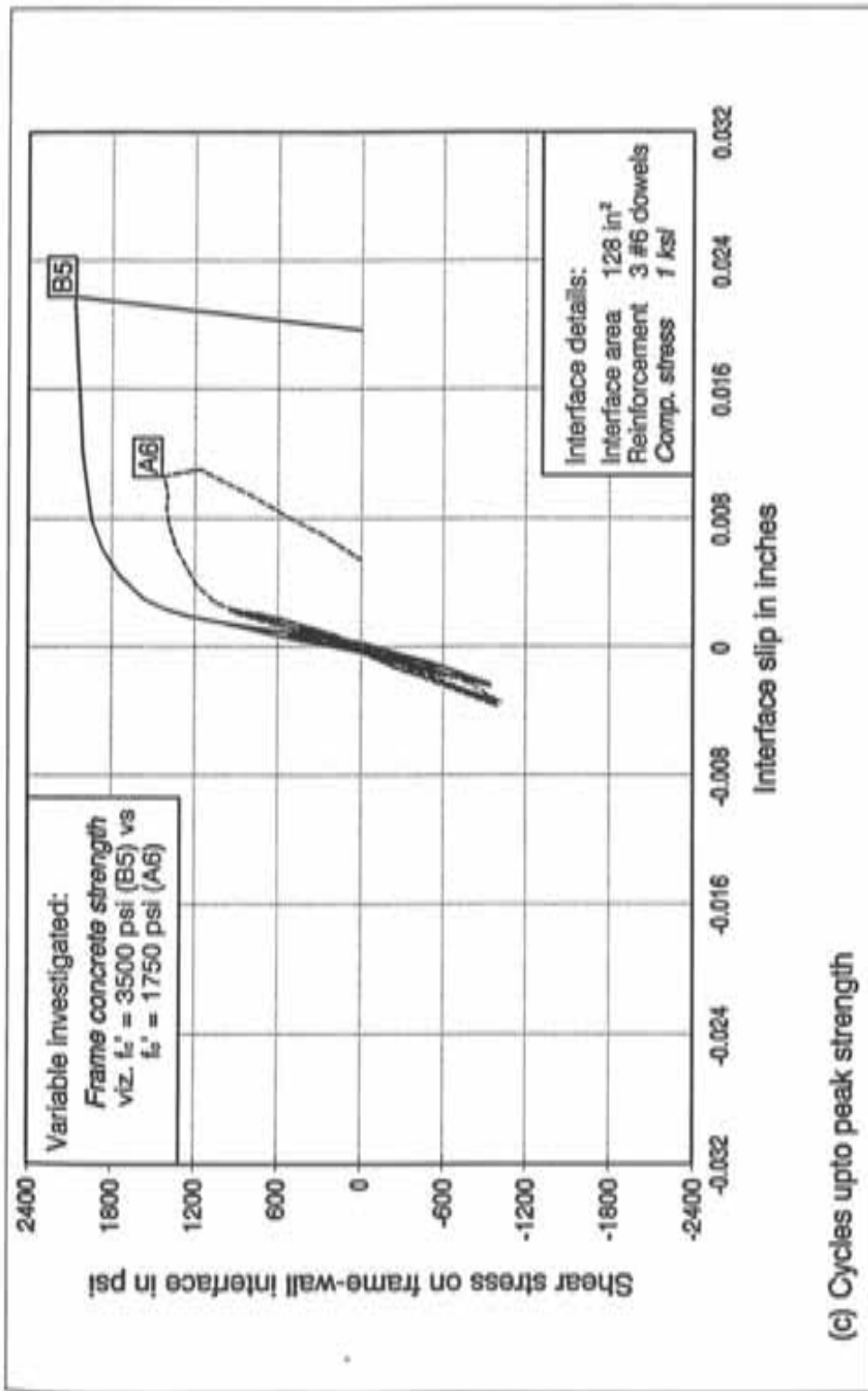


Figure 8.11 Performance of test specimens with compressive stress for different frame strengths

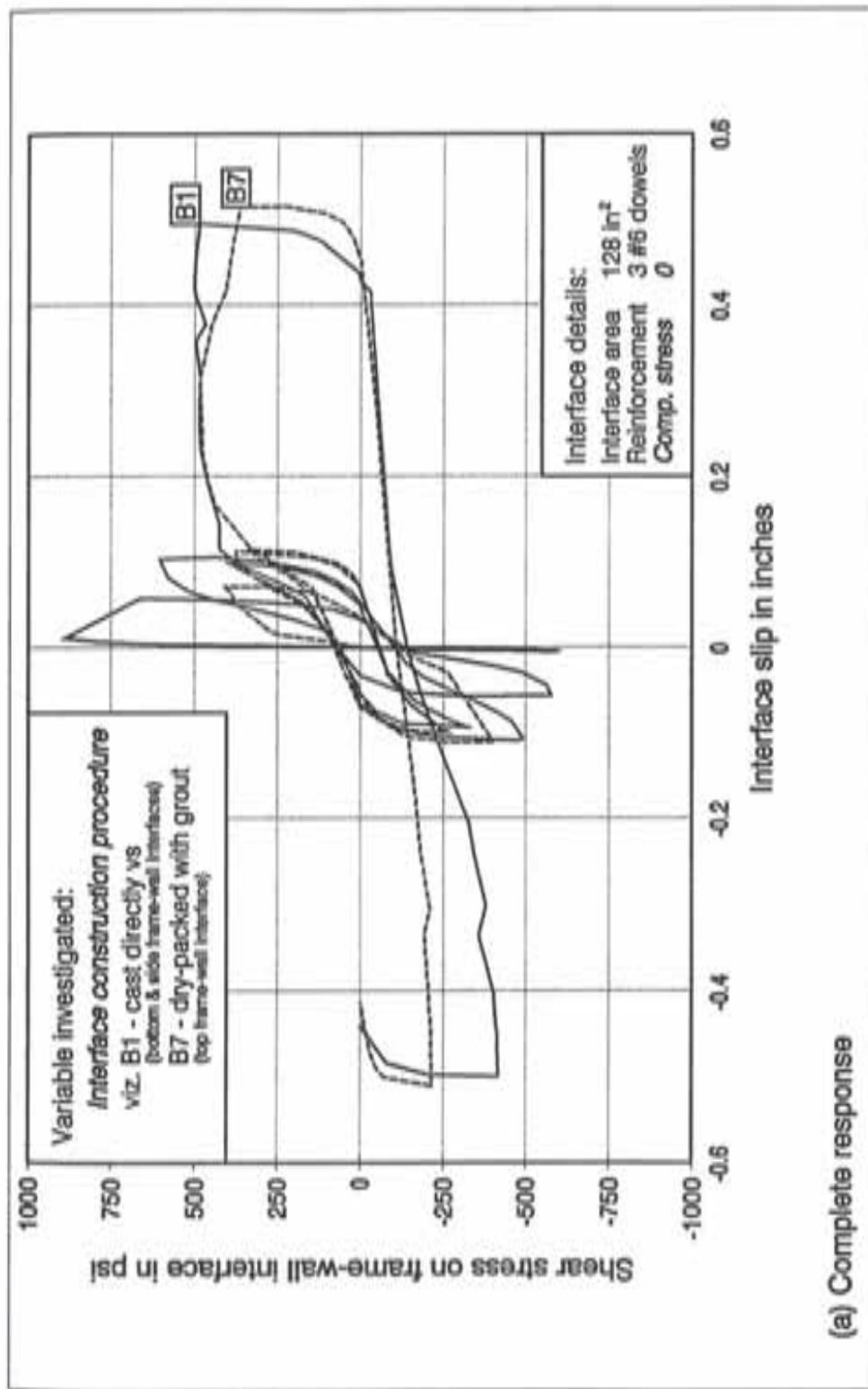


Figure 8.12 Performance of test specimens without compressive stress for frame-wall interfaces constructed using different procedures (contd.)

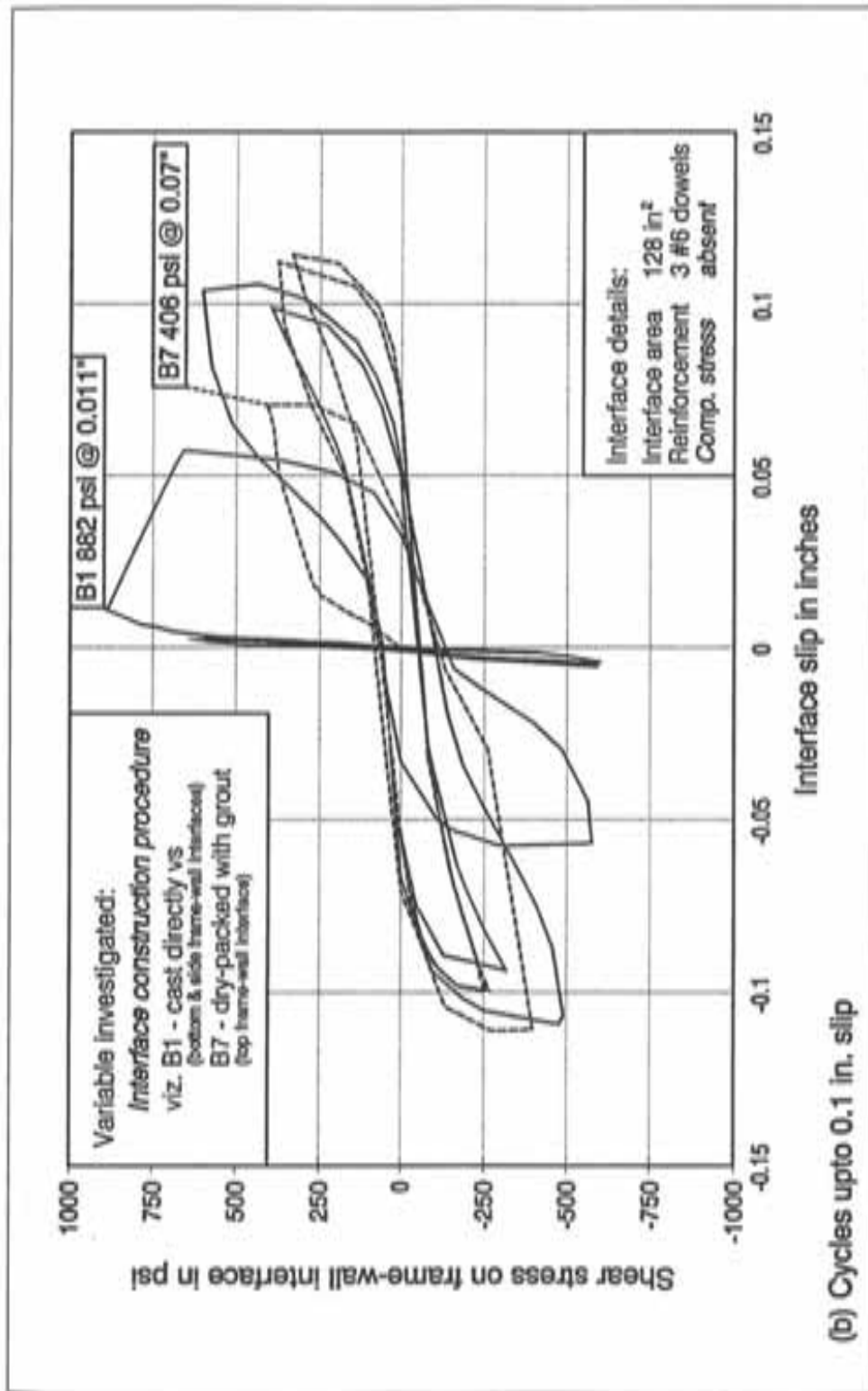


Figure 8.12 Performance of test specimens without compressive stress for frame-wall interfaces constructed using different procedures (contd.)

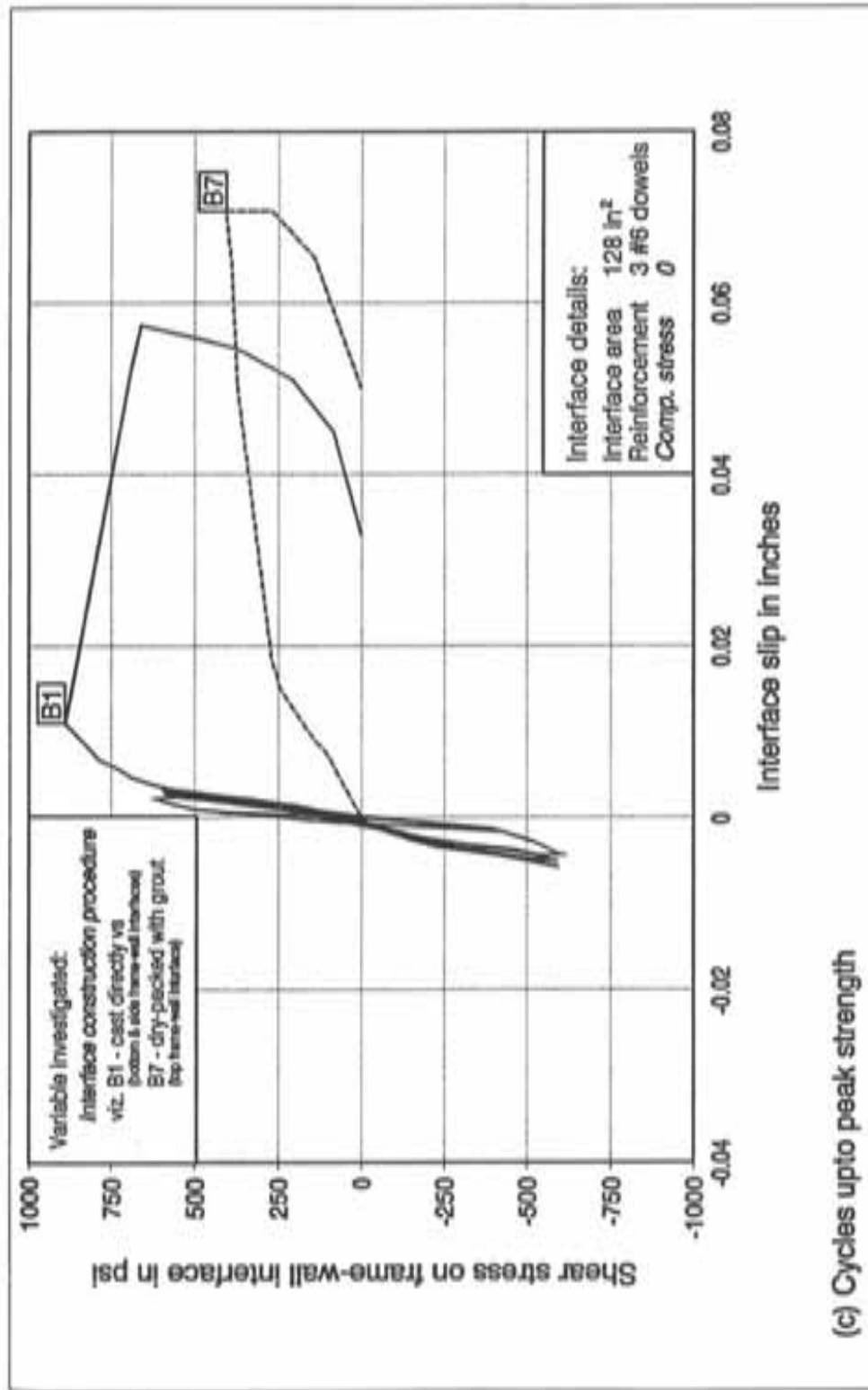


Figure 8.12 Performance of test specimens without compressive stress for frame-wall interfaces constructed using different procedures

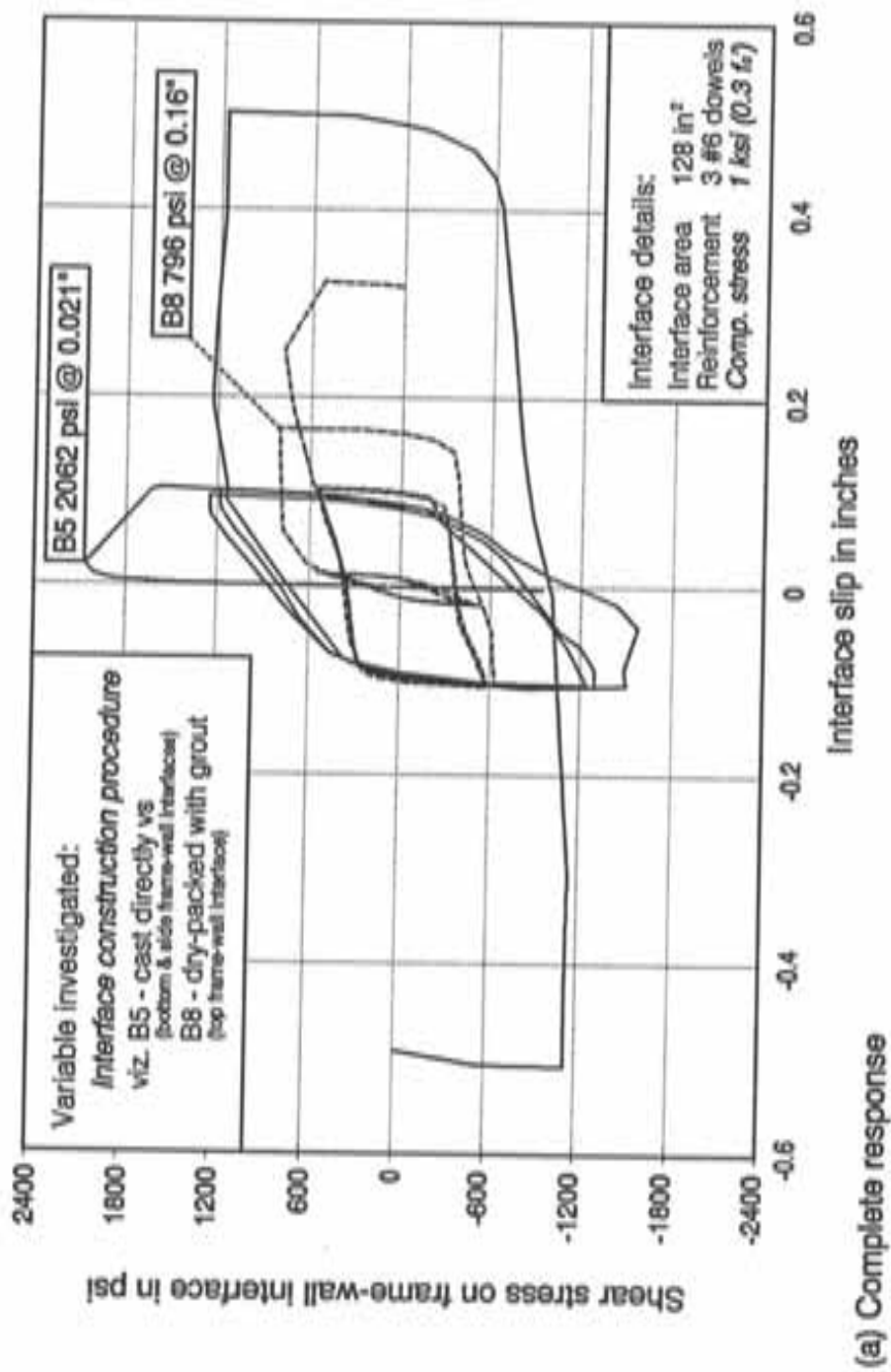


Figure 8.13 Performance of test specimens with compressive stress for frame-wall interfaces constructed using different procedures (contd.)

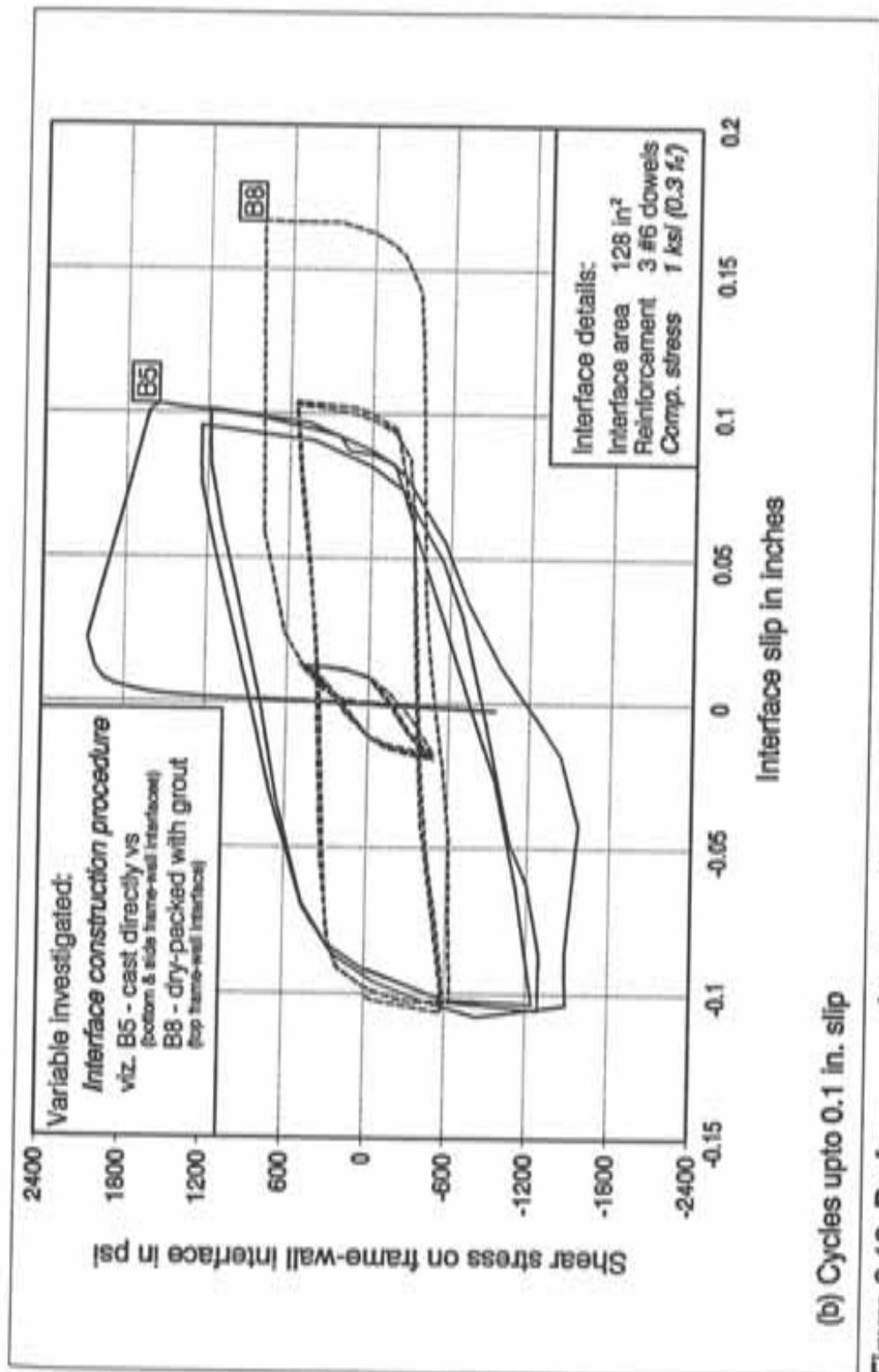


Figure 8.13 Performance of test specimens with compressive stress for frame-wall interfaces constructed using different procedures (contd.)

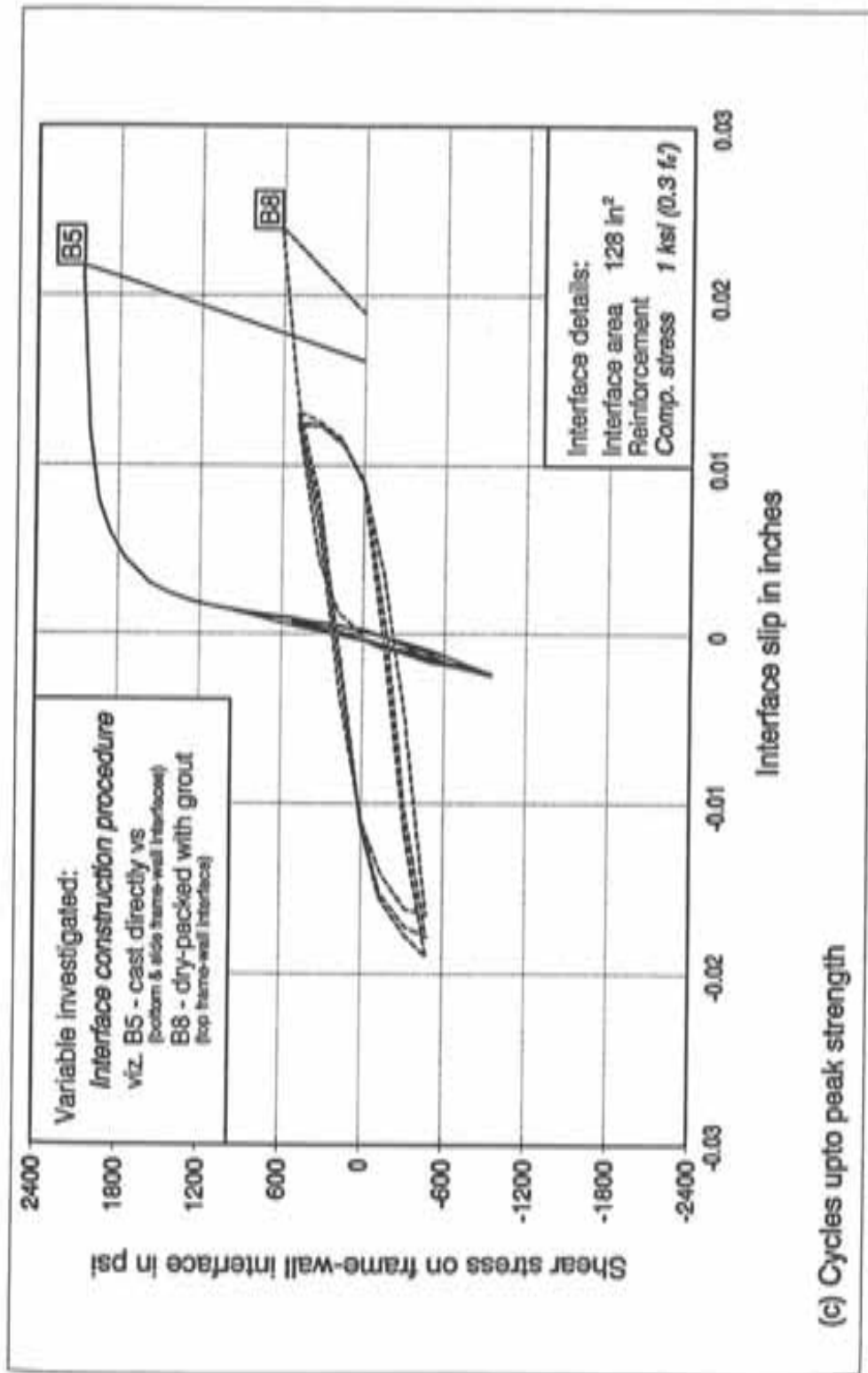


Figure 8.13 Performance of test specimens with compressive stress for frame-wall interfaces constructed using different procedures

CHAPTER 9

A REVIEW ON SHEAR-FRICTION PROVISIONS IN SECTION 11.7 OF ACI 318-89

9.1 INTRODUCTION

Section 11.7 of ACI 318-89 [3] defines design values for conditions where direct shear transfer through shear-friction should be considered. Such conditions include an interface between concretes cast at different times, and an interface between concrete and steel.

The shear-friction concept is based on the assumption that a crack will form in a plane which contains shear forces and that reinforcement must be provided across the crack to resist relative displacements along the crack. When shear acts along a crack, one crack face slips relative to the other. If the crack faces are rough and irregular, this slip is accompanied by separation of the crack faces. The separation is assumed to be sufficient to stress the reinforcement crossing the crack to its yield point. The reinforcement thus provides a clamping force of $A_{vf} f_y$ (where A_{vf} is the area of shear-friction reinforcement across the interface, and f_y is the specified yield strength of shear-friction reinforcement) across the crack faces. The applied shear is then resisted by friction between the crack faces, by resistance to the shearing off of protrusions on the crack faces, and by dowel action of the reinforcement crossing the cracks.

The test results discussed in Chap. 8 warrant a review of ACI 318 provisions on shear-friction (refer to Appendix D). Relevant sections of the code presented below are for comparison with test results:

11.7.4.1 When shear-friction reinforcement is perpendicular to shear plane, shear strength V_n shall be computed by,

$$V_n = A_{vf} f_y \mu \quad (11-26)$$

where, μ is coefficient of friction in accordance with 11.7.4.3. Different coefficients of friction are recommended for various cases so that the calculated shear strengths will be in reasonable agreement with test results.

11.7.4.3 The coefficient of friction μ in Eq. (11-26) shall be

| | |
|---|---------------|
| Concrete placed monolithically | 1.4 λ |
| Concrete placed against hardened concrete with surface intentionally roughened as specified in 11.7.9 | 1.0 λ |
| Concrete placed against hardened concrete not intentionally roughened | 0.6 λ |
| Concrete anchored to as-rolled structural steel by headed studs or by reinforcing bars (see 11.7.10) | 0.7 λ |

where $\lambda = 1.0$ for normal weight concrete, 0.85 for "sand-lightweight" concrete and 0.75 for "all lightweight" concrete. Linear interpolation is permitted when partial sand replacement is used.

- 11.7.5 Shear strength V_n shall not be taken greater than $0.2 f_c' A_c$ nor $800 A_c$ in pounds, where A_c is area of concrete section resisting shear transfer.
- 11.7.7 Net tension across shear plane shall be resisted by additional reinforcement. Permanent net compression across shear plane may be taken as additive to the force in the shear-friction reinforcement $A_{vf} f_y$ when calculating required A_{vf} .
- 11.7.8 Shear-friction reinforcement shall be appropriately placed along the shear plane and shall be anchored to develop the specified yield strength on both sides by embedment, hooks, or welding to special devices.

11.7.9 *For the purpose of 11.7, when concrete is placed against previously hardened concrete, the interface for shear transfer shall be clean and free of laitance. If μ is assumed equal to 1.0A, interface shall be roughened to a full amplitude of approximately 1/4 in.*

The ACI 318 shear-friction provisions are reviewed from two points of view; new construction and retrofit.

9.2 EVALUATION OF ACI SHEAR-FRICTION PROVISIONS USING CURRENT TEST RESULTS

Test results from the current study are utilized to review the validity of shear-friction provisions in the ACI code. Variations between test data and code-predicted resistances are discussed and suitable modifications are proposed. Measured and estimated shear strengths for all test specimens are presented in Table 9.1. Estimated shear strengths under column "(1)" refer to strengths estimated using the shear-friction equation $V_n = A_{vf} f_y \mu$ as given in Section 11.7.4.1 of ACI 318-89 [3]. Those under column "(2)" refer to strengths estimated using the shear-friction equation $V_n = 0.8 A_{vf} f_y + A_c K_1$ as given in Section R11.7.3 of the ACI 318 commentary [3]. Values under column "(3)" are based on the specified upper limit of $0.2 f_c' A_c$ or $800 A_c$, whichever is less, as given in Section 11.7.5 of the code.

The shear-friction equations presented in the ACI code are based on the specified yield strength of shear-friction reinforcement (f_y). The assumption behind the use of f_y is that the shear-friction reinforcement is anchored to develop the specified yield strength on both sides of the interface as required by Section 11.7.8 of the ACI code. The #6 dowels provided as shear-friction reinforcement across the interface in the current study had an embedment depth of 6 inches. Such embedment lengths are typical in retrofit schemes where it is not possible to anchor the reinforcement into the existing frame to develop yield strength. In some cases, difficulties arise from congestion of reinforcement in the existing structural elements. For #6 dowels with 6 in. embedment in concrete having compressive

strengths of 1750 and 3500 psi, the estimated pull out strengths can be calculated as follows:

In Section 12.2.3.6 of ACI 318-89 [3], basic development length is given as,

$$l_{db} = \frac{0.03 d_b f_y}{\sqrt{f'_c}}$$

In order to obtain the pull out strength of reinforcement, the above equation may be rewritten as,

$$f_s = \frac{l_e \sqrt{f'_c}}{0.03 d_b}$$

- where f_s = stress developed in reinforcement prior to pull out in psi,
 l_e = embedment length in inches,
 f'_c = compressive strength of concrete in psi, and
 d_b = reinforcing bar diameter in inches.

For #6 dowels with 6 in. embedment in concrete having $f'_c = 1750$ psi,

$$\begin{aligned} f_s &= 11.2 \text{ ksi} \\ &= 0.19 f_y \text{ where } f_y = \text{specified yield strength of shear-friction reinforcement} = 60 \text{ ksi.} \end{aligned}$$

For #6 dowels with 6 in. embedment in concrete having $f'_c = 3500$ psi,

$$\begin{aligned} f_s &= 15.8 \text{ ksi} \\ &= 0.26 f_y \end{aligned}$$

However, simple pull out tests (presented in Appendix C) showed that average tensile (pull out) strengths of epoxy-grouted #6 dowels embedded in concrete having

compressive strengths of 1750 and 3500 psi were 42 (0.7 f_y) and 48.2 (0.8 f_y) ksi respectively. Better tensile strengths for epoxy-grouted #6 dowels can be attributed to the increased bond interface because bond failures occurred typically at the interface between the epoxy grout and surrounding concrete (Fig. C.2 in Appendix C). In addition, it is likely that anchorage capacity does not increase linearly with embedment length even though not implied by development provisions in the code. Because tensile stresses in dowels must have been below yield at the onset of failure in direct shear tests, the specified yield strength of dowels in shear-friction equations (f_y) was replaced by the actual tensile (pull out) stress in bars (f_s) as established from simple pull out tests. In the following sections, various issues related to the ACI code provisions and test results from the current study are discussed.

9.2.1 Shear-Friction Hypothesis in Section 11.7.7 of ACI Code

As provided in Section 11.7.7, permanent net compression across the shear plane was added to the tensile strength of shear-friction reinforcement for the calculations in columns *(1)* and *(2)* of Table 9.1. The addition of N and $A_v f_y$ is justified in the code because it is assumed that shear-friction reinforcement would yield in tension whether or not there was permanent net compression across the interface. However, test results from the current study do not confirm this hypothesis.

Specimens A8, A6, and A7 had the same magnitude of permanent net compression but had different numbers of dowels across the interface; specimen A8 had no dowels, specimen A6 had 3-#6 dowels, and specimen A7 had 6-#6 dowels. Estimated shear strengths were 128, 183, and 238 kips for specimens A8, A6, and A7, respectively. Measured shear strengths were 201, 182, and 213 kips, respectively. Measured shear strengths of specimens A6 (3-#6 dowels) and A7 (6-#6 dowels) did not differ significantly from the measured shear strength of specimen A8 which contained no shear-friction reinforcement across the interface. Also, for specimens B3 (no dowels), B5 (3-#6 dowels), and B6 (6-#6 dowels) which had the same magnitude of permanent net compression across the interface, the estimated shear strengths were 128, 191, and 255 kips, respectively. The measured shear strengths were 254, 264, and 274 kips, respectively. Dowels did not have an appreciable influence on shear strength when there was permanent

net compression of 128 kips ($0.57 f'_c$ for specimens A8, A6, and A7 and $0.29 f'_c$ for specimens B3, B5, and B6) across the interface (also refer to discussion in Art. 8.2.3). These six tests indicate that consideration of cumulative contribution of permanent net compression and shear-friction reinforcement across the interface, as specified by the ACI code, would be inaccurate.

Two extreme cases illustrate the problem with current provisions. Specimens B1 and B2, which had only shear-friction reinforcement and no permanent net compression, were governed by tensile strength of shear-friction reinforcement (failure modes of specimens B1 and B2 in Table 7.1). For specimens B5 and B6, permanent net compression of $0.29 f'_c$ controlled shear strength through direct shear failure, despite the presence of shear-friction reinforcement across the interface. The contribution of shear-friction reinforcement to shear strength of each test specimen, as observed from test results, was insignificant. In transition between the two extremes, the shear strength of an interface may be contributed by compression and shear-friction reinforcement. That is, cracks can develop along the interface and stress the shear-friction reinforcement despite the existence of some low-level compression. For example, the shear strength of specimen B10, which had a net compression of $0.1 f'_c$ (f'_c refers to concrete strength of weaker concrete) across the interface, was controlled by pull out failure of dowels; cracks developed despite the existence of compression across the interface (Figs. B.50 and 51 in Appendix B).

Using the available test data, it was not possible to determine the transition point where the contribution of shear-friction reinforcement becomes insignificant due to the presence of permanent net compression across the interface. However, it is evident that the strength of specimen B10 was contributed by both compression on the interface and shear-friction reinforcement, with the magnitude of the former being $0.1 f'_c$. In light of the current test data, the following modification to the shear-friction provisions is proposed:

$$V_n = (A_v f_y + N) \mu \quad (11-26-A)$$

$$V_n = N \mu \quad \text{when } N > 800 A_v \quad (11-26-B)$$

where, V_n = nominal shear capacity of connection in pounds,
 A_v = area of shear-friction reinforcement across the shear plane
 in sq. in.,

| | | |
|-------|---|--|
| f_y | = | specified yield strength of shear-friction reinforcement in psi, |
| N | = | permanent net compression across the shear plane in pounds, |
| μ | = | coefficient of friction in accordance with Section 11.7.4.3 of ACI 318-89 [3], and |
| A_c | = | area of concrete section resisting shear transfer in sq. in. |

It may also be observed from Table 9.1 that specimen B8 with a cementitious dry-pack interface reached only 40 percent of the shear strength of specimen B5 in which the interface was cast directly against the hardened concrete. Both test specimens had similar details; 3 #6 dowels and 1000 psi permanent net compression. It is therefore recommended that the presence of permanent net compression be neglected in calculating the estimated shear strengths of connections whose interfaces are grouted using cementitious dry-pack materials.

9.2.2 Friction Coefficients μ Specified in ACI Code

Section 11.7.4.3 of ACI code specifies different friction coefficients μ for various interface construction methods. The code is not clear on μ values for interfaces formed with dry-packed cementitious grout. For specimens B7 and B8, interfaces of hardened concrete in both test specimens were roughened in accordance with Section 11.7.9 of ACI code before dry-packing was carried out. A value of $\mu = 1.0$ seemed appropriate and was used in calculating the estimated shear strengths of specimens B7 and B8 in column "(1)" of Table 9.1. However, current test results show that dowel action was the major contributor to shear strengths of both test specimens (refer to discussion in Art. 8.2.5). The code specifies a $\mu = 0.6$ for concrete placed against hardened concrete with the interface not roughened intentionally. Specification of $\mu = 0.6$ for such a case is attributed to dowel action which is assumed to be a major contributor to shear strength. Since dowel action was indeed the major contributor to shear

strength of interfaces which were grouted using a cementitious dry-pack material, $\mu = 0.6 \lambda$ should be more appropriate whether or not the interface in hardened concrete was roughened intentionally. Concretes of different strength and age with the interface grouted using cementitious dry-pack materials can be included in Section 11.7.4.3 of ACI code with a friction coefficient of $\mu = 0.6 \lambda$ specified for such a case.

9.2.3 Upper Limit on Shear Strength Specified by ACI Code

Section 11.7.5 of ACI code specifies an upper limit on the shear strength of connections. According to the specifications, shear strength of a connection shall not be taken greater than $0.2 f_c' A_c$ nor $800 A_c$ in pounds, where A_c is area of concrete section resisting shear transfer. Current test results show that the limit is overly conservative especially when the shear planes are subjected to permanent net compression. In Fig. 9.1, the measured shear strengths of test specimens and the code-specified upper limit on shear strength of connections are compared. Measured shear strengths are plotted against the sum of permanent net compression and tensile strength of shear-friction reinforcement across the shear plane (as currently specified by Section 11.7.7 of ACI code). It may be seen from the figure that the shear strengths of test specimens with permanent net compression were much better than the code-estimated strengths which were always controlled by this upper limit. Table 9.1 also shows that the estimated shear strengths of test specimens were in most cases controlled by this upper limit. The specified upper limit should be modified to reflect test results.

Modified upper limits are proposed for the shear strengths which are estimated using the modified equations proposed in Art. 9.2.1.

Case 1: For $V_n = (A_v f_y + N) \mu$ as proposed in Eqn. (11-26-A).

The ratios of measured to estimated shear strengths (using a limit of $0.2 f_c' A_c$ or $800 A_c$, whichever is less) of specimens A2, A3, A4, B2, and B10 ranged from 1.46 to 2.05 (refer to Table 9.1). If the upper limit is modified as $0.25 f_c' A_c$ or $800 A_c$, whichever is less, the ratios of measured to

estimated shear strengths would range from 1.27 to 1.64 for the test specimens under consideration (refer to Table 9.3). Based on the discussion, it may be recommended that shear strength V_n not be taken greater than $0.25 f'_c A_c$ nor $800 A_c$ in pounds, where A_c is area of concrete section resisting shear transfer.

Case 2: For $V_n = N \mu$ when $N > 800 A_c$ as proposed in Eqn.(11-26-B).

It may be seen from Table 9.1 that the upper limits specified by the current ACI code were overly conservative when $N > 800 A_c$. The ratios of measured to estimated shear strengths of specimens A5, A6, A7, A8, B3, B4, B5, and B6 ranged from 2.85 to 4.84. It must be noted that the estimated shear strengths of all test specimens under consideration were controlled by the code-specified upper limit.

In Table 9.2 the measured shear strengths of test specimens with compression greater than $800 A_c$ across the interface are compared with the shear strengths estimated using the modified shear-friction equation proposed in Eqn. (11-26-B) of Art. 9.2.1. It may be noted that the ratios of measured to estimated shear strengths ranged from 1.42 to 2.14. The code-specified upper limit must therefore be selected in such a way that it would not make strength in this range even more conservative than it is by using Eqn. (11-26-B). Specimen A8 had no shear-friction reinforcement but had permanent net compression of about $0.6 f'_c A_c$ ($1000 A_c$) across its interface. Compressive strength of concrete in the weaker segment of test specimen was only 1750 psi. Specimen A8 developed shear strength 57 % higher than the strength estimated using Eqn. (11-26-B). It must be noted that the estimated shear strength of specimen A8 (about $0.6 f'_c A_c$) was as much as the magnitude of permanent net compression across the specimen interface since the value of μ was equal to 1 for this case. Therefore, the measured shear strength of specimen A8 was 57 % higher than the magnitude of permanent net compression across its interface. Since specimen A8 can be considered as the worst case in the current test

series, $0.6 f_c' A_c$ is recommended as an upper limit on shear strengths estimated by the modified shear-friction equation (Eqn. 11-26-B). It must however be noted that $0.6 f_c' A_c$ may not be a conservative upper limit for concretes of higher compressive strengths. Maximum compressive strength of concrete (in the weaker segment of test specimens) used in the current study was 3500 psi. For concrete of 3500 psi compressive strength, $0.6 f_c' A_c$ would be $2100 A_c$ pounds. It may be seen from Table 9.2 that specimens B3, B5, and B6 with compression of $0.29 f_c' A_c$ ($1000 A_c$) had measured shear strengths of $1984 A_c$, $2062 A_c$, and $2140 A_c$ pounds respectively. Using Eqn. (11-26-B), the estimated shear strengths were only $1000 A_c$ pounds and therefore conservative. Also specimen B4 which had compression of $0.43 f_c' A_c$ ($1500 A_c$) reached a shear strength of $2273 A_c$ pounds while estimated shear strength was $1500 A_c$ pounds. Since test specimens with 0.29 and $0.43 f_c'$ ($f_c' = 3500$ psi) compression measured shear strengths close to $0.6 f_c' A_c$ ($= 2100 A_c$) pounds, an upper limit of $2100 A_c$ pounds is considered appropriate for concretes with f_c' equal or greater than 3500 psi. Any increase in the limit of $2100 A_c$ must be verified by tests on specimens with f_c' of weaker concrete greater than 3500 psi. Based on the discussion, it may be recommended that shear strength V_n not be taken greater than $0.6 f_c' A_c$ nor $2100 A_c$ in pounds, where A_c is area of concrete section resisting shear transfer.

For concretes of different strength and age with the interface dry-packed using cementitious grouts or other special materials, f_c' to be used in the upper limits shall be the f_c' of weaker concrete or grout material, whichever is less.

9.2.4 Useful Upper Limit on Amount of Shear-Friction Reinforcement

Section 11.7 of ACI 318-89 [3] on shear-friction does not specify any upper limit on the amount of shear-friction reinforcement, A_{vf} . Tests from current study show that the improvement in shear strength was not in proportion with the increase in amount of

shear-friction reinforcement across the shear plane. For example, specimen B2 ($\rho = 0.02$) which contained twice the amount of shear-friction reinforcement in specimen B1 ($\rho = 0.01$), reached a strength only 15 percent higher than that of specimen B1 (refer to Table 9.1). In order to prevent over-estimation of interface shear strength, it is important to define an upper limit on the amount of shear-friction reinforcement.

Figure 9.2 shows the measured ultimate shear stresses against different amounts of shear-friction reinforcement across the shear plane. Test results from a study by Hofbeck [15] were used to develop Fig. 9.2 since strengths of test specimens used in the study were controlled by tensile yielding of shear-friction reinforcement and not by pull out failure of shear-friction reinforcement as observed in current tests.

It may be observed from Fig. 9.2 that the shear strength of test specimens with initially-uncracked shear planes improved significantly with the increase in the amount of shear-friction reinforcement up to a limit of $\rho f_y = 900$ psi ($\rho = 0.015$ for 60 ksi steel). However, the improvement in shear strength of test specimens which had initially-cracked shear planes was significant up to a limit of $\rho f_y = 1200$ psi ($\rho = 0.02$ for 60 ksi steel). Also, reduction in strength due to the presence of pre-existing cracks along the shear planes decreased with the increase in ρf_y and became almost insignificant beyond $\rho f_y = 1200$ psi ($\rho = 0.02$ for 60 ksi steel).

In view of the possibility of pre-existing cracks (formed by factors unrelated to shear) along the shear planes, an upper limit of 1200 psi on ρf_y ($\rho = 0.02$ for 60 ksi steel) seems appropriate. However, it must be remembered that the maximum value of ρf_y allowed by the ACI code is 800 psi. Therefore, no limit on ρf_y needs to be specified in the code.

9.3 MODIFIED SHEAR-FRICTION PROVISIONS FOR SECTION 11.7 OF ACI 318-89

9.3.1 Introduction

The modifications proposed in Art. 9.2 are incorporated into the current ACI 318-89 [3] provisions for shear-friction. The code format is maintained here to facilitate easy follow-up of the proposed modifications. The current ACI shear-friction provisions are presented in Appendix D. Major modifications to the code are *italicized* and minor changes are *bolded and italicized*. Some of the words proposed for removal from the current ACI code are ~~struck-out~~.

MODIFIED SHEAR-FRICTION PROVISIONS FOR SECTION 11.7 OF ACI 318-89

11.0 Notation (terms to be added or changed)

N = permanent net compression across the shear plane, pounds

μ = coefficient of friction. See 11.7.4.4

11.7 - Shear-friction

11.7.1 - Provisions of 11.7 are to be applied where it is appropriate to consider shear transfer across a given plane, such as: an existing or potential crack, an interface between dissimilar materials or an interface between two concretes cast at different times.

11.7.2 - Design of cross sections subject to shear transfer as described in 11.7.1 shall be based on Eq. (11-1), where V_n is calculated in accordance with provisions of ~~11.7.3~~ or 11.7.4.

11.7.3 - A crack shall be assumed to occur along the shear plane considered. The required area of shear-friction reinforcement A_{vf} across the shear

R11.7 - Shear-friction

R11.7.1 - With the exception of 11.7, virtually all provisions regarding shear are intended to prevent diagonal tension failures rather than direct shear-transfer failures. The purpose of 11.7 is to provide design methods for conditions where shear transfer should be considered: an interface between concretes cast at different times, an interface between concrete and steel, reinforcing details for precast concrete structures, and other situations where it is considered appropriate to investigate shear transfer across a plane in structural concrete. (See References 11.23 and 11.24).

R11.7.3 - Although uncracked concrete is relatively strong in direct shear there is always the possibility that a crack will form in an unfavorable location.

plane shall be designed using either 11.7.4 or any other shear transfer design methods that result in prediction of strength in substantial agreement with results of comprehensive tests.

11.7.3.1 - Provisions of 11.7.5 through 11.7.9 shall apply for all calculations of shear transfer strength.

The shear friction concept assumes that such a crack will form, and that reinforcement must be provided across the crack to resist relative displacement along it. When shear acts along a crack, one crack face slips relative to the other. If the crack faces are rough and irregular, this slip is accompanied by separation of the crack faces. At ultimate, the separation is sufficient to stress the reinforcement crossing the crack to its yield point. The reinforcement provides a clamping force $A_{vf} f_y$ across the crack faces. The applied shear is then resisted by friction between the crack faces, by resistance to the shearing off of protrusions on the crack faces, and by dowel action of the reinforcement crossing the crack. Successful application of 11.7 depends on proper selection of the location of an assumed crack.^{11,12,11,23}

The direct shear-transfer strength of a shear plane can be determined using various relationships. Eq. (11-26), (11-27), and (11-28) of 11.7.4 are based on the shear-friction model. This gives a conservative prediction of shear-transfer strength. Other relationships which give a closer estimate of shear-transfer strength^{11,12,11,26,11,28} can be used under the provisions of 11.7.3.

11.7.4 - Shear-friction design method

Shear strength V_n shall be calculated in accordance with provisions of 11.7.4.1 through 11.7.4.4.

11.7.4.1 - Shear strength V_n

(a) If the shear-friction reinforcement is perpendicular to the shear plane,

R11.7.4 - Shear-friction design method

Experimental studies^{11,24,11,49} indicate that when a resultant compressive force acts permanently across a shear plane, the shear transfer strength is a function of the sum of the resultant compressive force N , and the force $A_{vf} f_y$ in the shear-friction reinforcement. Recent tests^{11,49} show that contribution of shear-friction reinforcement becomes insignificant when N is greater than $800 A_{vf}$. In

$$V_n = (A_{vf} f_y + N) \mu \quad (11-26)$$

(b) If the shear-friction reinforcement is inclined to the shear plane, such that the shear force produces tension in shear-friction reinforcement,

$$V_n = A_{vf} f_y (\mu \sin \alpha_f + \cos \alpha_f) + N \mu \quad (11-27)$$

where α_f is angle between shear-friction reinforcement and shear plane.

(c) V_n from Eq. (11-26) or (11-27) shall not be taken greater than $0.25 f'_c A_c$ nor $800 A_c$ in pounds, where f'_c is the smallest of the concrete(s) or grout material(s) at the interface.

11.7.4.2 - Shear strength V_n , when $N > 800 A_c$

$$V_n = N \mu \quad (11-28)$$

V_n from Eq. (11-28) shall not be taken greater than $0.6 f'_c A_c$ nor $2100 A_c$ in pounds, where f'_c is the smallest of the concrete(s) or grout material(s) at the interface.

design, advantage may be taken of the presence of permanent net compression across the shear plane to reduce the amount of shear-friction reinforcement required. In cases, where no shear-friction reinforcement is needed due to the presence of permanent net compression, structural integrity reinforcement must still be provided across the shear plane.

When the shear-friction reinforcement is inclined to the shear plane, such that the component of the shear force parallel to the reinforcement tends to produce tension in the reinforcement, as shown in Fig. 11.7.4, part of the shear is resisted by the component parallel to the shear plane of the tension force in the reinforcement.¹¹⁻²⁶ Eq. (11-27) must be used only when the shear force component parallel to

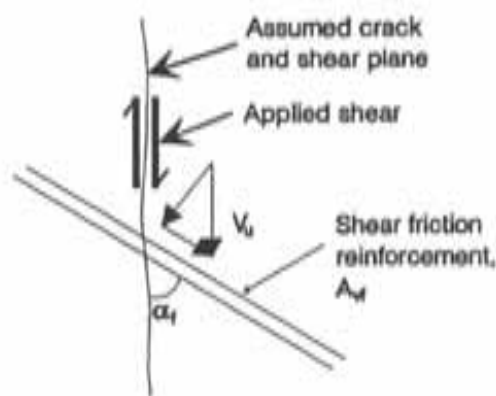


Fig. 11.7.4 - Shear-friction reinforcement at an angle to assumed crack

the reinforcement produces tension in the reinforcement, as shown in Fig. 11.7.4. When α_f is greater than 90 deg, the relative movement of the

surfaces tends to compress the bar and Eq. (11-27) is not valid.

Upper limits on shear strength V_n are specified because, experimental data^{11.23, 11.24, 11.48, 11.49} show that Eq. (11-26), (11-27), and (11-28) become unconservative if V_n has a greater value. The upper limit of $0.6 f_c A_c$ or $2100 A_c$, whichever is less, is considered appropriate for V_n calculated from Eq. (11-28). Tests^{11.24, 11.49} show that concrete-to-concrete interfaces having permanent net compression N greater than $800 A_c$ have much better resistance to shear than those with N less than or equal to $800 A_c$ pounds.

11.7.4.3 - N shall be taken as zero in Eq. (11-26) and (11-27) when the interface is grouted using cementitious dry-pack materials. Eq. (11-28) shall not be valid for this case.

R11.7.4.3 - It has been verified experimentally^{11.49} that the presence of permanent net compression across the shear plane did not result in substantial improvement in shear transfer strength of interfaces, which were grouted using cementitious dry-pack materials.

11.7.4.4 - The coefficient of friction μ in Eq. (11-26), (11-27), and Eq. (11-28) shall be

R11.7.4.4 - In the shear-friction method of calculation, it is assumed that all the shear resistance is due to the friction between the crack faces. It is, therefore, necessary to use artificially high values of the coefficient of friction in the shear-friction equations, so that the calculated shear strength will be in reasonable agreement with test results. For the case of concrete cast against hardened concrete not roughened in accordance with 11.7.8, shear resistance is primarily due to dowel action of the reinforcement and tests^{11.27} indicate that reduced value of $\mu = 0.6\lambda$ specified for this case is appropriate. Recent tests^{11.49} on interfaces grouted using cementitious dry-pack materials show that the resistance by cementitious grout to direct shear deteriorated rapidly. A value of $\mu =$

Concrete placed monolithically 1.4 λ

Concrete placed against hardened concrete with surface intentionally roughened as specified in 11.7.8 1.0 λ

Concrete placed against hardened concrete not intentionally roughened or interface between two hardened concretes grouted using cementitious dry-pack materials 0.6 λ

Concrete anchored to as-rolled structural steel by headed studs or by reinforcing bars

(see 11.7.9) 0.7λ

where $\lambda = 1.0$ for normal weight concrete, 0.85 for "sand-lightweight" concrete and 0.75 for "all-lightweight" concrete. Linear interpolation is permitted when partial sand replacement is used.

11.7.5 - Design yield strength of shear-friction reinforcement shall not exceed 60,000 psi.

11.7.6 - Net tension across shear plane shall be resisted by additional reinforcement.

0.6 λ is considered appropriate for this case since shear resistance is primarily due to dowel action.

The value of μ specified for concrete placed against as-rolled structural steel relates to the design of connections between precast concrete members, or between structural steel members and structural concrete members. The shear-transfer reinforcement may be either reinforcing bars or headed stud shear connectors; also, field welding to steel plates after casting of concrete is common. The design of shear connectors for composite action of concrete slabs and steel beams is not covered by these provisions, but should be in accordance with Reference 11.28.

R11.7.6 - If a resultant tensile force acts across a shear plane, reinforcement to carry that tension must be provided in addition to that provided for shear transfer. Tension may be caused by restraint of deformations due to temperature change, creep and shrinkage. Such tensile forces have caused failures, particularly in beam bearings.

When moment acts on shear plane, the flexural tension stresses and flexural compression stresses are in equilibrium. There is no change in the resultant compression $A_v f_v$ acting across the shear plane and the shear-transfer strength is not changed. It is therefore not necessary to provide additional reinforcement to resist the flexural tension stresses, unless the required flexural tension reinforcement exceeds

11.7.7 - Shear-friction reinforcement shall be appropriately placed along the shear plane and shall be anchored to develop the specified yield strength on both sides by embedment, hooks, or welding to special devices.

the amount of shear-transfer reinforcement provided in the flexural tension zone. This has been demonstrated experimentally.^{11.28}

R11.7.7 - If no moment acts across the shear plane, reinforcement should be uniformly distributed along the shear plane to minimize crack widths. If a moment acts across the shear plane, it is desirable to distribute the shear-transfer reinforcement primarily in the flexural tension zone.

Since the shear-friction reinforcement acts in tension, it must have full tensile anchorage on both sides of the shear plane. Further, the shear-friction reinforcement anchorage must engage the primary reinforcement, otherwise a potential crack may pass between the shear-friction reinforcement and the body of the concrete. This requirement applies particularly to welded headed studs used with steel inserts for connections in precast and cast-in-place concrete. Anchorage may be developed by bond, by a welded mechanical anchorage, or by threaded dowels and screw inserts. Space limitations often require a welded mechanical anchorage. For anchorage of headed studs in concrete see Reference 11.13.

In situations where the shear-friction reinforcement is not anchored to develop the specified yield strength on both sides of the shear plane, f_v shall be replaced by f_s , which may be (1) calculated as the ratio of the anchorage length provided for the shear-friction reinforcement to the code-specified development length times f_v , or (2) determined from actual tests. Actual tests are recommended whenever possible. Also, for post-

installed anchors, f_a can be determined from actual tests.

11.7.8 - For the purpose of 11.7, when concrete is placed against previously hardened concrete, the interface for shear transfer shall be clean and free of laitance. If μ is assumed equal to 1.0 λ , interface shall be roughened to a full amplitude of approximately 1/4 in.

11.7.9 - When shear is transferred between as-rolled steel and concrete using headed studs or welded reinforcing bars, steel shall be clean and free of paint.

References (to be added)

11.48. Hofbeck, J.A., Ibrahim, I.O., and Mattock, A.H., "Shear Transfer in Reinforced Concrete," *Journal of the American Concrete Institute*, Vol. 66, No. 2, February 1969, pp. 119-128.

11.49. Valluvan, R., "Issues Involved in Seismic Retrofit of Reinforced Concrete Frames Using Infilled Walls," Ph.D. dissertation, University of Texas at Austin, December 1993.

9.4 COMPARISON OF TEST RESULTS FROM CURRENT AND PREVIOUS RESEARCH WITH MODIFIED SHEAR-FRICTION PROVISIONS

In this section, test results from current and previous experimental studies are compared against the modified shear-friction provisions. The objective is to ensure that the modified shear-friction provisions are conservative for all available, relevant test data.

(1) Experimental data from current tests are compared against modified shear-friction provisions in Table 9.3 and Fig. 9.3. It may be seen that the modified shear-friction provisions yield conservative values for nominal shear strengths of test specimens. Figure 9.4 is a histogram that compares current ACI code and modified code provisions (on shear-friction) based on current test results. The modified shear-friction provisions offer conservative predictions while considering the significant benefit afforded by permanent net compression across shear plane.

(2) Extensive tests were conducted by Hofbeck [15] and Mattock [25] on direct shear transfer. All test specimens used in the study were cast monolithically. Most of the test specimens were precracked along the shear plane in order to study the effect of pre-existing cracks on shear transfer.

Figure 9.5 shows the distribution of test data with respect to the modified shear-friction provisions. The modified provisions offer conservative estimates on shear strengths of test specimens used in the study. A histogram of test results by Mattock [25] based on current and modified code provisions is shown in Fig. 9.6. All test specimens included in the histogram had shear-friction reinforcement and permanent net compression across their shear planes. It may be observed that the modified shear-friction provisions give conservative strength values for test specimens which had permanent net compression across their shear plane.

(3) Test results from experimental study by Bass [7, 8, 9] are compared with modified shear-friction provisions in Fig. 9.7. The study included test specimens with different amounts of shear-friction reinforcement across shear plane. It can be seen from

the figure that the modified code provisions offer conservative estimates on nominal shear strengths of test specimens used in the study.

The modified shear-friction provisions produce conservative but more accurate strength estimates of all test data available to date.

9.5 USE OF MODIFIED FRICTION COEFFICIENTS μ AND MODIFIED STRENGTH UPPER LIMITS FOR RETROFIT SCHEMES

Shear-friction provisions presented in Section 11.7 of ACI 318-89 [3] are intended to be conservative. The purpose of having conservative provisions is to prevent direct shear failures from being the weak links in a structure. Provision of shear-friction reinforcement across shear planes is inexpensive for new construction since the shear reinforcement can be easily placed during casting. However in retrofit schemes, the shear-friction reinforcement must be anchored across the shear plane between existing structural elements and new strengthening elements. Anchoring the reinforcement may be labor intensive and costlier since holes have to be drilled in the existing elements to place the shear-friction reinforcement. Also, the shear-friction reinforcement has to be set into the holes using a strong grout such as epoxy. In view of the overall costs involved in retrofit schemes, it is desirable to design shear planes to be safe but not overly conservative.

In current test series, two kinds of shear planes were investigated; (1) concrete placed directly against roughened interface of hardened concrete, and (2) concretes of different strength and age with the interface grouted using cementitious dry-pack material. The two cases are typical in retrofit schemes. The modified shear-friction provisions recommend μ values of 1.0λ and 0.6λ for both cases respectively. It may be seen from Fig. 9.8 that the modified shear-friction provisions with modified μ values of 1.4λ and 0.8λ respectively yield safe values of nominal strengths for shear planes. It may therefore be recommended that modified friction coefficients of 1.4λ and 0.8λ be used for retrofit schemes. Also, an increase in strength upper limits; from $0.25 f_c' A_c$ or $800 A_c$, whichever is less to $0.3 f_c' A_c$ or $1000 A_c$, whichever is less would still result in safe strength estimates (Fig. 9.8). Therefore,

for retrofit schemes, the upper limit on shear strength V_n (calculated using Eqn. 11-26-A in Art. 9.2.1) shall be recommended as $0.3 f_c' A_c$ or $1000 A_c$, whichever is less.

9.6 SUMMARY, CONCLUSIONS AND RECOMMENDATIONS

Current ACI code provisions for shear-friction are reviewed. Disagreements between test data and code values are identified and suitable modifications to the code are proposed. Test values from current and previous research are utilized to verify the suitability of modified provisions. The following conclusions and recommendations are made based on the study:

(1) Shear-friction provisions in Section 11.7 of ACI 318-89 [3] do not reflect test results especially when there is permanent net compression across the shear plane. The modified provisions produce conservative but more accurate strength estimates for all available, relevant test data to date.

(2) Code assumptions regarding cumulative contribution of shear-friction reinforcement and permanent net compression across the shear plane to shear transfer strength are not justified in all cases. The modified provisions present a more accurate representation on contribution of shear reinforcement and compression.

(3) Even though code upper limits on shear strength are generally conservative, they become overly conservative when there is permanent compression across the shear plane. The upper limits proposed in modified provisions take the benefit of compression into account.

(4) The modified provisions present friction coefficients for grouted shear planes.

(5) Modified shear-friction provisions offer a better tool for estimating shear transfer strengths.

(6) Different (less conservative) friction coefficients and strength upper limits may be specified for retrofit purposes.

Table 9.1 Comparison of test results from current study with ACI 318-89 provisions on shear-friction

| Specimen | $V_{measured}$ (peak strength) kips (psi) | Interface details | | $A_v f_v$ for dowels kips | Perm. comp. force N kips | Estimated shear strengths | | | V_{ACI} least of (1) or (2) or (3) kips | Ratio of $V_{measured}$ to V_{ACI} |
|----------|---|-------------------|--------------------------|------------------------------------|--------------------------------------|----------------------------------|----------------------------------|----------------------------------|---|---|
| | | Dowels | Comp. stress (psi) | | | (1) $V_{ACI 208.8}^1$ kips | (2) $V_{ACI 208.8}^2$ kips | (3) $V_{ACI 208.8}^3$ kips | | |
| A2 | 76 (553) | 3 #6 | 0 | 55 | 0 | 55 | 95 | 44 | 44 | 1.73 |
| A3* | 76 (553) | 3 #6 | 0 | 55 | 0 | 55 | 95 | 44 | 44 | 1.73 |
| A4 | 90 (703) | 6 #6 | 0 | 111 | 0 | 111 | 139 | 44 | 44 | 2.05 |
| A5* | 204 (1553) | none | 1000 | 0 | 128 | 128 | 153 | 44 | 44 | 4.64 |
| A6 | 182 (1421) | 3 #6 | 1000 | 55 | 128 | 183 | 197 | 44 | 44 | 4.14 |
| A7 | 213 (1664) | 6 #6 | 1000 | 111 | 128 | 238 | 242 | 44 | 44 | 4.84 |
| A8 | 201 (1570) | none | 1000 | 0 | 128 | 128 | 153 | 44 | 44 | 4.57 |
| B1 | 113 (882) | 3 #6 | 0 | 63 | 0 | 63 | 102 | 89 | 63 | 1.79 |
| B2 | 130 (1015) | 6 #6 | 0 | 127 | 0 | 127 | 152 | 89 | 89 | 1.46 |

+ Indicates monotonic loading * bond (pull out) strength of #6 dowels (embedment depth = 6 in.)

contd.

Table 9.1 Comparison of test results from current study with ACI 318-89 provisions on shear-friction (cont'd.)

| Specimen | $V_{measured}$ (peak strength) kips (psi) | Interface details | | $A_v f_s$ for dowels kips | Perm. comp. force N kips | Estimated shear strengths | | | V_{ACI} least of (1) or (2) or (3) kips | Ratio of $V_{measured}$ to V_{ACI} |
|--------------|---|-------------------|--------------------------|------------------------------------|--------------------------------------|-----------------------------------|-----------------------------------|-----------------------------------|---|---|
| | | Dowels | Comp. stress (psi) | | | (1) $V_{ACI 318-89}^1$ kips | (2) $V_{ACI 318-89}^2$ kips | (3) $V_{ACI 318-89}^3$ kips | | |
| B3 | 254 (1984) | none | 1000 | 0 | 128 | 128 | 153 | 89 | 89 | 2.85 |
| B4 | 291 (2273) | none | 1500 | 0 | 192 | 192 | 204 | 89 | 89 | 3.27 |
| B5 | 264 (2062) | 3 #6 | 1000 | 63 | 128 | 191 | 204 | 89 | 89 | 2.97 |
| B6 | 274 (2140) | 6 #6 | 1000 | 127 | 128 | 255 | 255 | 89 | 89 | 3.08 |
| B7 (grouted) | 52 (402) | 3 #6 | 0 | 63 | 0 | 63 | 50 | 89 | 50 | 1.04 |
| B8 (grouted) | 102 (796) | 3 #6 | 1000 | 63 | 128 | 191 | 153 | 89 | 89 | 1.15 |
| B9 | 254 (1984) | 3 #6 | 1000 (cyclic) | 63 | 0 | 63 | 102 | 89 | 63 | 4.03 |
| B10 | 167 (1304) | 3 #6 | 350 | 63 | 44 | 107 | 137 | 89 | 89 | 1.88 |

1 $V_s = (A_v f_s + N) \mu$ where $A_v f_s =$ area of shear-friction reinforcement in in^2 , $f_s =$ bond (pull out) strength of shear-friction reinforcement in psi, $N =$ permanent net compression in pounds, and $\mu =$ coefficient of friction as specified in Sect. 11.7.4.3 of ACI 318-89 [3]

2 $V_s = 0.8 (A_v f_s + N) + A_c K_1$ where $A_c =$ area of conc. section resisting shear in in^2 and K_1 as in Sect. R11.7.3 of ACI 318-89 [3]

3 $V_s =$ lesser of $0.2 f_c' A_c$ or $800 A_c$ where $f_c' =$ specified compressive strength of weaker concrete in psi

Table 9.2 Comparison of current test results with modified shear-friction equation proposed in Eqn. (11-26-B) of Art. 9.2.1

| Specimen | Frame f'_c (psi) | Wall f'_c (psi) | Compressive stress across specimen interface | | $V_{measured}$ kips (psi) | $V_n = N \mu$ $\mu = 1.0$ kips | $V_{measured} / V_n$ |
|----------|--------------------|-------------------|--|---------------|---------------------------|--------------------------------------|----------------------|
| | | | magnitude, N kips (psi) | $\times f'_c$ | | | |
| A5 | 1750 | 5100 | 128 (1000) | 0.57 | 204 (1583) | 128 | 1.59 |
| A6 | 1750 | 5100 | 128 (1000) | 0.57 | 182 (1421) | 128 | 1.42 |
| A7 | 1750 | 5100 | 128 (1000) | 0.57 | 213 (1664) | 128 | 1.66 |
| A8 | 1750 | 5100 | 128 (1000) | 0.57 | 201 (1570) | 128 | 1.57 |
| B3 | 3500 | 6000 | 128 (1000) | 0.29 | 254 (1994) | 128 | 1.96 |
| B4 | 3500 | 6000 | 192 (1500) | 0.43 | 291 (2273) | 192 | 1.52 |
| B5 | 3500 | 6000 | 128 (1000) | 0.29 | 264 (2062) | 128 | 2.06 |
| B6 | 3500 | 6000 | 128 (1000) | 0.29 | 274 (2140) | 128 | 2.14 |

Note: All test specimens had permanent net compression, N greater than 800 A_c pounds across their interfaces

Table 9.3 Comparison of test results from current study with modified shear-friction provisions

| Specimen | $V_{measured}$ (peak strength) kips (psi) | Interface details | | $A_v f_y$ [*] for dowels kips | Perm. comp. force N kips | Estimated shear strengths | | $V_{modified}$ least of (1) or (2) or (3) kips | Ratio of $V_{measured}$ to $V_{modified}$ |
|-----------------|---|-------------------|--------------------------|---|--------------------------------------|---------------------------------|---------------------------------|--|--|
| | | Dowels | Comp. stress (psi) | | | (1) $V_{measured}^1$ kips | (2) $V_{measured}^2$ kips | | |
| A2 | 76 (593) | 3 #6 | 0 | 55 | 0 | 55 | 56 | 56 | 1.36 |
| A3 ⁺ | 76 (593) | 3 #6 | 0 | 55 | 0 | 55 | 56 | 56 | 1.36 |
| A4 | 90 (703) | 6 #6 | 0 | 111 | 0 | 111 | 56 | 56 | 1.61 |
| A5 ⁺ | 204 (1593) | none | 1000 | 0 | 128 | 128 | 134 | 128 | 1.59 |
| A6 | 182 (1421) | 3 #6 | 1000 | 0 | 128 | 128 | 134 | 128 | 1.42 |
| A7 | 213 (1664) | 6 #6 | 1000 | 0 | 128 | 128 | 134 | 128 | 1.66 |
| A8 | 201 (1570) | none | 1000 | 0 | 128 | 128 | 134 | 128 | 1.57 |
| B1 | 113 (882) | 3 #6 | 0 | 63 | 0 | 63 | 102 | 63 | 1.79 |
| B2 | 130 (1015) | 6 #6 | 0 | 127 | 0 | 127 | 102 | 102 | 1.27 |

+ indicates monotonic loading

* bond (pull out) strength of #6 dowels (embedment depth = 6 in.)

contd.

Table 9.3 Comparison of test results from current study with modified shear-friction provisions (contd.)

| Specimen | $V_{measured}$ (peak strength) kips (psi) | Interface details | | $A_d f_c$ for dowels kips | Perm. comp. force N kips | Estimated shear strengths | | $V_{modified}$ least of (1) or (2) or (3) kips | Ratio of $V_{measured}$ to $V_{modified}$ |
|--------------|---|-------------------|--------------------------|------------------------------------|--------------------------------------|---------------------------------|---------------------------------|--|--|
| | | Dowels | Comp. stress (psi) | | | (1) $V_{modified}^1$ kips | (2) $V_{modified}^2$ kips | | |
| B3 | 254 (1984) | none | 1000 | 0 | 128 | 128 | 268 | 128 | 1.98 |
| B4 | 291 (2273) | none | 1500 | 0 | 192 | 192 | 268 | 192 | 1.52 |
| B5 | 264 (2062) | 3 #6 | 1000 | 0 | 128 | 128 | 268 | 128 | 2.06 |
| B6 | 274 (2140) | 6 #6 | 1000 | 0 | 128 | 128 | 268 | 128 | 2.14 |
| B7 (grouted) | 52 (406) | 3 #6 | 0 | 63 | 0 | 38 | 102 | 38 | 1.37 |
| B8 (grouted) | 102 (796) | 3 #6 | 1000 | 63 | 0 | 38 | 102 | 38 | 2.68 |
| B9 | 254 (1984) | 3 #6 | 1000 (cyclic) | 63 | 0 | 63 | 102 | 63 | 4.03 |
| B10 | 167 (1304) | 3 #6 | 350 | 63 | 44 | 107 | 102 | 102 | 1.64 |

1 $V_n = (A_d f_c + N) \mu$ and $V_n = N \mu$ when $N > 800 A_d$, pounds2 $V_n = \text{lesser of } 0.25 f_c' A_c \text{ or } 800 A_d \text{, and } V_n = \text{lesser of } 0.6 f_c' A_c \text{ or } 2100 A_d \text{, when } N > 800 A_d \text{, pounds}$

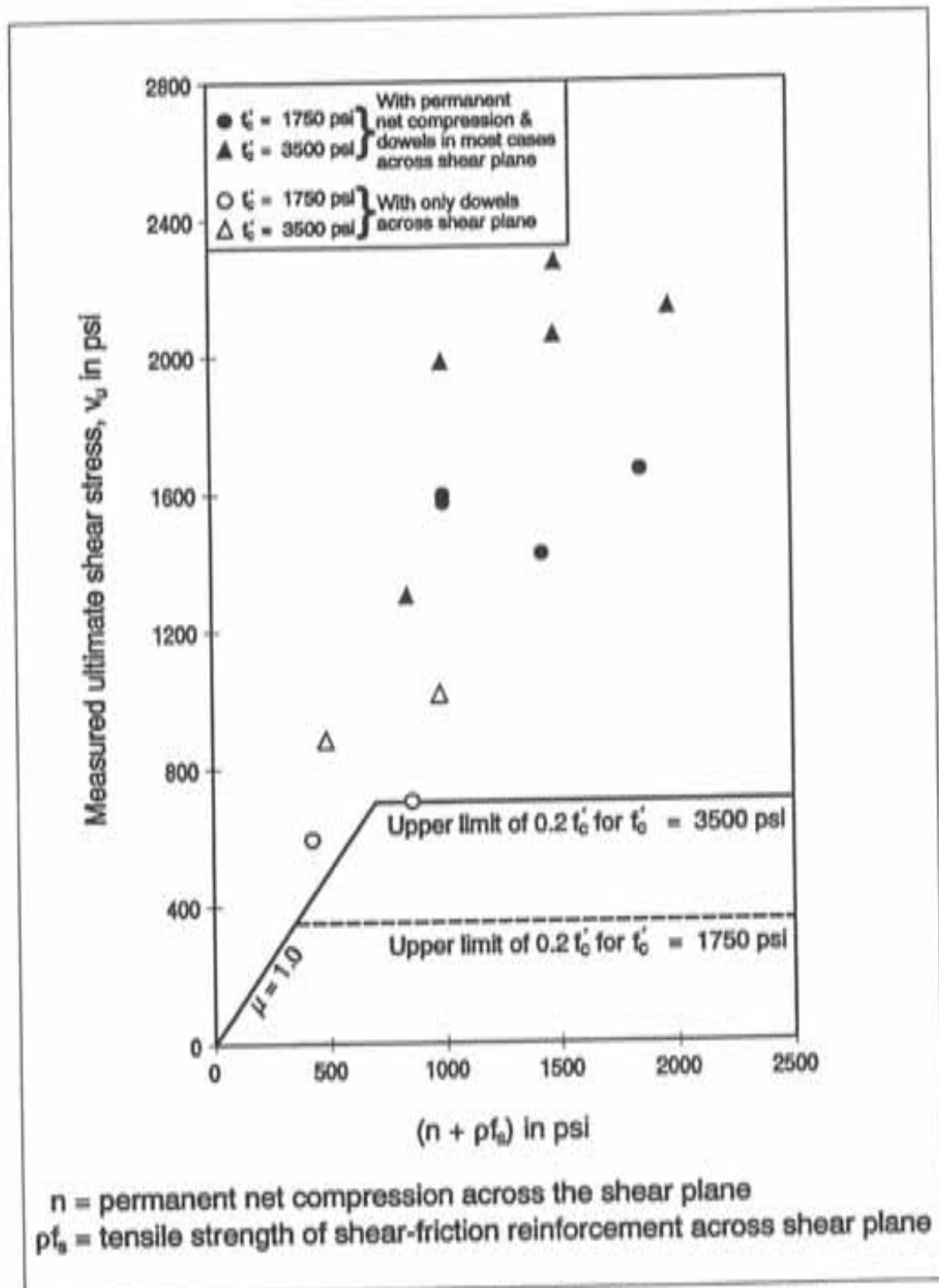


Figure 9.1 Comparison of test results with ACI recommended upper limits for nominal shear stress

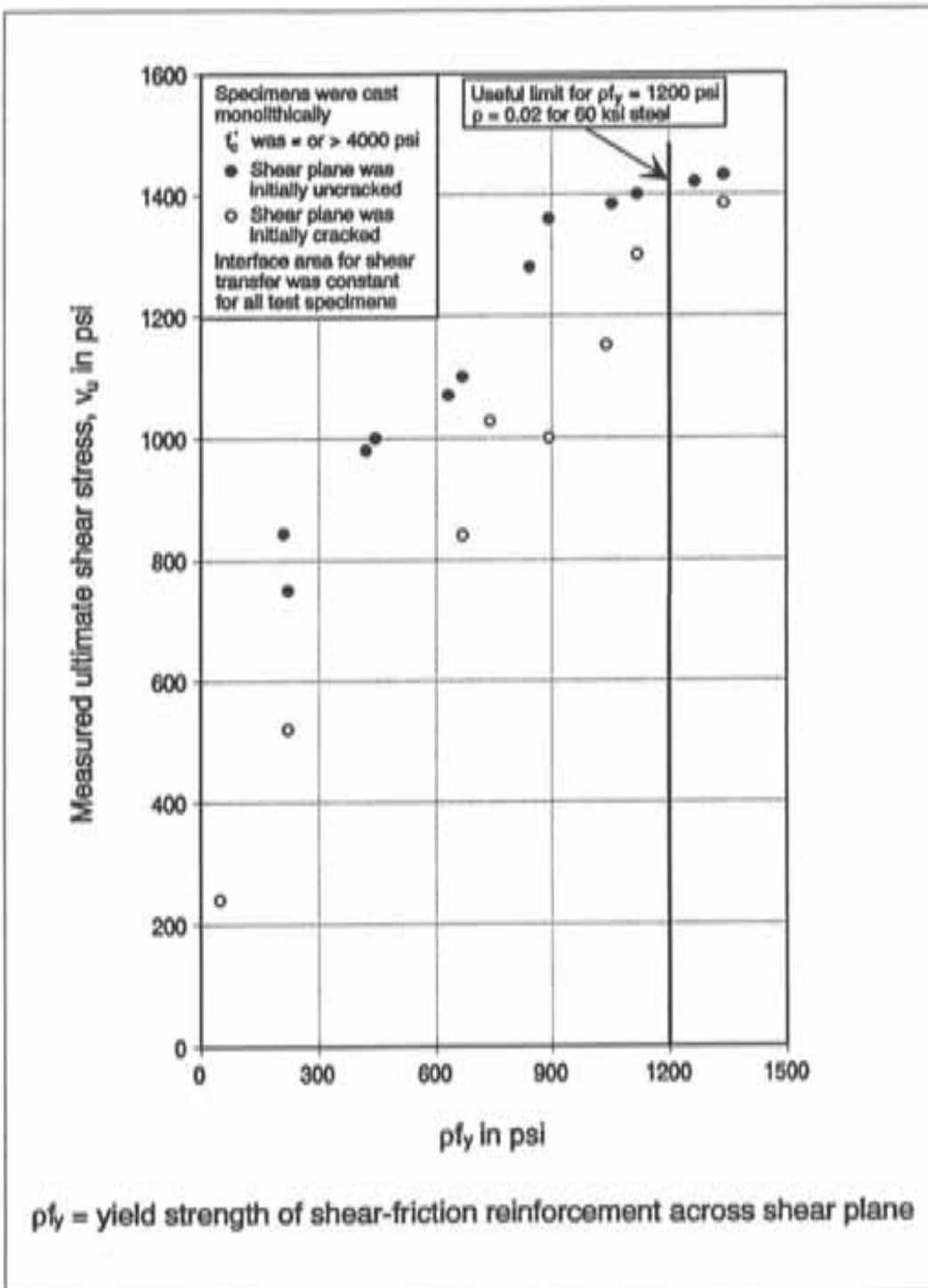


Figure 9.2 Influence of amount of shear-friction reinforcement on interface shear transfer as established from tests by Hofbeck [15]

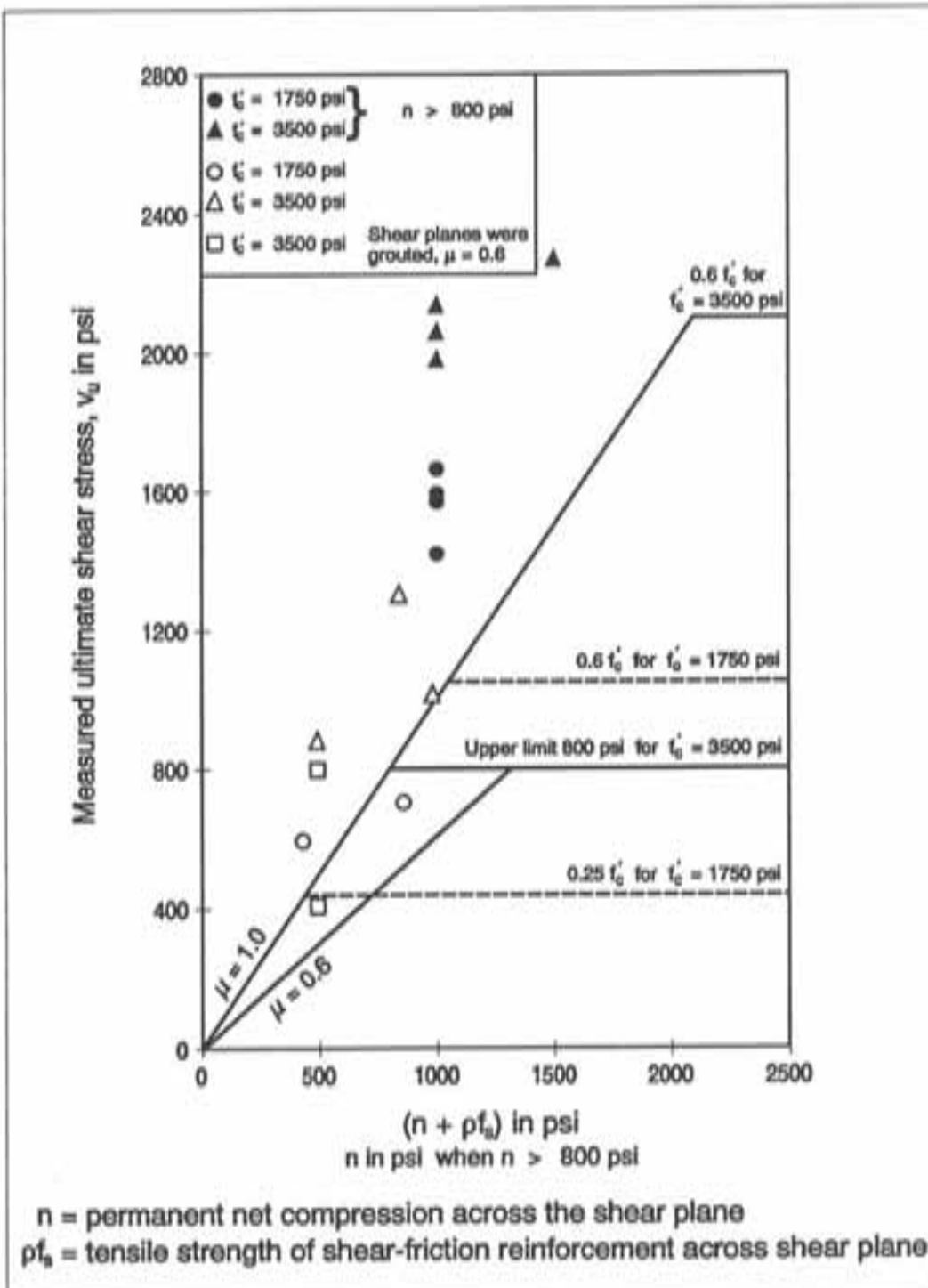


Figure 9.3 Comparison of current test results with modified shear-friction provisions

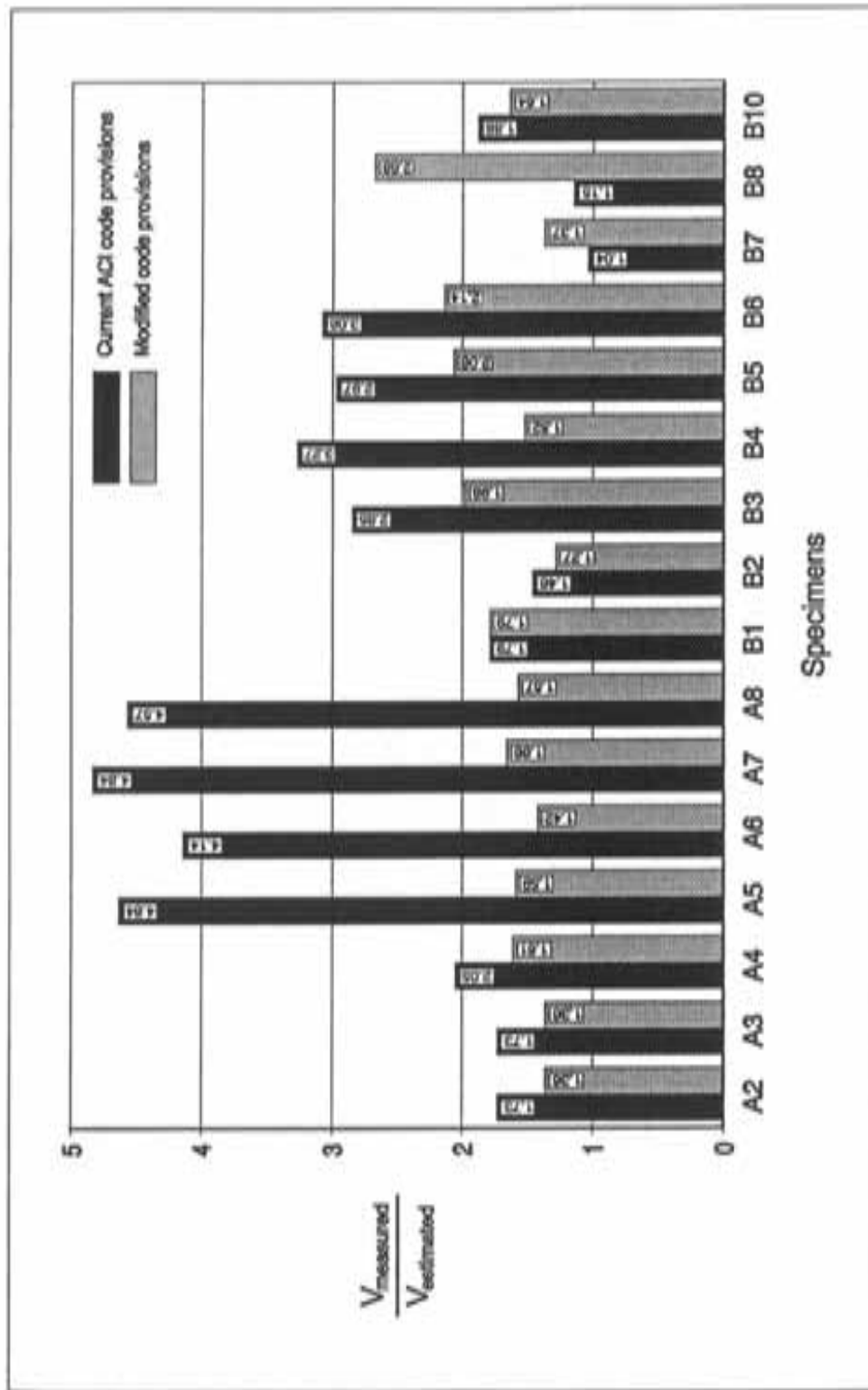


Figure 9.4 Comparison of current ACI code and modified code provisions based on current test results

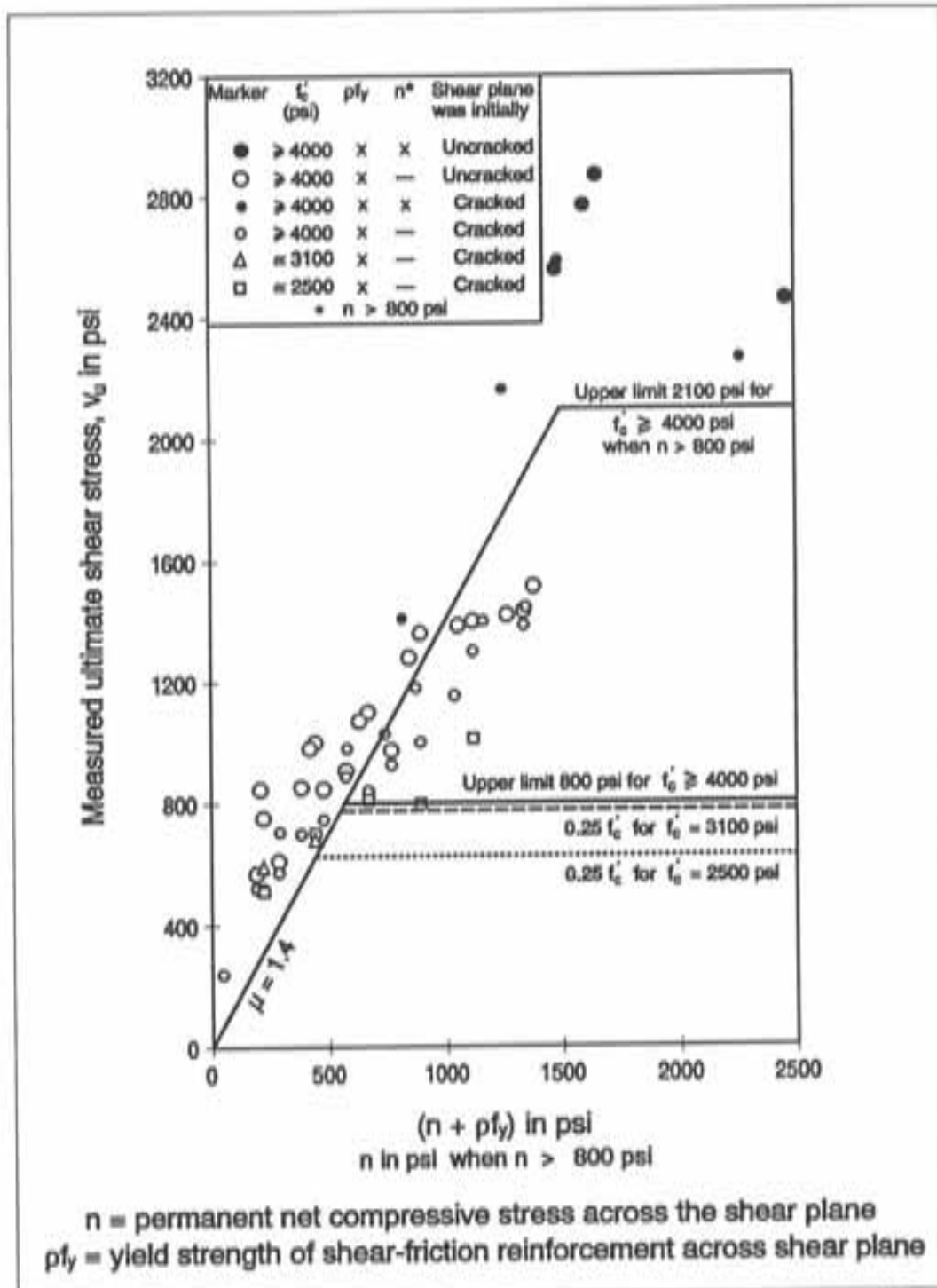


Figure 9.5 Comparison of test results by Hofbeck [15] & Mattock [25] with modified shear-friction provisions

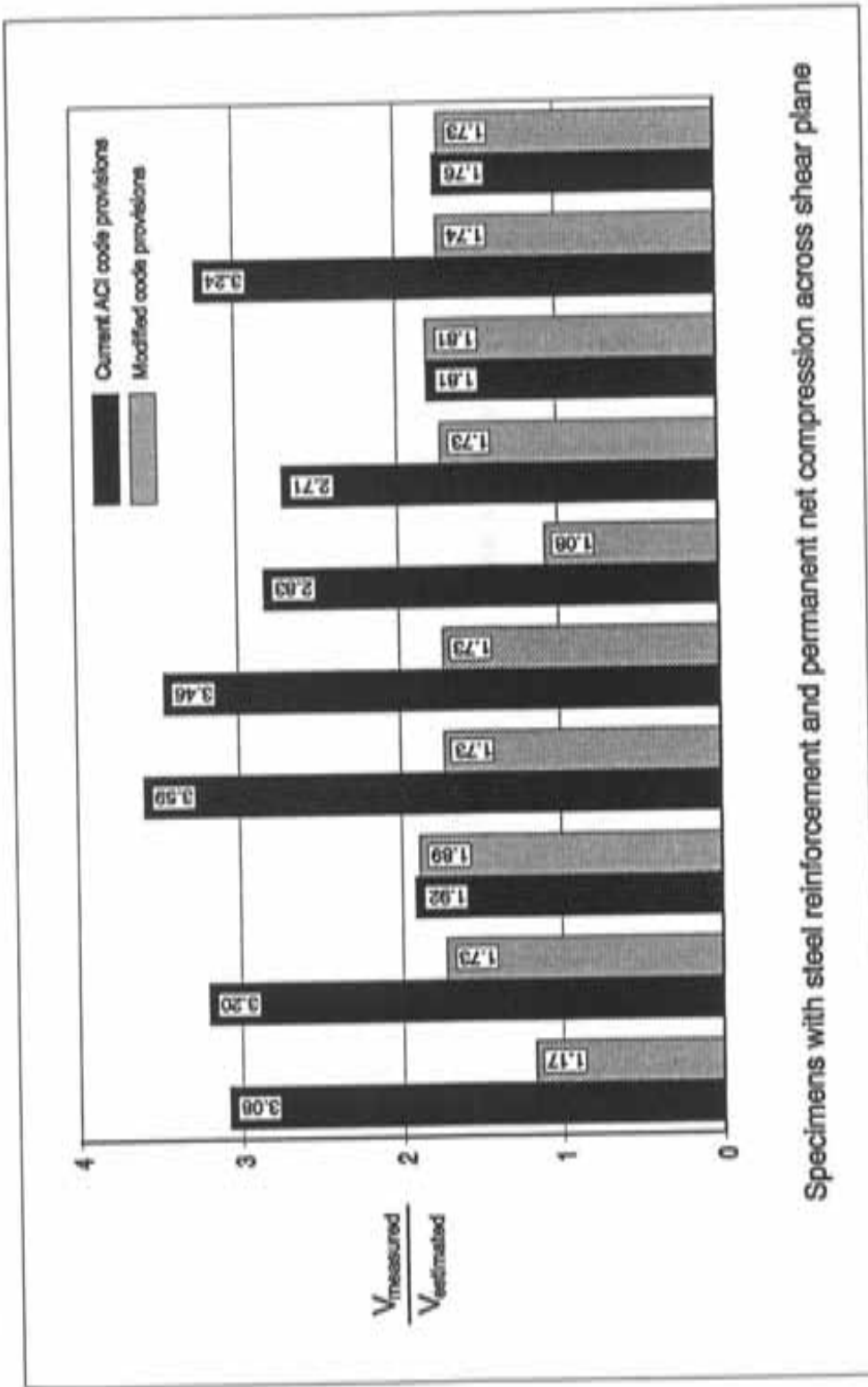


Figure 9.6 Comparison of current ACI code and modified code provisions based on test results by Mattock [25]

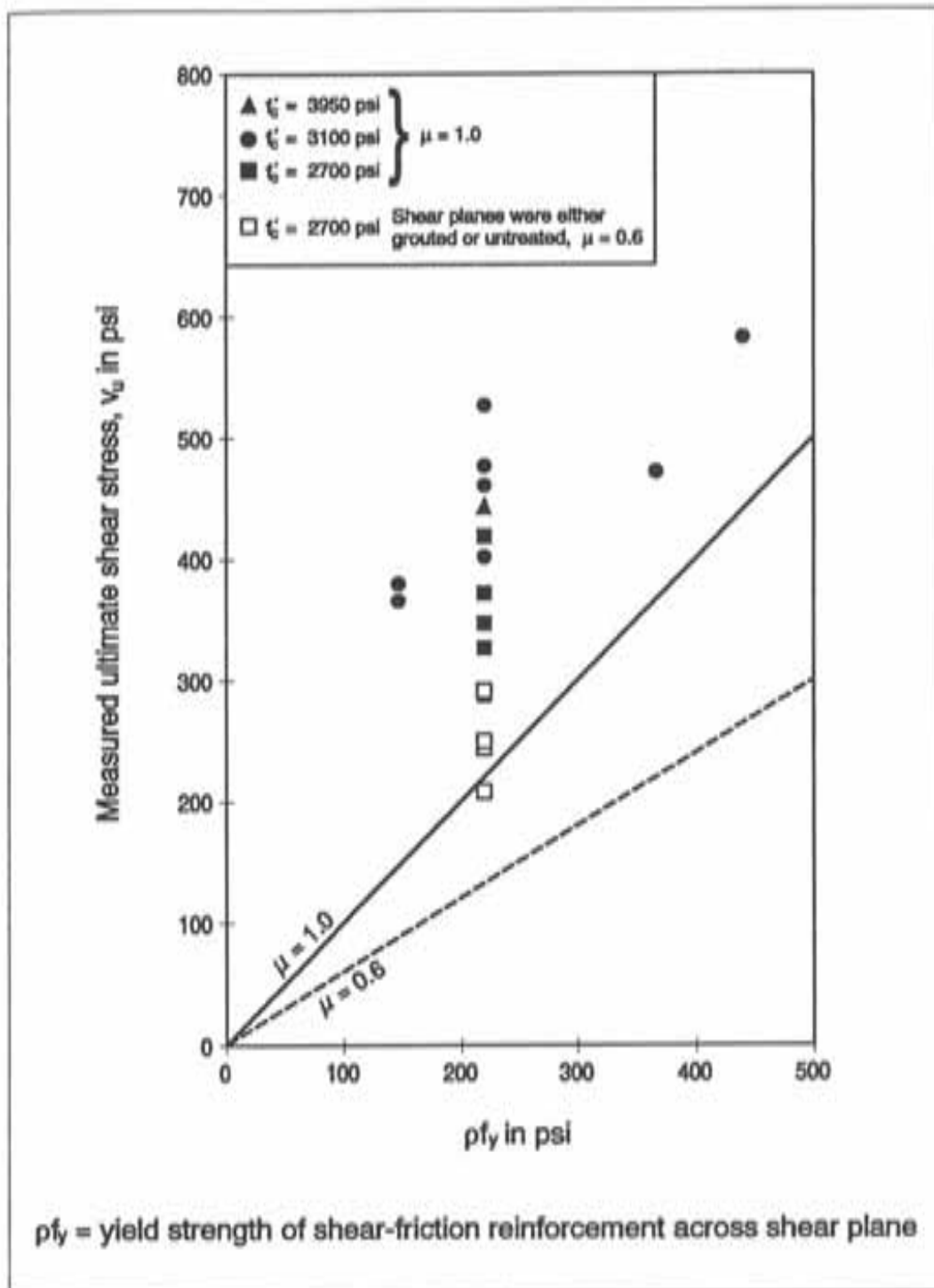


Figure 9.7 Comparison of test results by Bass [7, 8, 9] with modified shear-friction provisions

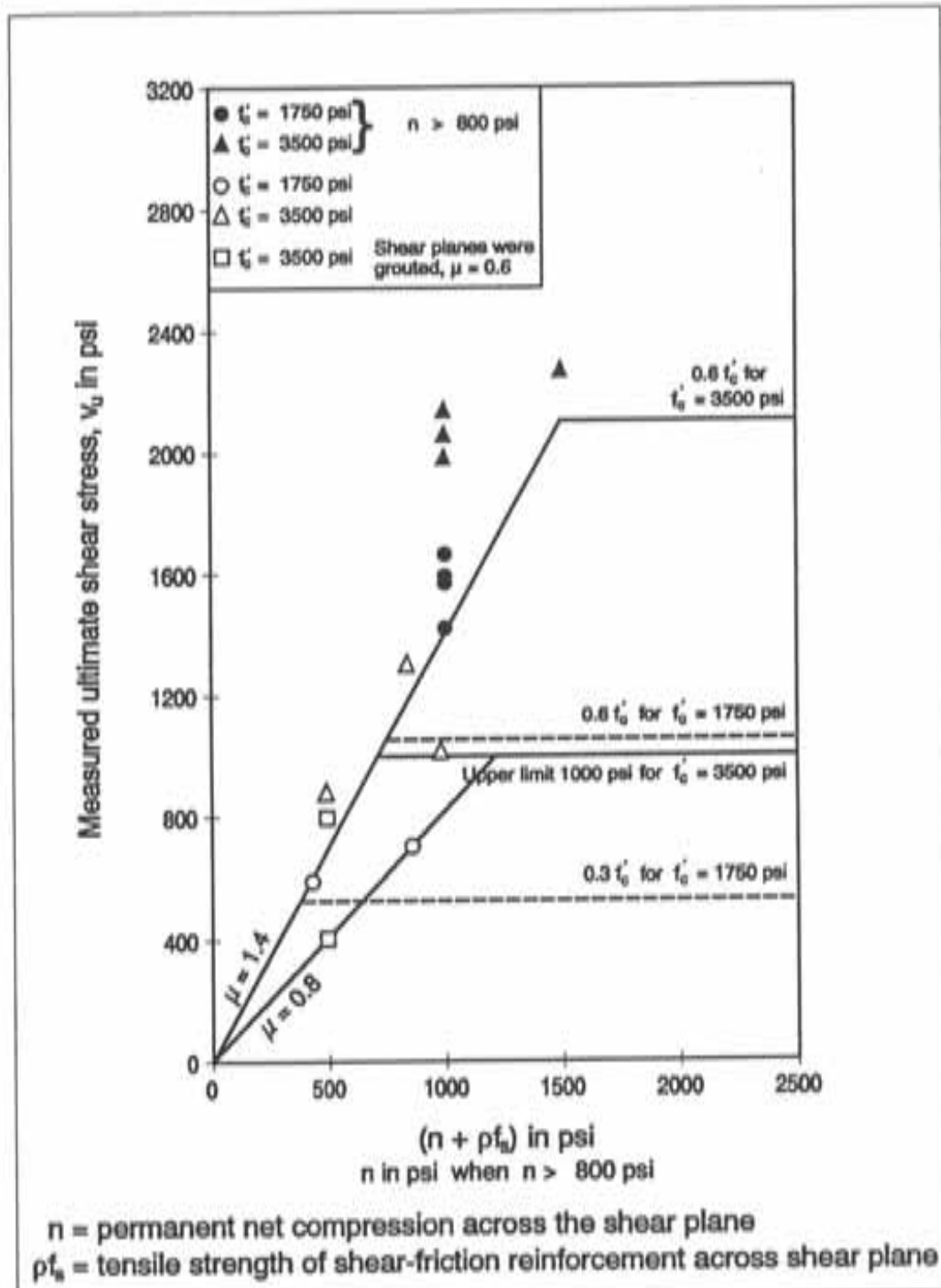


Figure 9.8 Comparison of current test results with modified μ and modified strength upper limits for retrofit purposes

CHAPTER 10

CONCLUSIONS AND RECOMMENDATIONS

The current experimental investigation focussed on the issues involved in seismic retrofit of non-ductile, moment-resisting reinforced concrete frames using infilled walls. Issues investigated were: (1) retrofit techniques for strengthening short, compression lap splices in the existing columns to enable column longitudinal reinforcement to develop the tensile strength and the column to sustain significant inelastic deformations; and (2) the direct shear transfer mechanism across frame-wall interfaces. In the first phase of the study, column-splice specimens were strengthened using a variety of selected retrofit techniques and were tested to investigate the seismic performance of retrofitted column splices. For the second phase, test specimens representative of a portion of a frame-wall interface were constructed and the mechanism of reversed, cyclic shear transfer directly across the specimen interface was studied in detail. Test results from the second phase were used to verify and extend the application of shear-friction provisions currently incorporated in Sect. 11.7 of ACI 318-89 [3]. The conclusions and recommendations presented below are based on the study.

(1) Retrofitting of Column Splices

(a) Column lap splices designed for axial compression and little or no flexure cannot develop the tensile strength of column longitudinal reinforcement and do not permit significant inelastic deformations in the column region when the structure is subjected to lateral seismic loads.

(b) Non-ductile RCMRF retrofitted for seismic forces using an infill wall may not satisfy performance goals due to the premature failure of lap splices in the existing columns.

(c) External reinforcement (steel elements or ties) around the splice region significantly improved confinement resulting in substantial increases in splice tensile strength and ductility. External reinforcement must be grouted to ensure effective confinement of the splice region.

(d) Addition of only internal ties to the splice region was not an effective technique for strengthening column splices. Removal of concrete cover resulted in microcracking of the concrete core and reduction in effectiveness of concrete cover which reduced the gains in splice strength and ductility provided by the added ties.

(e) Providing continuity in the splice region by welding the spliced bars enabled column reinforcement to yield in tension and improved column ductility. However, it was necessary to add internal ties to restrain the outward thrust produced by the eccentricity between spliced bars.

(2) Shear Transfer Across Frame-Wall Interface

(a) Permanent net compression across an interface improved significantly interface performance for direct shear transfer. The higher the level of compression, the better were peak shear strength, peak-to-peak shear stiffness, and residual shear capacity of the interface.

(b) Cyclic compression resulting across an interface from such forces as seismic loads may not be considered for calculating direct shear transfer capacity because its influence on interface performance for direct shear transfer was not substantial.

(c) Dowels provided as shear connectors across an interface must be anchored on both sides of the interface to develop tensile yield strength or more dowels should be provided to account for premature pull out failures.

(d) Frame-wall interfaces with frames having low-strength concrete should be provided with more dowels since their strength will be governed by disintegration of the low-strength concrete around the dowels.

(e) Grouting of frame-wall interfaces using cementitious dry-pack materials should be avoided if possible. Dry-pack grout interfaces will not develop aggregate interlock. Better means for closing the gap between interfaces should be explored and resorted to.

(3) Modifications for Shear-Friction Provisions in Section 11.7 of ACI 318-89 [3]

(a) Shear-friction provisions in Section 11.7 of ACI 318-89 [3] do not reflect the behavior of test specimens, especially when there is permanent net compression across the shear plane. The modified provisions presented in chapter 9 produce conservative but more accurate strength estimates for all available, relevant test data to date.

(b) Code assumptions regarding cumulative contribution of shear-friction reinforcement and permanent net compression across the shear plane to shear transfer strength are not justified in all cases. The modified provisions present a more accurate representation of the contribution of shear reinforcement and compression.

(c) Even though code upper limits on shear strength are generally conservative, they become overly conservative when there is permanent compression across the shear plane. The upper limits proposed in modified provisions take into account the benefit of compression.

(d) The modified provisions present friction coefficients for grouted shear planes.

(e) The modified shear-friction provisions offer a better tool for estimating shear transfer strengths.

(f) Different (less conservative) friction coefficients and strength upper limits, as presented in chapter 9, may be specified for retrofit purposes.

APPENDIX A

RETROFITTING OF COLUMN SPLICES

DESIGN OF RETROFIT SCHEMES

A.1 DESIGN CRITERIA

Design of retrofit schemes providing additional confinement in the splice region was based primarily on the transverse reinforcement requirements for lap splices as proposed by Orangun [26]. One of the schemes, besides being designed to comply with Orangun's recommendations, was also designed to meet the transverse reinforcement requirements as specified by chapter 21 of ACI 318-89 [3] for boundary elements of structural walls. The scheme that provided continuity between lap spliced bars was designed to transfer the load by shear.

A.2 STEEL ANGLES AND STRAPS

The technique was used widely in Mexico City following the 1985 earthquake. Its performance was however not verified through experimental studies. Design of steel angles and straps scheme was based on Orangun's equation, which specifies a limiting factor that represents the confinement in the splice region. The equation recommends that,

$$\frac{A_v f_{yt}}{500 s d_b} \leq 3 \quad (A-1)$$

where,

- A_v = area of transverse reinforcement across the splitting plane divided by the number of splices in sq. in.,
- f_{yt} = yield strength of transverse reinforcement in psi,
- s = spacing of transverse reinforcement in inches, and
- d_b = splice bar diameter in inches

In order to ensure adequate confinement, the factor given in Eqn. (A-1) must be greater than 3.

$$\begin{aligned} \frac{A_{st} f_{yt}}{500 s d_b} &\geq 3 \\ A_{strap} \times 36,000 &\geq 3 \times 500 \times 6 \times 0.75 \\ A_{strap} &\geq 0.188 \text{ in.}^2 \end{aligned}$$

∴ Straps of 1" × 1/4" cross section (area = 0.25 in²) were used.

Steel angles were designed to enable the straps to yield in tension. From Fig. A.1c,

$$\begin{aligned} W &= \sqrt{2} P_y \\ &= \sqrt{2} (A_{strap} f_{yt}) \\ &= \sqrt{2} (0.25 \times 36,000) \\ &= 12,728 \text{ lbs.} \end{aligned}$$

Assuming that the radially outward stresses, produced by reinforcing bar lugs, were uniform along the splice region, the steel angle would be subjected to a uniformly distributed load of W divided by the strap spacing, s . Also, the angle-strap connections could be assumed as rigid. With the assumptions made,

$$\begin{aligned} \text{Maximum flexural moment on the angle} &= \frac{(W/s) \times s^2}{12} \\ &= \frac{(12.728 \text{ K} / 6 \text{ in.}) \times (6 \text{ in.})^2}{12} \\ &= 6.36 \text{ K-in.} \end{aligned}$$

$$\begin{aligned}
 S_{required} &= \frac{M}{F_y} \\
 &= \frac{6.36}{36} \\
 &= 0.17 \text{ in.}^3
 \end{aligned}$$

Choosing L 2 × 2 × 1/4 from LRFD (p. 1-58), $S_{provided} = 0.17 \text{ in.}^3$

$$\begin{aligned}
 \therefore \text{Factor of safety against yielding} &= \frac{S_{provided}}{S_{required}} \\
 &= 0.17 / 0.17 \\
 &= 1.0
 \end{aligned}$$

Therefore, O. K.

Summary: *Angles* = 2" x 2" x 1/4" A36 Grade
 Straps = 12" x 1" x 1/4" A36 Grade

A.3 EXTERNAL REINFORCING BAR TIES

"External reinforcing bar ties" scheme was designed to provide the splice region with additional transverse reinforcement that would comply with the requirements of Chapter 21 of ACI 318-89 [3] for boundary elements of structural walls. While the tie spacing was governed by code requirements, its size was determined using Orangun's equation.

From Section 21.4.4.6 of ACI 318-89 [3],

Tie spacing ≤ Smaller of six times the diameter of the column longitudinal bar or 6 in.

$$\begin{aligned} &\leq \text{Smaller of } 6 \times 0.75 \text{ in. (\#6 bar)} = 4.5 \text{ in.} \\ &\quad \text{or } 6 \text{ in.} \\ &\leq 4.5 \text{ in.} \end{aligned}$$

Therefore, tie spacing of 3 in. was chosen.

Using Orangun's equation,

$$\begin{aligned} \frac{A_v f_y}{500s d_b} &\geq 3 \\ A_v \times 70,000 &\geq 3 \times 500 \times 3 \times 0.75 \\ A_v &\geq 0.048 \text{ in}^2 \end{aligned}$$

Providing #4 ties, $A_v = 0.20 \text{ in}^2$ and therefore, O. K.

Summary: 9 #4 ties were provided at 3 in. spacing over the splice region.

A.4 ADDITIONAL INTERNAL TIES

The scheme was selected as it would not change the column dimensions. Such a scheme might be resorted to in situations, where changes to column dimensions must be strictly avoided.

Spacing of additional internal ties could not be selected in compliance with the transverse reinforcement requirements of ACI 318-89 [3] for boundary elements of structural walls. Closer spacing of ties would have required removal of significant amount of concrete cover and caused extensive damage to concrete core, and hence a tie spacing of 8 in. (wider than the code requirement) was selected as an optimum spacing considering the practical implications.

Since #2 ties (at 12 in. spacing) were existing in the splice region, the available confinement was estimated using Orangun's equation as,

$$\begin{aligned} \left(\frac{A_v f_{yt}}{500 s d_b} \right)_{\text{available}} &= \frac{0.049 \times 71,000}{500 \times 12 \times 0.75} \\ &= 0.77 \\ \therefore \left(\frac{A_v f_{yt}}{500 s d_b} \right)_{\text{required}} &\geq 3 - 0.77 \\ &\geq 2.23 \\ A_v \text{ required} &\geq \frac{2.23 \times 500 \times 8 \times 0.75}{70,000} \\ &\geq 0.1 \text{ in}^2 \end{aligned}$$

Providing #3 ties, $A_v = 0.11 \text{ in}^2$ and therefore, O. K.

Summary: 3 #3 ties were provided at 8 in. spacing over the splice region.

A.5 WELDED SPLICES

The scheme was designed to provide continuity between lap spliced bars through shear. It facilitates direct transfer of forces without relying on the bond strength between spliced bars and surrounding concrete. Reinforcing bars of #3 size had to be used as fillers between lap spliced bars, since the splices were constructed as non-contact splices (with 1/4 in. gap between them) to represent field conditions where the lap spliced bars are not in contact with each other after construction is completed.

Lap spliced bars, when welded together and loaded, produces an outward thrust on the surrounding concrete due to the eccentricity between them. As a result, the concrete cover surrounding the splice region would be subjected to extensive damage. The non-contact splices were constructed to simulate the increased outward thrust produced by larger eccentricity between the splice bars.

From Fig. A.2c, throat thickness of weld, a = $0.4 \times$ filler bar diameter
 = 0.15 in.

Measured yield strength of a column bar = Bar area \times measured yield stress
 = 0.44×69
 = 30.4 kips

Strength of weld = $\phi \times a \times l \times$ shear strength of weld

where,

ϕ = under strength factor,
 a = throat thickness of weld in inches, and
 l = length of the weld in inches

= $0.75 \times 0.15 \times l \times$
 (0.6 \times 90)
 = $6.1 l$

For a safe design, strength of weld \geq Measured yield strength of a column bar
 $6.1 l \geq 30.4$
 $l \geq 5$ in.

Weld of 6 in. length was used.

Summary: Weld length = 6 in.
 Weld electrode type = AWS E9018-M

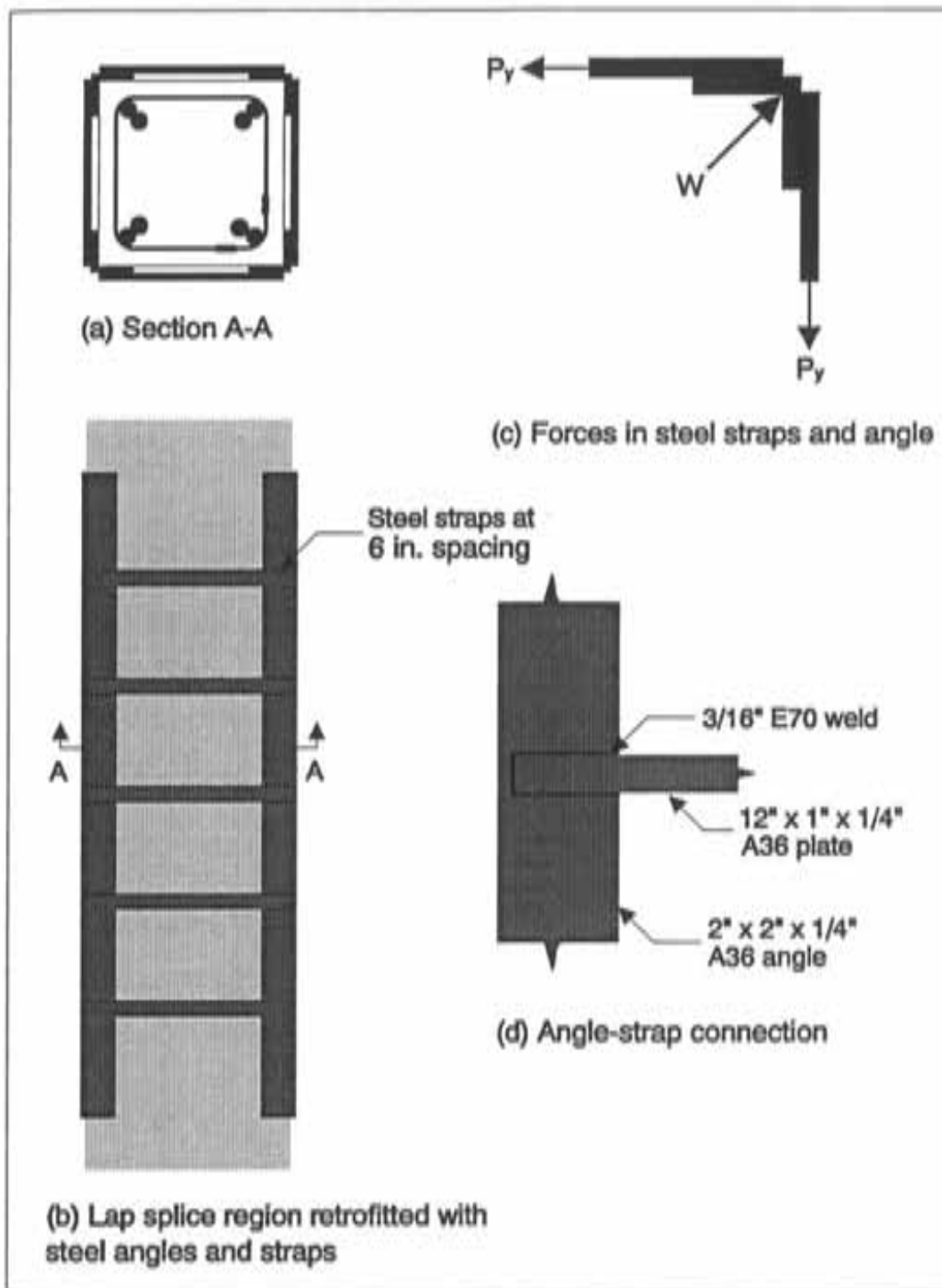


Figure A.1 Details of retrofit scheme with steel angles and straps

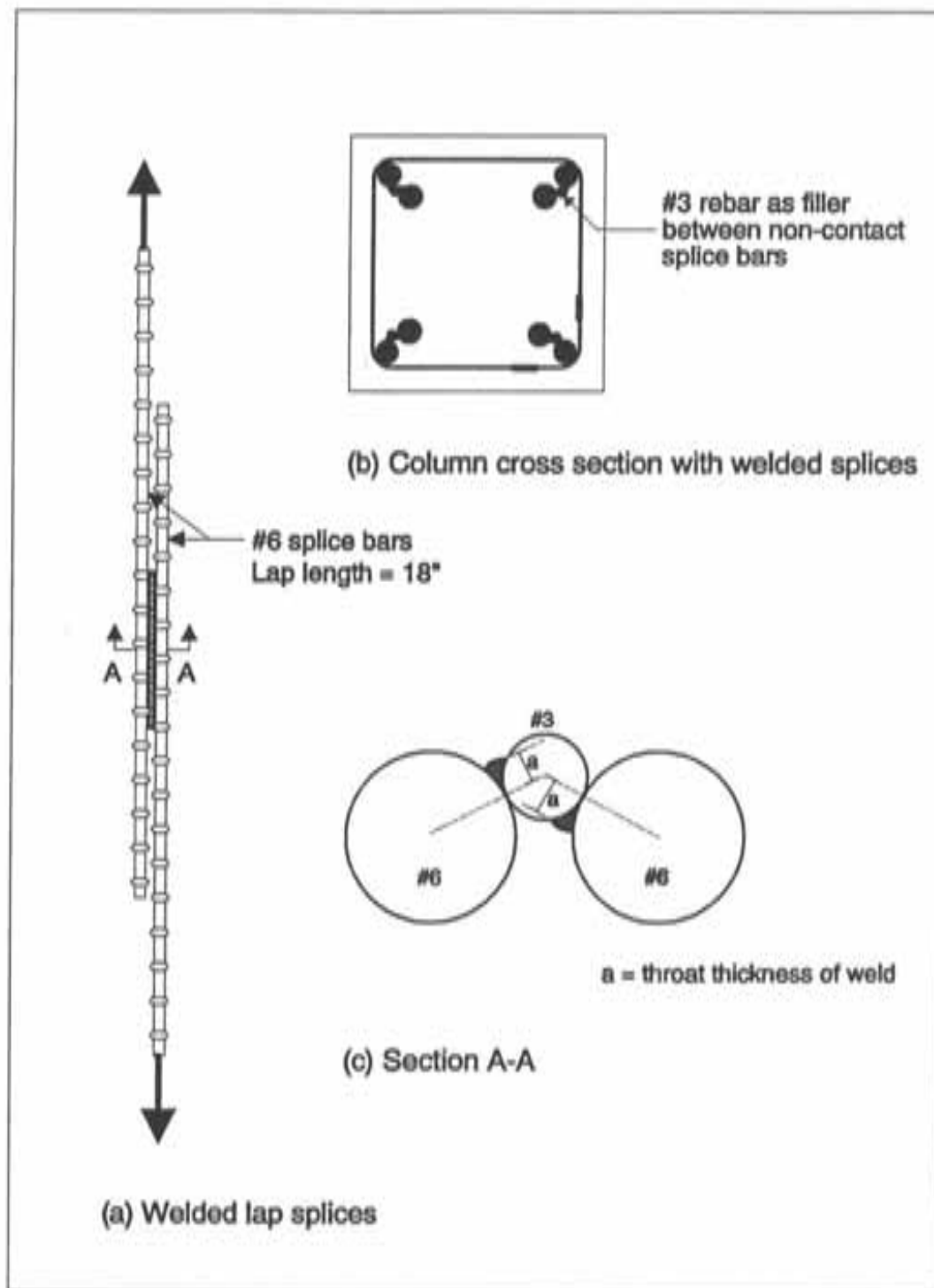


Figure A.2 Details of welded lap splices

APPENDIX B
SHEAR TRANSFER ACROSS FRAME-WALL INTERFACES
LOAD-DEFORMATION RELATIONSHIPS
FOR ALL TEST SPECIMENS

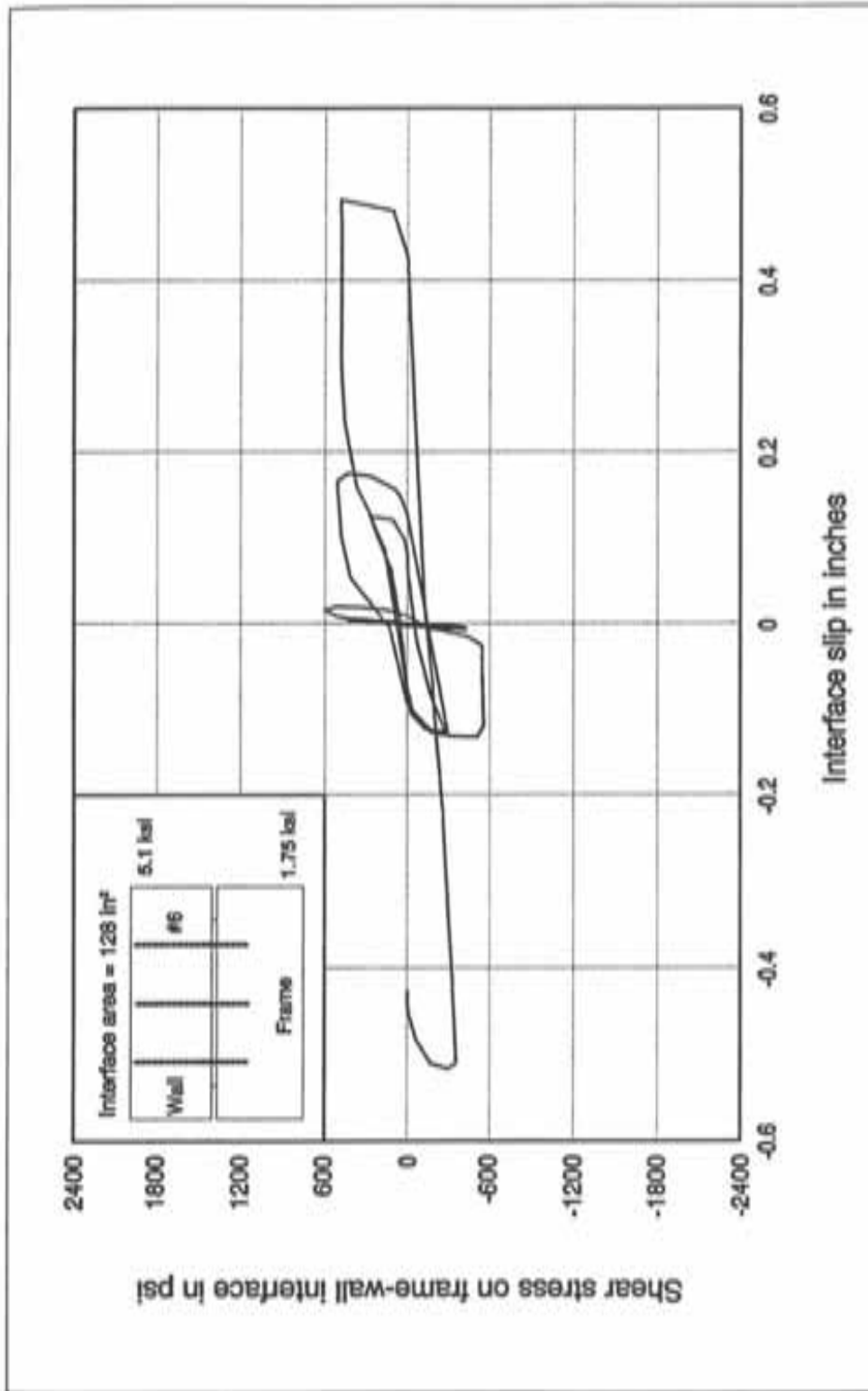


Figure B.1 Performance of shear specimen A2

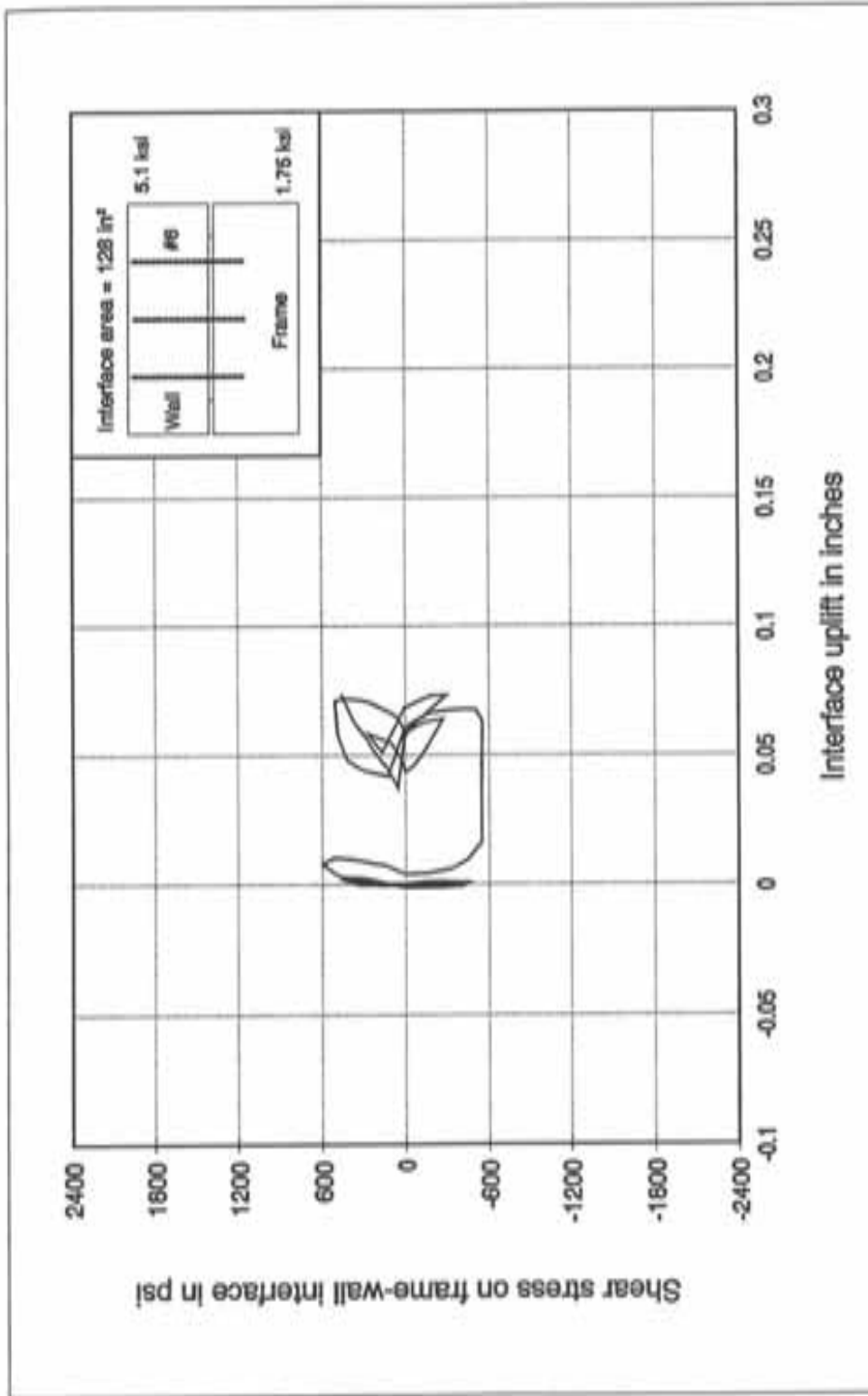


Figure B.2 Interface uplift on north side of shear specimen A2

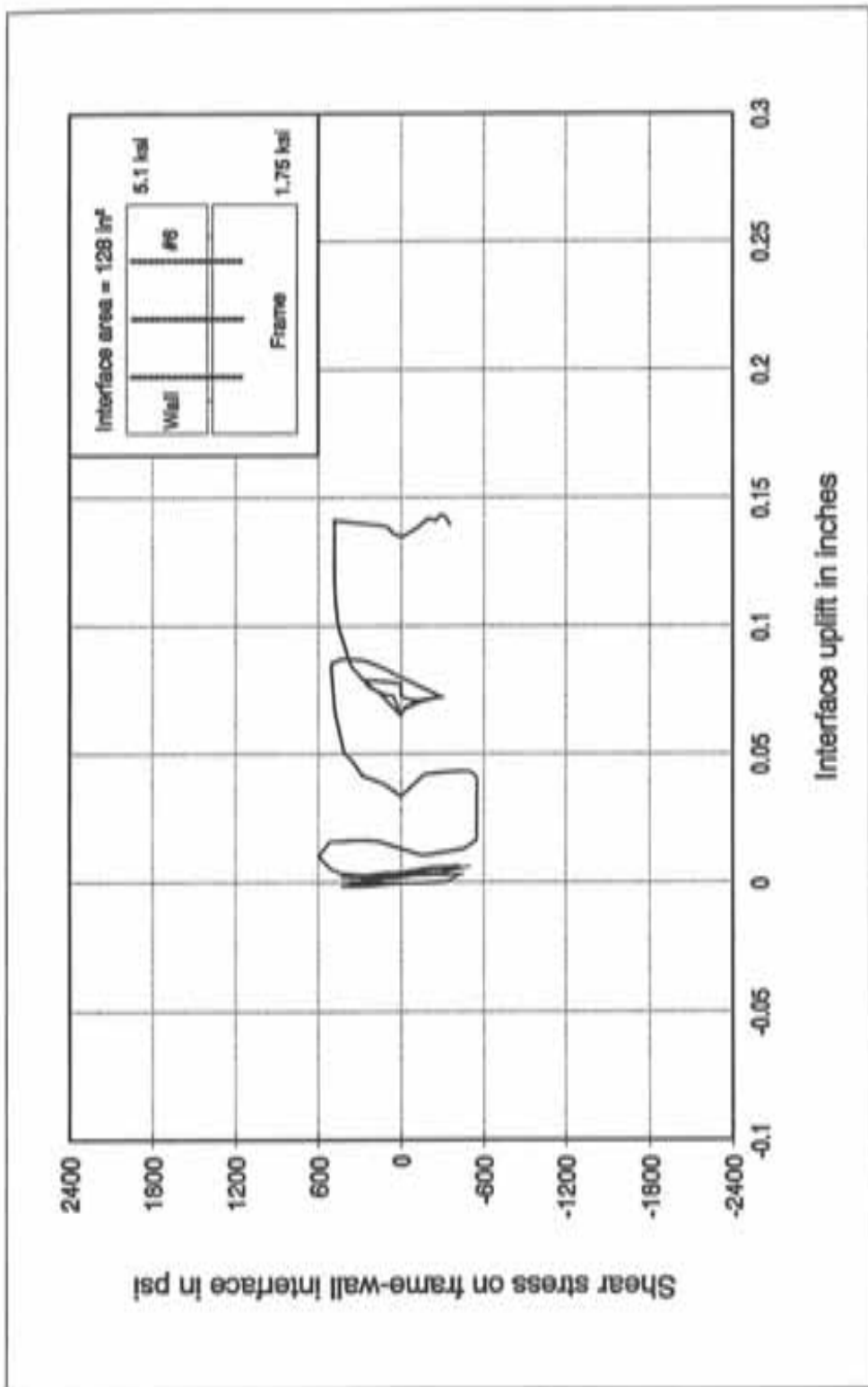


Figure B.3 Interface uplift on south side of shear specimen A2

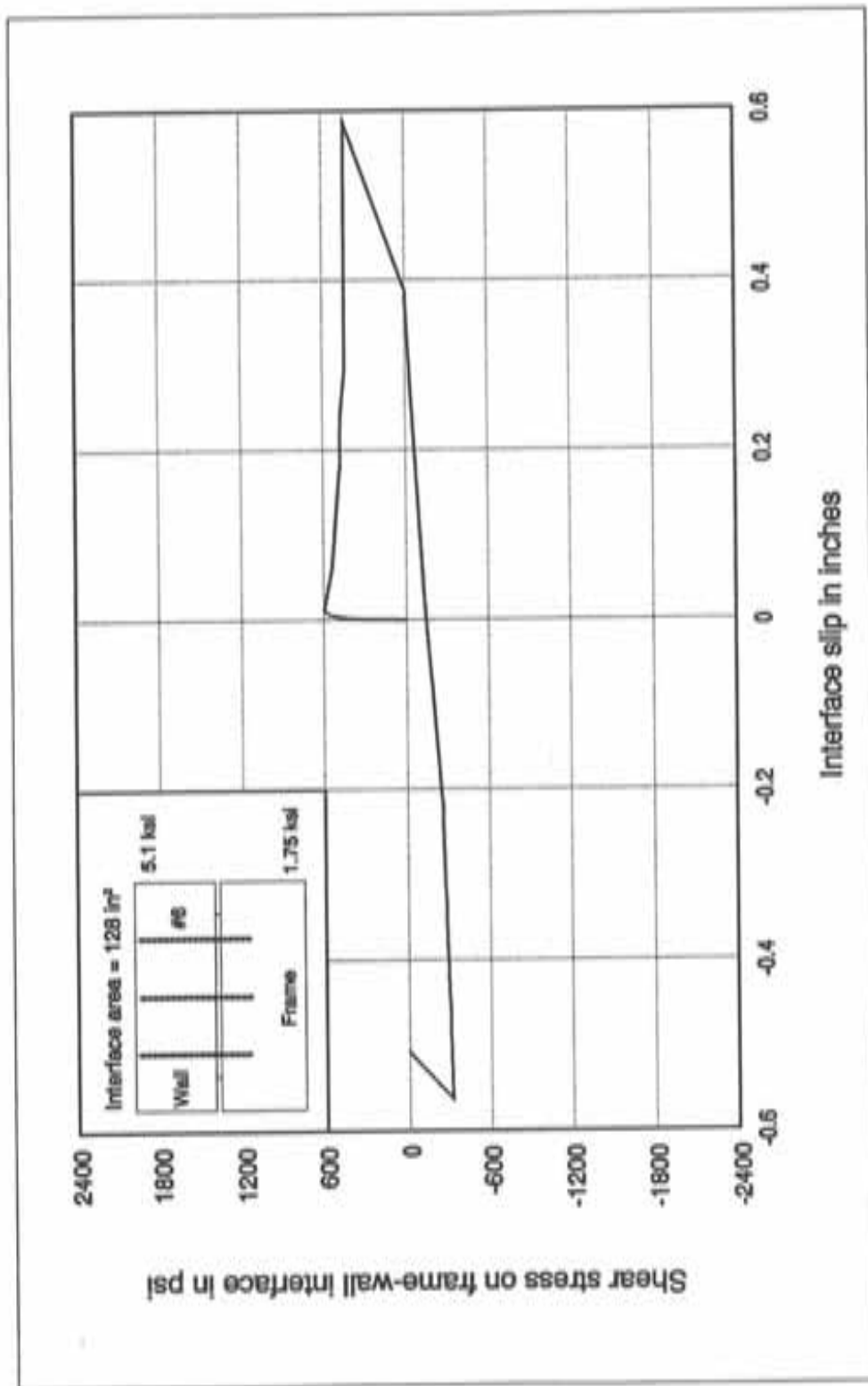


Figure B.4 Performance of shear specimen A3

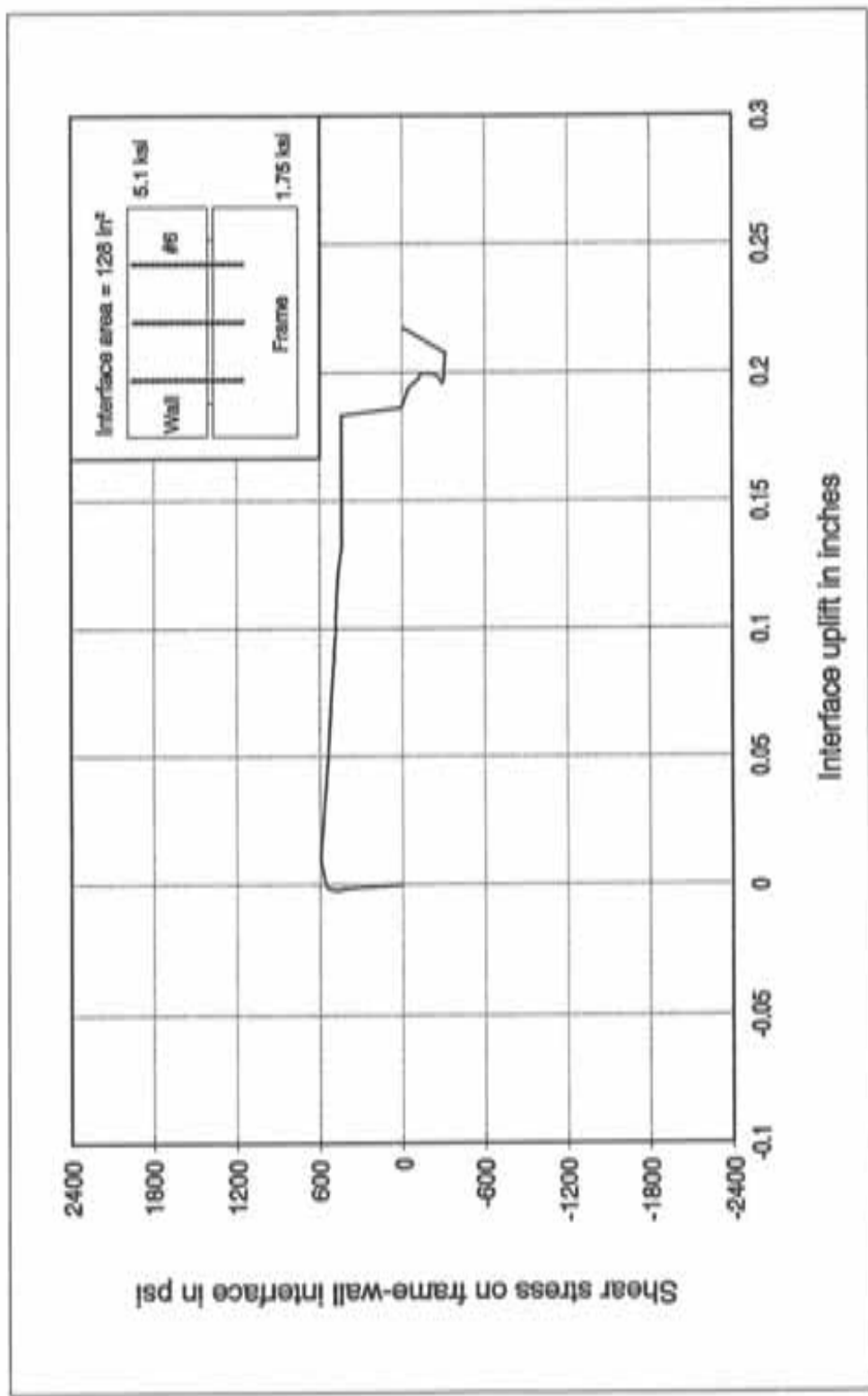


Figure B.5 Interface uplift on north side of shear specimen A3

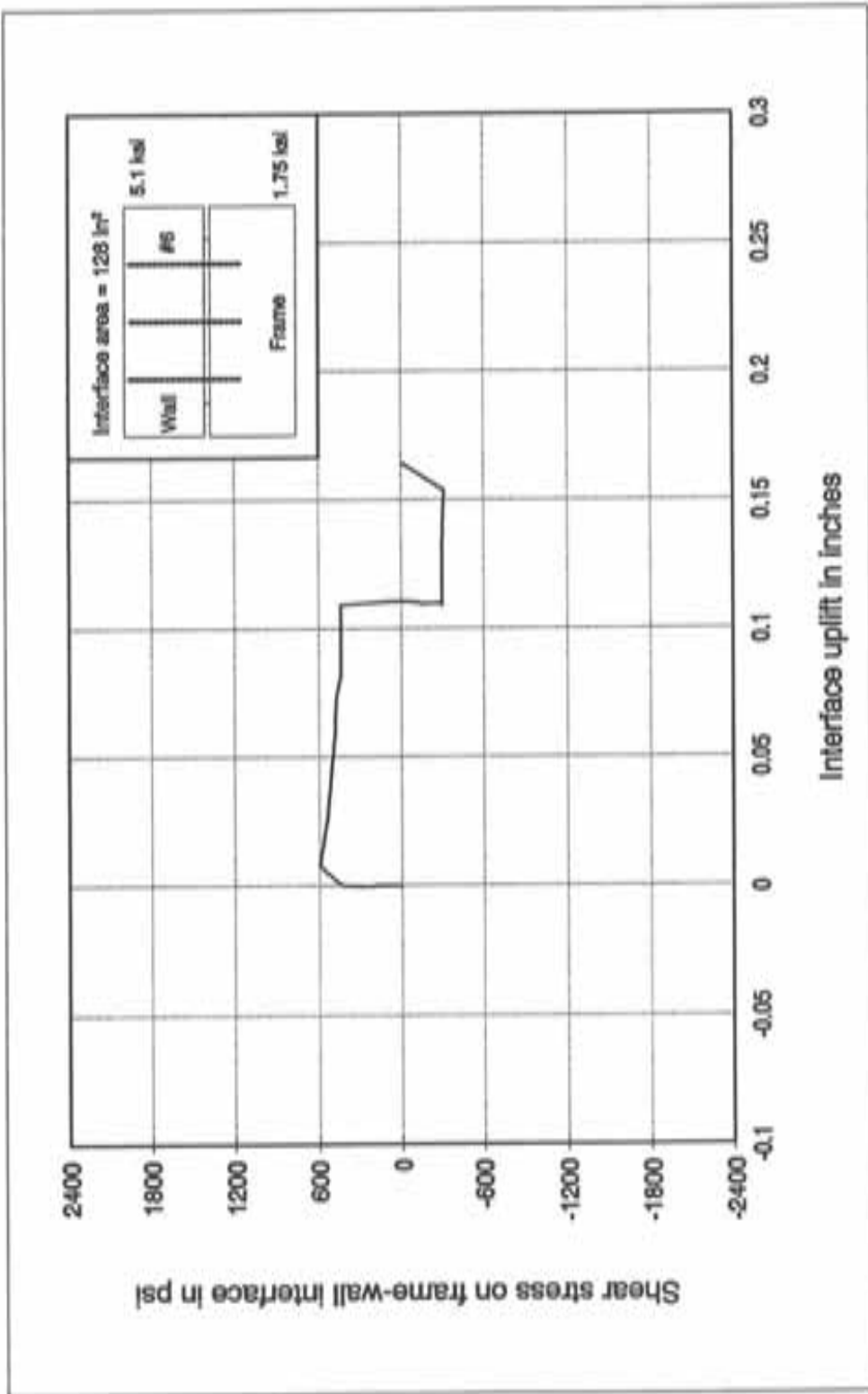


Figure B.6 Interface uplift on south side of shear specimen A3

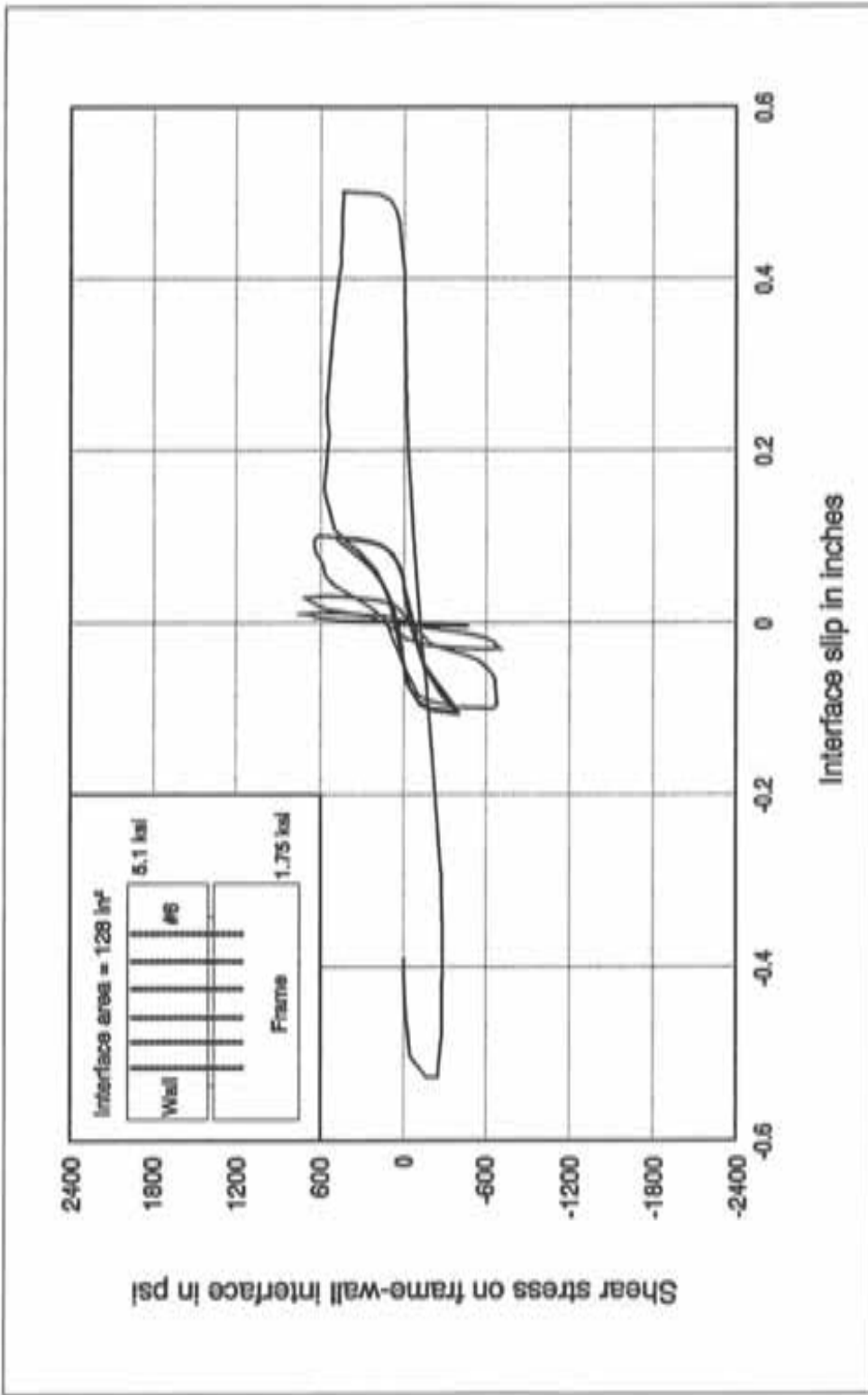


Figure B.7 Performance of shear specimen A4

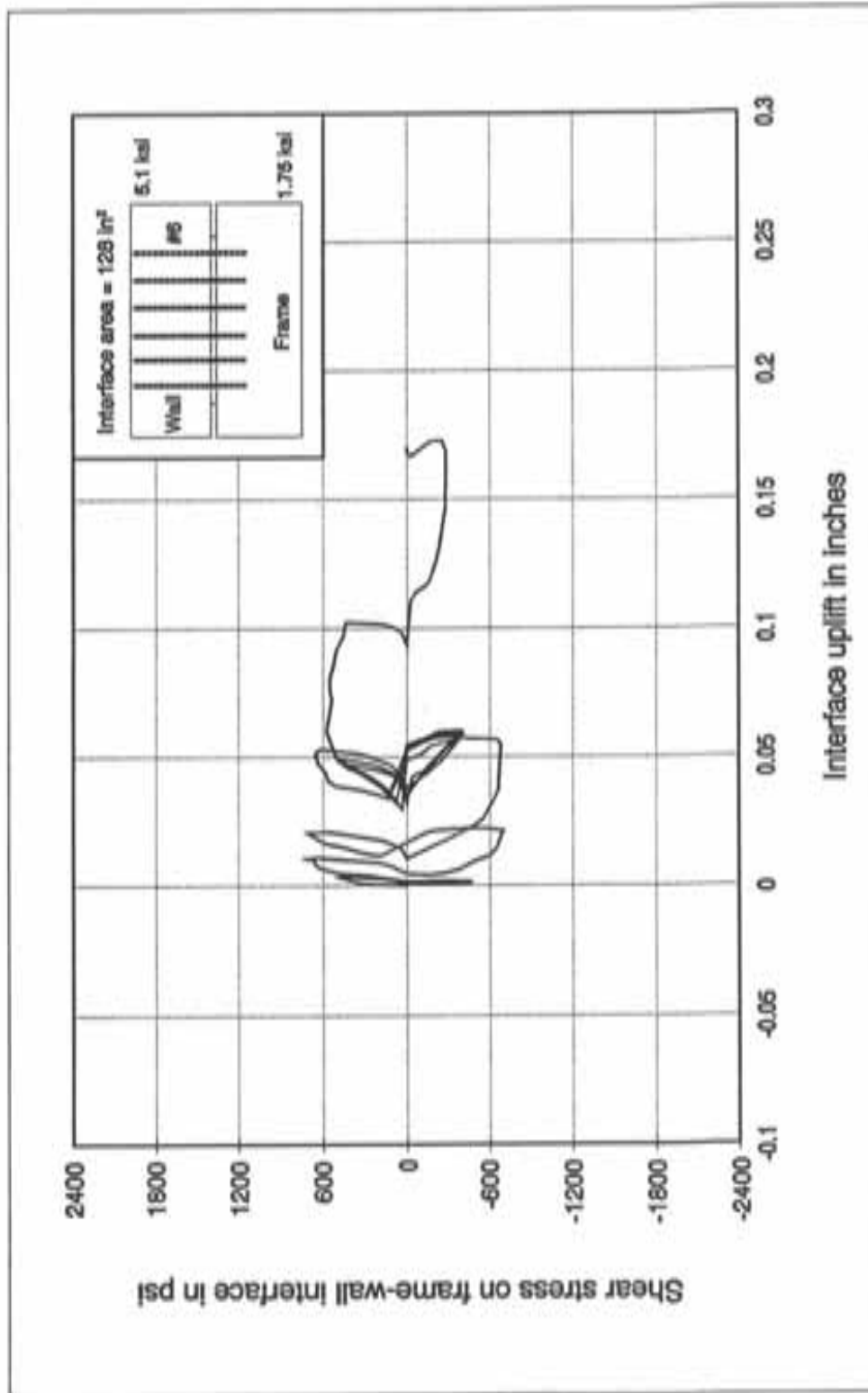


Figure B.8 Interface uplift on north side of shear specimen A4

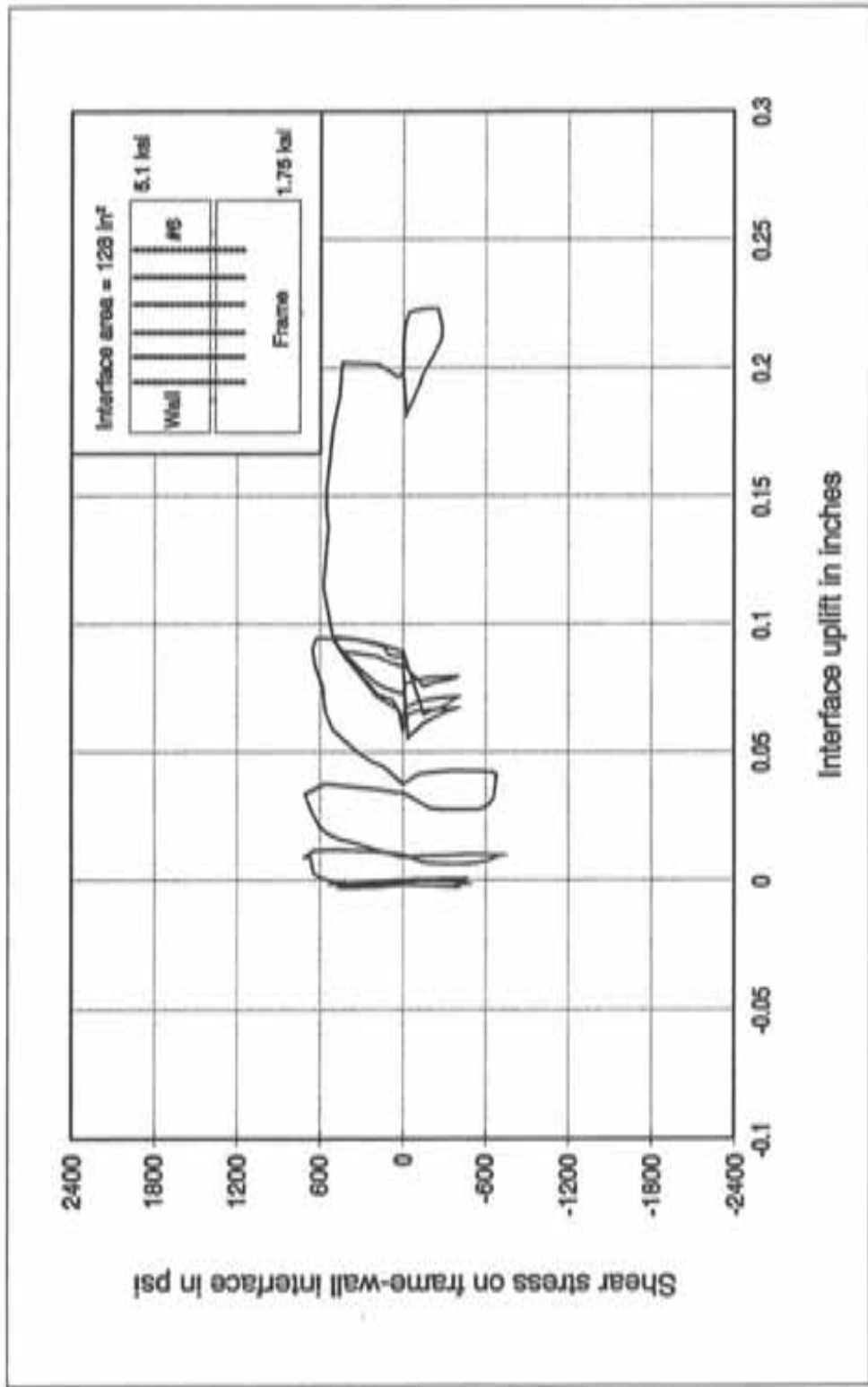


Figure B.9 Interface uplift on south side of shear specimen A4

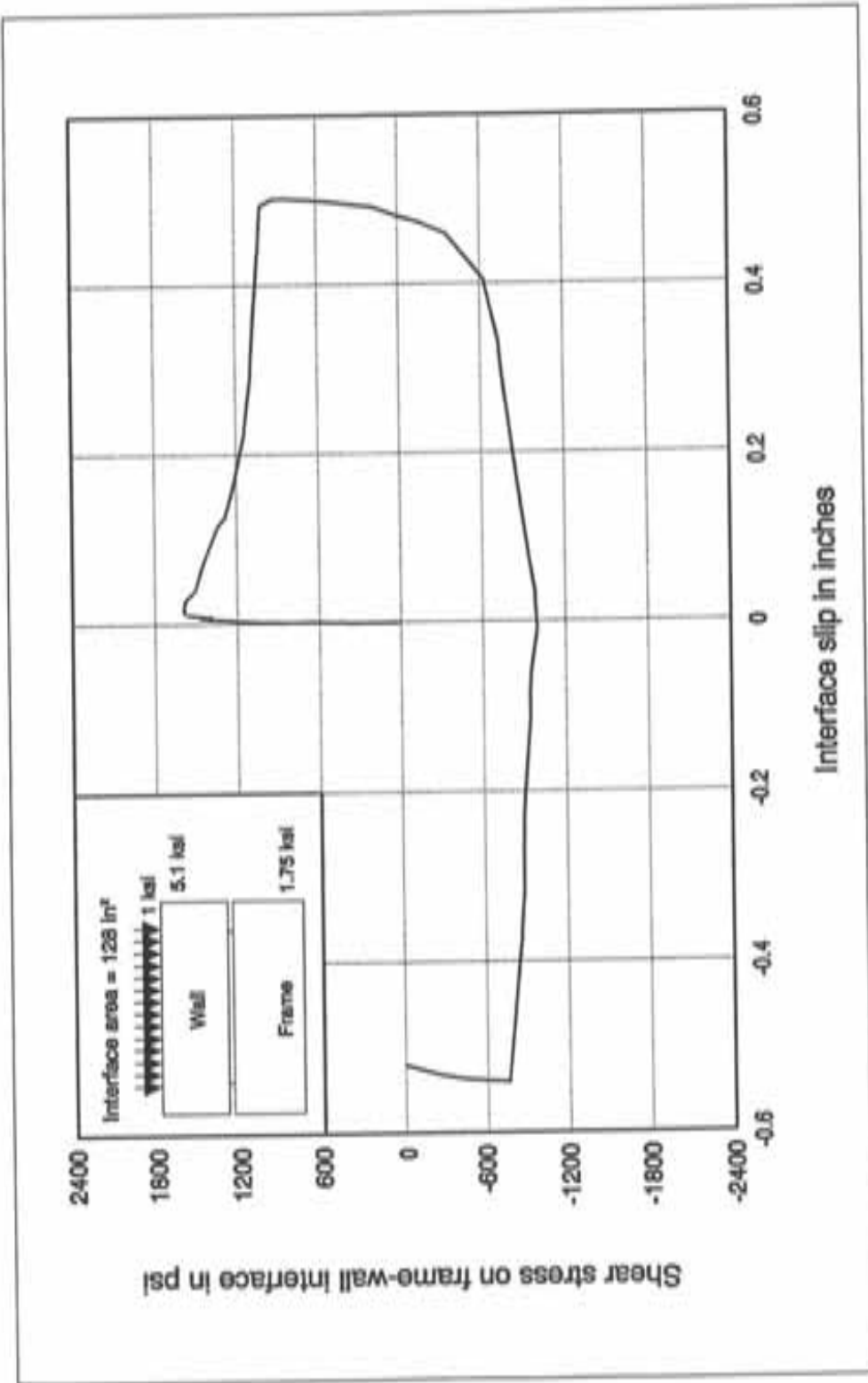


Figure B.10 Performance of shear specimen A5

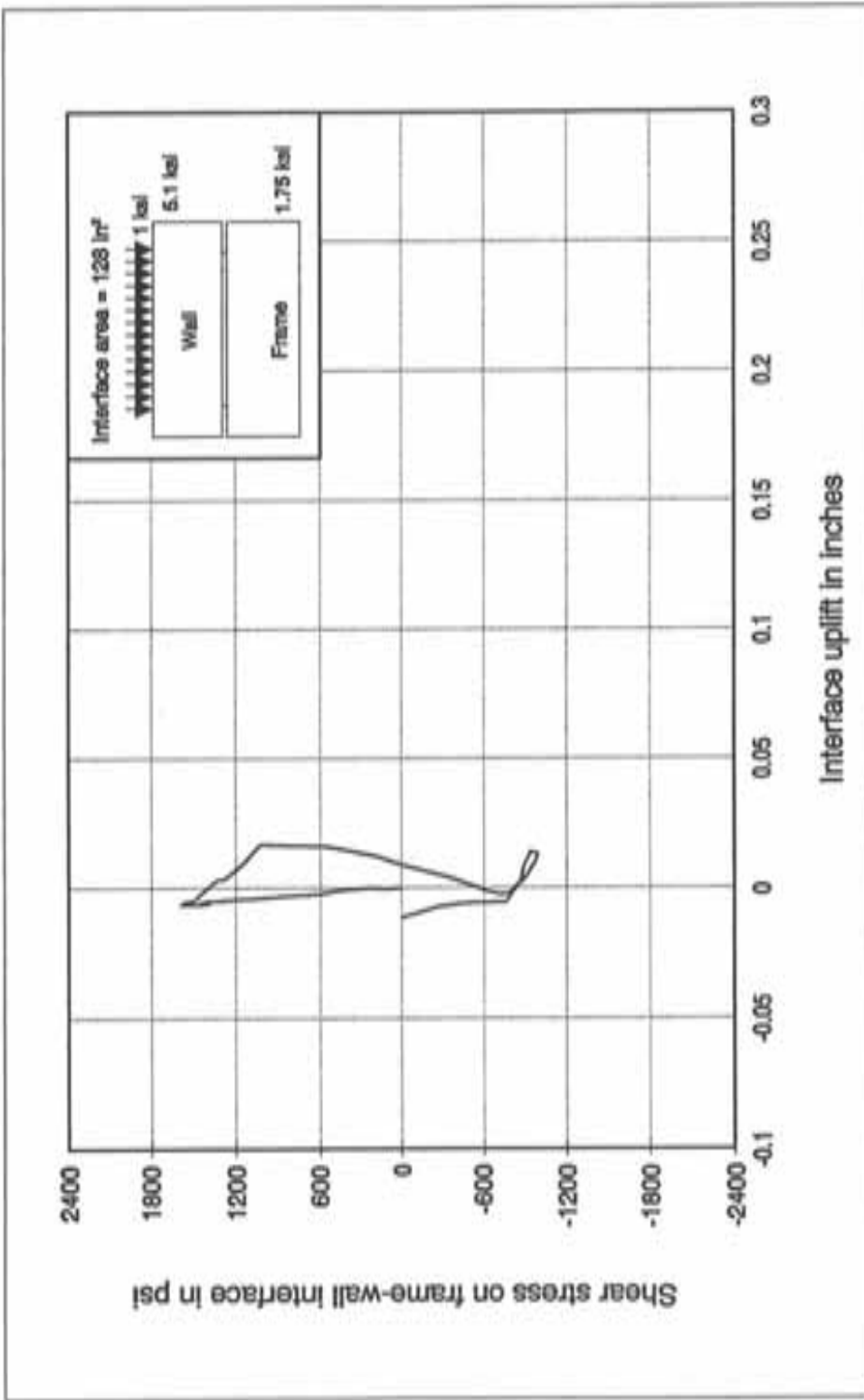


Figure B.11 Interface uplift on north side of shear specimen A5

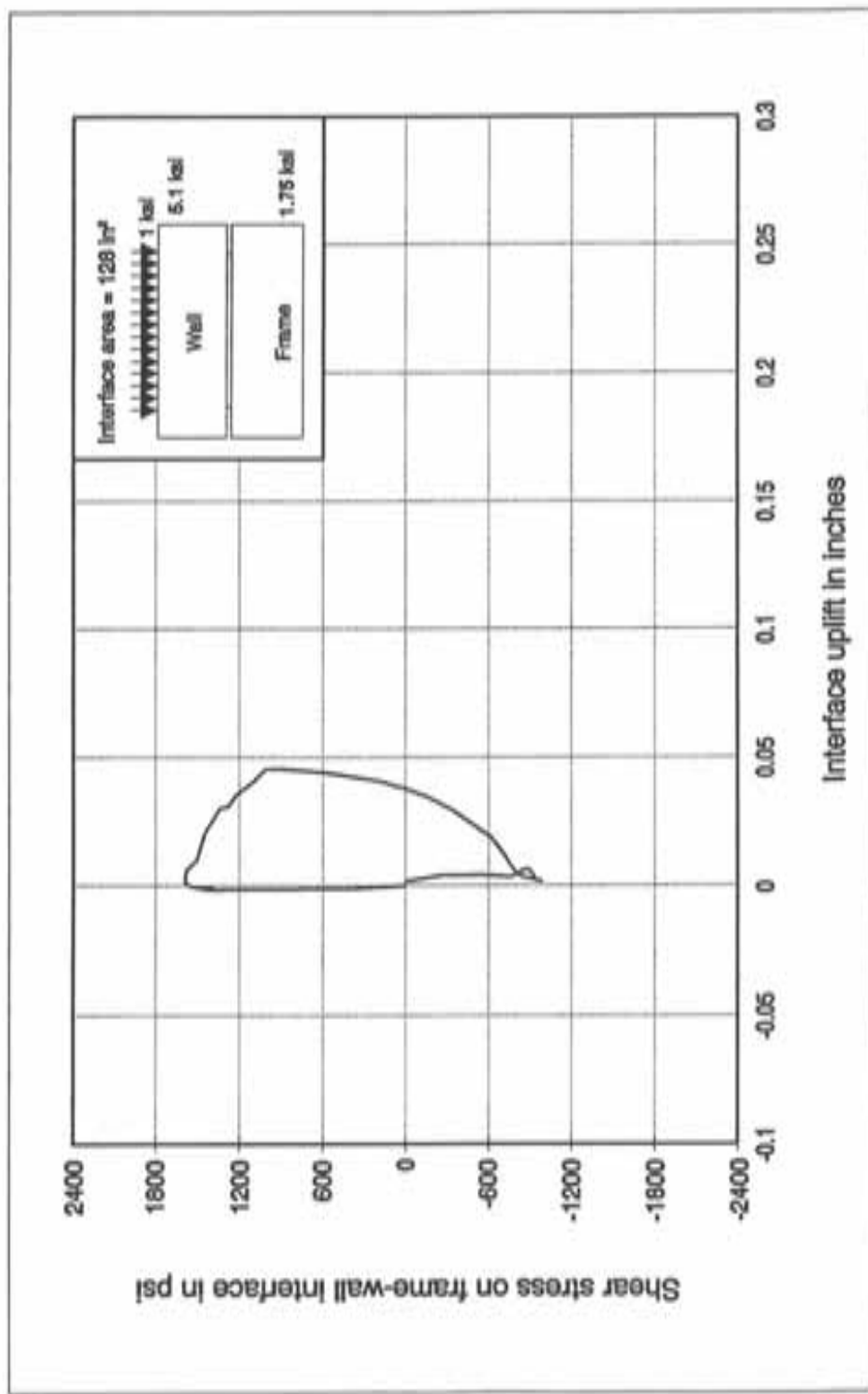


Figure B.12 Interface uplift on south side of shear specimen A5

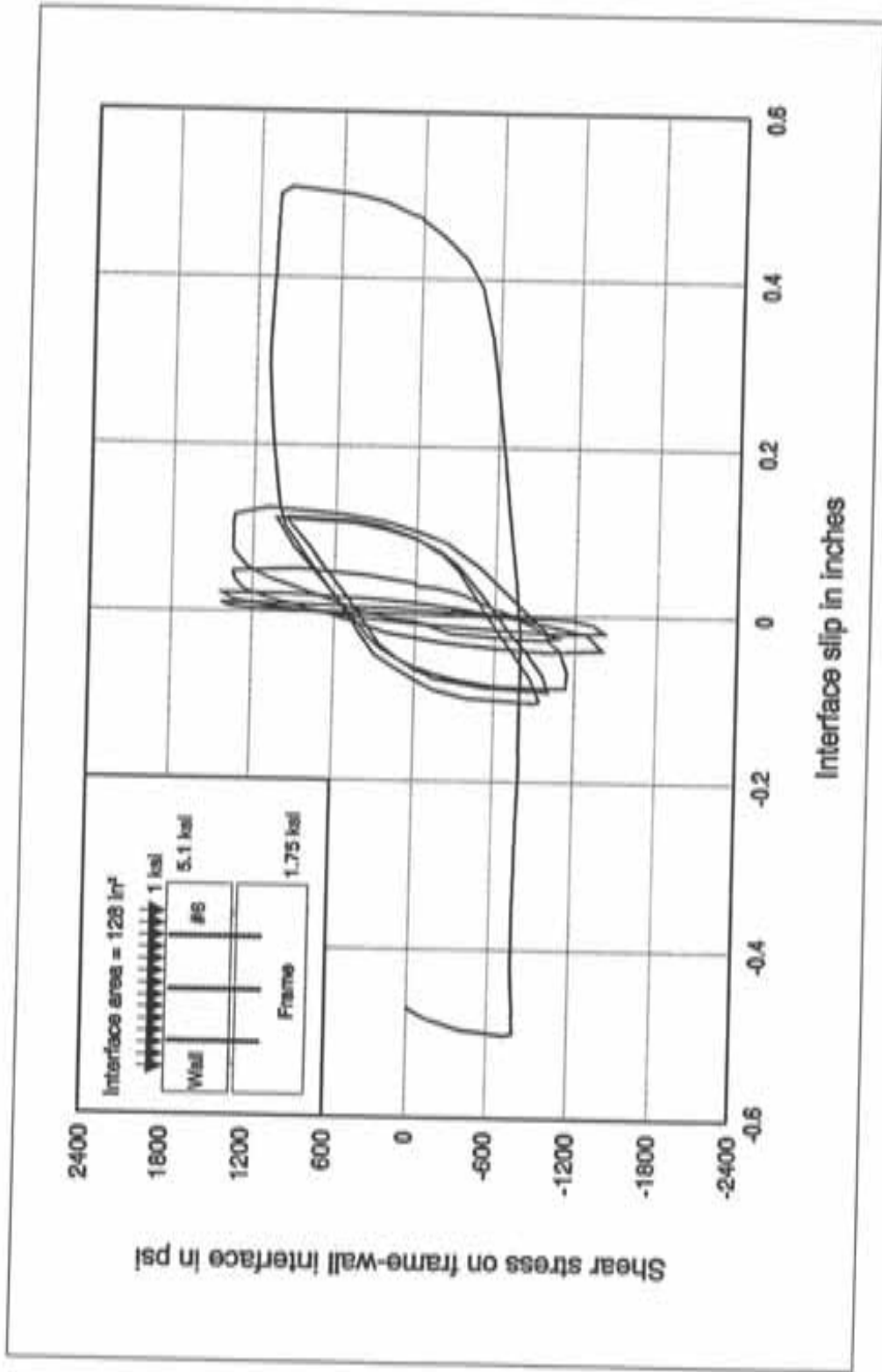


Figure B.13 Performance of shear specimen A6

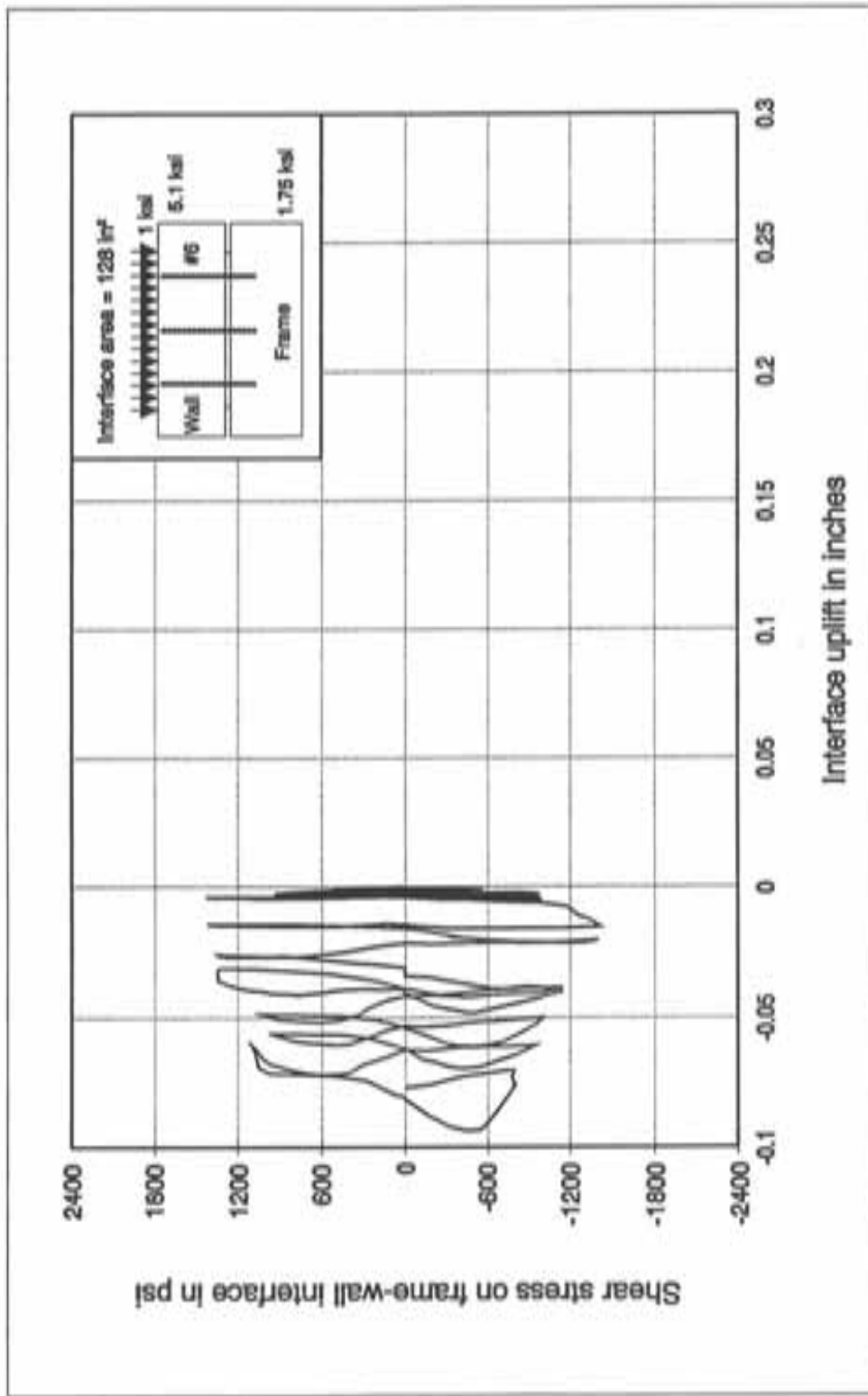


Figure B.14 Interface uplift on north side of shear specimen A6

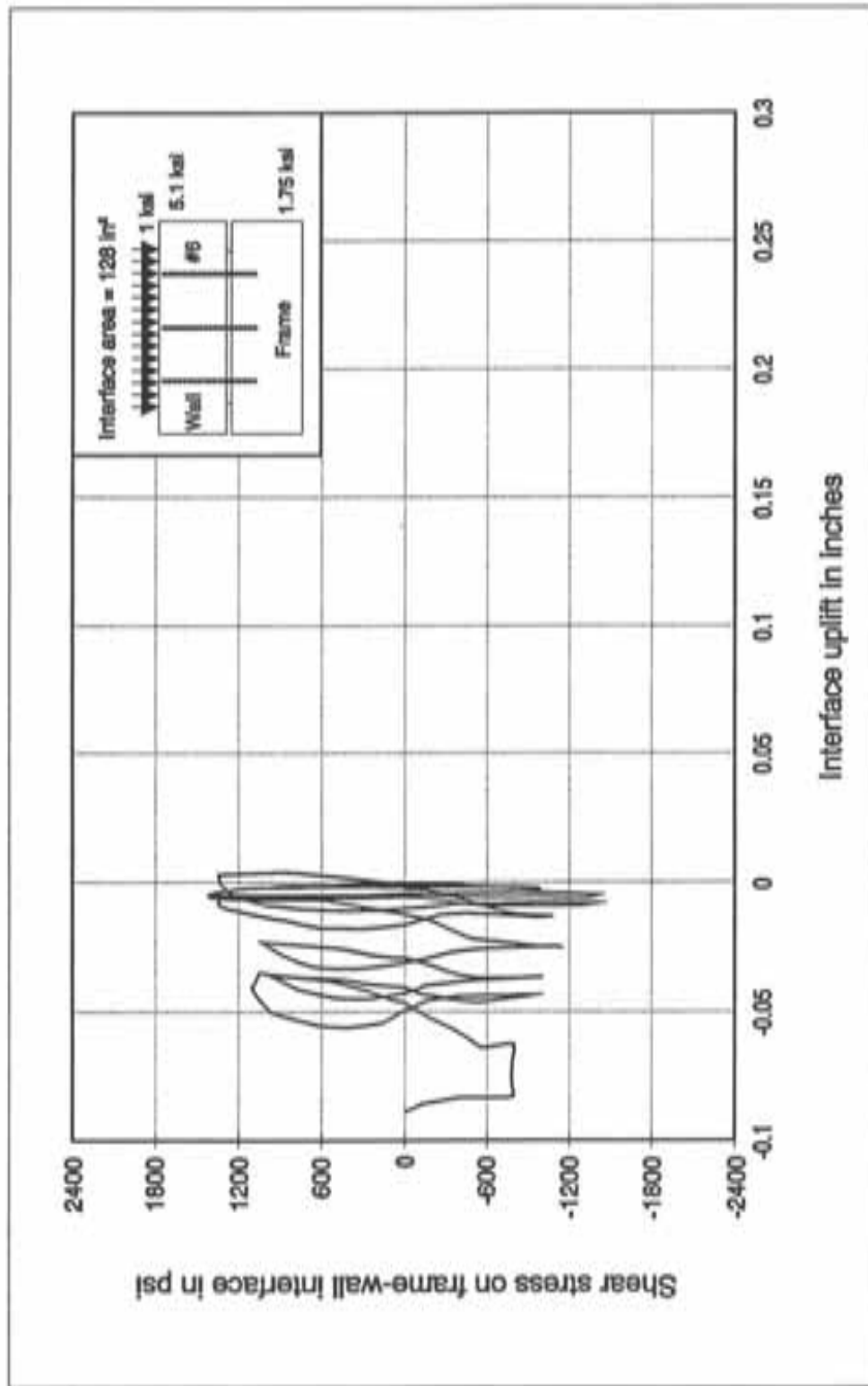


Figure B.15 Interface uplift on south side of shear specimen A6

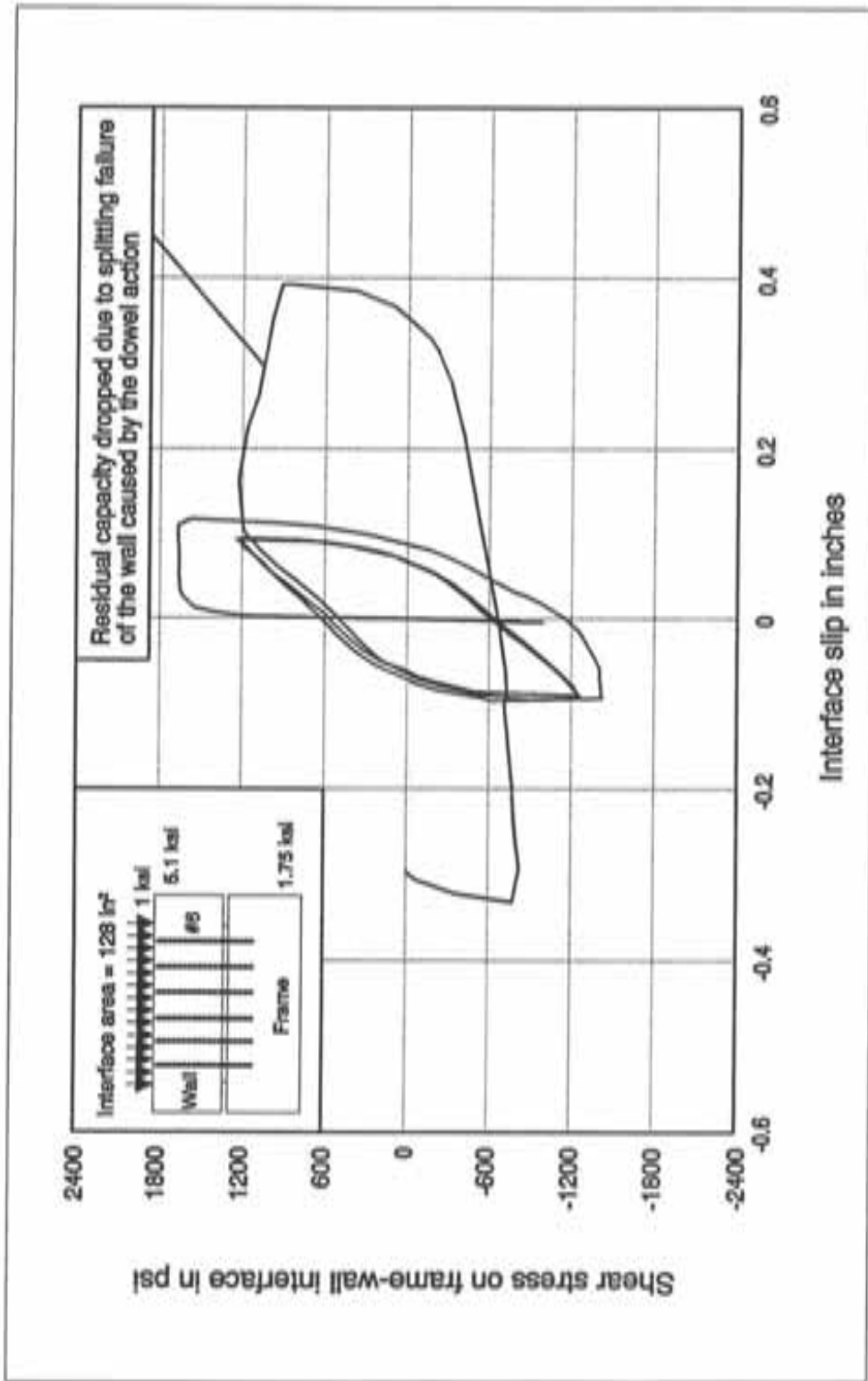


Figure B.16 Performance of shear specimen A7

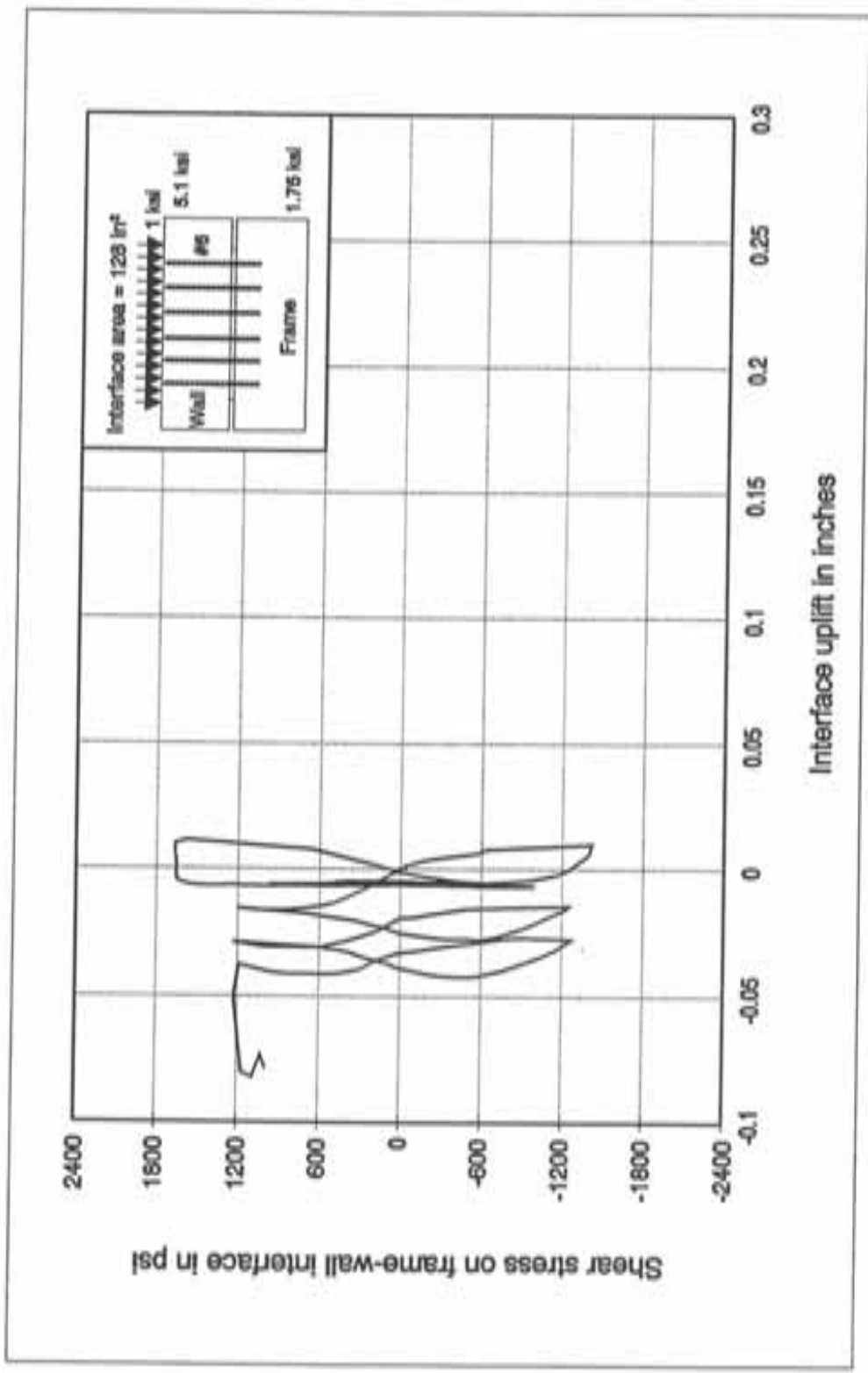


Figure B.17 Interface uplift on north side of shear specimen A7

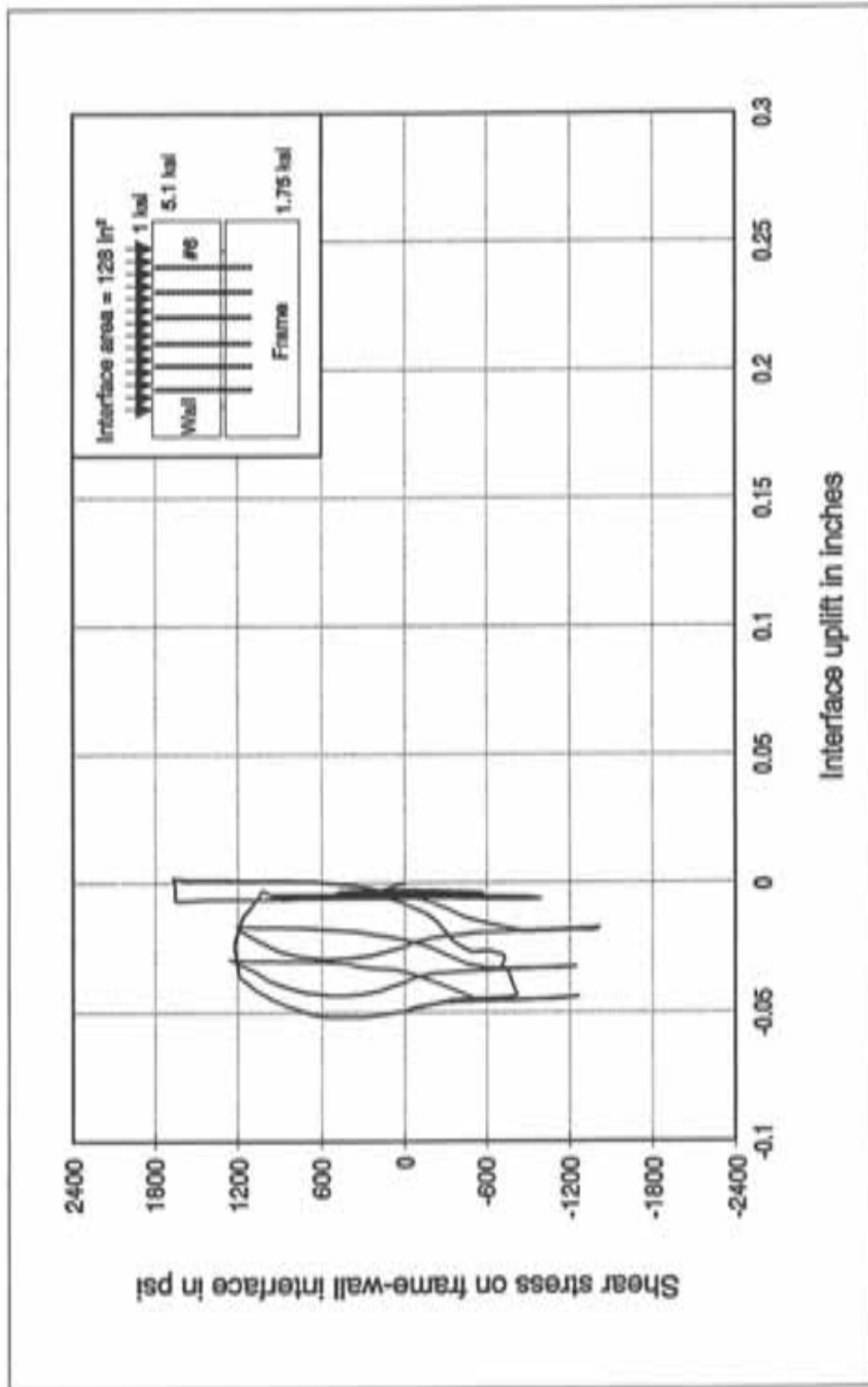


Figure B.18 Interface uplift on south side of shear specimen A7

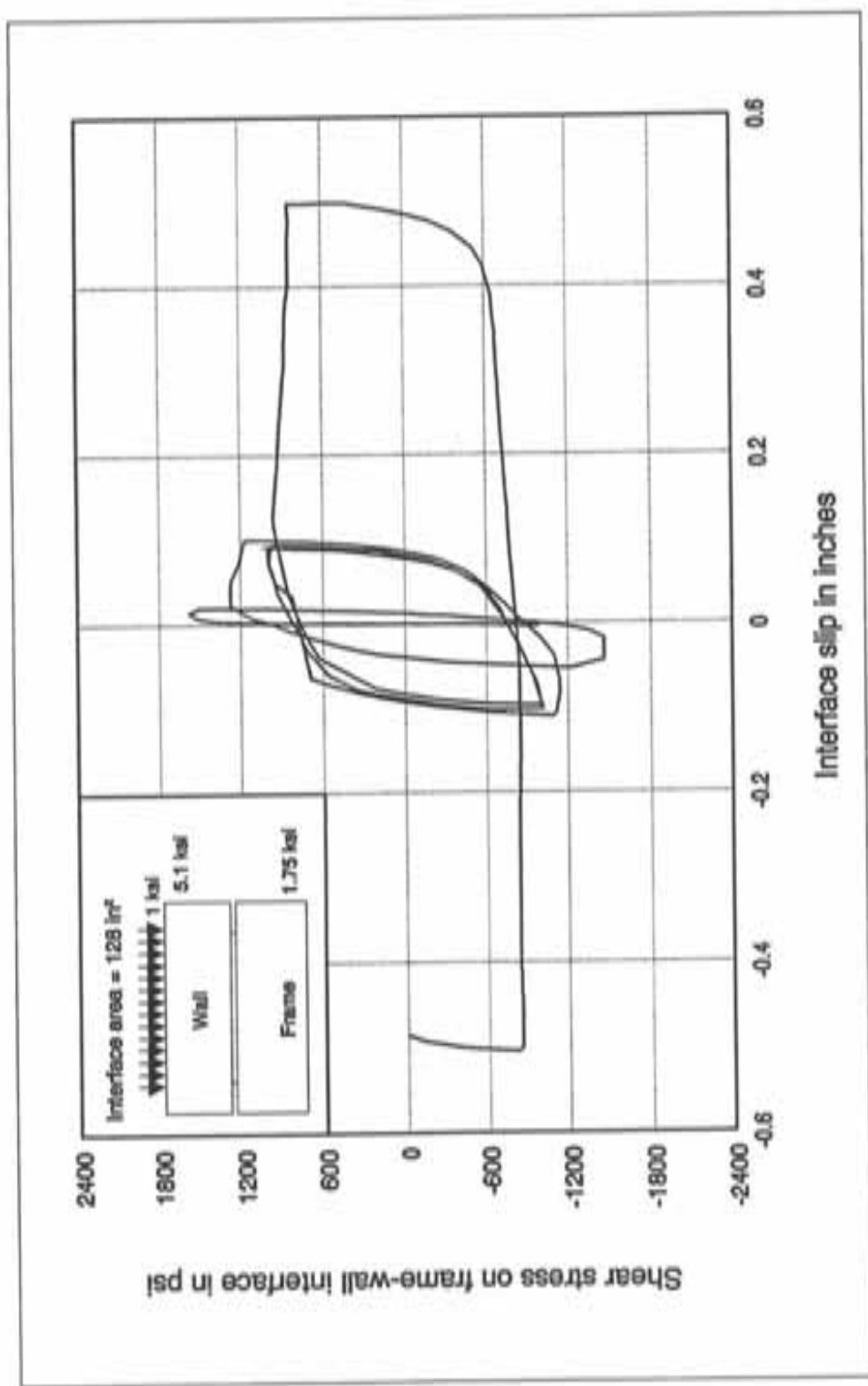


Figure B.19 Performance of shear specimen A8

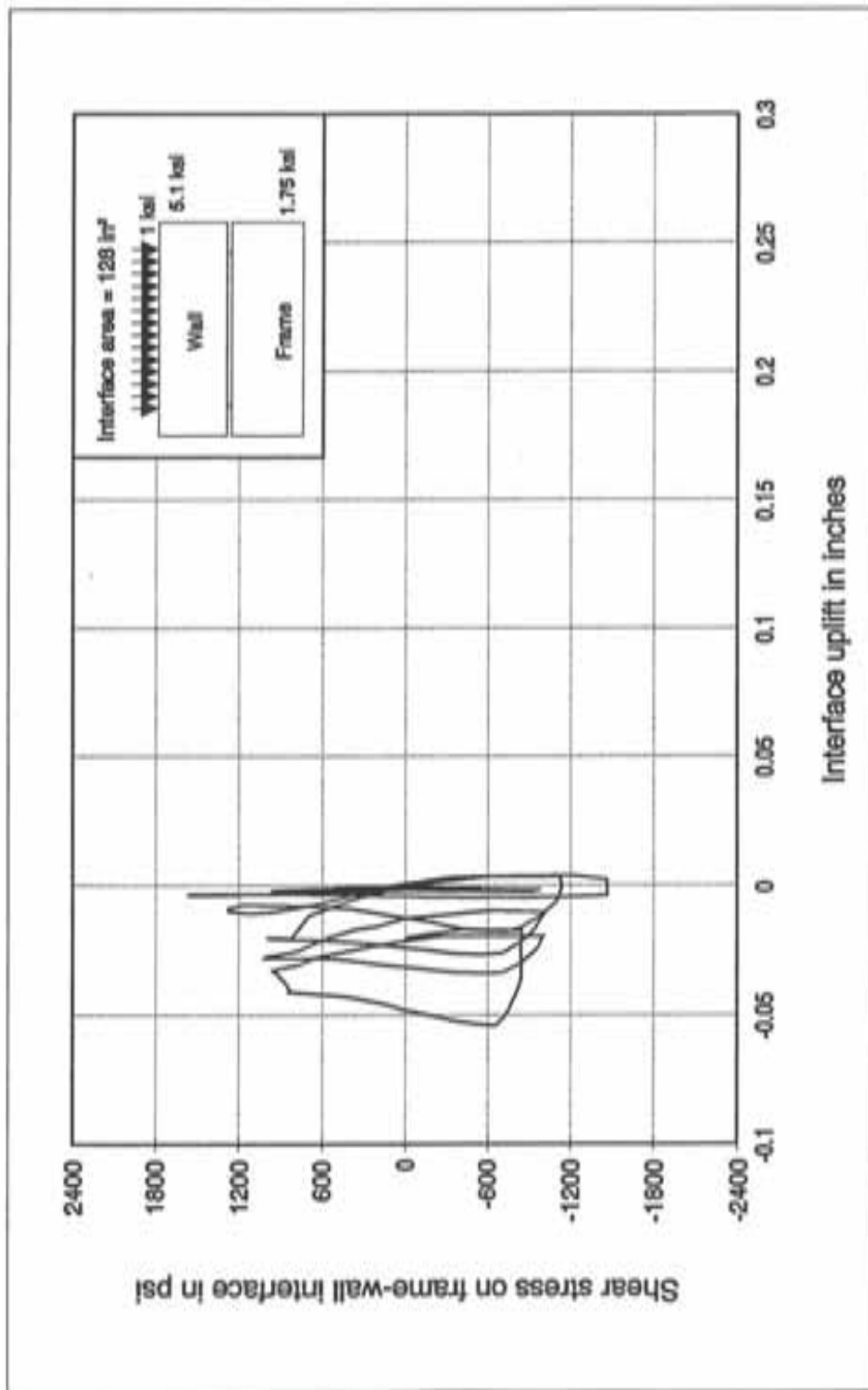


Figure B.20 Interface uplift on north side of shear specimen A8

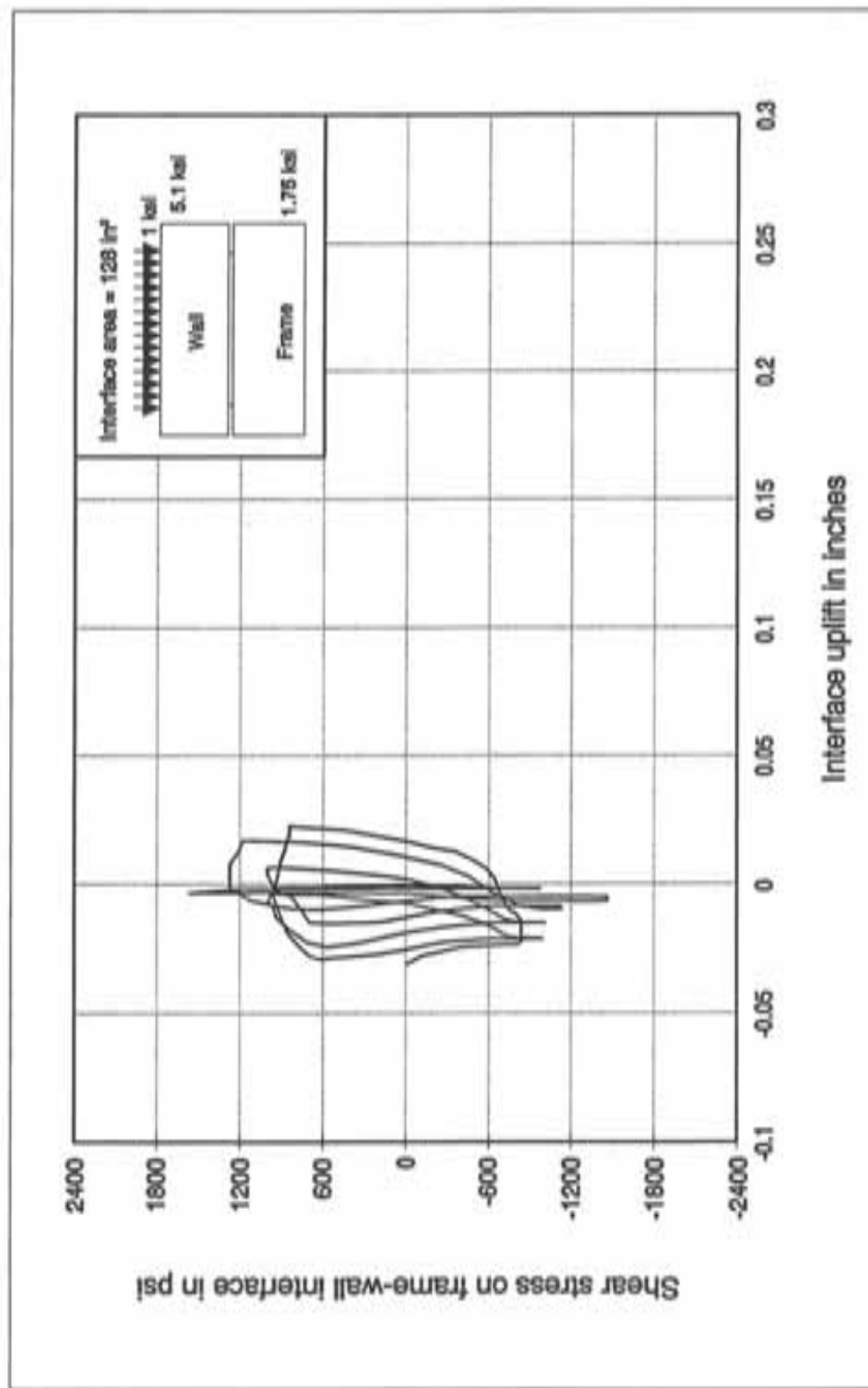


Figure B.21 Interface uplift on south side of shear specimen A8

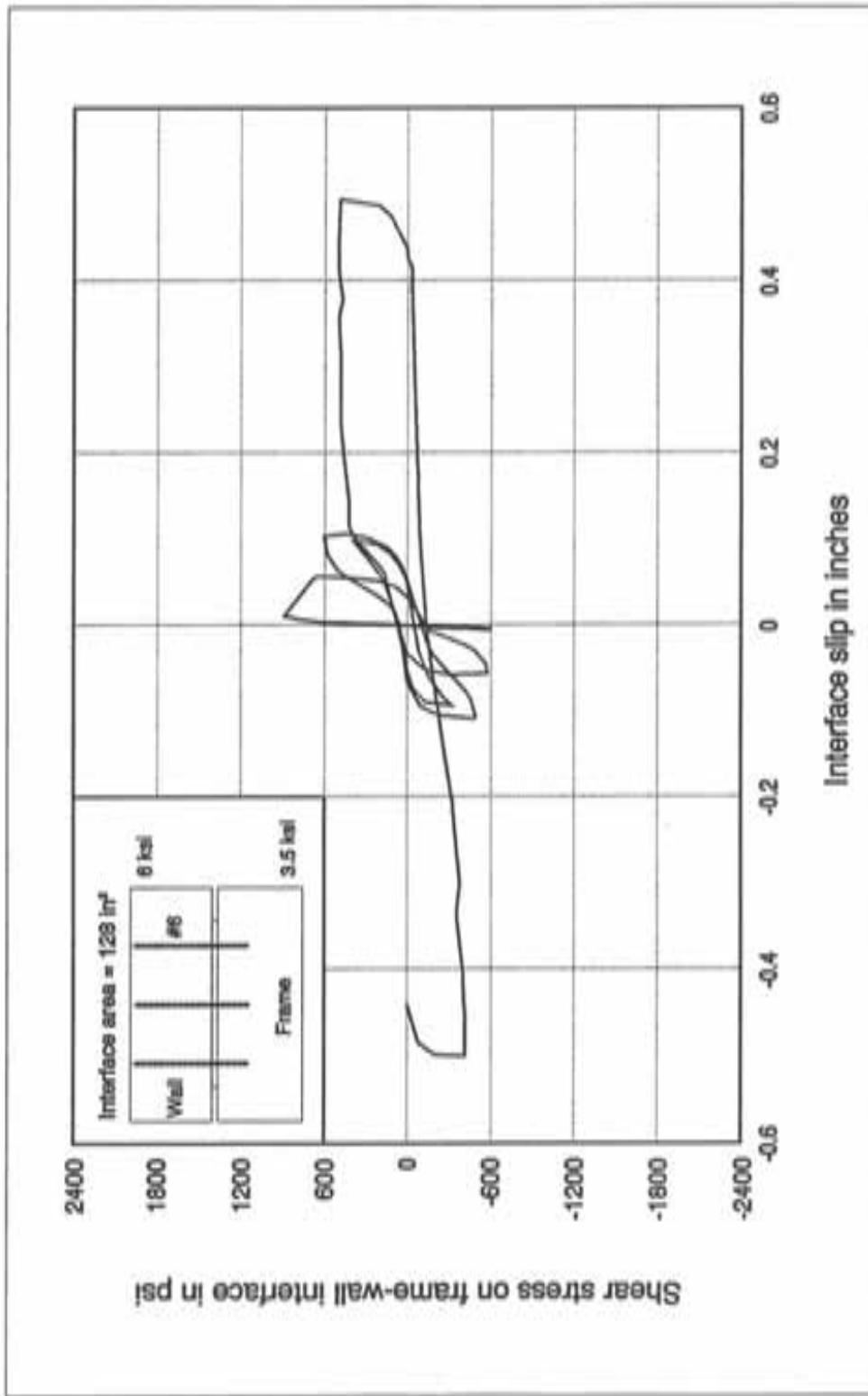


Figure B.22 Performance of shear specimen B1

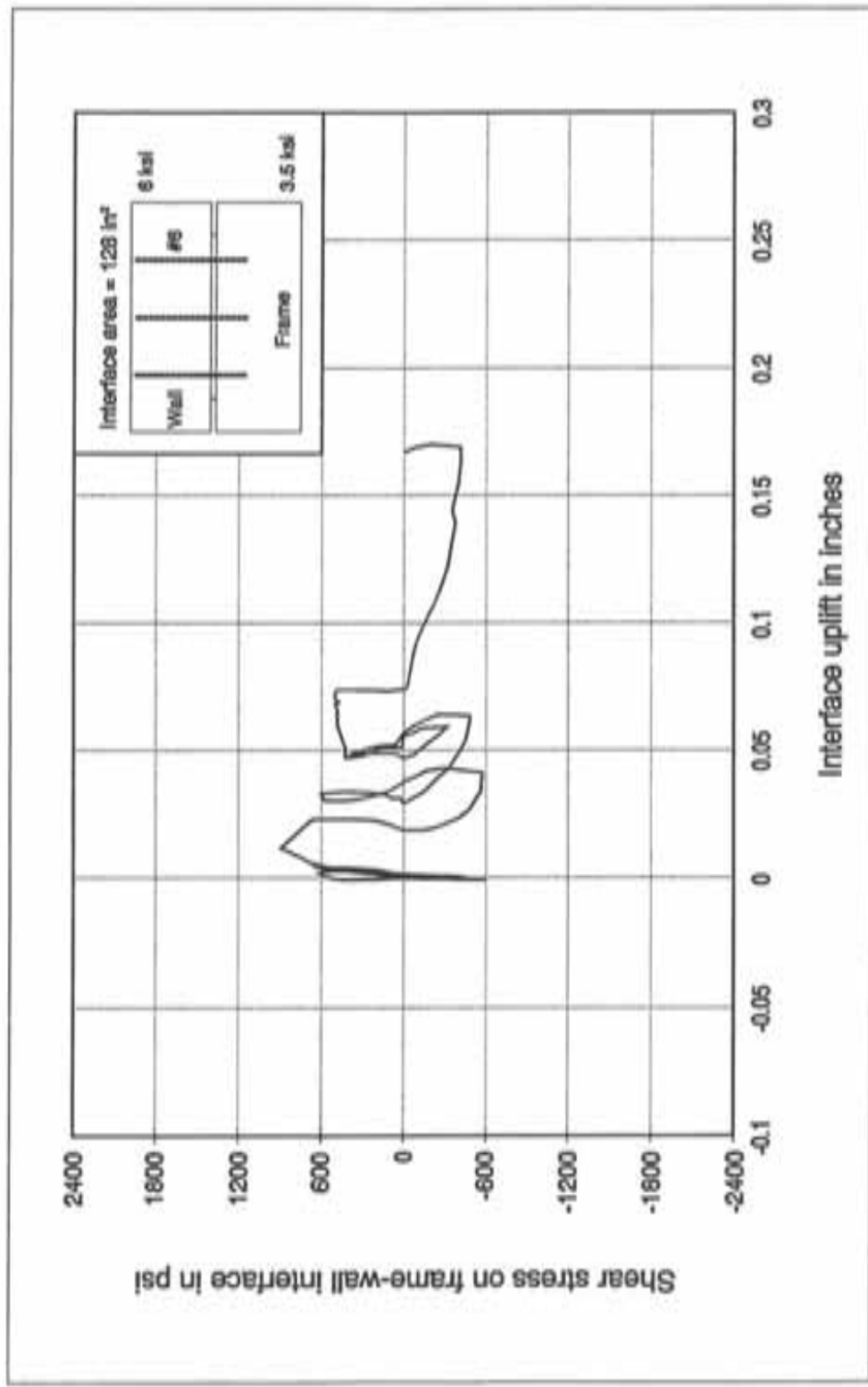


Figure B.23 Interface uplift on north side of shear specimen B1

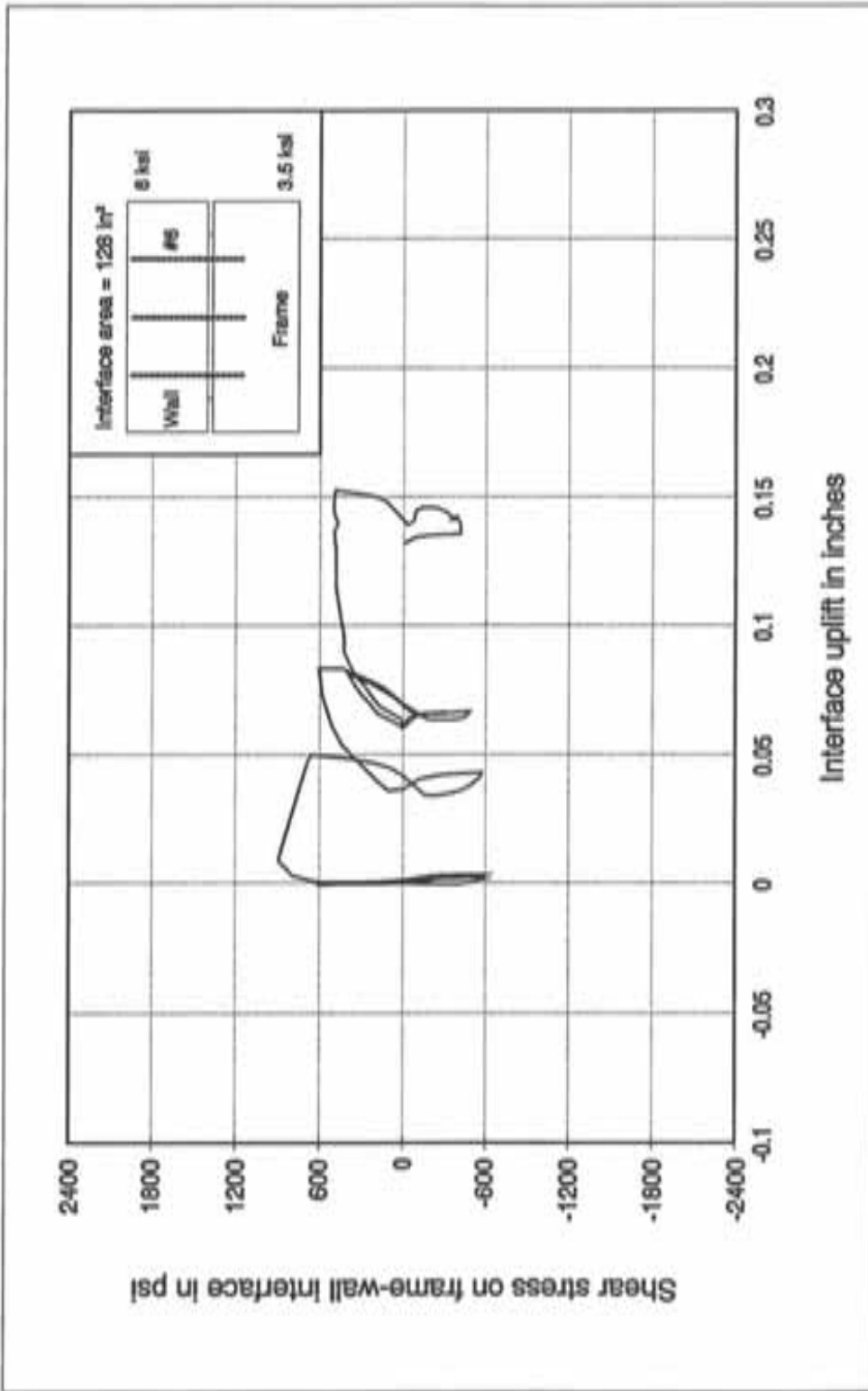


Figure B.24 Interface uplift on south side of shear specimen B1

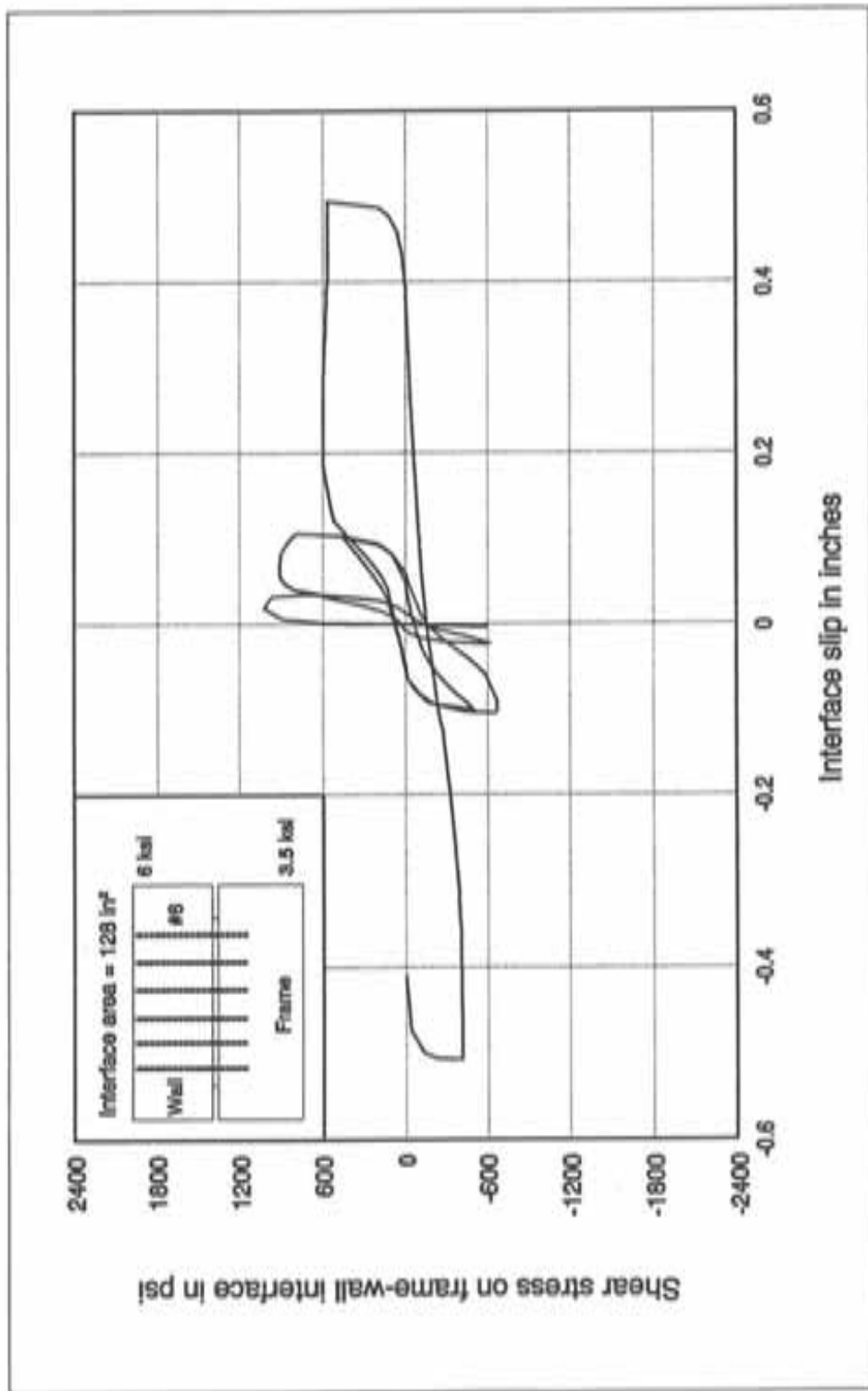


Figure B.25 Performance of shear specimen B2

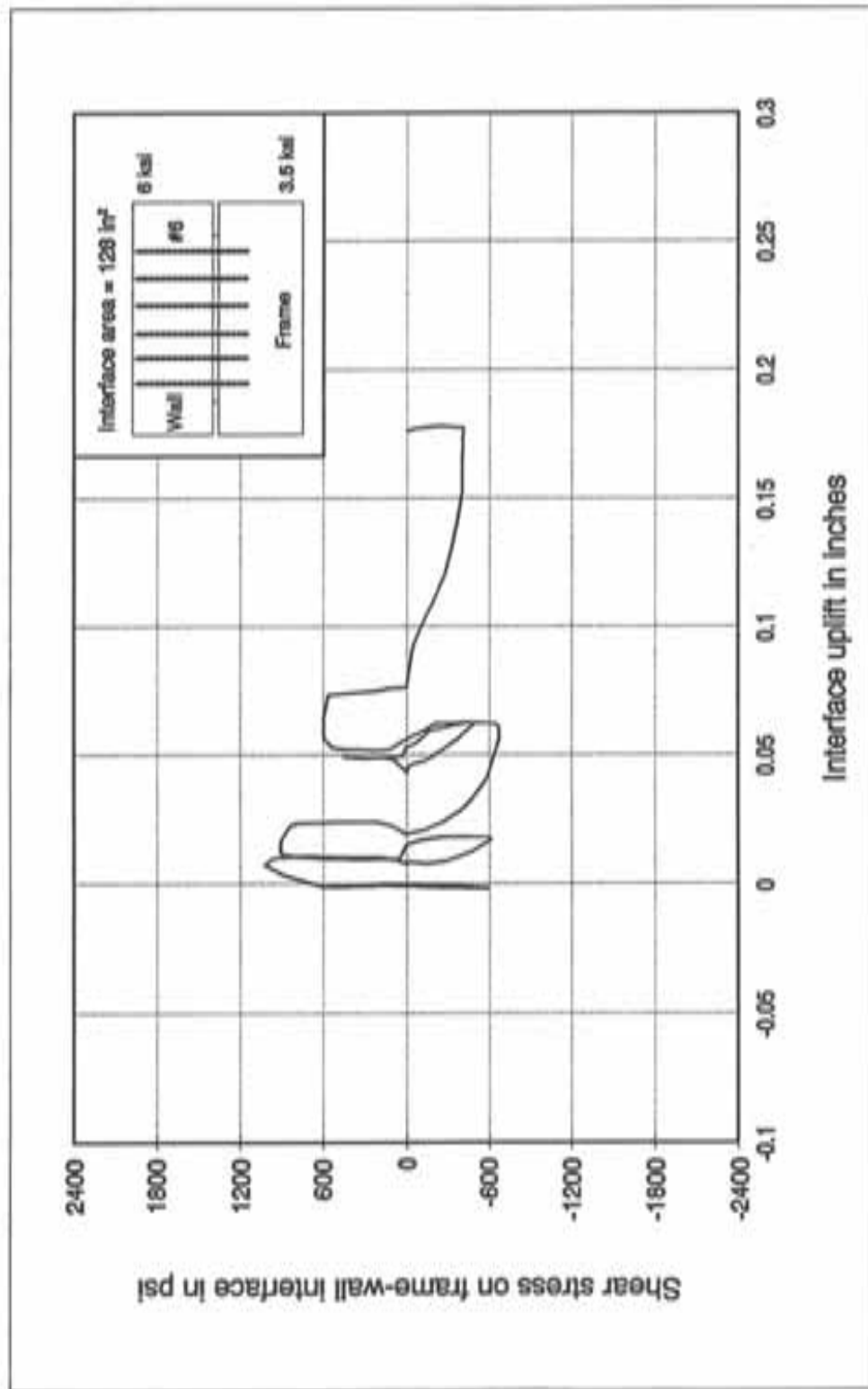


Figure B.26 Interface uplift on north side of shear specimen B2

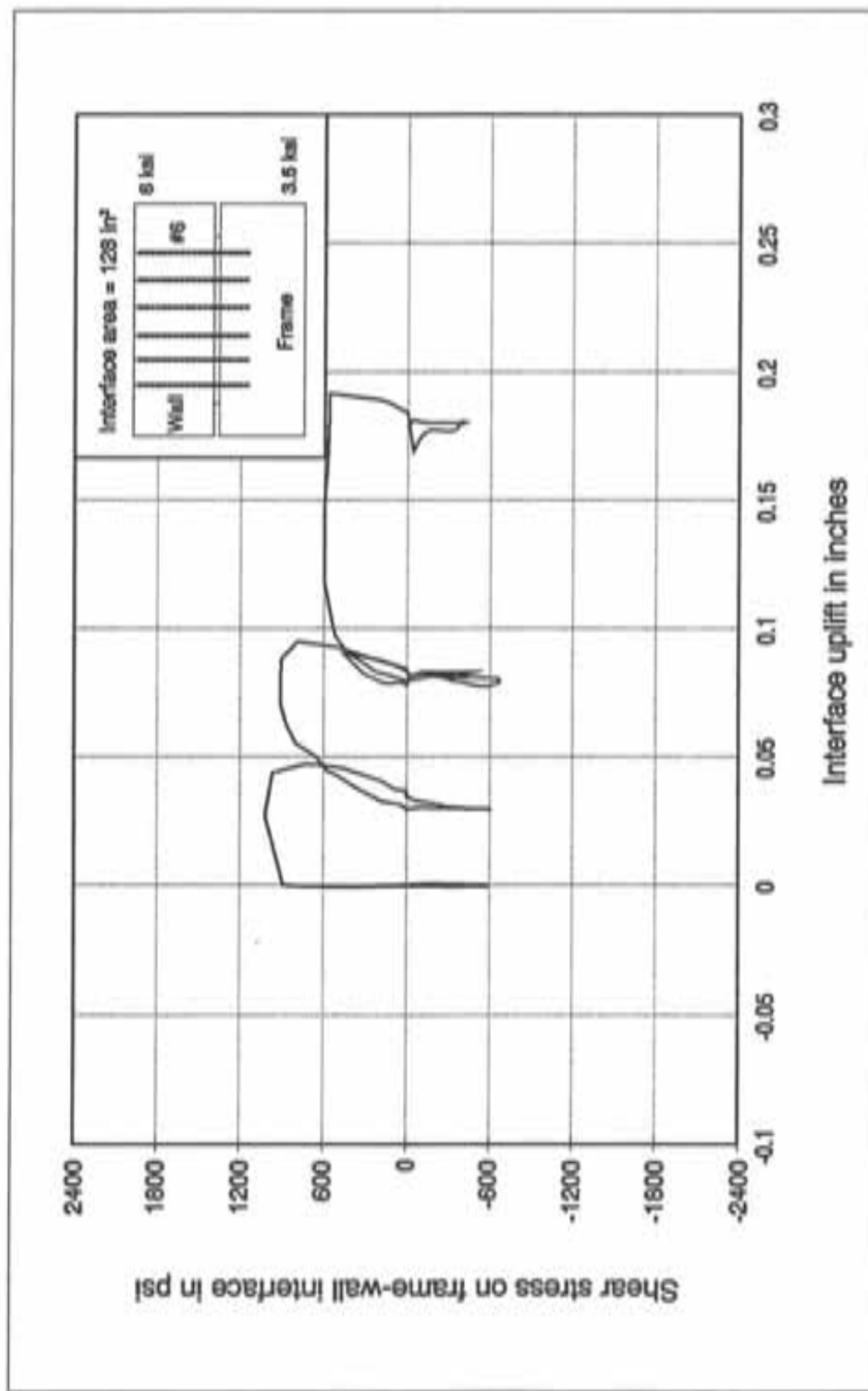


Figure B.27 Interface uplift on south side of shear specimen B2

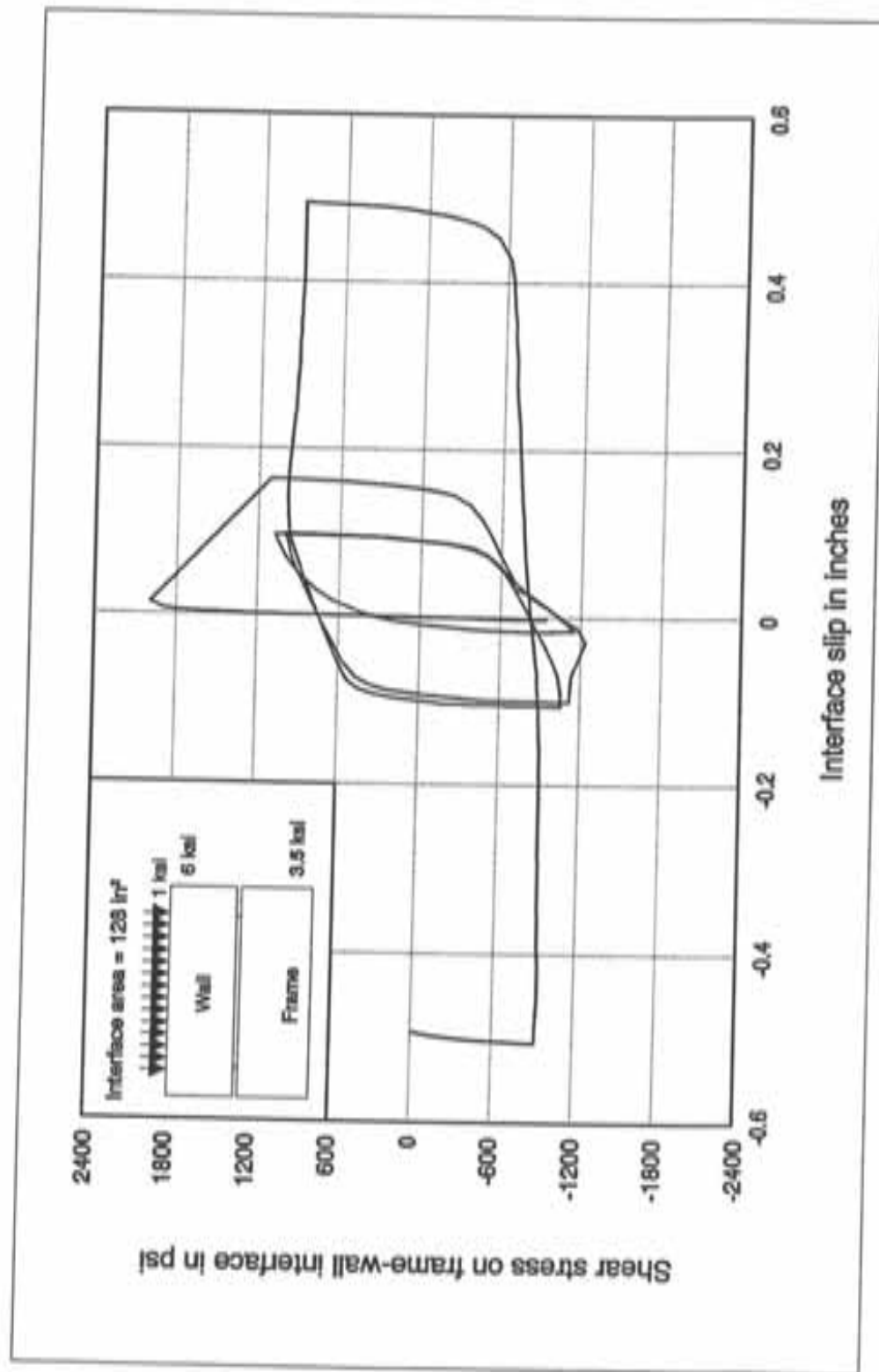


Figure B.28 Performance of shear specimen B3

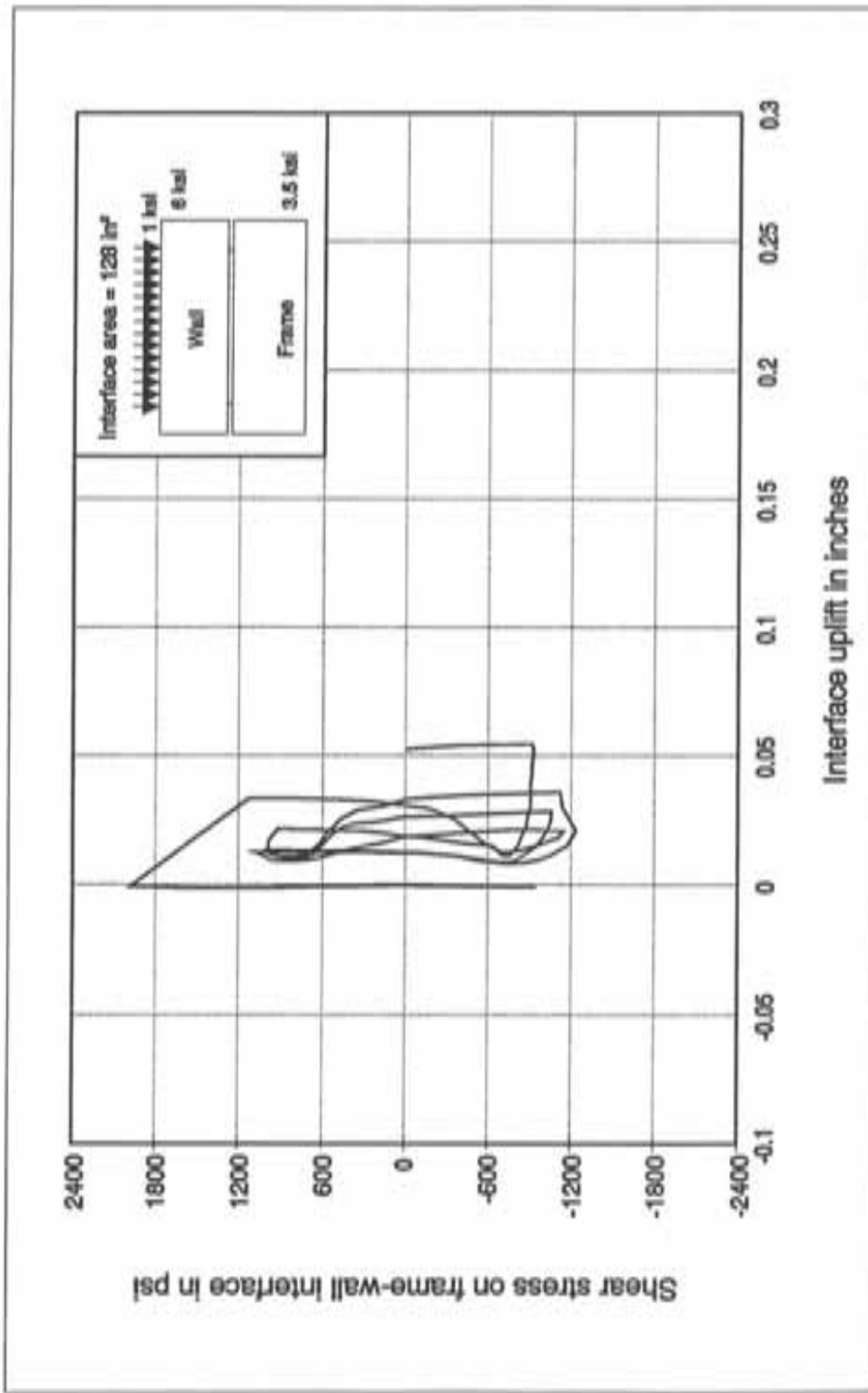


Figure B.29 Interface uplift on north side of specimen B3

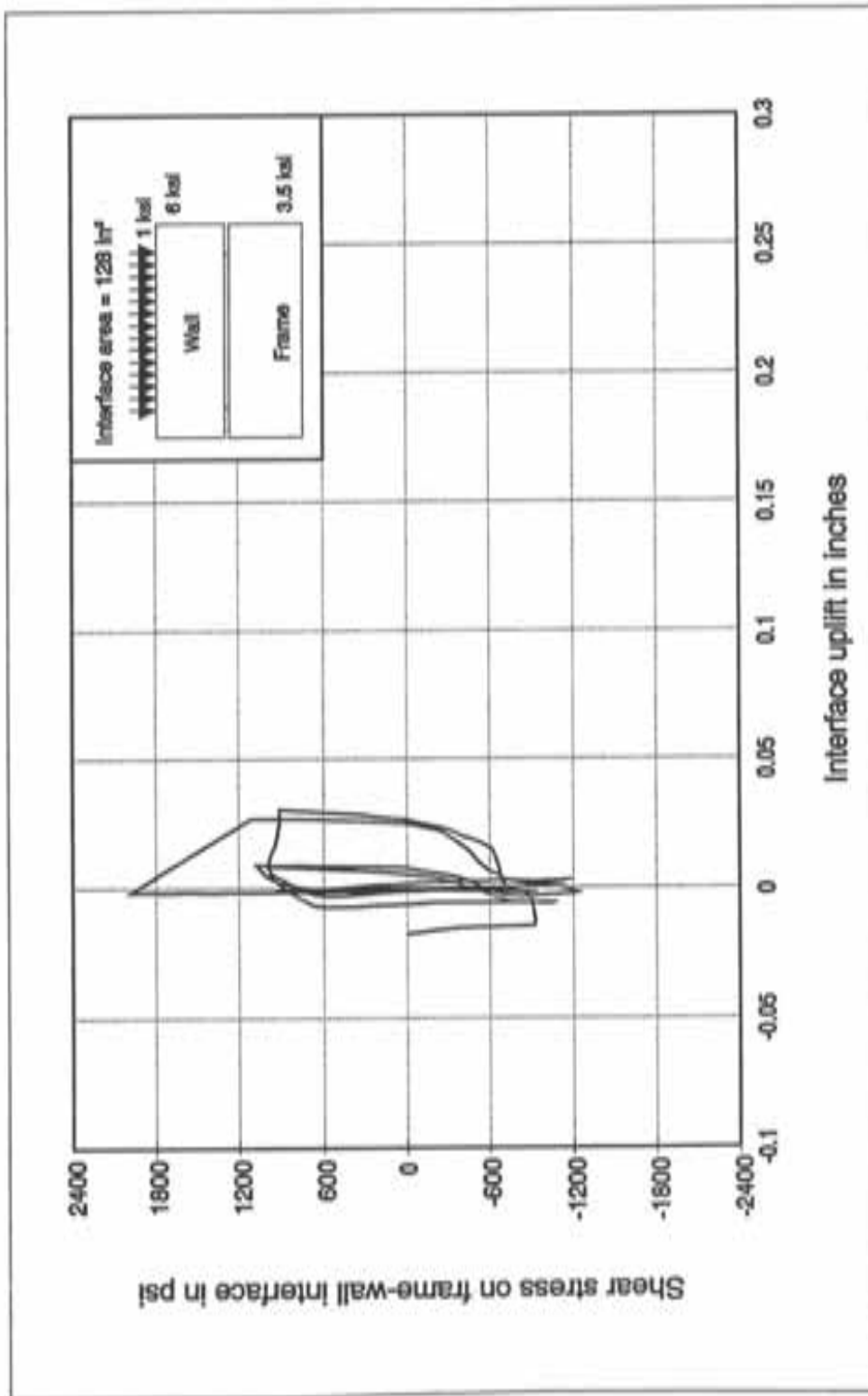


Figure B.30 Interface uplift on south side of specimen B3

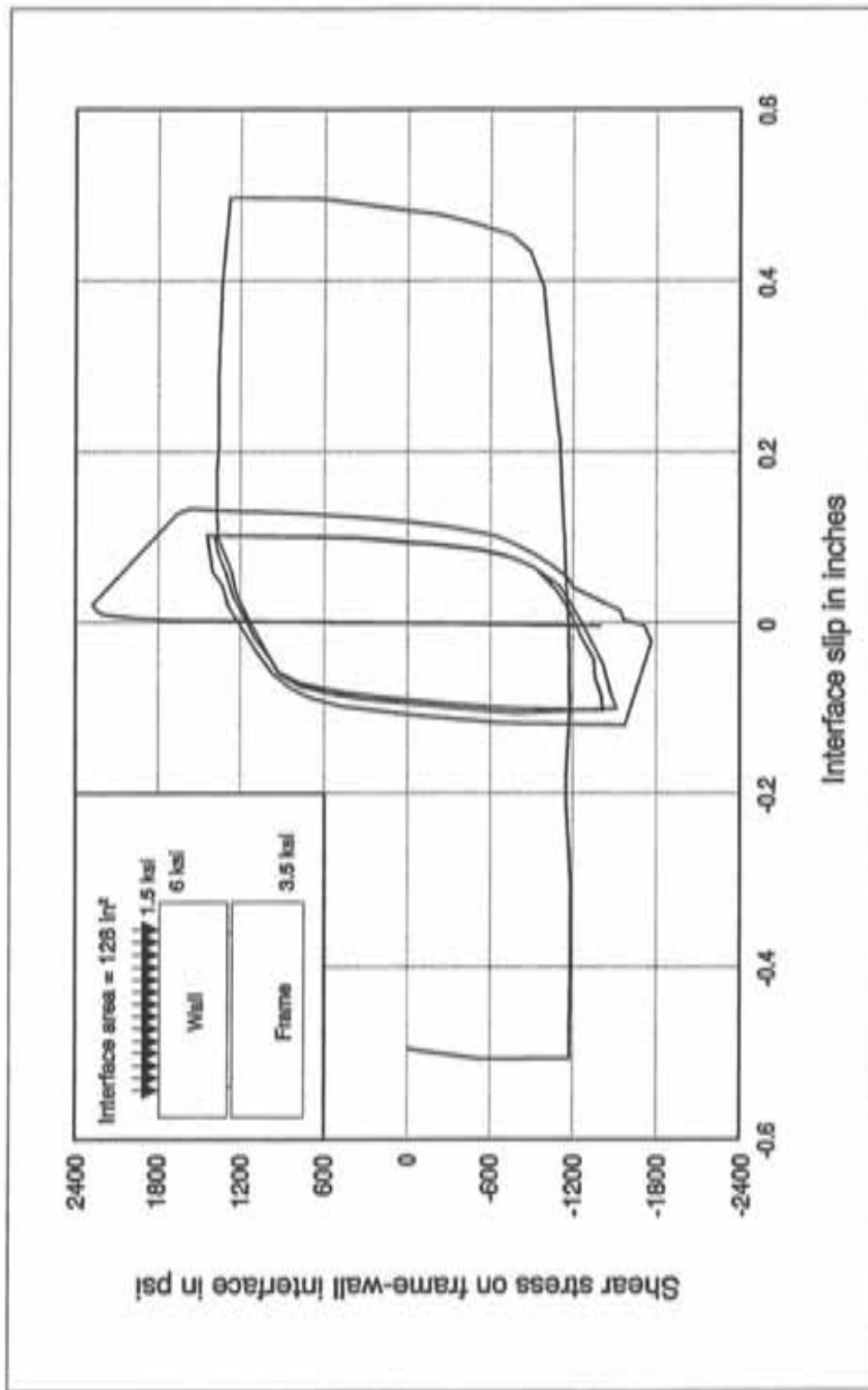


Figure B.31 Performance of shear specimen B4

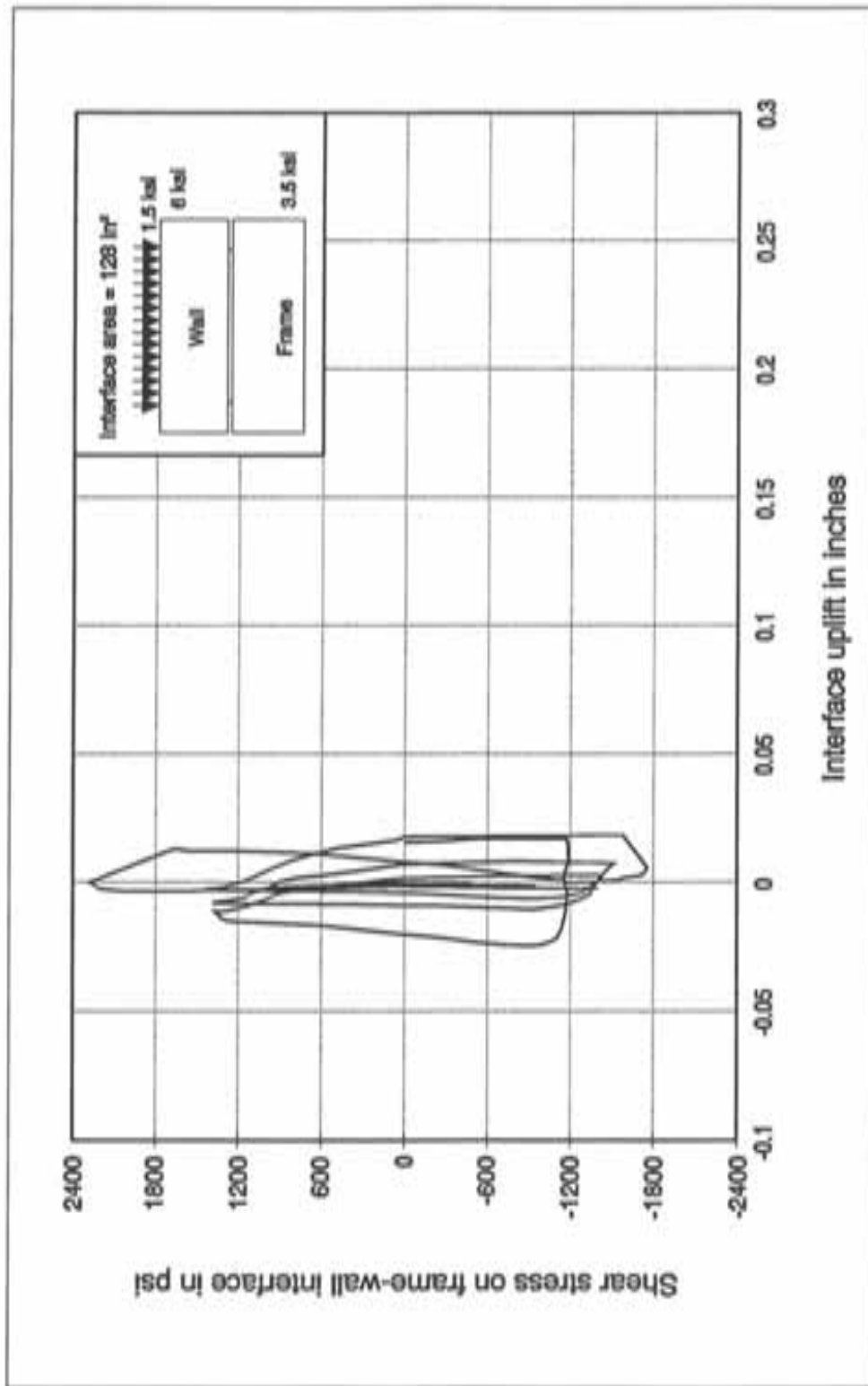


Figure B.32 Interface uplift on north side of shear specimen B4

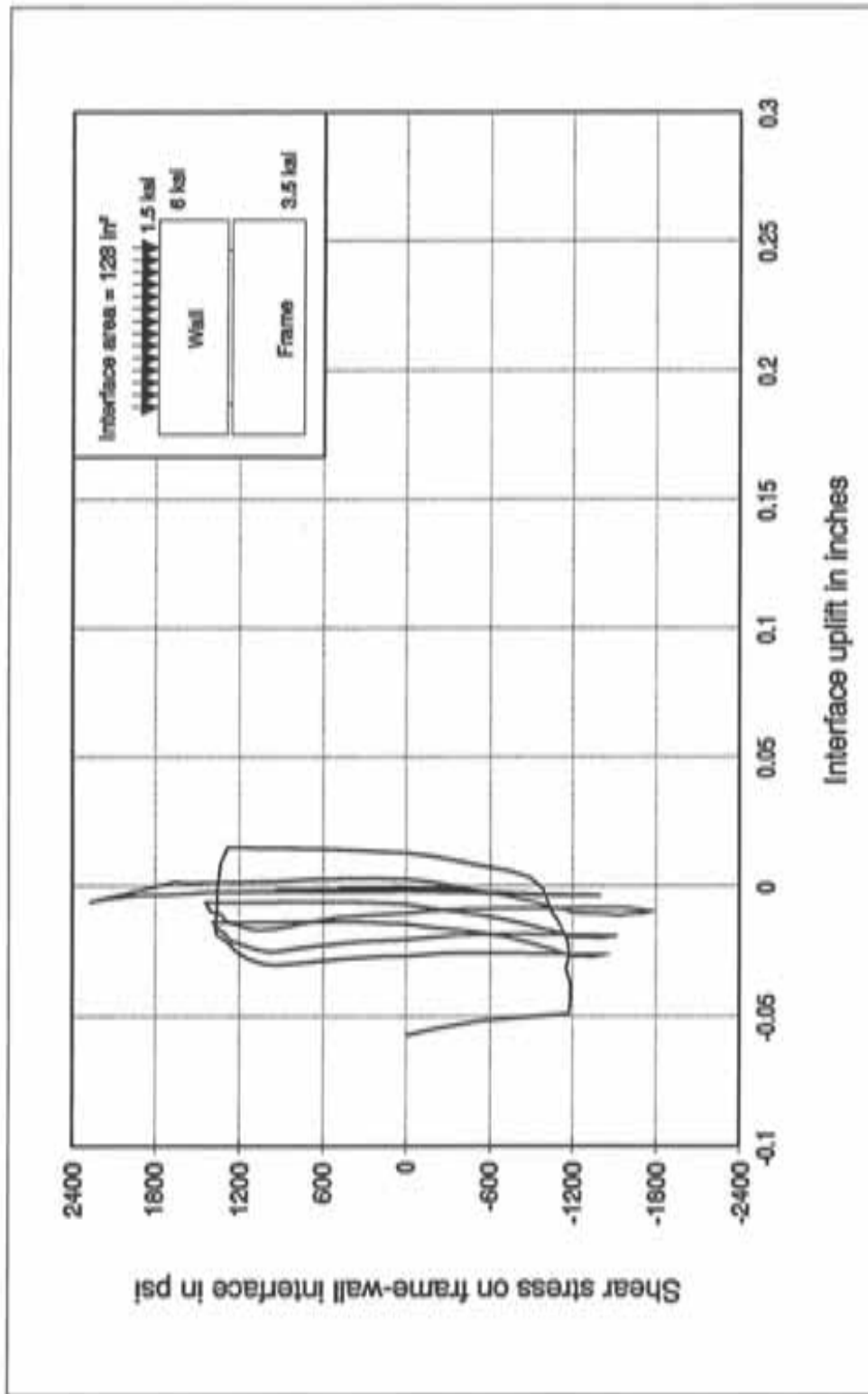


Figure B.33 Interface uplift on south side of shear specimen B4

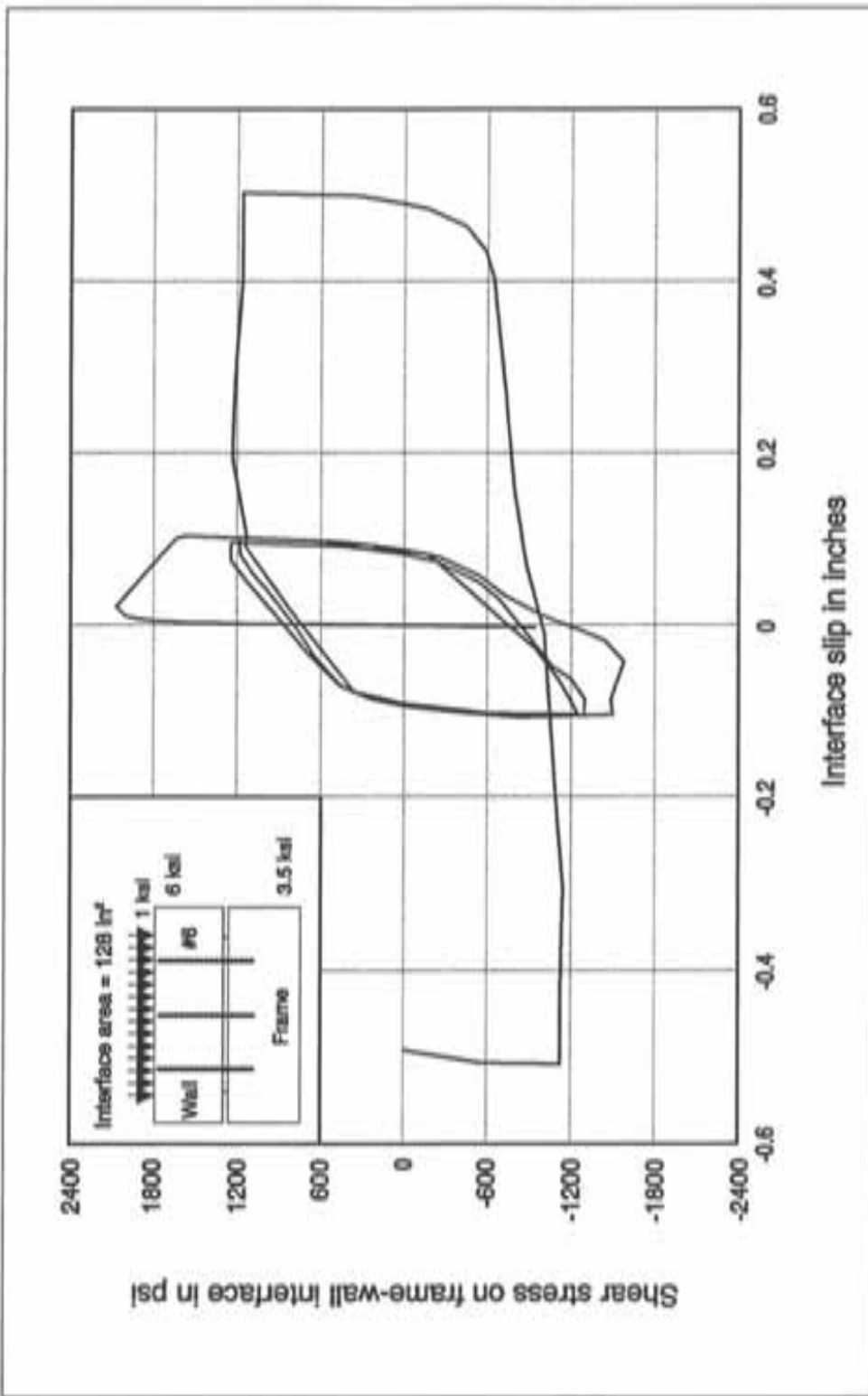


Figure B.34 Performance of shear specimen B5

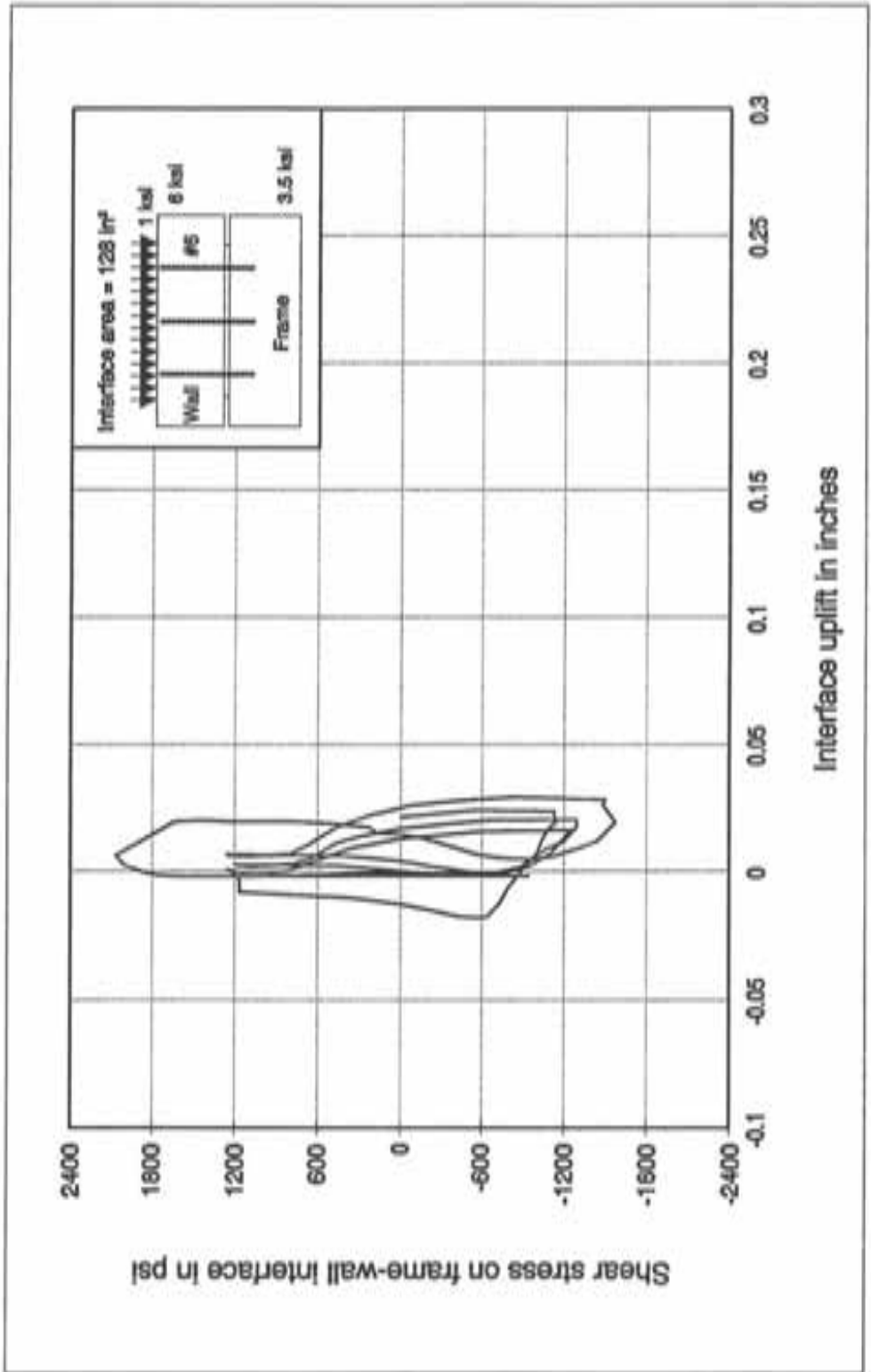


Figure B.35 Interface uplift on north side of shear specimen B5

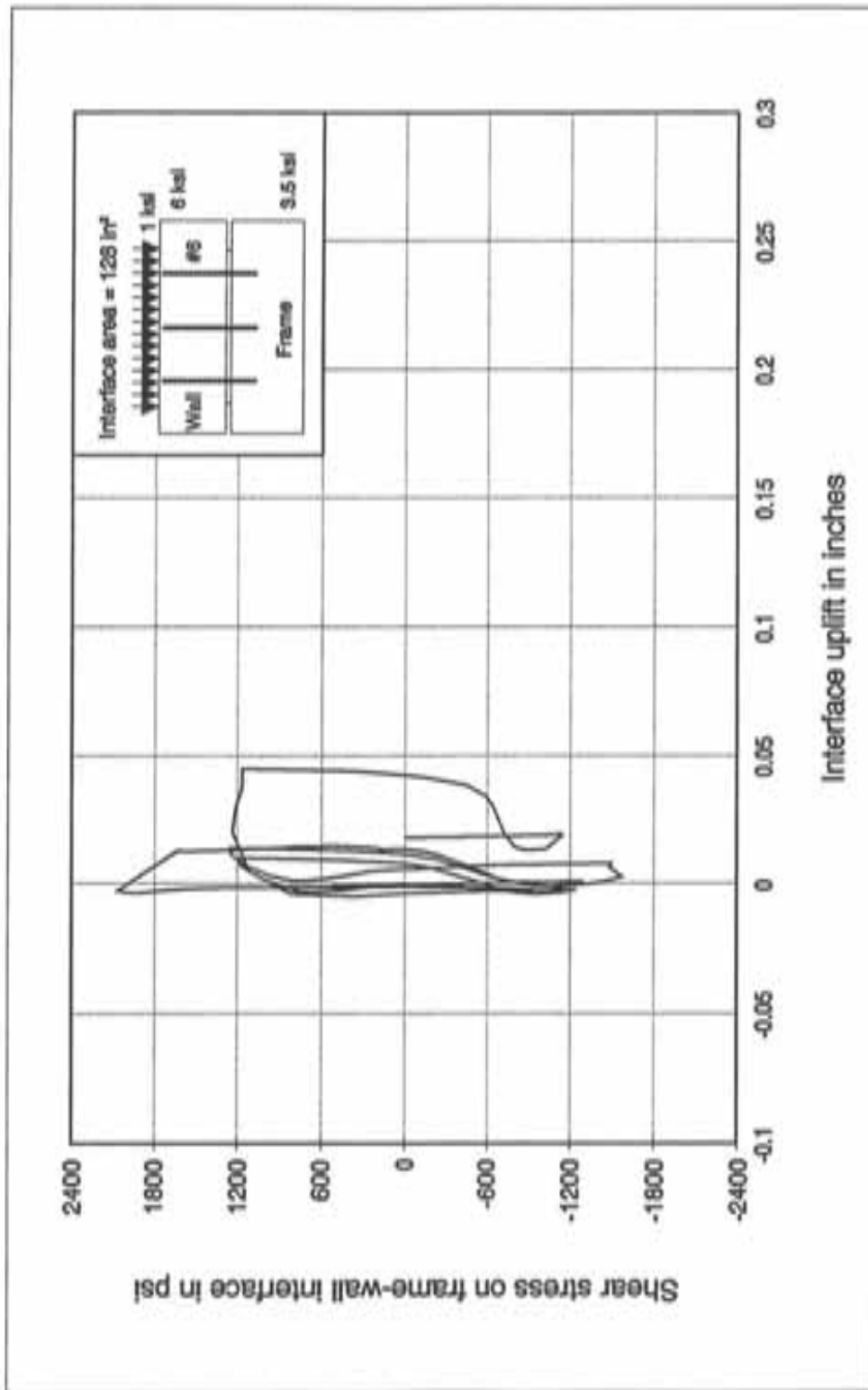


Figure B.36 Interface uplift on south side of shear specimen B5

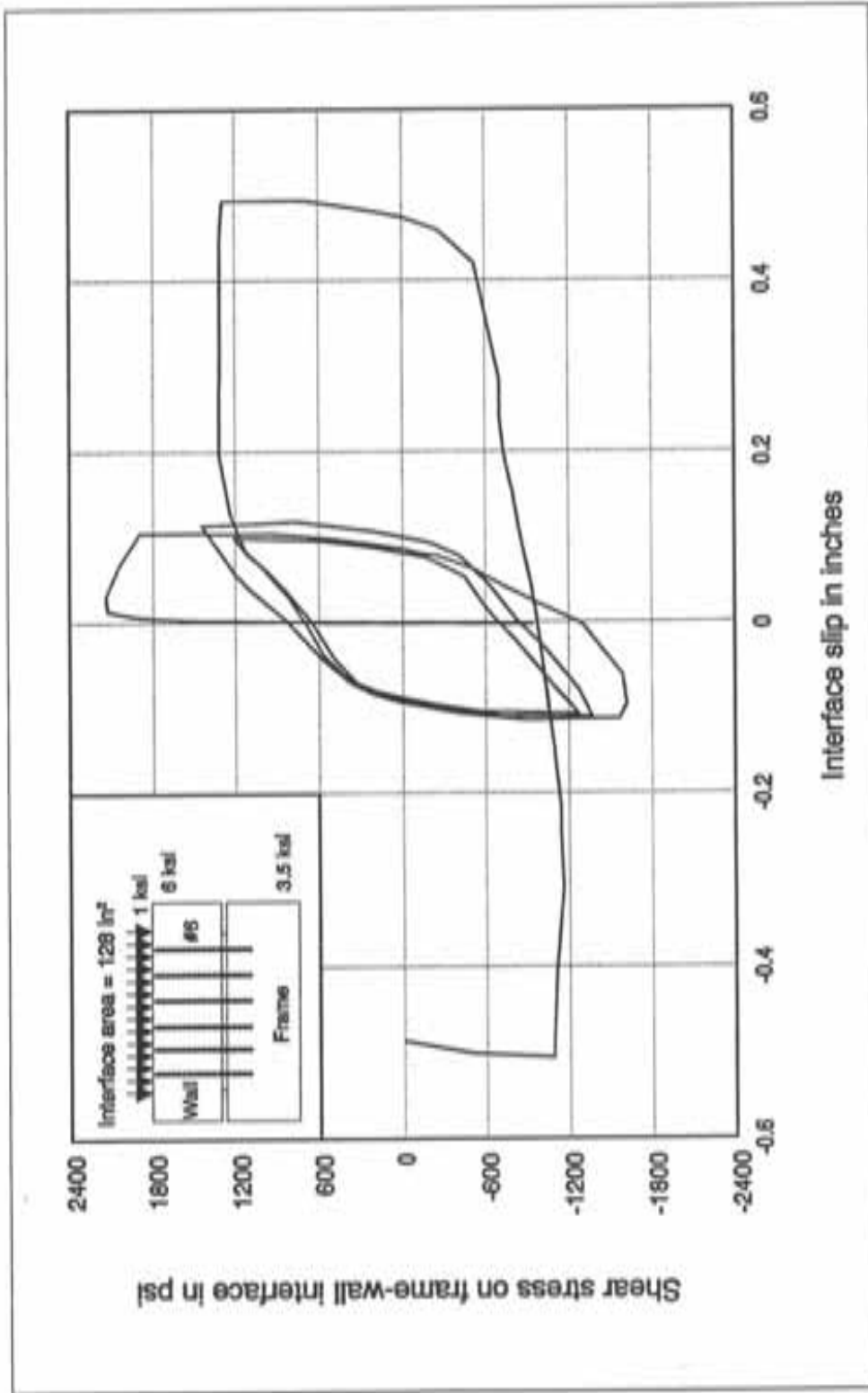


Figure B.37 Performance of shear specimen B6

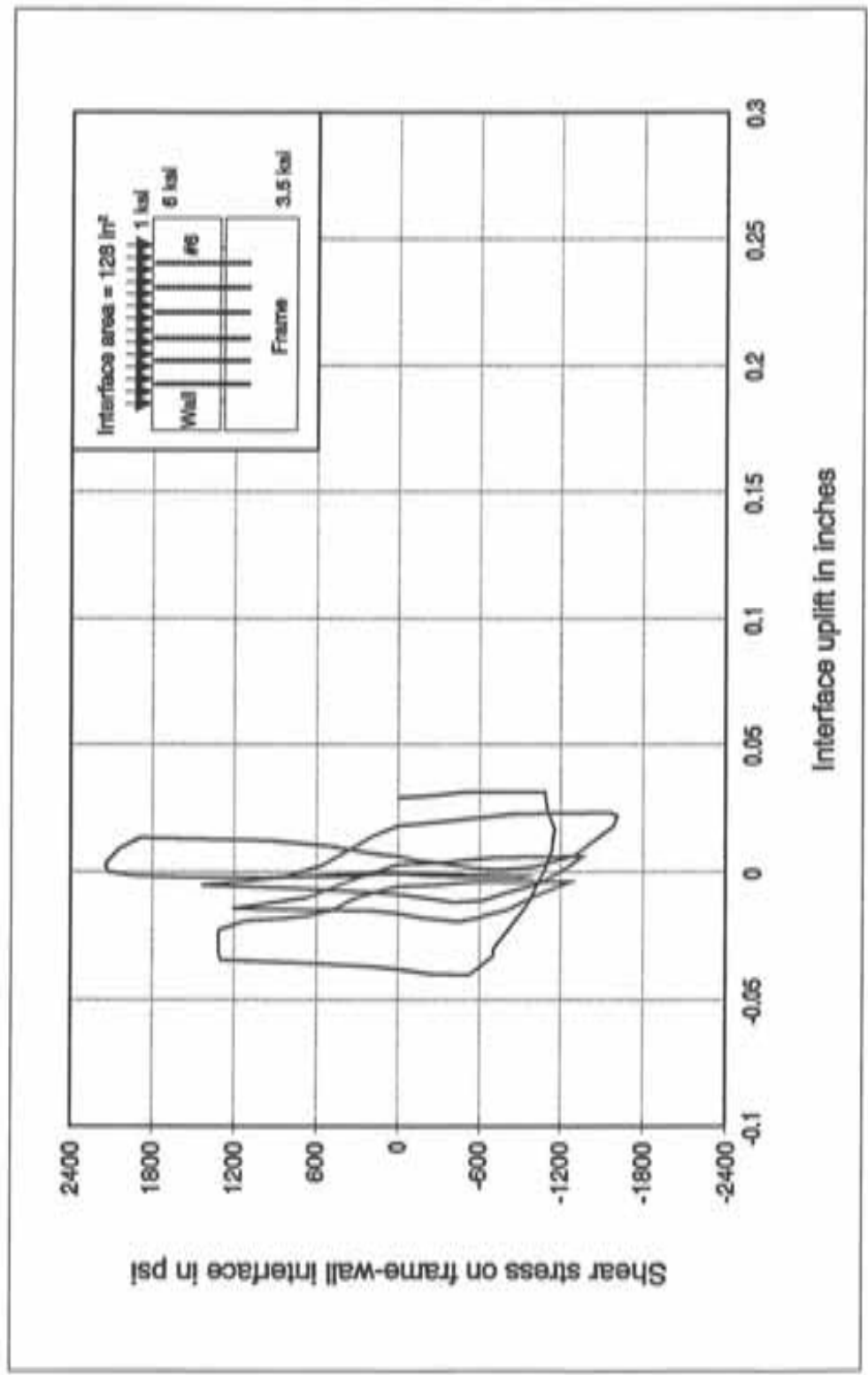


Figure B.38 Interface uplift on north side of shear specimen B6

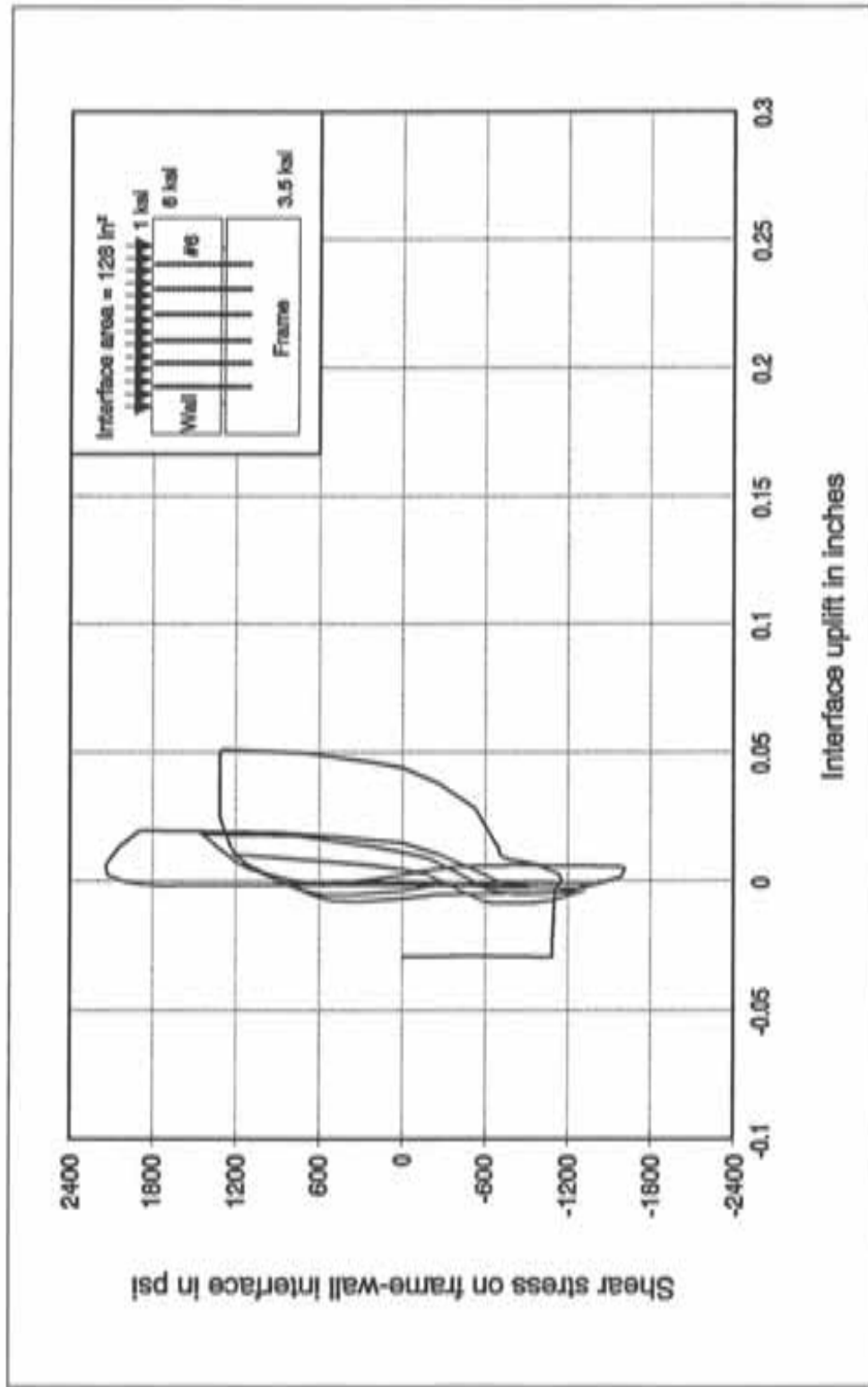


Figure B.39 Interface uplift on south side of shear specimen B6

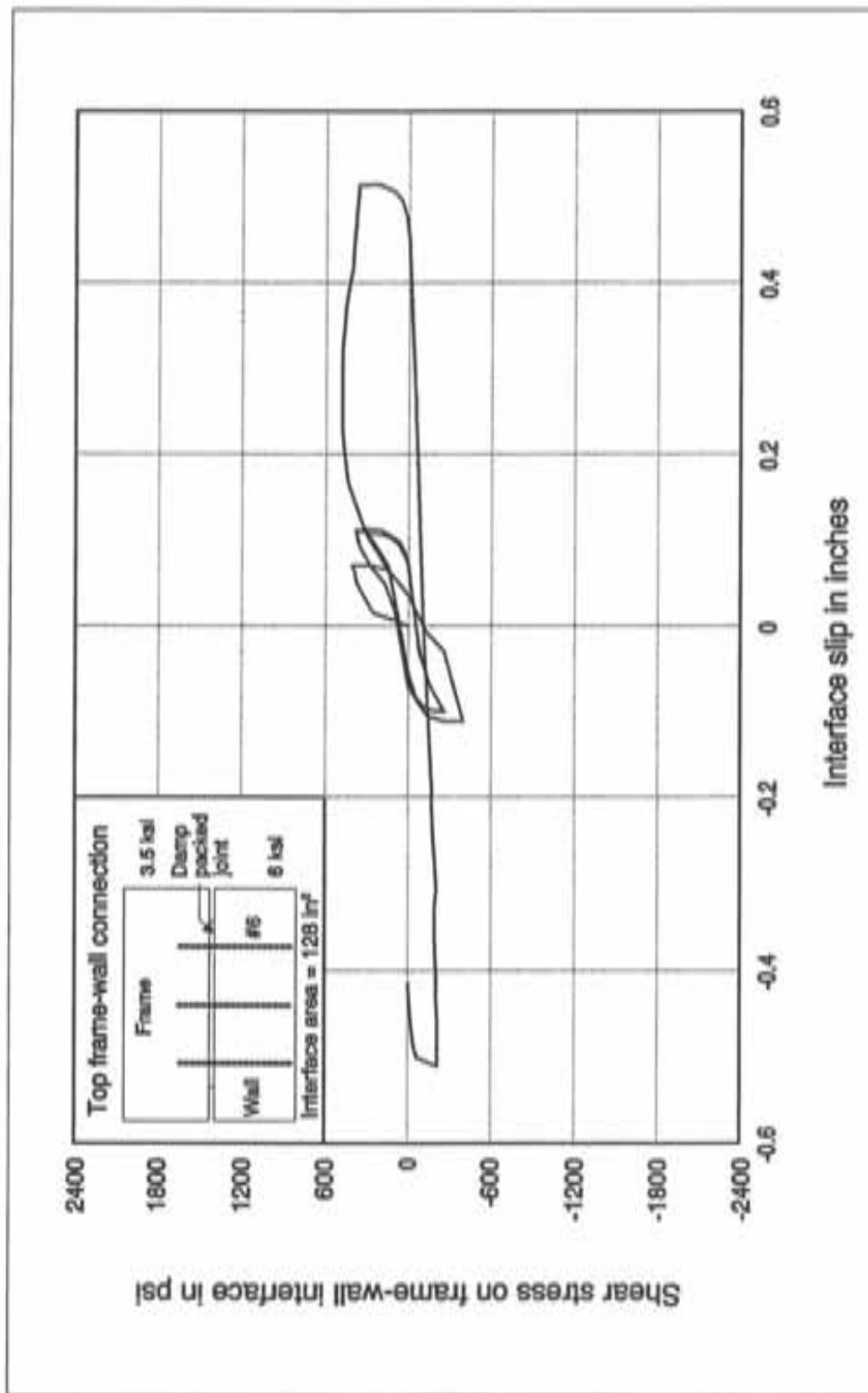


Figure B.40 Performance of shear specimen B7

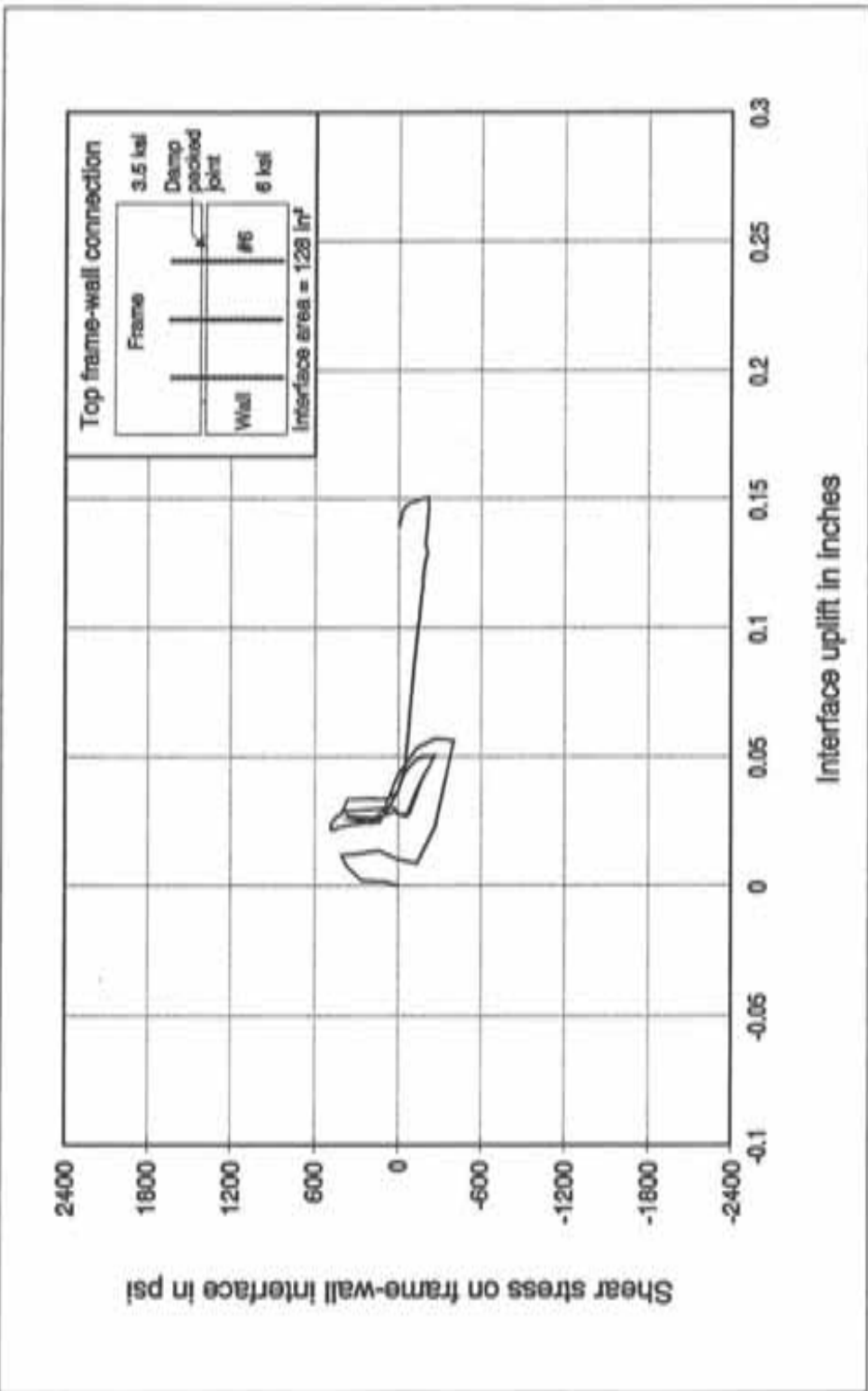


Figure B.41 Interface uplift on north side of shear specimen B7

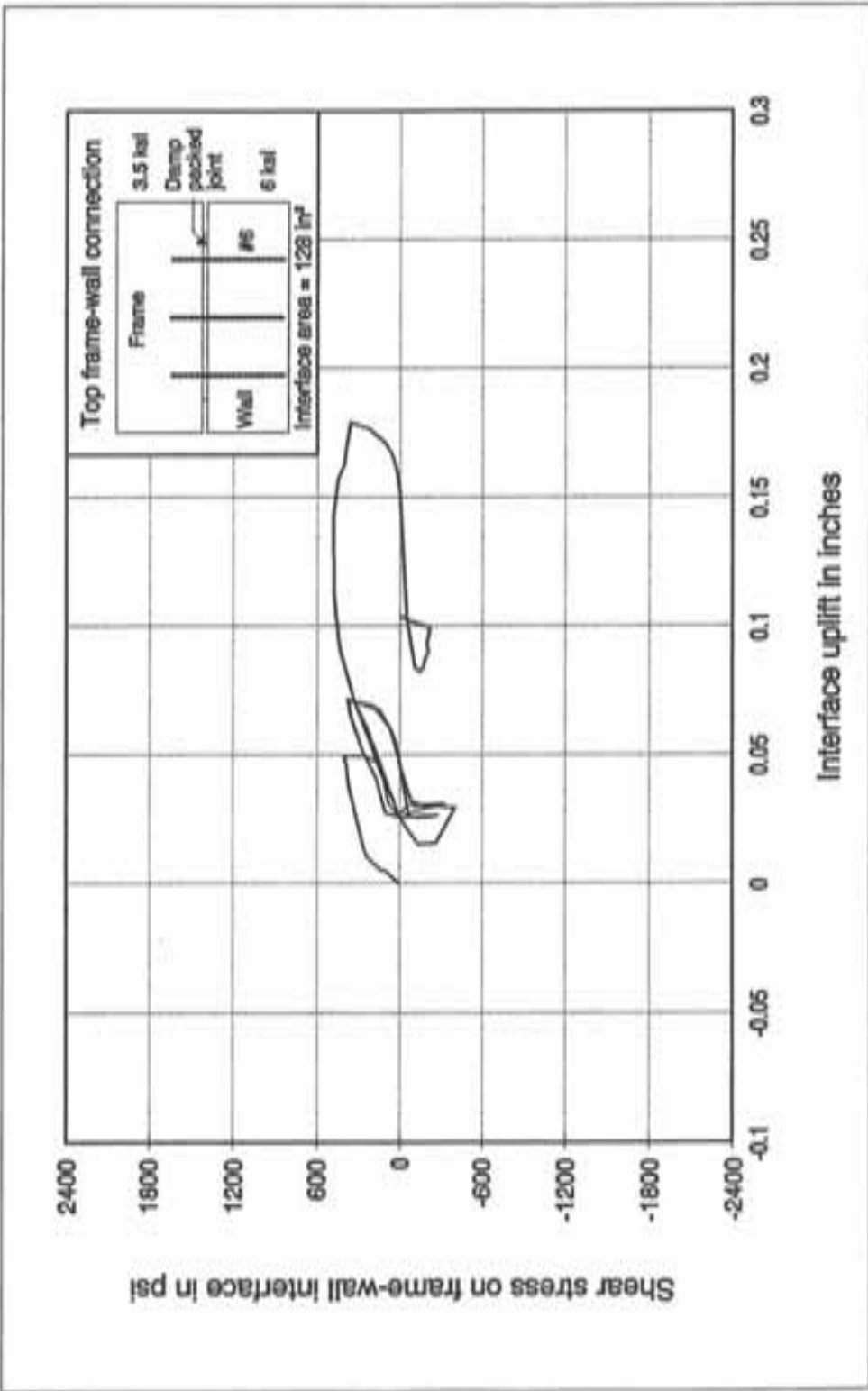


Figure B.42 Interface uplift on south side of shear specimen B7

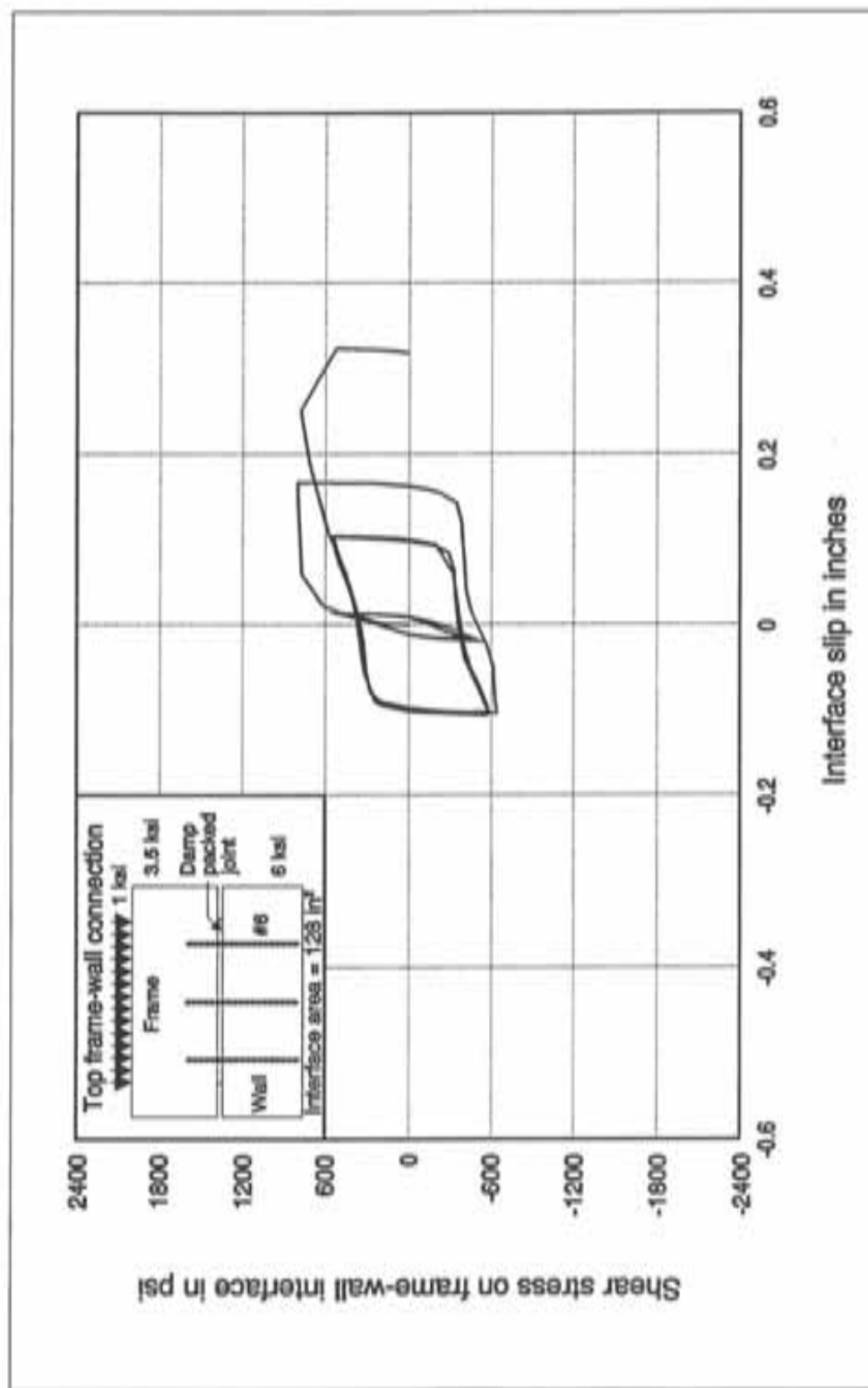


Figure B.43 Performance of shear specimen B8

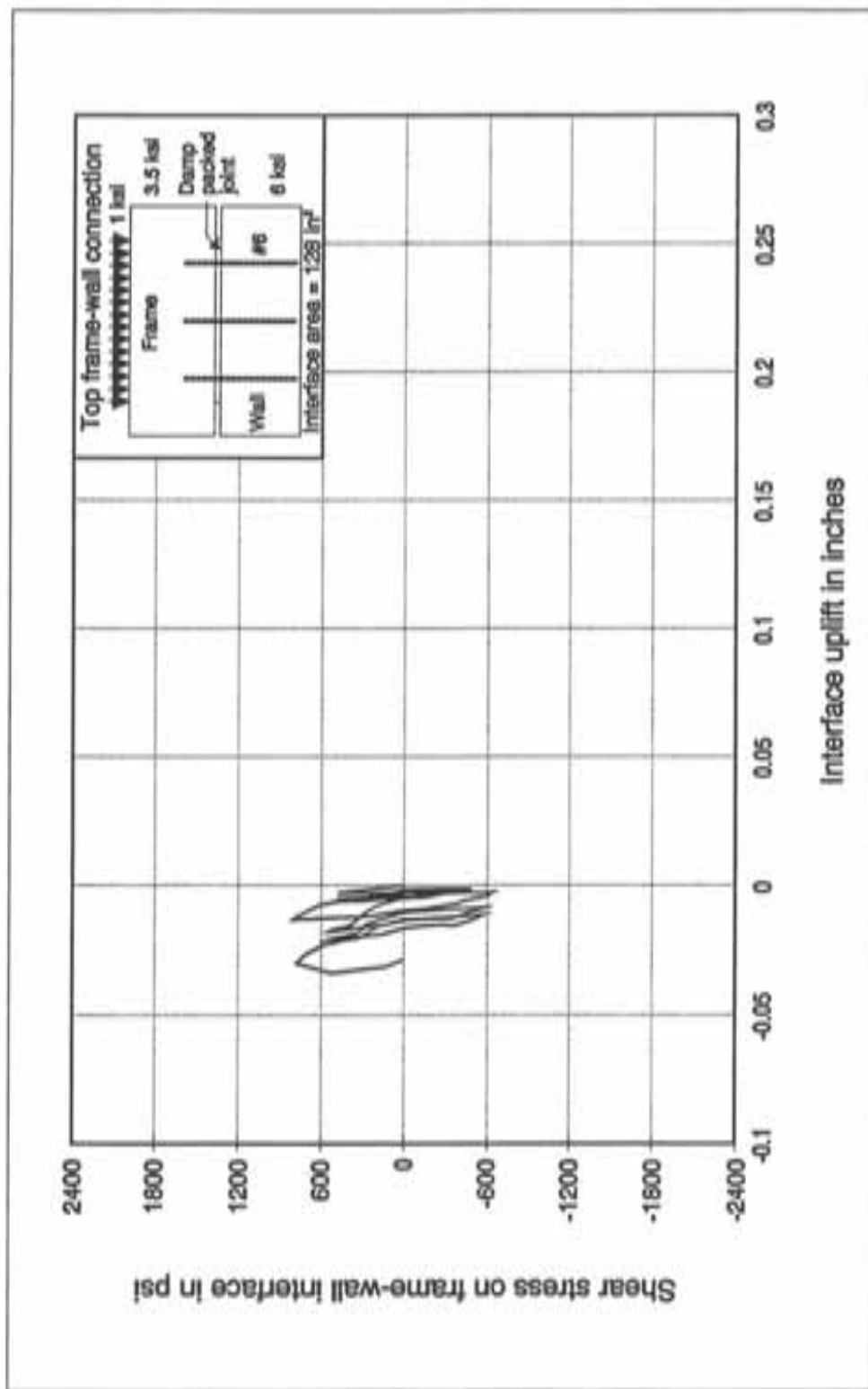


Figure B.44 Interface uplift on north side of shear specimen B8

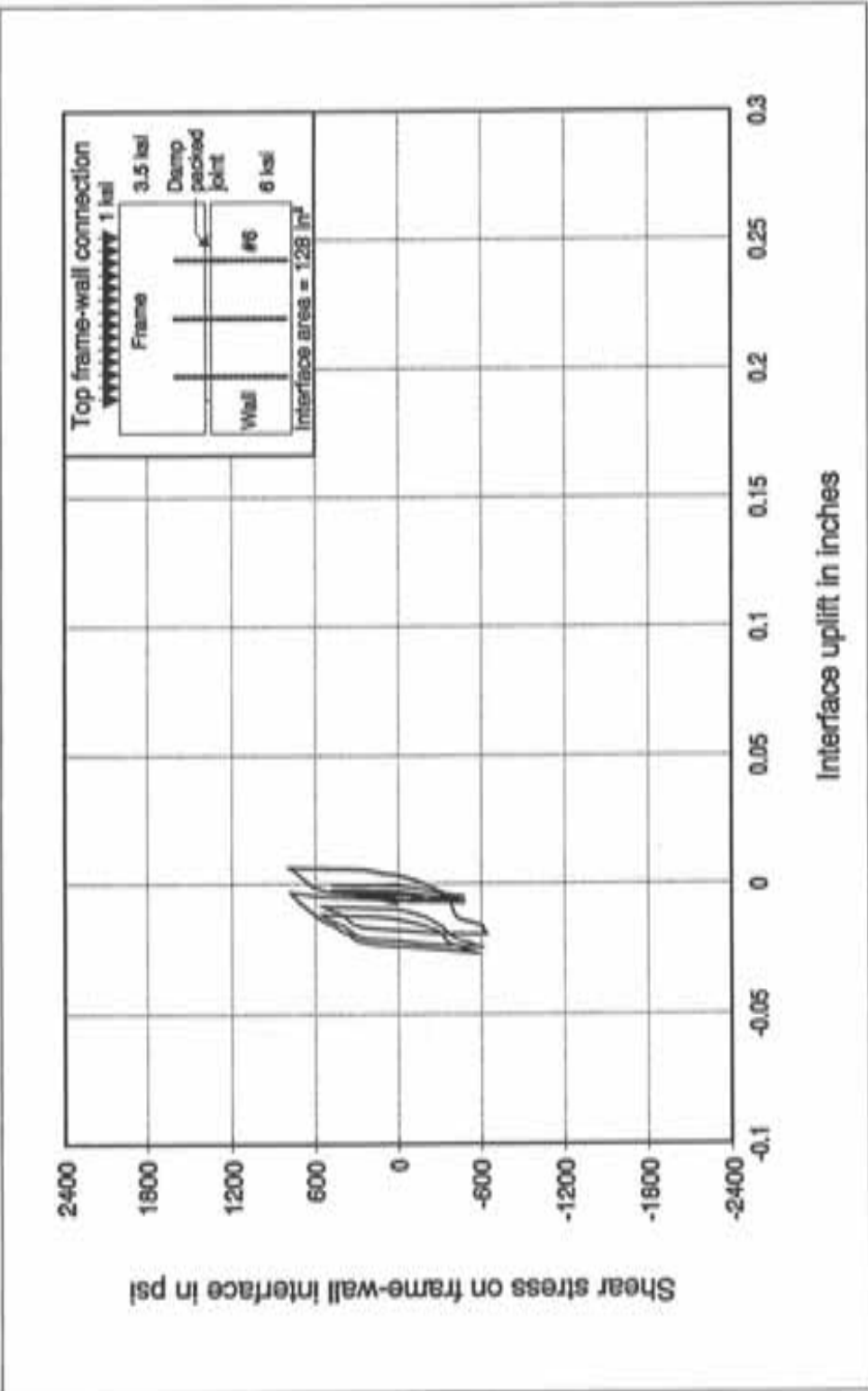


Figure B.45 Interface uplift on south side of shear specimen B8

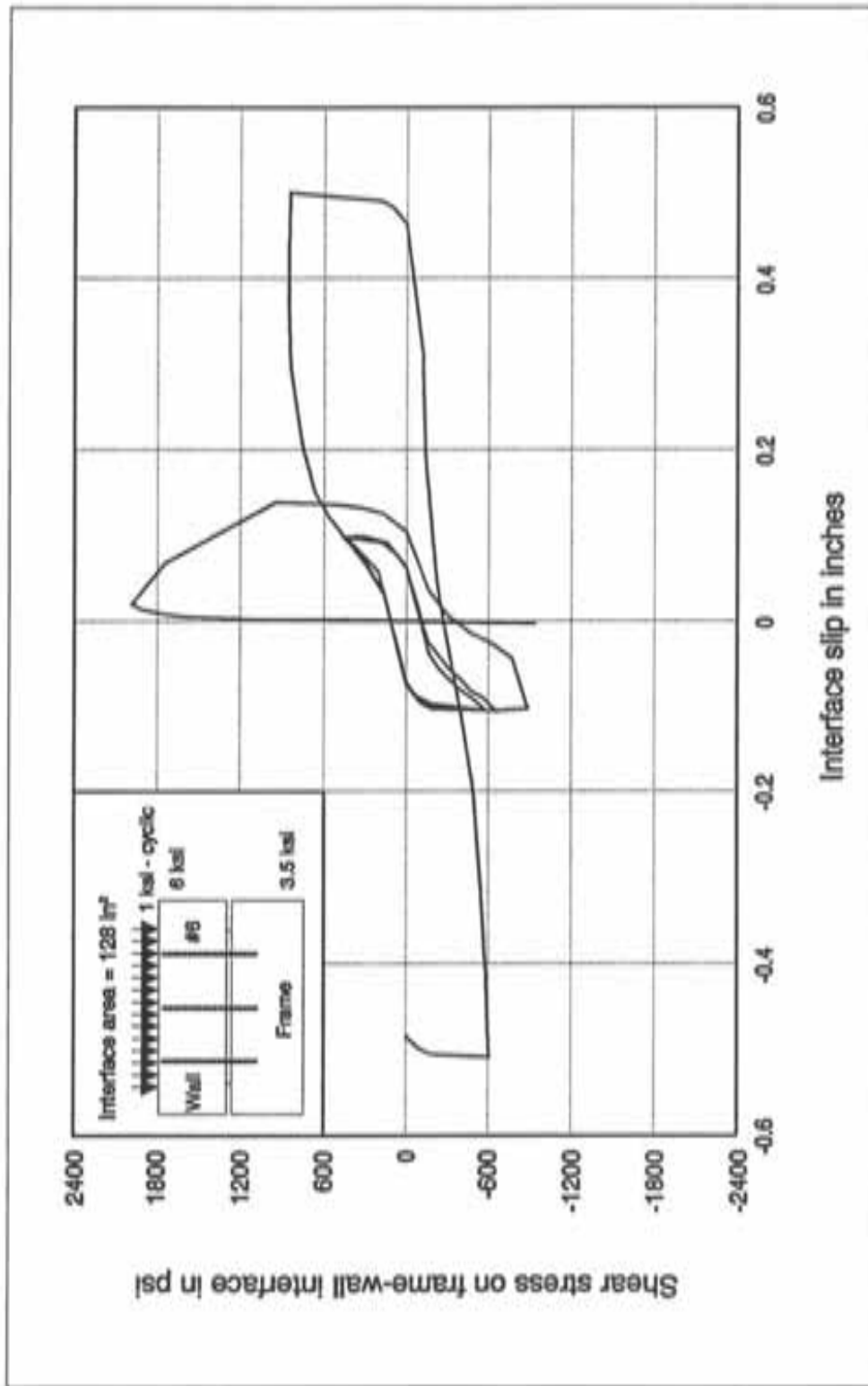


Figure B.46 Performance of shear specimen B9

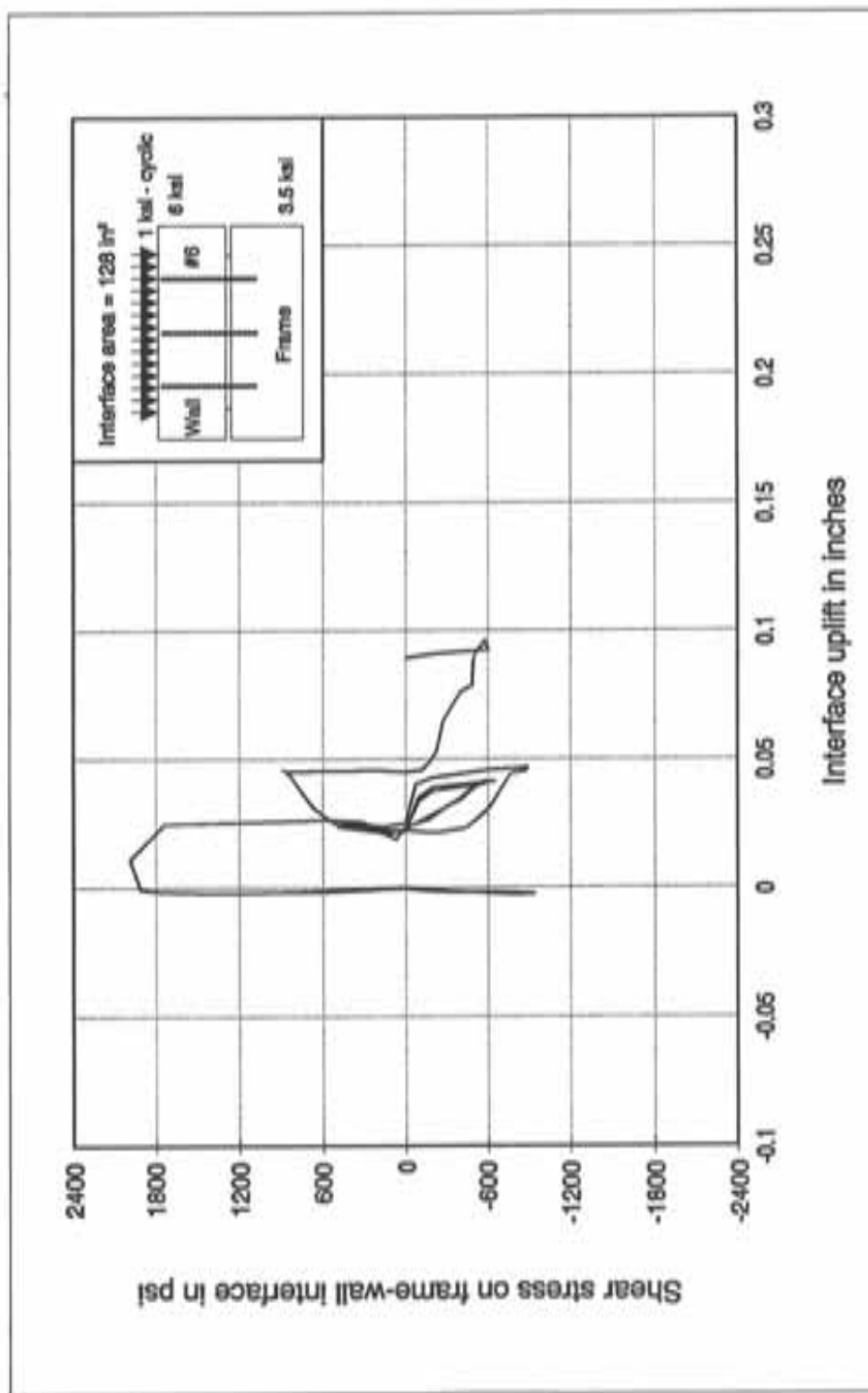


Figure B.47 Interface uplift on north side of shear specimen B9

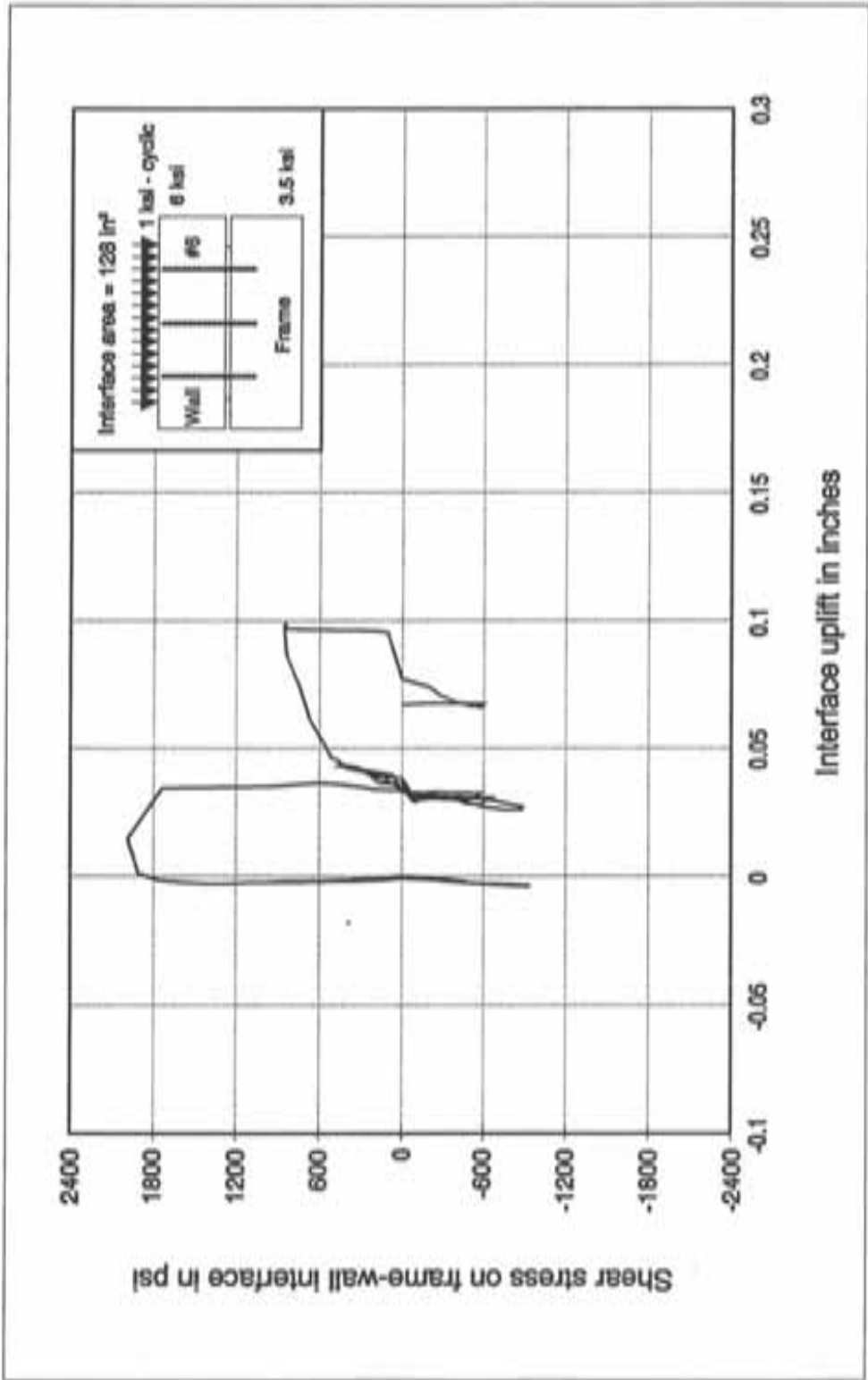


Figure B.48 Interface uplift on south side of shear specimen B9

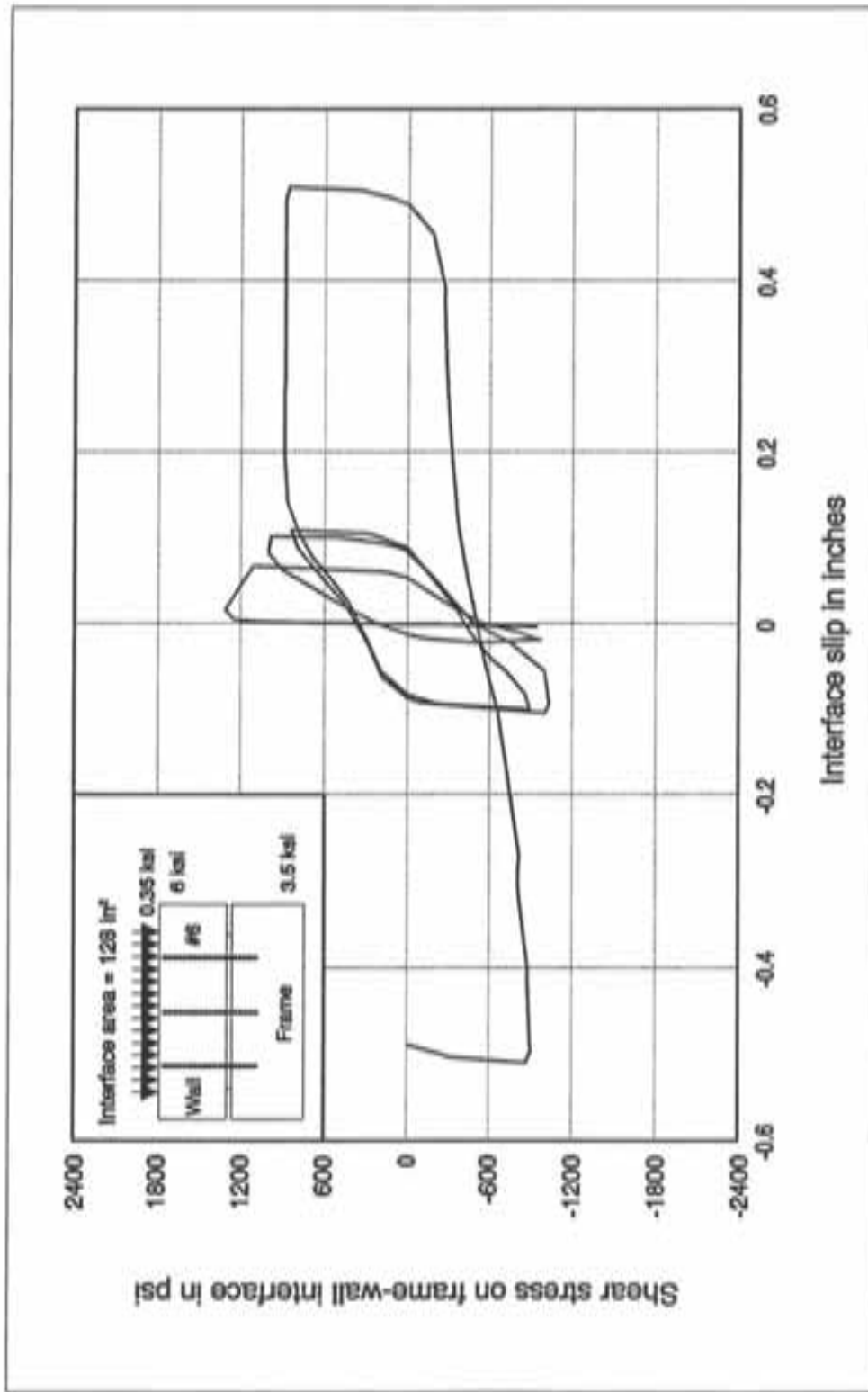


Figure B.49 Performance of shear specimen B10

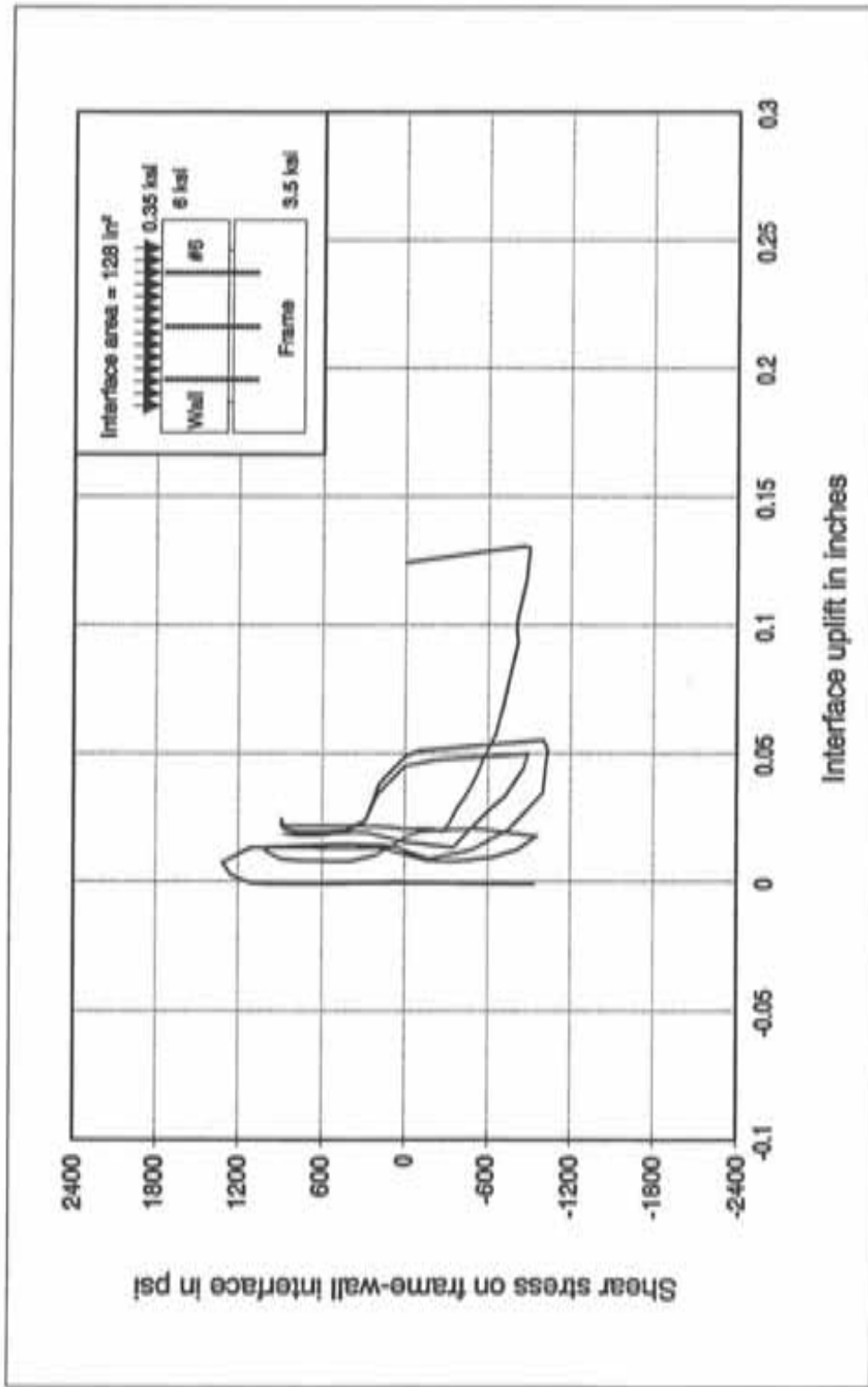


Figure B.50 Interface uplift on north side of shear specimen B10

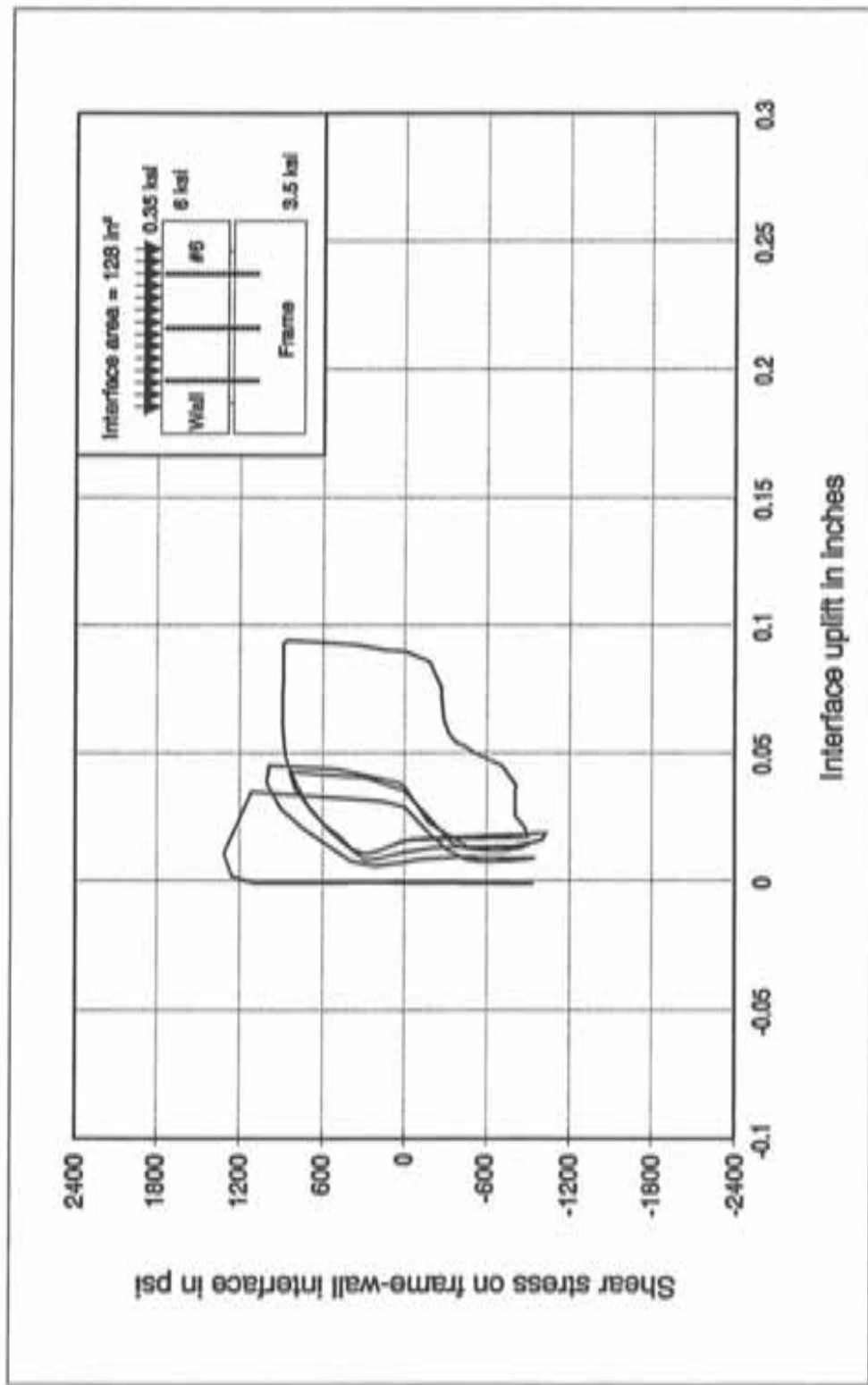


Figure B.51 Interface uplift on south side of shear specimen B10

APPENDIX C

SHEAR TRANSFER ACROSS FRAME-WALL INTERFACES

PULL OUT TEST RESULTS

C.1 PULL OUT TESTS

Simple pull out tests were proposed and conducted on the unused faces of frame segments of shear test specimens. Holes were drilled in the frame segments of specimens A4, A5, A8, B1, B2, and B5 and were cleaned with stiff brushes and a vacuum cleaner. Rebar dowels of #6 size were set into the cleaned 6 in. (8 bar diameters) deep holes using the same epoxy that was used to embed the dowels (as interface shear connectors) in the frame segments of shear test specimens.

Test setup shown in Fig. *.1 was used to determine the pullout strengths of dowels. Tension on the dowels was applied using a 60 kips capacity hydraulic ram. Applied load was monitored by a pressure transducer and a pressure gage. Displacement transducers measured the slip in dowels.

C.2 PULL OUT TEST RESULTS

Dowels in all test specimens pulled out and failed prematurely without reaching their nominal (60 ksi) or measured (69 ksi) yield strengths. Failure patterns (see Fig. *.2) consisted of different failure interfaces; (1) interface between rebar surface and epoxy, (2) interface between epoxy and surrounding concrete, and (3) conical failure of concrete surrounding the dowels. Pull out strengths as established by the tests are presented in Table *.1.

Table C.1 Summary of pull out test results

| Sl. no. | Specimen Index | Frame f'_c (psi) | Pull out strength | | Ratio of pull out strength to | |
|---------|----------------|--------------------|-------------------|--------|---------------------------------|----------------------------------|
| | | | In kips | In ksi | nominal yield strength (60 ksi) | measured yield strength (69 ksi) |
| 1 | A4 | 1750 | 17.0 | 38.6 | 0.64 | 0.56 |
| 2 | A5 | 1750 | 18.4 | 41.8 | 0.70 | 0.61 |
| 3 | A8 | 1750 | 20.1 | 45.7 | 0.76 | 0.66 |
| 4 | B1 | 3500 | 19.9 | 45.2 | 0.75 | 0.66 |
| 5 | B2 | 3500 | 23.2 | 52.7 | 0.88 | 0.76 |
| 6 | B5 | 3500 | 20.5 | 46.6 | 0.78 | 0.68 |

Dowels were of #6 rebars (area = 0.44 in.²)
Dowel embedment depth = 6 in. (8 bar diameters)

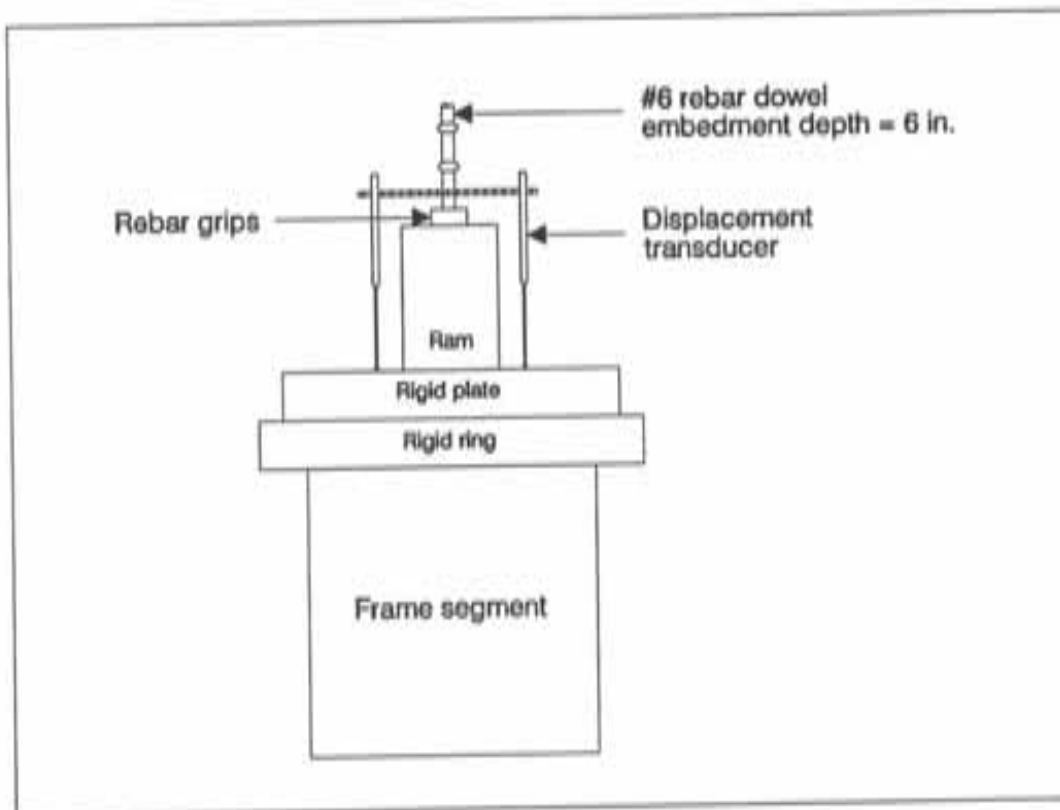
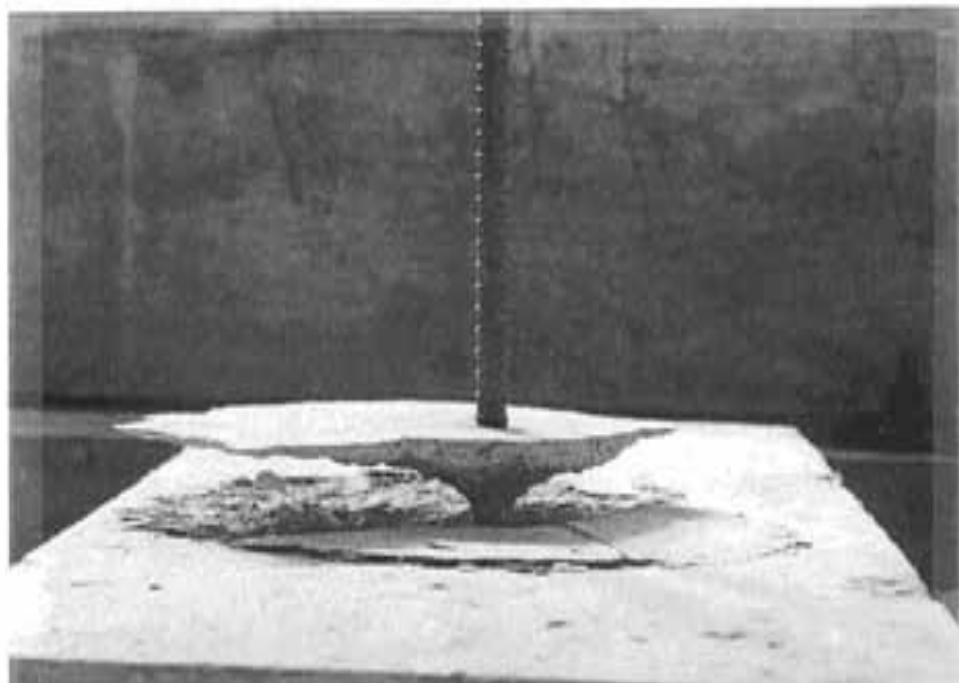
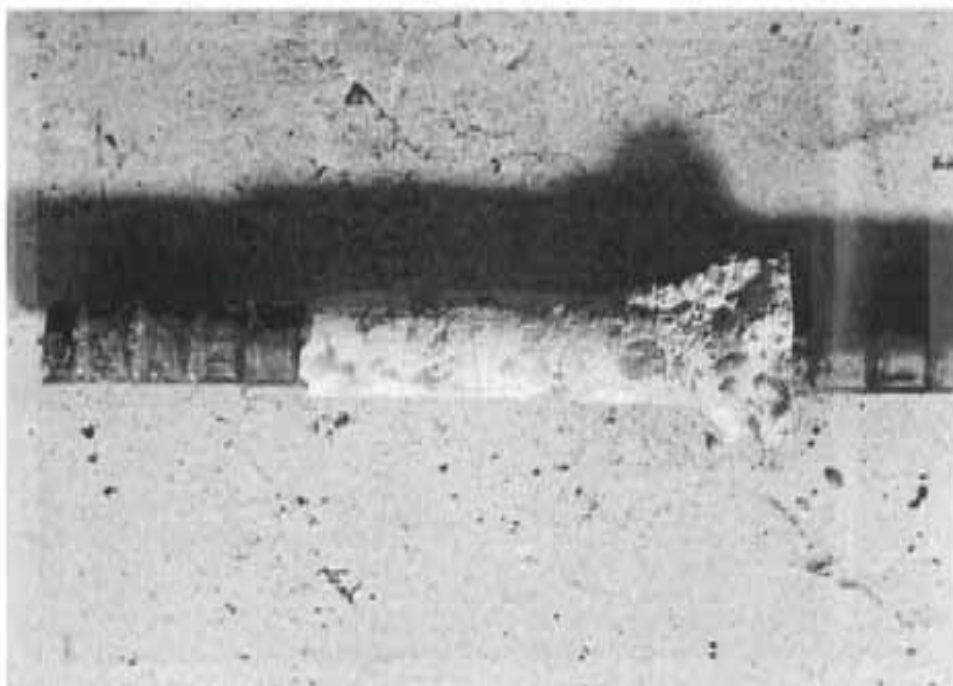


Figure C.1 Pull out test setup

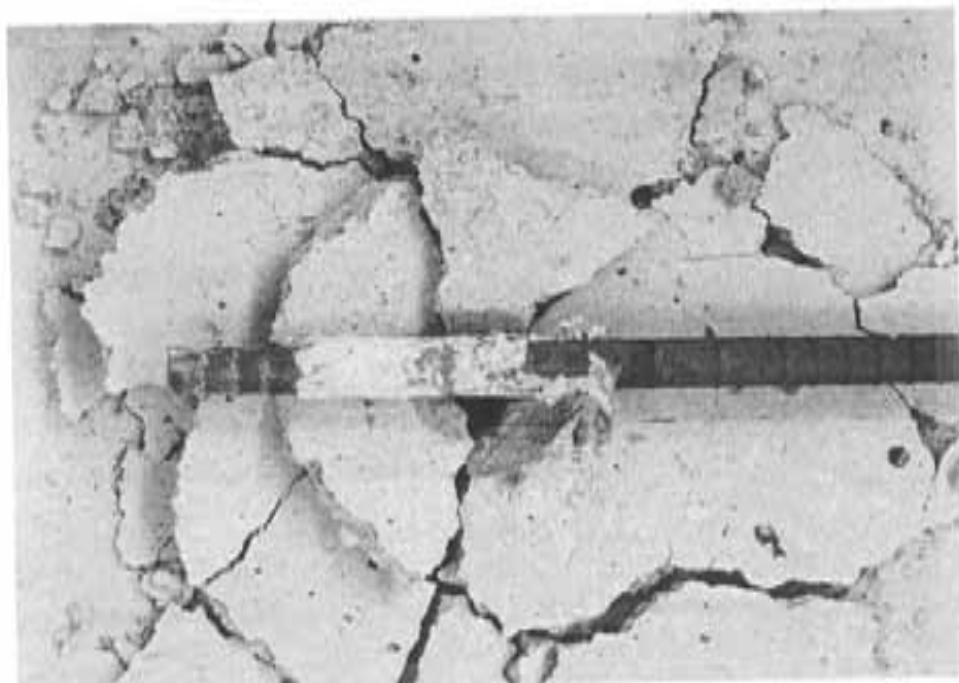


(a) Failure pattern of dowel in test specimen A8



(b) Failure pattern of dowel in test specimen B2

Figure C.2 Pull out failure patterns of dowels (contd.)



(c) Failure pattern of dowel in test specimen B5

Figure C.2 Pull out failure patterns of dowels

APPENDIX D

SHEAR-FRICTION PROVISIONS IN SECTION 11.7 OF ACI 318-89

D.1 INTRODUCTION

The ACI code provisions on shear-friction are presented here without making any changes in section numbers as specified by the code. The intention is to facilitate easy follow-up of discussions made in chapter 9.

11.7 - Shear-friction

11.7.1 - Provisions of 11.7 are to be applied where it is appropriate to consider shear transfer across a given plane, such as: an existing or potential crack, an interface between dissimilar materials or an interface between two concretes cast at different times.

11.7.2 - Design of cross sections subject to shear transfer as described in 11.7.1 shall be based on Eq. (11-1), where V_u is calculated in accordance with provisions of 11.7.3 or 11.7.4.

11.7.3 - A crack shall be assumed to occur along the shear plane considered. The required area of shear-friction reinforcement A_w across the shear

R11.7 - Shear-friction

R11.7.1 - With the exception of 11.7, virtually all provisions regarding shear are intended to prevent diagonal tension failures rather than direct shear-transfer failures. The purpose of 11.7 is to provide design methods for conditions where shear transfer should be considered: an interface between concretes cast at different times, an interface between concrete and steel, reinforcing details for precast concrete structures, and other situations where it is considered appropriate to investigate shear transfer across a plane in structural concrete. (See References 11.23 and 11.24).

R11.7.3 - Although uncracked concrete is relatively strong in direct shear there is always the possibility that a crack will form in an unfavorable location.

plane shall be designed using either 11.7.4 or any other shear transfer design methods that result in prediction of strength in substantial agreement with results of comprehensive tests.

11.7.3.1 - Provisions of 11.7.5 through 11.7.10 shall apply for all calculations of shear transfer strength.

The shear friction concept assumes that such a crack will form, and that reinforcement must be provided across the crack to resist relative displacement along it. When shear acts along a crack, one crack face slips relative to the other. If the crack faces are rough and irregular, this slip is accompanied by separation of the crack faces. At ultimate, the separation is sufficient to stress the reinforcement crossing the crack to its yield point. The reinforcement provides a clamping force $A_v f_y$ across the crack faces. The applied shear is then resisted by friction between the crack faces, by resistance to the shearing off of protrusions on the crack faces, and by dowel action of the reinforcement crossing the crack. Successful application of 11.7 depends on proper selection of the location of an assumed crack.^{11.13, 11.23}

The relationship between shear-transfer strength and the reinforcement crossing the shear plane can be expressed in various ways. Eq. (11-26) and (11-27) of 11.7.4 are based on the shear-friction model. This gives a conservative prediction of shear-transfer strength. Other relationships which give a closer estimate of shear-transfer strength^{11.13, 11.26, 11.28} can be used under the provisions of 11.7.3. For example, when the shear-friction reinforcement is perpendicular to the shear plane, the shear strength V_n is given by^{11.26, 11.28}

$$V_n = 0.8 A_v f_y + A_c K_1 \quad (1b)$$

where A_c is the area of concrete section resisting shear transfer (sq. in.) and $K_1 = 400$ psi for normal weight concrete, 200 psi for "all lightweight" concrete, and 250 psi for "sand lightweight" concrete. These values of

K_1 apply to both monolithically cast concrete and to concrete cast against hardened concrete with a rough surface, as defined in 11.7.9.

In this equation, the first term represents the contribution of friction to shear-transfer resistance (0.8 representing the coefficient of friction). The second term represents the sum of: (1) the resistance to shearing of protrusions on the crack faces, and (2) the dowel action of the reinforcement.

When the shear-friction reinforcement is inclined to the shear plane, such that the shear force produces tension in that reinforcement, the shear strength V_n is given by

$$V_n = A_{vf} f_y (0.8 \sin \alpha_f + \cos \alpha_f) + A_c K_1 \sin^2 \alpha_f$$

where α_f is the angle between the shear-friction reinforcement and the shear plane, (i.e. $0 < \alpha < 90$ deg).

When using the modified shear-friction method, the terms $(A_{vf} f_y / A_c)$ or $(A_{vf} f_y \sin \alpha_f / A_c)$ must not be less than 200 psi for the design equations to be valid.

11.7.4 - Shear-friction design method

11.7.4.1 - When shear-friction reinforcement is perpendicular to shear plane, shear strength V_n shall be computed by

$$V_n = A_{vf} f_y \mu \quad (11-26)$$

where μ is coefficient of friction in accordance with 11.7.4.3.

R11.7.4 - Shear-friction design method

R11.7.4.1 - The required area of shear-transfer reinforcement A_{vf} is computed using

$$A_{vf} = \frac{V_u}{\phi f_y \mu}$$

The specified upper limit on shear strength must also be observed.

11.7.4.2 - When shear-friction reinforcement is inclined to shear plane, such that the shear force produces tension in shear-friction reinforcement, shear strength V_n shall be computed by

$$V_n = A_{vf} f_y (\mu \sin \alpha_f + \cos \alpha_f) \quad (11-27)$$

where α_f is angle between shear-friction reinforcement and shear plane.

R11.7.4.2 - When the shear-friction reinforcement is inclined to the shear plane, such that the component of the shear force parallel to the reinforcement tends to produce tension in the reinforcement, as shown in Fig. 11.7.4, part

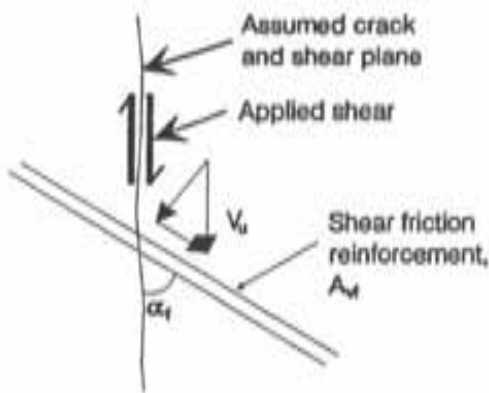


Fig. 11.7.4 - Shear-friction reinforcement at an angle to assumed crack

of the shear is resisted by the component parallel to the shear plane of the tension force in the reinforcement.^{11,26} Eq. (11-27) must be used only when the shear force component parallel to the reinforcement produces tension in the reinforcement, as shown in Fig. 11.7.4. When α_f is greater than 90 deg, the relative movement of the surfaces tends to compress the bar and Eq. (11-27) is not valid.

11.7.4.3 - The coefficient of friction μ in Eq. (11-26) and Eq. (11-27) shall be

Concrete placed monolithically 1.41

R11.7.4.3 - In the shear-friction method of calculation, it is assumed that all the shear resistance is due to the friction between the crack faces. It is, therefore, necessary to use artificially high values of the coefficient of friction in the shear-friction equations, so that the calculated shear strength will be in reasonable

Concrete placed against hardened concrete with surface intentionally roughened as specified in 11.7.9 1.0λ

Concrete placed against hardened concrete not intentionally roughened 0.6λ

Concrete anchored to as-rolled structural steel by headed studs or by reinforcing bars (see 11.7.10) 0.7λ

where $\lambda = 1.0$ for normal weight concrete, 0.85 for "sand-lightweight" concrete and 0.75 for "all light-weight" concrete. Linear interpolation is permitted when partial sand replacement is used.

11.7.5 - Shear strength V_n shall not be taken greater than $0.2 f_c' A_c$ nor $800 A_w$ in pounds, where A_w is area of concrete section resisting shear transfer.

11.7.6 - Design yield strength of shear-friction reinforcement shall not exceed 60,000 psi.

11.7.7 - Net tension across shear plane shall be resisted by additional reinforcement. Permanent net compression across shear plane may be taken as additive to the force in the shear-friction reinforcement $A_{vf} f_y$ when calculating required A_{vf} .

agreement with test results. For the case of concrete cast against hardened concrete not roughened in accordance with 11.7.9, shear resistance is primarily due to dowel action of the reinforcement and tests^{11.27} indicate that reduced value of $\mu = 0.6\lambda$ specified for this case is appropriate.

The value of μ specified for concrete placed against as-rolled structural steel relates to the design of connections between precast concrete members, or between structural steel members and structural concrete members. The shear-transfer reinforcement may be either reinforcing bars or headed stud shear connectors; also, field welding to steel plates after casting of concrete is common. The design of shear connectors for composite action of concrete slabs and steel beams is not covered by these provisions, but should be in accordance with Reference 11.28.

R11.7.5 - This upper limit on shear strength is specified because Eq. (11-26) and (11-27) become unconservative if V_n has a greater value.

R11.7.7 - If a resultant tensile force acts across a shear plane, reinforcement to carry that tension must be provided in addition to that provided for shear transfer. Tension may be caused by restraint of deformations due to temperature change, creep and shrinkage. Such tensile forces have caused failures, particularly in beam bearings.

When moment acts on shear plane, the flexural tension stresses and flexural compression stresses are in equilibrium. There is no change in the resultant compression $A_v f_y$ acting across the shear plane and the shear-transfer strength is not changed. It is therefore not necessary to provide additional reinforcement to resist the flexural tension stresses, unless the required flexural tension reinforcement exceeds the amount of shear-transfer reinforcement provided in the flexural tension zone. This has been demonstrated experimentally.^{11,28}

It has also been demonstrated experimentally^{11,24} that if a resultant compressive force acts across a shear plane, the shear-transfer strength is a function of the sum of the resultant compressive force and the force $A_v f_y$ in the shear-friction reinforcement. In design, advantage should be taken of the existence of a compressive force across the shear plane to reduce the amount of shear-friction reinforcement required, only if it is absolutely certain that the compressive force is permanent.

11.7.8 - Shear-friction reinforcement shall be appropriately placed along the shear plane and shall be anchored to develop the specified yield strength on both sides by embedment, hooks, or welding to special devices.

R11.7.8 - If no moment acts across the shear plane, reinforcement should be uniformly distributed along the shear plane to minimize crack widths. If a moment acts across the shear plane, it is desirable to distribute the shear-transfer reinforcement primarily in the flexural tension zone.

Since the shear-friction reinforcement acts in tension, it must have full tensile anchorage on both sides of the shear plane. Further, the shear-friction reinforcement anchorage must engage the primary reinforcement, otherwise a potential crack may pass between the shear-friction reinforcement and the

body of the concrete. This requirement applies particularly to welded headed studs used with steel inserts for connections in precast and cast-in-place concrete. Anchorage may be developed by bond, by a welded mechanical anchorage, or by threaded dowels and screw inserts. Space limitations often require a welded mechanical anchorage. For anchorage of headed studs in concrete see Reference 11.13.

11.7.9 - For the purpose of 11.7, when concrete is placed against previously hardened concrete, the interface for shear transfer shall be clean and free of laitance. If μ is assumed equal to 7.0λ , interface shall be roughened to a full amplitude of approximately 1/4 in.

11.7.10 - When shear is transferred between as-rolled steel and concrete using headed studs or welded reinforcing bars, steel shall be clean and free of paint.

REFERENCES

1. **ACI Committee 318**, "Building Code Requirements for Reinforced Concrete (ACI 318-56)," American Concrete Institute, Detroit, Michigan, 1956, 74 pp.
2. **ACI Committee 318**, "Building Code Requirements for Reinforced Concrete (ACI 318-63)," American Concrete Institute, Detroit, Michigan, 1963, 144 pp.
3. **ACI Committee 318**, "Building Code Requirements for Reinforced Concrete (ACI 318-89)," American Concrete Institute, Detroit, Michigan, 1989, 353 pp.
4. **Altin, S., Ersoy, U., and Tankut, T.**, "Seismic Strengthening of Reinforced Concrete Frames with Reinforced Concrete Infills," Report No. METU/SML-90/01, Structural Mechanics Laboratory, Middle East Technical University, Ankara, Turkey, June 1990, 81 pp.
5. **Anderson, R.A.**, "Composite Designs in Precast and Cast-in-Place Concrete," *Progressive Architecture*, V. 41, No. 9, Sept. 1960, pp. 172-179.
6. **Bakhoun, M.M., Buyukozturk, O., and Beattie, S.M.**, "Structural Performance of Joints in Precast Concrete Segmental Bridges," Report No. R89-26, Massachusetts Institute of Technology, November 1989, 239 pp.
7. **Bass, R.A.**, "An Evaluation of the Interface Shear Capacity of Techniques Used in Repair and Strengthening Reinforced Concrete Structures," Master of Science thesis, The University of Texas at Austin, August 1984, 229 pp.
8. **Bass, R.A., Carrasquillo, R.L., and Jirsa, J.O.**, "Interface Shear Capacity of Concrete Surfaces Used in Strengthening Structures," PMFSEL Report No. 85-4, The University of Texas at Austin, December 1985, 82 pp.
9. **Bass, R.A., Carrasquillo, R.L., and Jirsa, J.O.**, "Shear Transfer across New and Existing Concrete Interfaces," *ACI Structural Journal*, V. 86, No. 4, July - August 1989, pp. 383-393.
10. **Birkeland, P.W., and Birkeland, H.W.**, "Connections in Precast Concrete Construction," *ACI Journal, Proceedings*, V.63, No. 3, Mar. 1966, pp. 345-368.
11. **Bouadi, A., Engelhardt, M.D., Jirsa, J.O., and Kreger, M.E.**, "Use of Eccentric Steel Bracing for Strengthening of R/C Frames," *Proceedings on Structural Engineering in Natural Hazards Mitigation, ASCE Structures Congress*, Vol. 1, Apr. 1993, pp. 307-312.

12. **Gambarova, P.G., and Prisco, M.D.**, "Behavior and Analysis of R.C. Structures Under Alternate Actions Inducing Inelastic Response; Chapter 5 - Interface Behavior," CEB - GTG 22, Draft presented at CEB Plenary Session, Wien, September 1991, 55 pp.
13. **Gaynor, P.J.**, "The Effect of Openings on the Cyclic Behavior of Reinforced Concrete Infilled Shear Walls," Master of Science thesis, The University of Texas at Austin, August 1988, 245 pp.
14. **Hanson, N.W.**, "Precast - Prestressed Concrete Bridges 2. Horizontal Shear Connections," Development Department Bulletin D35, Portland Cement Association, 1960, pp. 38-58.
15. **Hofbeck, J.A., Ibrahim, I.O., and Mattock, A.H.**, "Shear Transfer in Reinforced Concrete," *Journal of the American Concrete Institute*, Vol. 66, No. 2, February 1969, pp. 119-128.
16. **Holmes, W.T.**, Private Communication, Meeting of NSF Repair and Rehabilitation Research Program, The University of Texas at Austin, November 1991.
17. **Jimenez, L.**, "Strengthening of Reinforced Concrete Frame Using an Eccentric Shear Wall," Master of Science thesis, The University of Texas at Austin, May 1989, 67 pp.
18. **Jimenez, R., Perdikaris, P., and White, R.**, "Interface Shear Transfer and Dowel Action in Cracked Reinforced Concrete Subject to Cyclic Shear," Report No. 78-2, Cornell University, Ithaca, May 1978, pp. E1-E10.
19. **Jordan, R.M.**, "Evaluation of Strengthening Schemes for Reinforced Concrete Moment-Resisting Frame Structures subjected to Seismic Loads," Ph.D. dissertation, The University of Texas at Austin, May 1991, 207 pp.
20. **Koseki, K., and Breen, J.E.**, "Exploratory Study of Shear Strength of Joints For Precast Segmental Bridges," Report No. CTR 3-5-80-248-1, Center For Transportation Research, The University of Texas at Austin, September 1983, 94 pp.
21. **Kriz, L.B., and Raths, C.H.**, "Connections in Precast Concrete Structures - Strength of Corbels," *Journal of the Prestressed Concrete Institute*, Vol. 10, No. 1, Feb. 1965, pp. 16-61.
22. **Lukose, K., Gergely, P., and White, R.N.**, "A study of Lapped Splices in Reinforced Concrete Columns Under Severe Cyclic Loads," Report No. 81-11, Cornell University, Ithaca, July 1981.

23. **Mast, R.F.**, "Auxiliary Reinforcement in Concrete Connections," Proceedings, ASCE, Vol. 94, ST6, June 1968, pp. 1485-1504.
24. **Mattock, A.H.**, "Shear Transfer in Concrete Having Reinforcement at an Angle to the Shear Plane," Shear in Reinforced Concrete, SP-42, American Concrete Institute, Detroit, 1974, pp. 17-42.
25. **Mattock, A.H., and Hawkins, N.M.**, "Shear Transfer in Reinforced Concrete - Recent Research," Journal, Prestressed Concrete Institute, V. 17, No. 2, March - April 1972, pp. 55-75.
26. **Orangun, C.O., Jirsa, J.O., and Breen, J.E.**, "A Re-Evaluation of Test Data on Development Length and Splices," ACI Journal, Proceedings, March 1977, V. 74, pp. - 114-122.
27. **Panahshahi, N., White, R.N., and Gergely, P.**, "Compression and Tension Lap Splices in Reinforced Concrete Members Subjected to Inelastic Cyclic Loading," Report No. 87-2, Cornell University, Ithaca, April 1987.
28. **Paulay, T., and Loeber, P.J.**, "Shear Transfer by Aggregate Interlock," Shear in Reinforced Concrete, SP-42, American Concrete Institute, Detroit, 1974, pp. 1-15.
29. **Paulay, T., Park, P., and Phillips, M.H.**, "Horizontal Construction Joints in Cast-In-Place Reinforced Concrete," Shear in Reinforced Concrete, SP-42, American Concrete Institute, Detroit, 1974, pp. 599-616.
30. **Pincheira, J.A.**, "Seismic Strengthening of Non-Ductile Reinforced Concrete Frames using Post-Tensioned Bracing Systems," Ph.D. dissertation, The University of Texas at Austin, May 1992.
31. **Prestressed Concrete Institute**, "PCI Design Handbook - Precast and Prestressed Concrete," 3rd Edition, Prestressed Concrete Institute, Chicago, 1985.
32. **Sagan, V. E., Gergely, P., and White, R.N.**, "Behavior and Design of Noncontact Lap Splices Subjected to Repeated Inelastic Tensile Loading," ACI Structural Journal, V. 88, No. 4, July - August 1991, pp. 420-431.
33. **Shah, S.**, "Evaluation of Infill Wall Strengthening Schemes for Non-Ductile Reinforced Concrete Buildings," Master of Science thesis, The University of Texas at Austin, May 1989, 68 pp.

34. Sivakumar, B., Gergely, P., and White, R.N., "Behavior and Design of Reinforced Concrete Column-Type Lapped Splices Subjected to High-Intensity Cyclic Loading," Report No. 82-11, Cornell University, Ithaca, October 1982.
35. Sivakumar, B., Gergely, P., and White, R.N., "Suggestions for the Design of R/C Lapped Splices for Seismic Loading," *Concrete International: Design & Construction*, V. 5, No. 2, Feb. 1983, pp. 46-50.
36. Structural Welding Committee, "Structural Welding Code - Reinforcing Steel," AWS D1.4, American Welding Society, 3rd edition, Miami, 1979.
37. Sugano, S., "Guidelines For Seismic Retrofitting (Strengthening, Toughening, and/or Stiffening), Design of Existing Reinforced Concrete Buildings," Proceedings of the Second Seminar on Repair and Retrofit of Structures, Ann Arbor, Michigan, May 1981, pp. 189-246.
38. Suleiman, R.E., Ersoy, U., and Tankut, T., "Behavior of Jacketed R/C Columns Subjected to Combined Axial Load and Bending," Report No. METU/SML-91/04, Structural Mechanics Laboratory, Middle East Technical University, Ankara, Turkey, June 1991, 63 pp.
39. Vintzileou, E.N., and Tassios, T.P., "Behavior of Dowels Under Cyclic Deformations," *ACI Structural Journal*, V. 84, No. 1, January - February 1987, pp. 18-30.
40. White, R.N., and Gergely, P., "Shear Transfer in Thick Walled Reinforced Concrete Structures Under Seismic Loading," Report No. 78-2, Cornell University, Ithaca, May 1978.
41. Yamada, M., Kawamura, H., and Katagihara, K., "Reinforced Concrete Shear Walls Without Openings; Test and Analysis," *Shear in Reinforced Concrete*, SP-42, American Concrete Institute, Detroit, 1974, pp. 539-558.
42. Yamada, M., Kawamura, H., and Katagihara, K., "Reinforced Concrete Shear Walls With Openings; Test and Analysis," *Shear in Reinforced Concrete*, SP-42, American Concrete Institute, Detroit, 1974, pp. 559-578.

VITA

Rajalingam Valluvan was born in Jaffna, Sri Lanka on January 28, 1964, the son of Nallathamby Rajalingam and Maheswary Rajalingam. After completing his work at Jaffna Hindu College, Sri Lanka in 1983, he entered Anna University, Madras, India to pursue a Bachelor of Engineering (B.E.) degree in Civil Engineering. After completion of his undergraduate studies in 1987, he attended Imperial College of Science, Technology and Medicine, University of London, England, where he earned his D.I.C. and M.Sc. degrees in Concrete Structures in 1989. In September 1989, he entered the Graduate School of University of Texas at Austin to pursue his doctoral work. He married Naganimalini Rajaratnam on December 6, 1992.

Permanent address: 43 Galsborough House
Ayley Croft
Enfield, London EN1 1XY
United Kingdom

This dissertation was typed by the author.